NTNU – Trondheim
Norwegian University of
Science and Technology

Behavior and modeling of injection molded PP

Heine Havneraas Røstum

Department of Structural Engineering
Faculty of Engineering Science and Technology
NTNU- Norwegian University of Science and Technology

MASTER THESIS 2014

SUBJECT AREA:	DATE:	NO. OF PAGES:
Polymer engineering	11. feb. 2014	116+209

TITLE:

Behavior and modeling of injection-molded PP

Oppførsel og modellering av sprøytestøpt PP

BY:

Heine Havneraas Røstum

SUMMARY:

The structural impact laboratory (SIMLab) at NTNU has developed a constitutive material model to represent the behavior of brittle and ductile polymeric materials. The material model can be implemented into finite element solvers, e.g. LS-Dyna and Abaqus. In this thesis, the material model's ability to describe the behavior of an injection-molded polypropylene (PP), provided by TOYOTA, has been studied.

The injection-molded polypropylene displayed an inhomogeneous material behavior. During tensile loading, the material's core fractured prior to its outer section. This behavior had been observed for previous injection-molded polypropylenes, and is known as a "skin-core" effect.

To evaluate the accuracy of SIMLab's polymer model to predict the material's behavior, the material's mechanical properties at different sections and the material's morphology had to be identified. This was done through an array of experimental tests. To separate the material's mechanical properties at it's core from its skin, tensile loading tests were performed with and without a reduction in the test specimens' section thickness. The results from the experimental tests showed that the main difference in the material's mechanical properties of its skin and core section was that the skin had a higher yield stress and lower damage propagation than the core.

The validation of SIMLab polymer model's ability to represent the material's behavior was done by using the material model in a numerical simulation of a drop tower test performed using the injection-molded PP, where the material had been separated into a skin and a core part. The numerical simulation showed that SIMLab's polymer model could quite accurately represent the behavior of the injection-molded PP.

RESPONSIBLE TEACHER: Professor Arild H. Clausen

SUPERVISOR(S): Arild H. Clausen, David Morin, Ernesto Mottola

CARRIED OUT AT: SIMLab, NTNU and TOYOTA technical centre, Zaventem, Belgium

MASTER THESIS 2014

Heine Røstum

Behaviour and modelling of injection-moulded PP

(Oppførsel og modellering av sprøytestøpt PP)

As a part of the development of the finite element method, significant effort has been devoted to propose new material models which are able to represent the material behaviour at different conditions. Relevant parameters involve strain level, strain rate, temperature, and the material at hand may also exhibit pressure sensitivity, anisotropy, viscoelasticity etc. The material properties may also be dependent on the production process. In particular, injection moulded parts often exhibit an in-plane anisotropy and a skin-core layer effect.

The intention with this master thesis is to explore the behaviour of an injection-moulded PP provided by Toyota. The experimental work is going to be carried out at SIMLab, Department of Structural Engineering, NTNU, and involves material tests as well as some component tests. Careful post-processing of the results is an important part of the thesis. In the numerical study, the candidate is going to employ a material model developed at SIMLab. The aim is to evaluate the ability of the model to capture the behaviour observed in the experimental tests. The work related to this part of the thesis will be carried out in Brussels.

Possible keywords for activities in this master thesis research work may include:
- Literature: Injection-moulded polymers, material models, skin-core effect
- Experimental tests: Material and component tests. Presentation of test results
- Calibration: Identification of model coefficients
- Numerical modelling: Simulation of experimental tests. Evaluation of the model

The candidate may agree with the supervisors to pay particular attention to specific parts of the investigation, or include other aspects than those already mentioned.

The thesis is to be organized as a research report, recognising the guidelines provided by Department of Structural Engineering.

Supervisors at NTNU: David Morin and Arild Holm Clausen
Contact persons at Toyota: Yann Claude Ngueveu and Ernesto Mottola

The report is to be handed in not later than 1 March 2014.

NTNU, 1 September 2013

Arild Holm Clausen

Acknowledgments

I would like to express my sincere gratitude to Professor Arild H. Clausen and researcher Ph.D. David Morin, for the excellent guidance that I have received during my work. Thank you, David, for having an utmost patience and understanding when I have at times troubled you with too many questions.

I would also like to give a special thanks to Ph.D. Ernesto Mottola at TOYOTA motor Europe, for allowing me to do parts of my thesis at their office in Zaventem, and for providing me with valuable feedback.

Sharing desk with Yann Claude at TOYOTA has been a very good experience. Thank you Yann, for sharing your desk with me and for providing many interesting topics of discussion, both professional and non-professional. You and the other employees at TOYOTA made my stay in Brussels truly memorable.

My years of study at NTNU has now come to an end. I would like to thank everyone that have taken part in making my student years into maybe the best years of my life.

Abstract

The structural impact laboratory (SIMLab) at NTNU have developed a constitutive material model to represent the behavior of brittle and ductile polymeric materials. The material model can be implemented into finite element solvers, e.g. LS-Dyna and Abaqus. In this thesis, the material model's ability to describe the behavior of an injection molded polypropylene, provided by TOYOTA, has been studied.

The material had during previous experimental tests shown an inhomogeneous material behavior. As the material was loaded in uniaxial tensile, the core would fracture prior to it's outer section. This "skin-core" behavior has been observed for many injection molded polypropylenes, but the effect varies substantially due to differences in the molding process and the material additives. To determine how the material parameters would vary through the material's cross section, the "skin-core" effect had to be better understood.

To be able to separate the core from the skin, experimental tests were conducted using specimens with and without a reduction in its section thickness. The difference between the material parameters of the specimens with a full thickness and with a reduced thickness, was suggested to be the material parameters of the skin. The experimental tests showed that the main difference was linked to the specimens' yield stress and damage propagation. The specimens with a full section thickness had a higher yield stress and a lower damage propagation than the specimens with a reduced sections thickness.

Experimental tests were also performed to determine how the material's molding thickness would affect it's material properties. Three different molding thicknesses were used; 2mm, 3mm and 4mm. The tests indicated that the molding thickness mainly affected the damage propagation and yield stress of the material, the damage propagation increased and the yield stress decreased with an increase in the material's molding thickness. The tests suggested that the difference was larger for the material's skin than for it's core, which may be due to the distribution of particles.

To evaluate SIMLab polymer model's ability to describe the material's behavior, numerical simulations of the experimental tests were conducted. The numerical simulations ability to reproduce the behavior of the experimental tests would be used to determine the accuracy of the material model. The numerical models were composed of two sections; one for the core and one for the skin. Where the behavior of each section was controlled by it's own material card. The thickness of the skin was determined to be 0.2mm, based on visual evidence using an optical microscope.

Drop-tower tests and tensile loaded notched specimens were used for validation of the material model. The simulation results, indicated that SIMLab's polymer model could predict the material's behavior well, but that improving the formulation of the plastic flow will yield better results. The current formulation is not able to capture the material's transverse behavior and the material's behavior in compression.

Sammendrag

Structural impact laboratory (SIMLab) ved NTNU har utviklet en konstitutiv materialmodell for å beskrive oppførselen til sprø og duktile polymeriske materialer. Denne materialmodellen kan implementeres i elementmetodeprogrammer, slik som LS-Dyna og Abaqus. I denne oppgaven, vil materialmodellens evne til å beskrive oppførselen til et sprøytestøpt polypropylen, fra TOYOTA, undersøkes.

Material har ved tidligere forsøk vist en inhomogen oppførsel. Da materialet ble påført en enaksiell strekklast, startet bruddet i materialets kjerne før det spredte seg i tykkelsesretningen. Denne "skinn-kjerne" oppførselen har blitt observert for flere sprøytestøpte polypropylener, men effekten har variert betydelig som årsak av forskjell i støpeprosessen og tilsetningsstoffer. For å bestemme hvordan materialets parametere varierte gjennom tykkelsen, måtte "skinn-kjerne" effekten bli bedre forstått.

For å kunne separere kjernen fra skinnet, ble eksperimentelle tester utført hvor det på noen av prøvestykkene ble fjernet det ytterste laget. Forskjellen i materialparameterene til prøvestykkene med en redusert tykkelse og med en full tykkelse, ble tilegnet materialets skall. De eksperimentelle testene viste at hovedforskjellen lå i prøvenes flytespenning og skadeforplantning. Testene med full tykkelse hadde høyere flytespenning og en lavere skadeforplantning enn testene med en redusert tykkelse.

Det ble også utført forsøk for å bestemme hvordan materialets støpetykkelse ville påvirke materialegenskapene. Testene ble utført med tre ulike støpetykkelser; 2mm, 3mm og 4mm. Testene indikerte at støpetykkelsen i hovedsak påvirket materialets skadeforplantning og flytespenning. Materialets skadeforplantning økte, og flytespenning ble lavere ved økt støpetykkelse. Testene antydet at forskjellen var større for prøvestykkene med et fult tverrsnitt, enn for de med et redusert tverrsnitt, noe som kan skyldes fordelingen av partikler i materialet.

For å evaluere SIMLab sin polymer models evne til å beskrive materialets oppførsel, ble numeriske simuleringer av de eksperimentelle forsøkene gjennomført. De numeriske simuleringenes evne til å gjenskape oppførselen til de eksperimentelle forsøkene, ble brukt for å bestemme materialmodellens nøyaktighet. De numeriske modellene bestod av to deler; en for kjernen og en for skallet. Oppførselen i hver del ble bestemt av et eget materialkort. Tykkelsen av skallet ble bestemt til å være 0.2mm, basert på observasjoner gjort med et optisk mikroskop.

Drop-tower tester og prøvestykker med hakk, testet under strekk, ble brukt for å validere materialmodellen. Resultatene fra simuleringene indikerte at SIMLab sin polymermodell kunne anslå materialets oppførsel svært godt, men at en ny eller forbedret formulering av materialets plastiske støm vil gi bedre resultater. Den nåverende formuleringen klarer ikke å fange materialets transversale tøyninger, og heller ikke materialets oppførsel under trykk.

Contents

Chapter 1

Introduction

A large portion of new cars' shock-absorbing exterior is currently composed of polymers. For the car industry to safely engineer these parts of of their cars, they need a good understanding of the material's behavior, and an engineering tool that can be used to accurately reproduce this behavior. In this thesis, a polymer which is widely used in the car industry, and an engineering tool to describe it, has been studied.

The polymer studied herein, is a polypropylene with elastomer additives supplied by TOYOTA, which has been fabricated using an injection molding process. Earlier testings with the same material have displayed a "skin-core" behavior, the fractured surface of the test specimens had given indications of a non-homogeneous material behavior, that varied from the core of the specimens cross section to its surface [23]. Material skin-core effects have been observed for a number of injection molded polypropylenes, and it's affect on the material's mechanical properties is unquestionable [6, 13, 12]. The problem is that the skin-core effect varies with different additives, geometries and molding techniques. Thus the difference in the material's mechanical properties in the skin and the core that is mentioned in other articles, is not necessarily applicable for this material.

To better understand how the material's properties varied, different test methods has been applied for this thesis. An array of tests were conducted in which the material was loaded, and it was attempted to separate the mechanical properties of the skin from the core. The material's morphology was also investigated using different methods which included analyzing material specimens through electron scanning microscopy (SEM) and using an optical microscope.

The intention of the material tests, was to have more information from which finite element analyzes could be created. There are currently a number of finite element solver softwares; e.g LS-Dyna and Abaqus, that can be safely used for design purposes. These solvers have multiple material models that can be used to describe the material properties and behavior of metals, but the number of material models that can accurately describe polymers behavior, is far more rare. The structural impact laboratory (SIMLab) at NTNU has therefore developed a material model who's intended purpose is to describe the material behavior of brittle and ductile polymeric materials.

The SIMLab polymer material model allows the user to account for multiple material features, which includes; strain rate sensitivity, material hardening and softening, and fracture. Depending on the required accuracy of the model, some of these features may be turned on and off. A hypoe-

lastic co-rotational stress formulation has been used for it's implementation. The material model can be applied to both solid and shell elements.

The intention of this thesis has been to investigate the material behavior of the polypropylene supplied by TOYOTA, especially it's skin-core behavior, for the purpose of creating more accurate numerical simulations using finite element solvers with the SIMLab developed polymer material model. Experimental tests were performed to calibrate the material model, and to give a better understanding of the material's behavior. The aim of the work was to determine and evaluate the SIMLab polymer model's ability to accurately reproduce the behavior of the injection molded polypropylene.

The report starts with a description of the material, the injection molding process, and the material model. The method, post processing and results of the experimental testing is then presented, which is followed by a chapter concerning how the material parameters were calibrated. The modeling and results of the numerical models used to recreate the experimental tests is then described, before the report is ended with some final conclusions and recommendations for further work.

Chapter 2

Material and Material Model

As previously mentioned, the purpose of this thesis is to investigate the material behavior of an injection molded polypropylene, which has been provided by TOYOTA, in order to determine how well the polymer material model developed at SIMLab is able to reproduce the material's behavior. In this chapter, polypropylene and polymers in general will be described, as well as the procedure of injection molding. The equations and the principles of SIMLab's material model will be briefly presented in this chapter.

2.1 Material

The material investigated in this thesis is a polypropylene filled with elastomers, which means that rubber additives has been added to the material during the molding process. The polypropylene is at TOYOTA abbreviated as TSOP7, but will in this thesis be abbreviated to PP1.

2.1.1 Polypropylene

Polymers consists of multiple molecular chains, and each of these chains consists of numerous identical units called monomers. The monomer of polypropylene is propylene, which is also known as propene, and it has the molecular formula (C_3H_6). During the polymerisation of propene, the double binding between two of the carbon atoms is broken, allowing the monomers to create a chain, the polypropylene, with the molecular formula; $(C_3H_6)_n$. The polymerisation of propen to polypropylene is depicted in Figure 2.1. [11]

Figure 2.1: Polymerisation of propen to polypropylene

Polypropylene is a semi-crystalline thermoplastic polymer. A semi-crystalline material contains a

mixture of amorphous and crystalline regions, and a thermoplastic polymer consists of linear molecular chains. Instead of linear chains, there is also the possibility of covalent cross linking between the molecular chains. This cross linking is crucial for determining the mechanical properties of the material. Depending on the number of cross links, the polymer could either be an elastomer, also known as rubber, or a duromer, where elastomer has some cross links and the duromer has multiple [11]. The Van Der Waals bonds between the molecular chains are much weaker than the the covalent bonds between the monomers. As a result, the bonds between the molecular chains are broken prior to the covalent bonds between the atoms. In the unloaded state, the polymer chains are twisted and entangled.

During the elastic deformation, the covalent bonds in the molecular chains are stretched and deformed. At necking, the molecular chains are straightened as the weak Van der Waals bonds between the chains are broken. When all the molecular chains are completely straightened, the covalent bonds will break and the material will start to fracture. The characteristic behavior of polymers during uniaxial loading is shown in Figure 2.2.[1]

(a) Elastic   (b) Necking   (c) Prior to fracture
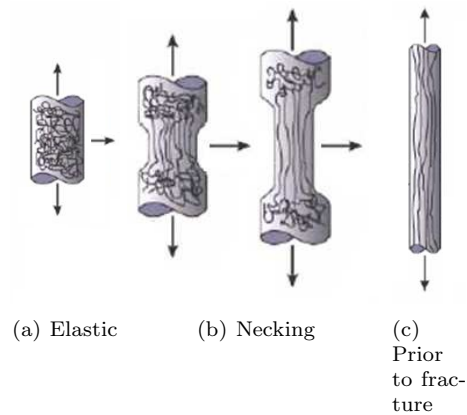
Figure 2.2: Deformation of polymers during tensile loading [1]

2.1.2   Injection molding

An injection molding machine consists of two main components; an injection unit and a clamping unit, as seen in Figure 2.3. The injection unit is heating and melting the the material, before it is transferred under high pressure into the mold, which is held shut by the clamping unit.

4
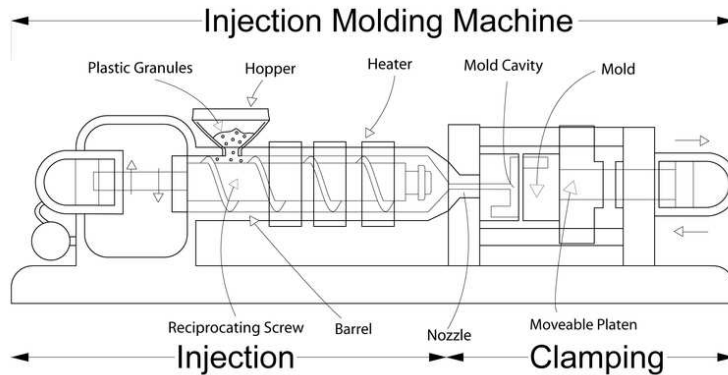
Figure 2.3: Injection molding machine [24]

The injection molding process

Not much information has been provided by TOYOTA concerning the injection molding process of the TSOP7, thus the process described in this section will be a general description of a typical operating sequence, which has been described in multiple articles [4, 7].

The process normally starts with the material being fed into the machine by gravity through the hopper. The rotation of the screw and external electric heating is melting the material. The design and rotation of the screw is important to ensure that the material has a homogeneous temperature and mixture, it is also pushing the material forward. The material is accumulated in front of the screw. When the injection unit is activated, the screw pushes the material through the nozzle and into the mold.

Initially the material is filled into the cavity of the mold at a relatively short time, this depends on the geometry and the material. When the mold is completely filled and the material starts to cool down, the material will start to shrink. More material is then injected into the mold to ensure a stable pressure. If performed correctly, this procedure can greatly increase the physical properties of the material.

When the material has achieved enough rigidity, it is ejected from the mold and the process is repeated.

Injection molding process' effect on material

The injection molding process' effect on the material properties is highly dependent on the material and the process itself. It has previously been observed, that due to the shear stress and rapid cooling close to the molds surface, the material closest to the surface will in general have a highly oriented low crystallinity micro structure [4]. The molecular chains will in this region be oriented in the materials flow direction during molding while the material's core will normally have a less oriented structure, and a higher degree of crystallinity.

During molding, a defect that may occur is weld lines [4]. The weld lines are caused by multiple insertion points into the mold, and will have a considerable effect on the materials mechanical

properties. It is almost impossible to avoid weld lines, but their affect can be greatly reduced by improving the processing conditions.

2.2 Material Model

Determining how well the material model developed at NTNU SIMLab is able to capture the material behavior of the material provided by TOYOTA, has been the aim of this thesis. The material model includes multiple features which is possible to switch on and off, based on the users purpose for the material model. In this section, only the features used for the numerical models in Chapter 5 will be described.

The material model contains two parts; one elastic and one plastic part. The description of SIMLab's material model is in this report highly based on the theory manual for SIMLab's polymer model [21]. The elastic part takes into account the intra molecular resistance of the material, see Figure 2.2a). The plastic part, accounts for the stretching and breaking of the molecular chains. This is the deformations which occurs in Figure 2.2b) and c). A rheoligical model, that illustrates the major features of SIMLab's polymer model, is shown in Figure 2.4.
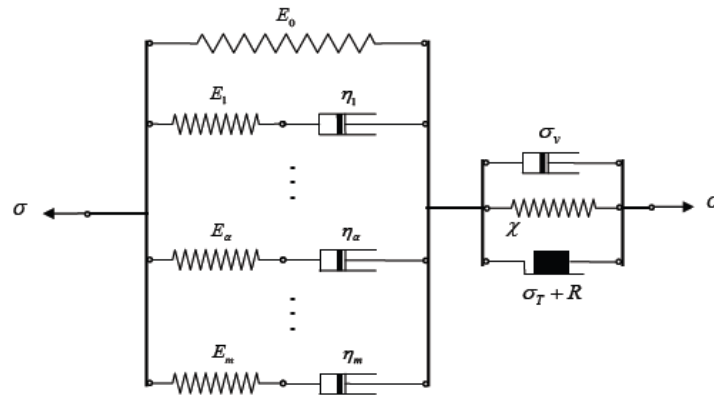
Figure 2.4: Principle of material model [21]

In the rheological model, the material is divided into one visco-elastic part, and a visco-plastic part. The total strain deformation of the material can be decomposed into:

$$\varepsilon = \varepsilon^e + \varepsilon^p \tag{2.1}$$

Where ε^e is the strain in the elastic region, and ε^p is the strain in the plastic region.

2.2.1 Elastic region

Calculating elastic stresses

The elastic region consists of a linear elastic spring with stiffness E_0, which is in parallel with multiple Maxwell elements with spring stiffness E_α and viscosity η_α. The elastic region of the Maxwell elements is decomposed into a linear elastic region, ε_α^e, and an inelastic region, ε_α^i:

$$\varepsilon^e = \varepsilon_\alpha^e + \varepsilon_\alpha^i \tag{2.2}$$

The stress distribution in the elastic region can be written as:

$$\sigma = \sigma_0 + \sum_{\alpha=1}^{m} \sigma_\alpha \qquad \text{where} \qquad \begin{cases} \sigma_0 = E_0 \varepsilon^e \\ \displaystyle\sum_{\alpha=1}^{m} \sigma_\alpha = \sum_{\alpha=1}^{m} \left(E_\alpha^e \varepsilon_\alpha^e + \eta_\alpha \dot{\varepsilon}_\alpha^i \right) \end{cases} \tag{2.3}$$

In this thesis, only the linear elastic part of the model will be considered. The focus of this thesis is in the plastic region of the material, as the experimental tests performed yielded few data points in the material's elastic region. It is therefore decided not to include any maxwell elements in the material model.

The linear elastic stress is calculated by assuming an isotropic material. With Newton notation, the elastic stress thus becomes:

$$\sigma_{ij} = \frac{\nu \mathrm{E}}{(1+\nu)(1-2\nu)} \varepsilon_{kk}^e \delta_{ij} + 2G \varepsilon_{ij}^e \tag{2.4}$$

Here ν, is Poisson's ratio, ε_{kk} is the strain in the principle directions, and G is the shear modulus. The stress in the first principle direction due to the elastic strain will be:

$$\sigma_{11} = \frac{\nu \mathrm{E}}{(1+\nu)(1-2\nu)} (\varepsilon_{11}^e + \varepsilon_{22}^e + \varepsilon_{33}^e) + 2G \varepsilon_{11}^e \tag{2.5}$$

The bulk modulus, K, and the shear modulus, G, is calculated using:

$$K = \frac{E}{2(1+\nu)} \tag{2.6a}$$

$$G = \frac{E}{3(1-2\nu)} \tag{2.6b}$$

Raghava's yield criterion

For polymers, Raghava's yield criterion is commonly used. Raghava's yield criterion is a modified von Mises yield criterion, which takes the difference in yield strength in tension and compression into consideration [20]. The Raghava yield surface may be expressed as:

$$(\sigma_1 - \sigma_2)^2 + (\sigma_2 - \sigma_3)^2 + (\sigma_3 - \sigma_1)^2 + 2(|\sigma_C| - |\sigma_T|)(\sigma_1 + \sigma_2 + \sigma_3) = 2|\sigma_T \sigma_C| \tag{2.7}$$

Here σ_C and σ_T are the yield stress in compression and tension, respectively. By introducing the total stress invariant, I_1, and the deviatoric stress invariant, J_2:

$$I_1 = \sigma_1 + \sigma_2 + \sigma_3 \tag{2.8a}$$

$$J_2 = \frac{1}{6} \left[(\sigma_1 - \sigma_2)^2 + (\sigma_2 - \sigma_3)^2 + (\sigma_3 - \sigma_1)^2 \right] \tag{2.8b}$$

7

The Raghava yield function may be written as:

$$f(I_1, J_2) = \alpha \sigma_T^2 - (\alpha - 1)I_1 \sigma_T - 3J_2 = 0 \qquad \text{,where} \quad \alpha = \left| \frac{\sigma_C}{\sigma_T} \right| \tag{2.9}$$

Which yields the following expression for the Raghava equivalent stress:

$$\sigma_{eq} = \frac{(\alpha - 1)I_1 + \sqrt{(\alpha - 1)^2 I_1^2 + 12 J_2 \alpha}}{2\alpha} \tag{2.10}$$

If the yield stress in compression is equal to the yield stress in tension, $\alpha = 1$, it will reduce Eq. (2.10) to von Mises:

$$\sigma_{Mises} = \sqrt{3J_2} = \sqrt{\frac{1}{2}[(\sigma_1 - \sigma_2)^2 + (\sigma_2 - \sigma_3)^2 + (\sigma_3 - \sigma_1)^2]} \tag{2.11}$$

In Figure 2.5, the yield surface using the von Mises and Raghava stress formulation in the I_1-J_2 plane have been depicted. From the graph, we see that the deviatoric stress invariant, J_2 will not be affected by changing the size or the direction of the total stress invariant, I_1, using the von Mises formulation. For the Raghava formulation on the other hand, the yield surface is greatly influenced by the size and direction of the total stress invariant.
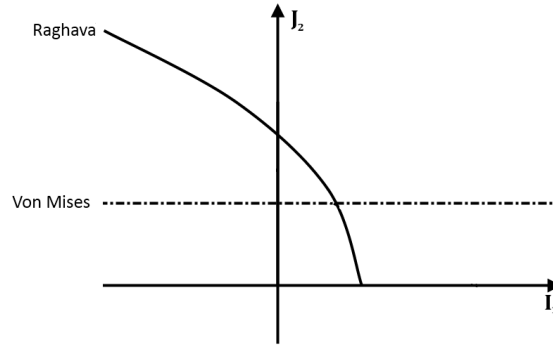
Figure 2.5: Raghava and von Mises yield surface in the I_1-J_2 plane

2.2.2 Plastic Region

Yield function and hardening

The material model's yield function, f, is given by the following relation:

$$f = \sigma_{eq} - (\sigma_0 + R) \tag{2.12}$$

Where σ_{eq} is the Raghava equivalent stress, σ_0 is the initial yield stress, and R is the hardening or softening of the material. The hardening/softening parameter, is defined using the following relation:

$$R(p) = \sum_{i=1}^{3} R_i(p) = \sum_{i=1}^{3} Q_{Ri} \left(1 - exp \left(-\frac{\theta_{Ri}}{Q_{Ri}} p \right) \right) \tag{2.13}$$

p, is the accumulated plastic strain, θ_{Ri} and Q_{Ri} are used to determine the slope of the hardening, and whether the material exhibits hardening or softening. If $\theta_{Ri} > 0$ and $Q_{Ri} > 0$, the material is hardening, and if $\theta_{Ri} < 0$ and $Q_{Ri} < 0$, the material exhibits softening.

Plastic flow rule

Previous testing have shown that an associated flow rule overestimates the volumetric strains [9]. An associated flow rule is obtained by using the yield function as the flow potential. A flow potential, that is not the yield function, which yields a none associated flow rule is therefor used in the material model:

$$\hat{D}^p = \dot{\lambda}\frac{\delta g}{\delta \sigma} \tag{2.14}$$

The flow potential used in the material model is very similar to the Raghava yield function, except that the parameter α, which is the ratio between tension and compression, is now a dilatation parameter, β. The flow potential, g, is defined by:

$$g = \frac{(\beta - 1)I_1 + \sqrt{(\beta - 1)^2 I_1^2 + 12 J_2 \beta}}{2\beta} \tag{2.15}$$

The parameter $\beta \geq 1$, controls the volumetric plastic strain. If $\beta = 1$, the material will exhibit no volumetric strain in the plastic region, and if $\beta = \alpha$, the flow potential will yield an associated flow rule.

Viscoplastic relation

The strain rate dependency in the plastic region of the model is taken into account by the following relation:

$$\dot{p} = \begin{cases} 0 & \text{if} \quad f \leq 0 \\ \dot{p}_0 \left\{ exp\left[\frac{1}{C}\left(\frac{\sigma_{eq}}{\sigma_0 + R} - 1\right)\right] - 1 \right\} & \text{if} \quad f > 0 \end{cases} \tag{2.16}$$

The parameter C, determines the rate sensitivity of the material in the plastic region. $\dot{p}_0$, is a reference plastic strain rate, σ_0 is the material's yield stress, and σ_{eq} is the equivalent stress. By rearranging Eq. (2.16), the equivalent stress outside of the yield surface may be determined by the following relation:

$$\sigma_{eq} = (\sigma_0 + R)\left[1 + C \ln\left(1 + \frac{\dot{p}}{\dot{p}_0}\right)\right] \quad \text{for} \quad f > 0 \tag{2.17}$$

2.2.3   Damage

The material model has the ability to include damage. The damage may occur as initial damage D_I, which is present in the material prior to loading, and/or as damage which occurs due to material deformations during loading. The damage formulation may either be coupled with the constitutive equations, or uncoupled. The damage should be uncoupled if the material does not exhibit substantial volumetric strains during loading, while damage coupling should be included if the material does exhibit large volumetric strains. For uncoupled damage, the constitutive response will only be affected at fracture. If the damage is coupled with the constitutive equation, the material will experience softening as the material's damage evolves.

Ductile damage

The materials flow rule will give plastic dilatation if $\beta > 1$. When the material expands, the material density will reduce which may lead to softening. As damage is irreversible, damage propagation only occurs in the materials plastic domain, and is calculated in the material model using the relation:

$$D = 1 - (1 - D_I)\exp(-\varepsilon_v^p) \tag{2.18}$$

ε_v^p, is the volumetric strain in the plastic region:

$$\varepsilon_v^p = \varepsilon_1^p + \varepsilon_2^p + \varepsilon_3^p \tag{2.19}$$

Coupled Damage

The damage coupling is formulated in the material model by calculating an effective stress, using the following relation for the stress in all the constitutive equations:

$$\sigma = \frac{\sigma}{1 - D} \tag{2.20}$$

Where D, is the damage variable, $0 \leq D < 1$. In Eq. (2.20), the effective stress goes to infinity as D approaches unity.

Fracture

The failure of the material is defined by a critical value, D_C. When an integration point reaches this critical value, the stress tensor is set to zero, thus the integration point is no longer able to carry any load. The failure criteria of the material model is formulated as:

$$D = D_C \qquad , \text{where} \quad D_C < 1 \tag{2.21}$$

2.2.4 Model Parameters

The model proposed by SIMLab can be divided into two main parts, the elastic and the plastic, and one sub part for damage. The parameters included in the various parts have been rendered below.

Elastic Region	
Parameter	**Description**
E	Youngs Modulus
ν	Poisson's Ratio
G	Shear modulus
K	Bulk Modulus

Plastic Region	
Parameter	**Description**
σ_0	Yield Stress
α	Uniaxial tension-compression yield stress ratio
β	Plastic dilatation
θ_{Ri}	Initial isotropic hardening moduli (i=1,2,3)
Q_{Ri}	Saturation value of R_i (i=1,2,3)
C	Rate sensitivity
$\dot{p}_0$	Reference strain rate

Damage	
Parameter	**Description**
D_I	Initial damage
D_C	Critical damage

Other features that is available in the material model, but has not been included is:

- Viscoelasticity

- Kinematic hardening

- Adiabatic heating

- Brittle damage and ECL ductile damage

Chapter 3

Material testing

Material tests were performed in order to determine the material's behavior and properties. Four different tests were done to determine and validate the material properties: Uniaxial tensile and compression tests were performed to calibrate and verify the parameters for the material model. Specimens with notches and drop-tower tests were done to validate the material model and it's parameters. Tests to better understand and determine the layers of the material was also performed. These included hardness tests, scanning electronic microscope (SEM) and optical microscope.

In this chapter the test methods, post processing and results will be described.

3.1 Uniaxile tensile tests

Uniaxile tensile tests were performed in two batches. In the first batch, tensile tests extruded from plates with a 3mm thickness was tested, and in the second batch, uniaxile tensile tests extruded from plates with a thickness of 2mm and 4mm were performed. The purpose of the tests with a different plate thicknesses, was to determine if the material's behavior was varying with different molding thicknesses. The tests extruded from the 3mm plate has been most thoroughly tested.

The specimens were tested with and without a reduced cross section, which will be described in more detail in the subsequent section. The full and reduced cross section of the 3mm plate was tested at three initial strain rates, $\dot{\varepsilon}_0$, while only the full cross section specimens of the 2mm and 4mm plates were tested at three velocities. The material was tested at different strain rates in order to determine the material's strain rate sensitivity.

3.1.1 Test methods

The materials were tested using a servo hydraulic loading machine, seen in Figure 3.1, which was connected to an Instron controller. The Instron controller logs the frame, time, force and displacement of the cross-head during loading. It was also set up two CCD cameras, which recorded the deformation history of the specimens' thickness and width surfaces. The images from the cameras was later used to determine the specimen's strain history during loading, using a method called digital image correlation, which will be described in further detail in the post processing section. The setup of the machine can be seen in Figure 3.1 a).

(a) Machine and equipment setup   (b) Specimen during loading
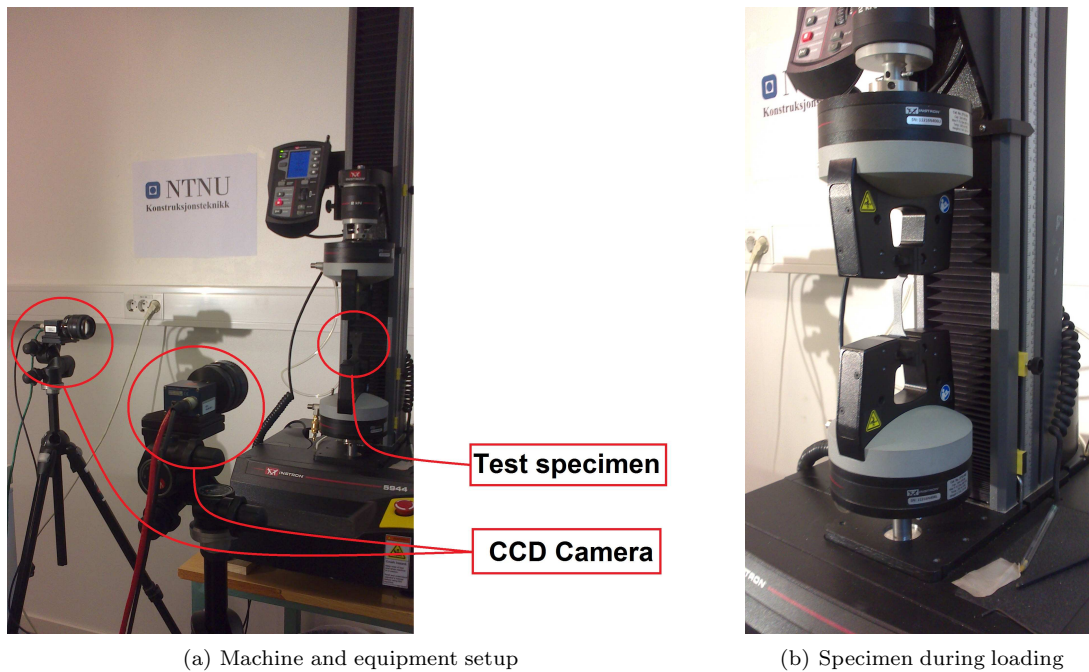
Figure 3.1: Servo hydraulic loading machine used for uniaxial tensile tests

The geometry of the test specimens used for the uniaxial tensile tests is what is known as a "dog bone" geometry, due to its particular geometrical shape. The geometrical specifications of the geometry can be seen in Figure 3.2 a). To test if the material exhibited anisotropic behavior, the plates were milled parallel and normal to the material flow during molding, as seen in Figure 3.2 b). To determine if the material experienced any temperature increase during milling, the surface temperature was measured during this process. The increase in surface temperature was found to be no more than $1^o c$, which will not affect the material properties of the milled specimens. The machine used to mill the specimens can be seen in Figure 3.2c).
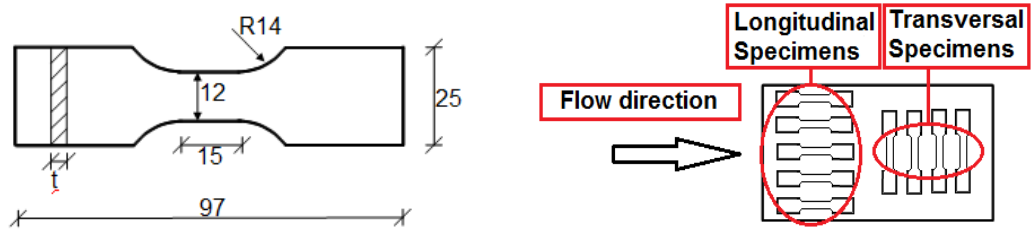
(a) Geometrical specifications

(b) Milling relative to molding direction

(c) Machine used to mill specimens

Figure 3.2: Geometrical specifications and the milling relative to the molding direction of the plate

The cross section was reduced for some tests to try to determine how the material properties would vary in the thickness direction of the material. The 3mm and 4mm thick plates were tested with a full cross section and with a section thickness that was reduced with 0.5mm on each side. The 2mm plate was tested with a full cross section, and with 0.25mm and 0.50mm removed from each side of the specimen. The reductions, and the corresponding abbreviations are shown in the table below.

Cross section	Abbreviation	Material removed from each side
Full	F	0.00mm
Medium	M	0.25mm
Reduced	R	0.50mm

Before testing, the specimens were fastened by clamps at each end, as seen in Figure 3.1b). As the test commenced, the bottom clamp would be held still throughout the test while the top end clamp would move with a constant velocity, v equal to:

$$v = \dot{\varepsilon}_0 l_0 \tag{3.1}$$

Here l_0 is the initial length of the specimens' gauge length, which is 15mm for the dog-bone specimens. $\dot{\varepsilon}_0$ is the true initial strain rate. Three different velocities were used when testing the specimens. The initial strain rate, the corresponding velocity, and the abbreviation used for test labeling is shown in the table below.

15

Initial strain rate, $[\dot{\varepsilon}_0]$	Velocity $[v]$	Abbreviation
$10^{-1}s^{-1}$	1.50 mm/s	V1
$10^{-2}s^{-1}$	0.15 mm/s	V2
$10^{-3}s^{-1}$	0.015 mm/s	V3

The specimens were labeled based on the initial plate thickness, strain rate, reduction of cross section, and the number of tests performed with the particular properties. The tests performed with specimens milled perpendicular to the material flow was marked with a "T" in the material abbreviation.

Material	Thickness	Reduction	Initial strain rate	Test No.
PP1(T)	T2	F	V1	#
			V2	#
			V3	#
		M	V2	#
		R	V2	#
	T3	F	V1	#
			V2	#
			V3	#
		R	V1	#
			V2	#
			V3	#
	T4	F	V1	#
			V2	#
			V3	#
		R	V2	#

As previously mentioned, the specimens' strain history was determined by using digital image correlation, DIC. For the DIC technique to work, the specimens must be given a speckled surface, because the DIC determines the specimens strain history based on the change in the surfaces' gray scale value. It must therefore be contrasts in the specimen's surface for the technique to work properly. The speckled surface is created by first applying a coat of white paint to the specimen's surface, see Figure 3.3b), before it is lightly sprayed with black paint to create the speckled surface seen in Figure 3.3c). It was important that the painting was not dry during loading, as this may cause it to crack as the specimen is deformed. The paint was therefore applied just before the specimens were tested.

(a) Initial surface   (b) White coated surface   (c) Final speckled surface
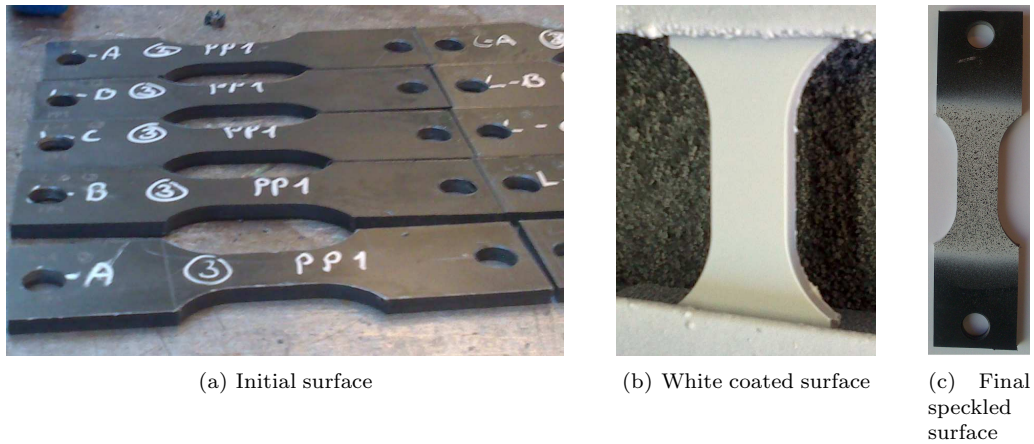
Figure 3.3: Facilitating the specimens for DIC

3.1.2 Post processing

The force-displacement history of the uniaxial tensile tests were obtained directly from the Instron controller, which was wired to the hydraulic loading machine. The stress-strain history was obtained by using the force from the Instron controller and the strains obtained from the digital image correlation.

Digital image correlation, DIC

By using eCorr, which is a digital image correlation tool created by PhD. Egil Fagerholt [5], the longitudinal and transversal strain history of the tensile tests could be determined from the images acquired by the CCD cameras. In eCorr, the user first discretizes a reference image. This is done by selecting the region which is to be analyzed, and then select the element size. The default element size is 25 pixels, which in most cases gives an accurate analyzes, but has herein been lowered to 20 pixels when analyzing the images taken in the specimen's thickness direction. A specimen discretized in eCorr is shown in Figure 3.4a). The strain history of the specimen is calculated on the basis of each updated picture's gray scale value relative to the reference image. Figure 3.4b) shows how the mesh has deformed with the specimen.

(a) Undeformed   (b) Deformed
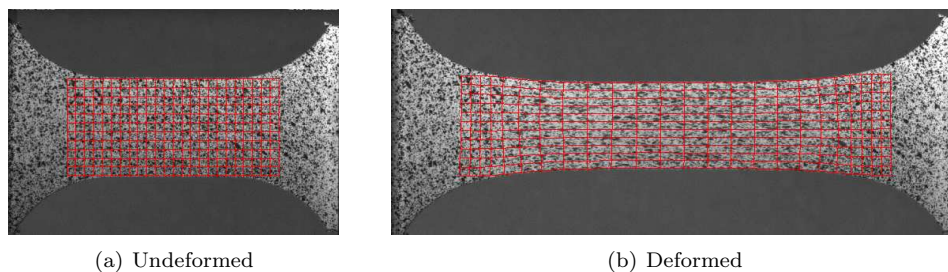
Figure 3.4: Discretization of test specimen in eCorr

The strain outputs from DIC is logarithmic strains, which is also known as true strains. The true

17

strain, ε_t, is calculated as the logarithm of the ratio between the current length, l, and it's initial length, l_0.

$$\varepsilon_t = \log\left(\frac{l}{l_0}\right) \tag{3.2}$$

Stress calculation

The images from the DIC were taken with the same frequency as the force-displacement was logged by the instron controller, which made the post processing somewhat easier as the force-displacement history then correlated well with that of the strain history. Scilab is a mathematical programming software which was used to determine the stress-strain history of the tests, as well as illustrate these results through graphs. The script used to determine the stress as well as removing noise from the results, is available in Appendix B.1.1.

The tests' true stress was calculated on the basis of the strain history acquired from the DIC-analyzes and from the force logged by the Instron controller. For most of the tests, images were taken from two sides, which yielded the transverse strains for both the thickness and width direction. The exception was the tests at the highest strain rate, $\dot{\varepsilon}_0 = 10^{-1}s^{-1}$. At this strain rate, the frequency of the images needed to be logged in order to have an accurate DIC analysis, was too great for the computer if two cameras were used. The transverse strains can be written as:

$$\varepsilon_2 = \log\left(\frac{w}{w_0}\right) \qquad \text{and} \qquad \varepsilon_3 = \log\left(\frac{t}{t_0}\right) \tag{3.3}$$

Here w and w_0 is the actual and initial width of the specimen, respectively. Similarly is the t and t_0 respectively the actual and initial thickness. For most of the tests, the stress history could be calculated using measured strains from two cameras. The true stress was then calculated by:

$$\sigma = \frac{F}{A} = \frac{F}{wt} = \frac{F}{w_0 t_0 \exp\left(\varepsilon_2\right)\exp\left(\varepsilon_3\right)} \tag{3.4}$$

Where F is the force logged by the Instron controller. When pictures were available for only one camera, isotropic behavior was assumed, which means that the transverse strains would be the same in both directions; $\varepsilon_2 = \varepsilon_3$. The stress was thus calculated using the following expression:

$$\sigma = \frac{F}{A} = \frac{F}{wt} = \frac{F}{w_0 t_0 \exp\left(\varepsilon_2\right)\exp\left(\varepsilon_3\right)} = \frac{F}{w_0 t_0 \exp\left(2\varepsilon_2\right)} \tag{3.5}$$

Eq. (3.5) and Eq. (3.4) is valid for uniaxial stress states, but as the specimen starts to neck it will transform into a triaxial stress state [9]. In the triaxial stress state it will no longer have a continues stress normal to the specimen's cross section. It is assumed that this variation will be very small for the dog-bone specimens, the effect of triaxiality has thus been neglected when calculating the stress history of the tests in this thesis.

3.1.3 Results

A total of 62 uniaxial tensile tests were performed. The results of each test can be seen in Appendix A.1, in this section the general behavior and trend of the tests will be presented and discussed. The results from the 3mm plate will be studied most thoroughly, as this was the plate thickness that was tested in the first batch and from which most tests were conducted. The test results from the 2mm and 4mm plate will primarily be used to study the effect of different molding thickness.

Basic results from 3mm plate with reduced cross section

All of the uniaxial tensile tests were run until failure. The tests' global behavior, represented by the tests force-displacement curves, at various velocities can be seen in Figure 3.5. What becomes apparent from the figure is that there is a significant variation in the test results, especially at the lowest strain rate. The peak force varies from 370N to 440N, and the displacement at fracture goes from 15mm to 55mm. The two other velocities show less variation in their peak force, though Figure 3.5b) also has a substantial variation in it's displacement at fracture. The fracture will be described more thoroughly in a subsequent section, while this section will look more closely at the general behavior of the uniaxial tests.

(a) $\dot{\varepsilon}_0 = 10^{-1}s^{-1}$

(b) $\dot{\varepsilon}_0 = 10^{-2}s^{-1}$

(c) $\dot{\varepsilon}_0 = 10^{-3}s^{-1}$
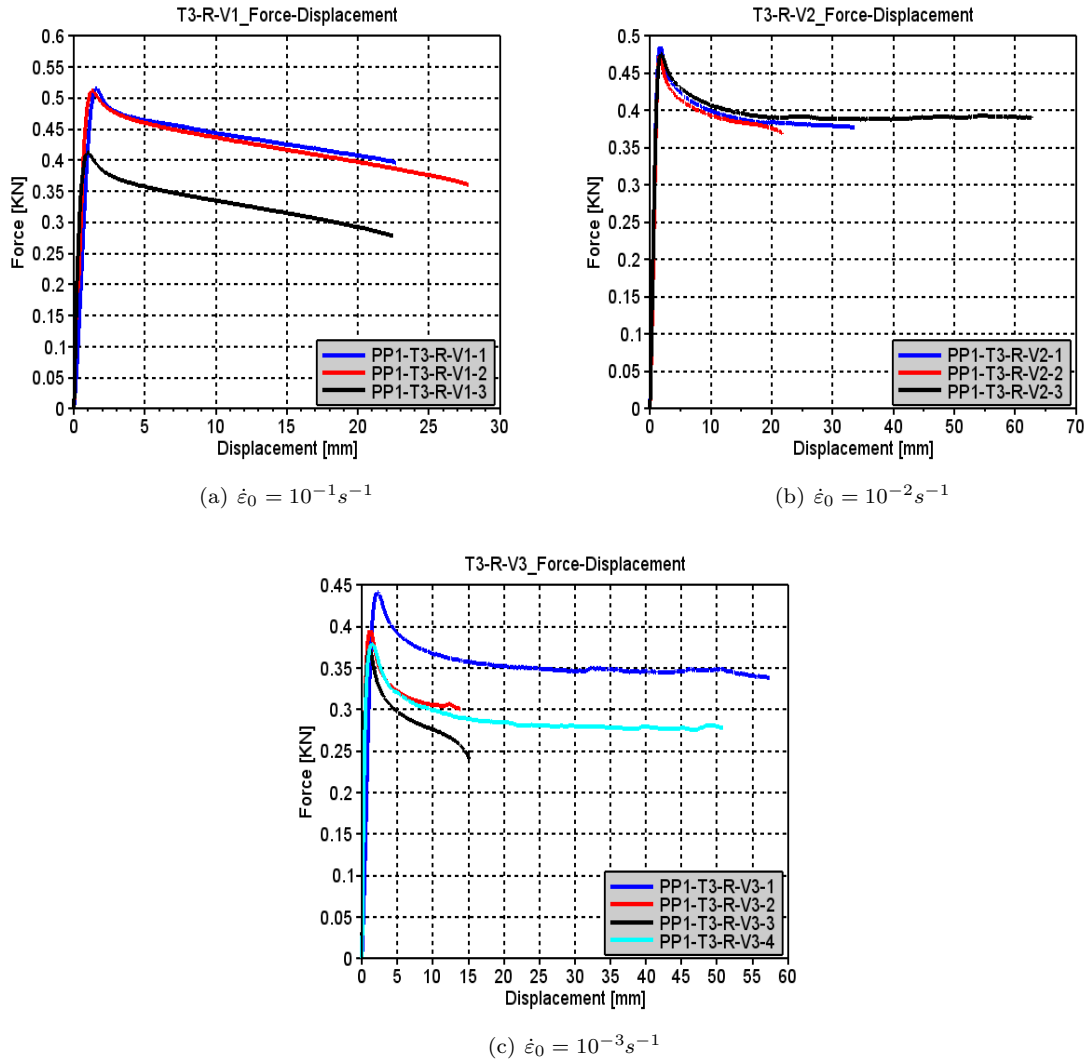
Figure 3.5: Force-displacement of reduced 3mm plate at different velocities

19

The specimens stress-strain curves can be seen in Figure 3.6, while the variation of the peak stress at the different initial strain rates can be seen in Figure 3.7. The stress curve displays a slight softening after it's peak stress before it re-hardens. The tests presented in Figure 3.6 suggests that the peak stress increases linearly with the logarithm of the velocity, which corresponds well with the relationship suggested by the material model in Eq. (2.17). The stress-strain curves in Figure 3.6 tend to exhibit less hardening with an increase in velocity. This decreased hardening may be due to an increase in the materials temperature due to adiabatic heating. Unfortunately, the specimens temperature was not measured during testing.
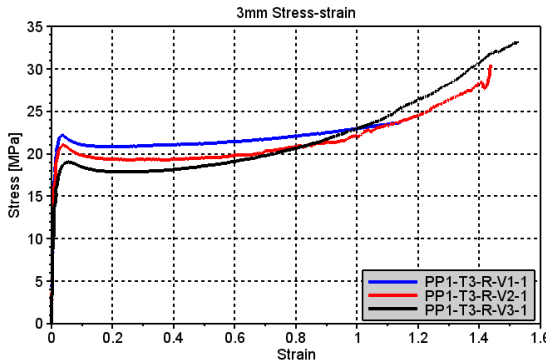
Figure 3.6: True stress-strain of 3mm plate
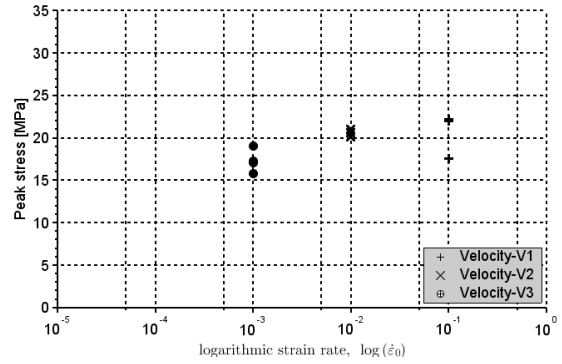
Figure 3.7: True peak stress relative to velocity, reduced 3mm

Basic results from 3mm plate with full cross section

The results from the 3mm with full cross section is shown in Figure 3.8 and Figure 3.9. The force-displacement of the tests is shown in Figure 3.8, and the stress-strain is shown in Figure 3.9. The figures indicate the same behavior as was observed for the specimens with a reduced cross section. We have a logarithmic linear relationship between the peak stress and the velocity, and the tests tend to soften at increased velocities.
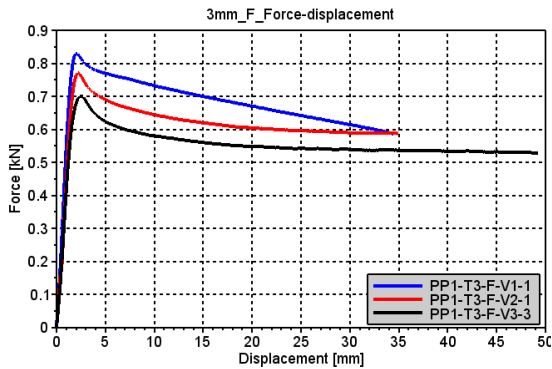
Figure 3.8: Force-displacement of 3mm full plate   Figure 3.9: True stress-strain of 3mm full plate
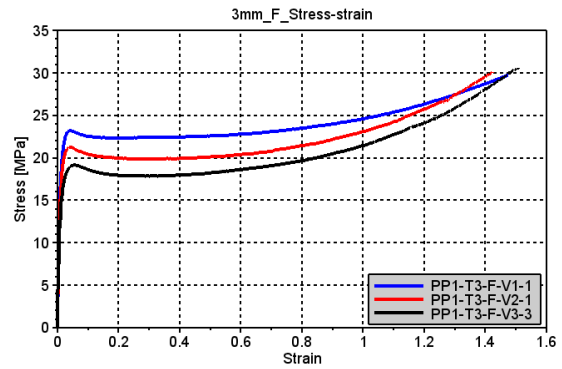
The tests in Figure 3.8 and Figure 3.9 gives a good indication of the general behavior of the tests with a full cross section. The tests with a full cross section showed less variation in their peak stress, as shown in Figure 3.10. The reduced scatter may be due to the neck that forms as the specimen is loaded in tension. When the uniaxial tensile tests deform, they develop a large neck. The fracture location in this neck will be very sensitive to imperfections in the specimens geometry and material structure. Because the specimens with a reduced cross section had their surfaces altered, this may have created some irregularities in the specimens surface which may have increased the scatter in the tests.
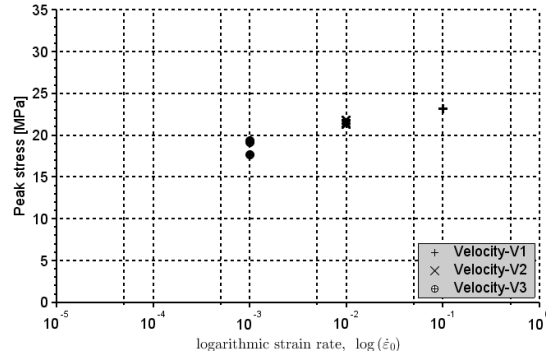
Figure 3.10: Peak stress relative to velocity, full 3mm

Transversal test specimens

In order to determine if the material exhibited anisotropic material behavior, test specimens which had been cut perpendicular to the materials flow direction during molding, was tested. In Figure 3.11, the specimens cut in the longitudinal direction is compared with those cut in the transverse direction. The specimens is tested at an initial strain rate of $10^{-2}s^{-1}$, and with a full cross section cut from a 3mm plate. The result clearly indicate that the transversal specimens have different material properties than the longitudinal specimens. The transverse tests have a lower peak stress and lower fracture strain, and in Figure 3.12 it is shown that the damage propagation in the transverse tests are higher. An anisotropic material behavior is thus clearly present.
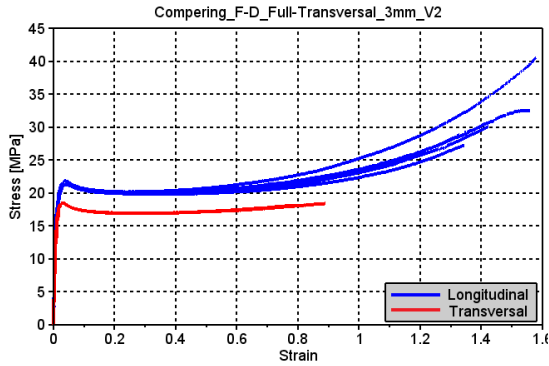
Figure 3.11: Transverse true stress-strain
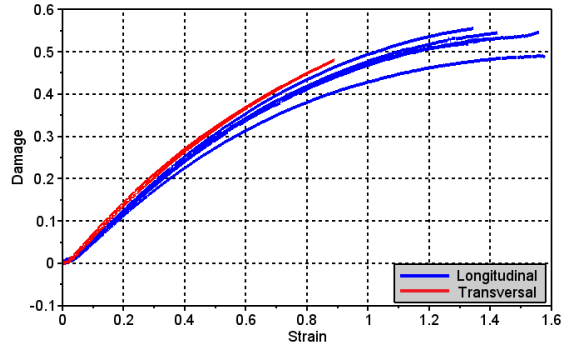
Figure 3.12: Transverse damage

Comparing results from the full and reduced cross section

The purpose of reducing the thickness of the specimens was to determine how the material properties would vary at different levels of the material's cross section. Figure 3.13a) displays the compressible stress-strain curves, and Figure 3.13b) the incompressible stress-strain curves of the reduced and full cross section. The incompressible stress-strain calculation does not take damage into account, the figure shows that the incompressible stress-strain relation of specimens with a full and reduced cross section is very similar, the only difference is that the curves of the specimens with a full cross section is located somewhat higher than the specimens with a reduced cross section. This would indicate that the specimens with a full cross section has a higher yield stress than the specimens with a reduced cross section. Because there is no significant difference in the hardening part for the full and reduced specimens calculated using incompressible stress, the difference seen in the hardening part of the compressible stress can only be due to damage.
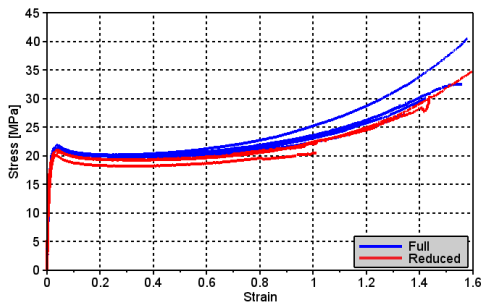
(a) Compressible stress
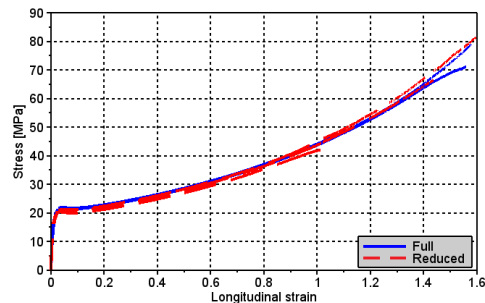
(b) Incompressible stress

Figure 3.13: Stress-strain relation of 3mm full and reduced specimens at $\dot{\varepsilon}_0 = 10^{-2}s^{-1}$

Different properties for the "skin" and "core" of polypropylene (PP), in the material's flow direction and normal to it's flow direction has previously been thoroughly studied. Fujiyama and Wakino studied this effect on a homoisotactic polypropylene [6]. They found that the yield stress in the skin

was 1.5 times higher than for the core, but that the core was much more ductile. The main reason for this was the orientation and the crystallization of the molecular chains' structure. As the skin was more rapidly cooled than the core, it had a different crystalline structure. The molecular chains in the skin was highly oriented in the molding direction, while the molecular chains in the core were not oriented to the same extent. This was due to the shear acting between the material and the mold. Multiple articles describe the "shish-kebab" structure of the skin layer. The "shishes" is oriented in the molding direction, while the "kebabs" are perpendicular to the shishes. The shishes consists of fibrous crystals, with higher strength than the kebabs, which is why the material has higher strength in the material's flow direction than in the transverse direction.

Limited information has been provided for the molding process of the polypropylene by Toyota. But it is very possible that during molding the initial temperature of the mold's surface was much lower than the material. As the material cools down, the skin will be cooled much more rapidly then the core creating different crystalline structures in the skin and the core, which explains why the material has a higher yield strength for the specimens with the full cross section, then with a reduced. The anisotropic material behavior shown in Figure 3.11 and Figure 3.12 is possibly due to a material "shish-kebab" structure.

Another possible reason for why the reduced cross section has a lower stress curve than the full cross section, is the amount of particles present in the specimens. Toyota has confirmed that the material contains particles [17]. As the material cools down, the skin will become solid before the core. Due to this, more particles may be trapped in the core, thus creating a higher concentration of particles in the core than in the skin. Figure 3.14 displays the damage propagation of specimens milled from 3mm plates tested at an initial strain rate of $10^{-2}s^{-1}$ with full and reduced cross sections. The figure shows that the damage increases faster for the core than for the skin, which may be due to the amount of particles, and/or the temperature gradient as the specimens solidifies during molding.
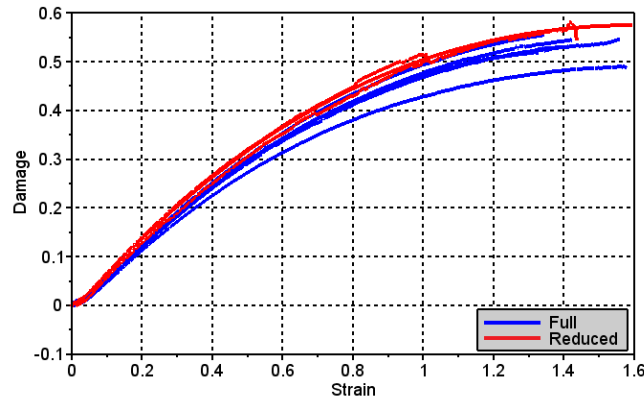
Figure 3.14: Damage propagation curve of 3mm full and reduced specimens at $\dot{\varepsilon}_0 = 10^{-2}s^{-1}$

In the article by Fujiyama and Wakino, they discovered that the skin had a higher melting temperature than the core. The stress-strain behavior of the 3mm reduced specimens in Figure 3.6 displays higher softening at increasing velocities than the specimens with a full cross section in

Figure 3.9. The specimens with a full cross section does not exhibit a significant increase in softening when the velocity is increased from V3 to V2, but the reduced specimens does. Figure 3.15 shows how the damage varies at different velocities for the full and reduced specimens. It is difficult to determine from the figure if there is any significant difference between the damage propagation of the reduced and full specimens at increasing velocities, due to the scatter in the damage propagation of the full specimens. Though it would seem that the velocity has a larger influence on the damage propagation of the reduced specimens.

(a) Reduced specimens   (b) Full specimens
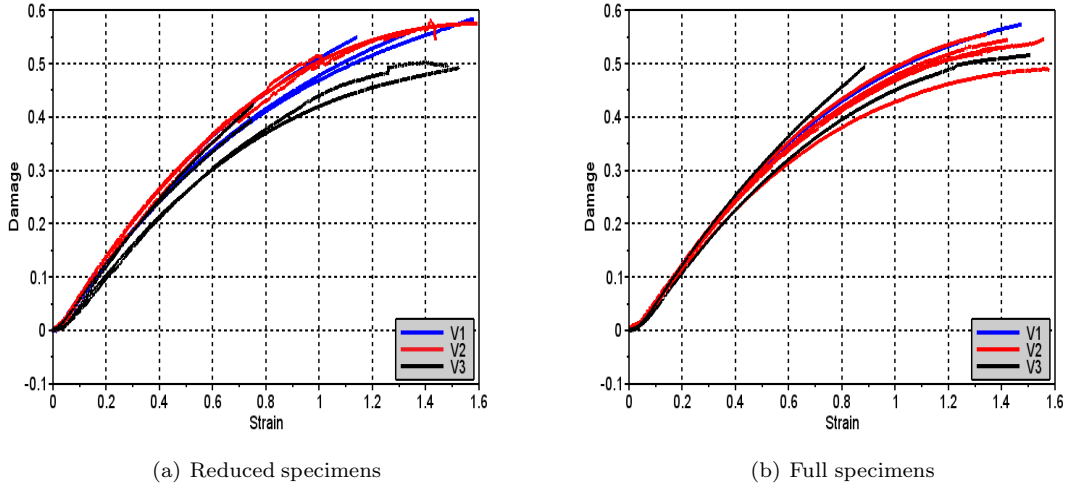
Figure 3.15: Damage at different velocities for specimens from 3mm plate

Basic results from 2mm tests

The global behavior, represented by the specimens' force-displacement curves, of the 2mm test specimens at different velocities is shown in Figure 3.16. The tests display a behavior which is very similar to what was observed for the specimens milled from a 3mm plate in Figure 3.8. There is a marked peak force before the specimens neck, which results in a sudden drop in the specimens' force. The tests at the velocities V3 and V2 display some increase in force after the neck is fully developed, which was not seen for the 3mm tests.
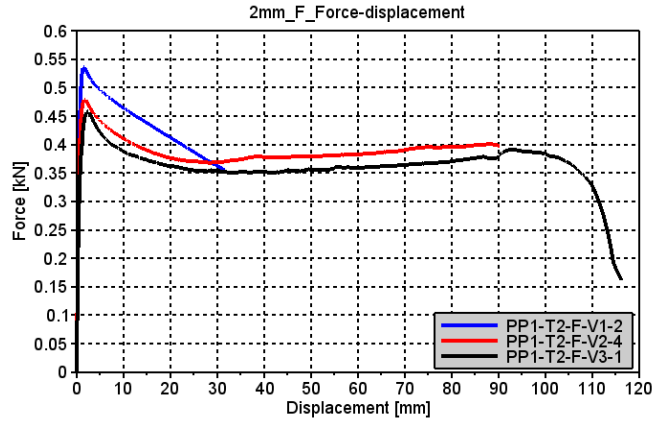
Figure 3.16: Force-displacement curves at different velocities for 2mm thick full specimens

In Figure 3.17a), the stress-strain curves at different velocities of the 2mm plate with a full cross section is showed. The shape of the curves is very similar to the 3mm plate's. The specimens have a marked peak stress before it softens and then re-hardens with a nonlinear curve shape. There is no significant increased material softening as the velocity is increased from V3 to V2, but as the velocity is increased to V1, there is a marked softening. The 2mm plate had a large variation in it's peak stress, as indicated by Figure 3.17b). At the lowest initial strain rate, $\dot{\varepsilon}_0 = 10^{-3}s^{-1}$, only a single test was performed, which is why there is no scatter in the peak stress at this strain rate. It s difficult to determine if the tests indicate that the peak stress increases linearly with the logarithm of the velocity, due to the scatter in the peak stress.

(a) Stress-strain

(b) Peak stress
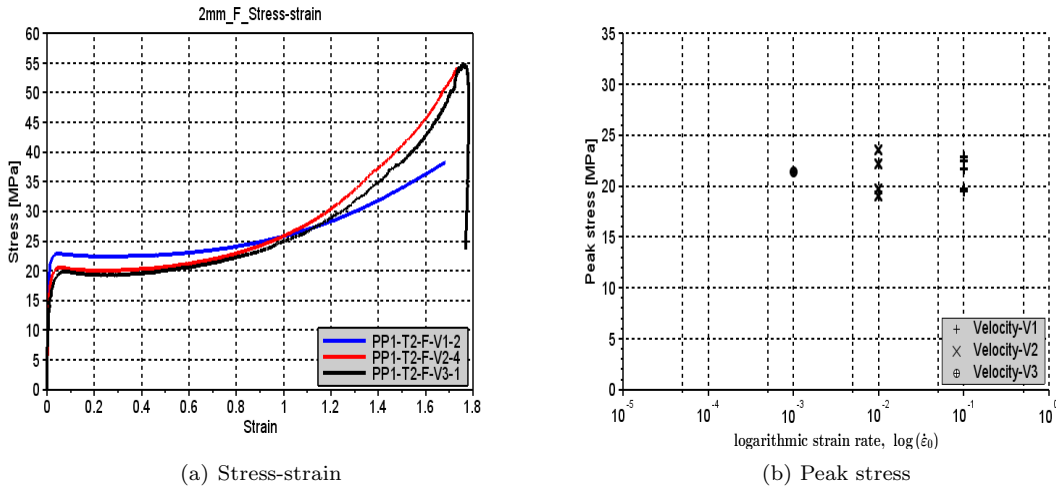
Figure 3.17: Stress-strain at different velocities for full 2mm specimens

Due to difficulties reducing the 2mm plates thickness by 0.50mm on each side, the specimens were

25

also reduced by 0.25mm on each side. Figure 3.18 and Figure 3.19 has been included to illustrate how the damage and peak stress is affected by reducing the specimens thickness. The tests included in these figures are all performed at the intermediate velocity, V2. The difference in the material's yield stress as the thickness is reduced is shown in Figure 3.18. It is difficult to determine how the yield stress is varying at different reductions, due to the scatter in the test results, but the yield stress seems to be decreasing as the specimens cross section is reduced. The damage propagation with different reductions is shown in Figure 3.19. The figure clearly shows that the damage propagation increases as more of the "skin" is removed. This corresponds well with the observations made for the 3mm plate.
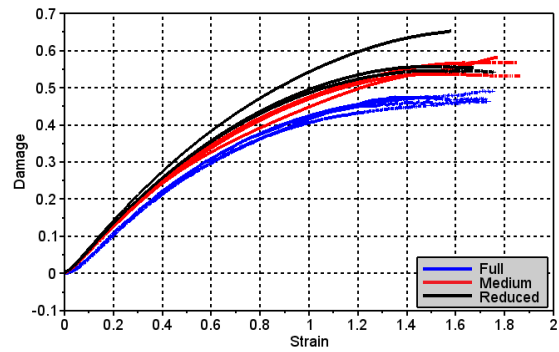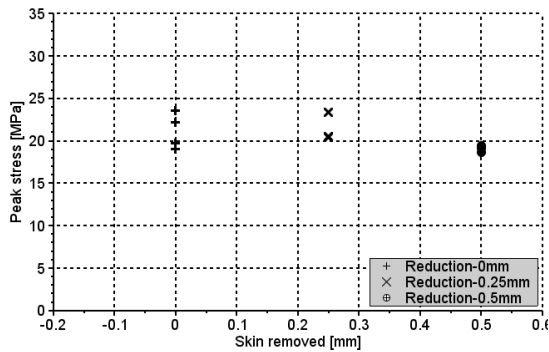
Figure 3.18: Peak stress at different reductions   Figure 3.19: Damage at different reductions

Basic results from 4mm tests

The force-displacement curves of tests performed at different velocities using specimens milled from plates with an initial thickness of 4mm, is shown in Figure 3.20. The force-displacement indicates the global behavior of the test specimens. The general behavior of the test specimens of the 4mm plate is very different from the 2mm and 3mm plates, respectively in Figure 3.16 and Figure 3.8. The curves from the two lowest velocities follows the same characteristics, an elastic hardening until the force reaches it's peak, then a steep drop in force as the material starts to neck. As the neck progresses, the slope of the curve is decreasing until there is another drop in the material's force, which is due to the onset of fracture that occurs in the specimen's core. It can be seen from the figure that the second drop in the force is shifted to the right as the velocity of the tests are increased, and that for the highest velocity it is not present.

26
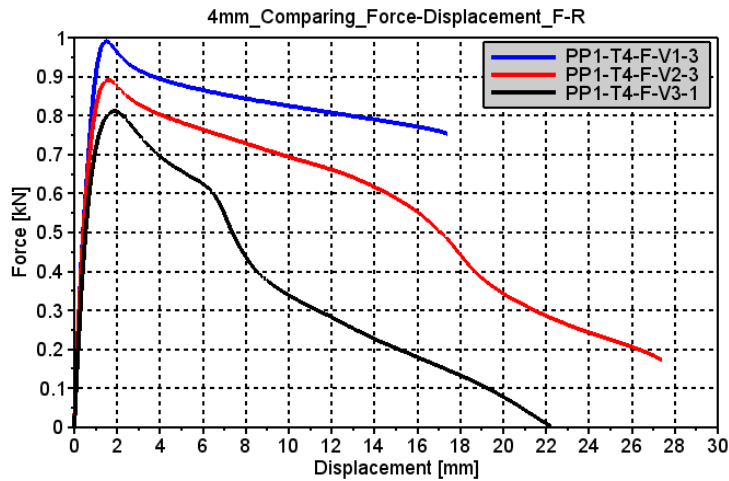
Figure 3.20: Force-displacement curves at different velocities for 4mm thick full specimens

In Figure 3.22a) the stress-strain history of the tests which were presented in Figure 3.20 is shown. The tests behavior is in this figure very different from what was observed for similar tests performed at test specimens with a plate thickness of 2mm and 3mm. In Figure 3.22a) the tests behave very similarly until the peak stress. After this point the tests at the lowest velocities softens but never re-hardens, they follow the shape of the force-displacement curve. The reason that the material does not re-harden, is because when the core fractures the decrease in area is not captured and taken into account when calculating the effective cross section area. The calculation of the effective cross section area is based on the DIC analyses. Figure 3.21 shows an image from a DIC analyses of a 4mm thick specimen were the core has fractured. What becomes evident from the figure is that the transverse strains from the DIC will not be very much effected by the fracture in the core, if anything it will just become somewhat more unstable.

Figure 3.21: Result from DIC analyses where the core has fractured

Figure 3.22b) displays the scatter in the specimens yield stress at different initial strain rates. The scatter is substantial, but it has a very clear trend that suggest a linear relationship between the peak stress of the material and the logarithm of the velocity.

(a) True stress-strain
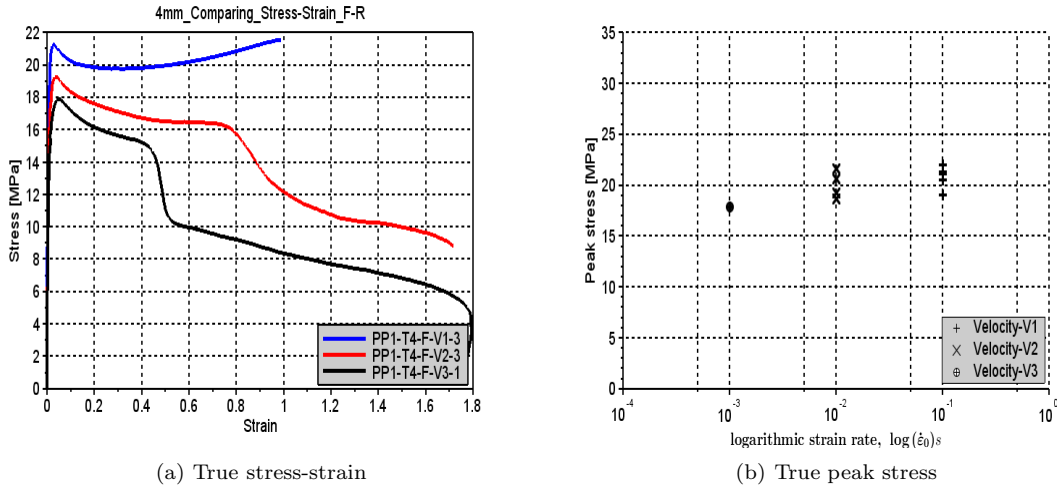
(b) True peak stress

Figure 3.22: Stress-strain at different velocities for full 4mm specimens

The peak stress for the 4mm tests with full and reduced cross section, performed at the intermediate velocity, is depicted in Figure 3.23. Though there is a substantial scatter in the results, it indicates that the peak stress decreases as the thickness of the specimen is reduced, which corresponds very well with the observations made for the 3mm and 2mm thick specimens. Figure 3.24 displays the damage propagation of the full and reduced 4mm thick specimens tested at the intermediate velocity. Similar to what has been observed for the 2mm and 3mm thick specimens, the specimens with a reduced cross section damage propagates faster than the specimens with a full cross section. What can also be observed, is that the reduced specimens from the 4mm thick material fractures at a much lower strain than the reduced specimens from the 2mm and 3mm plates.
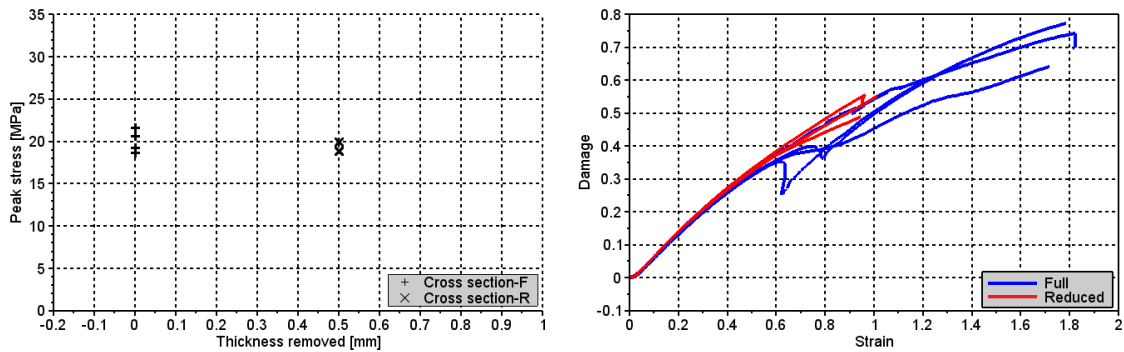
Figure 3.23: Peak stress at different reductions

Figure 3.24: Damage at different reductions

28

Molding thickness' effect on material properties

The peak stress of the specimens milled from plates with different initial plate thickness tested with an initial strain rate of $\dot{\varepsilon}_0 = 10^{-2}s^{-1}$ is shown in Figure 3.25. Figure 3.25a) shows the specimens with a full cross section. The figure indicates a slight decrease in the specimens peak stress as the material thickness is increased, but the variation in the 2mm specimens' peak stress is substantial. The peak stress of the specimens with a reduced cross section in Figure 3.25b), display a more constant peak stress. There is less scatter in the results, which makes it easier to verify the trend.

(a) Full cross section (b) Reduced cross section
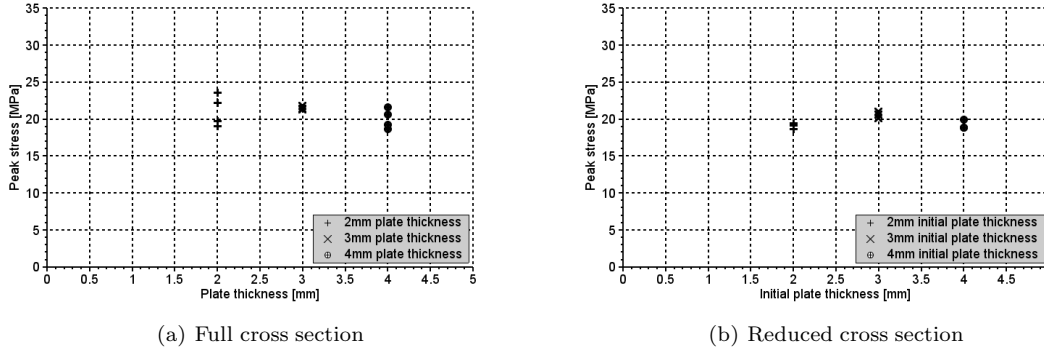
Figure 3.25: Peak stress of specimens with different thickness, $\dot{\varepsilon}_0 = 10^{-2}s^{-1}$

The average peak stress at different reductions with different plate thicknesses has been calculated and is displayed in the table below. The difference between the peak stress of the reduced and full specimens is relatively similar for the 3mm and 4mm specimens, but it is much higher for the 2mm specimens. The 2mm specimens has in general a much larger scatter in its results. The higher scatter in the 2mm plate may come as a result of a more random distribution of the particles in the 2mm plate, because the entire cross section may have reached a solid state faster than the 3mm and 4mm thick plates.

	Average peak stress at reduction			
Plate thickness	F	M	R	Difference between F and R
T4	20.04 MPa		19.20 MPa	0.84 MPa
T3	21.45 MPa		20.54 MPa	0.91 MPa
T2	21.13 MPa	21.43 MPa	19.08 MPa	2.05 MPa

The material tests has proved that the material's damage propagation is different for different thickness reductions. Figure 3.26a) and Figure 3.26b) displays how the material's damage propagation varies with different plate thicknesses. From the specimens with a full cross section, seen in Figure 3.26a), it is clear that the damage propagation increases with higher initial material thicknesses. While the trend is the same in Figure 3.26b), the increase in damage is lower at increased material thickness. As the material's thickness increases, the amount of particles will increase with the same ratio. One possibility for the behavior seen in Figure 3.26, is that the relative amount of particles is increasing in the skin, while a combination of a change in the material's cooling conditions and the amount of particles explains why the damage increase is less for the core specimens.

(a) Full thickness   (b) Reduced thickness
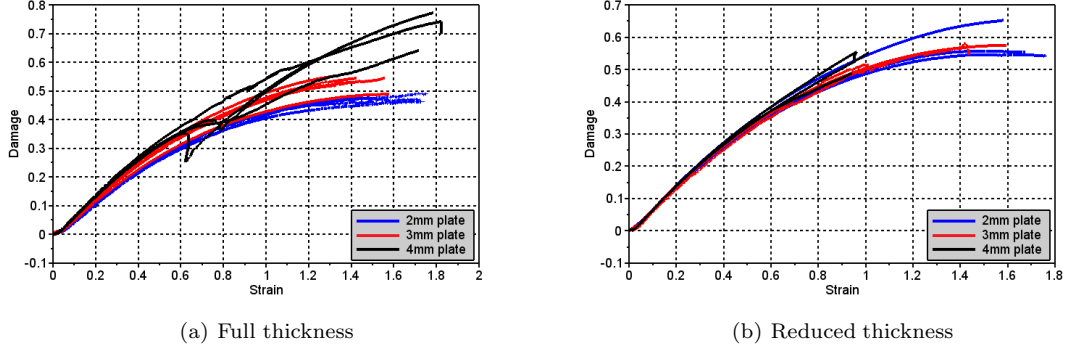
Figure 3.26: Damage propagation for different specimen thicknesses, $\dot{\varepsilon}_0 = 10^{-2}s^{-1}$

Fracture

The fracture of the uniaxial test specimens were determined on the basis of the specimens force-displacement relation. A MatLab script, which is available in Appendix B.2.2, was created to determine the strain at fracture. In the MatLab script, the change in the specimens' force is calculated numerically using the central difference theorem [2]:

$$\frac{dF}{dx}\bigg|_i = \frac{-F_{i+2} + 8F_{i+1} - 8F_{i-1} + F_{i-2}}{12\Delta x} \tag{3.6}$$

Here the change at the current step, i, is calculated on the basis of the values until two steps in front of the current value, F_{i+2}, and two steps before, F_{i-2}. The beginning of the last sudden drop of the force-curve is set as the point of fracture. Because the force was logged with the same frequency as images were taken, the force's frame number at fracture would be the same as the frame number in the DIC analyses, thus the fracture strain is easily obtained. When the strain at fracture was determined, the critical damage,D_c was determined using:

$$D_c = 1 - \frac{1}{e^{\varepsilon_{v,c}}} \tag{3.7}$$

$\varepsilon_{v,c}$ is the volumetric strain at fracture.

To illustrate the materials' fracture, the materials damage at fracture has been plotted with it's fracture strain. Figure 3.27 to Figure 3.28 displays the material's damage at fracture with different initial material plate thicknesses. The 3mm plate, in Figure 3.27, shows that though there is a substantial variation in the materials fracture strain, the damage at fracture shows less scatter. The fracture damage increases/decreases with the velocity of the test, but the average damage at fracture is about 0.55. From the 3mm plate results, it is not possible to say if the damage at fracture increases or decreases as the specimens cross section is reduced.

30
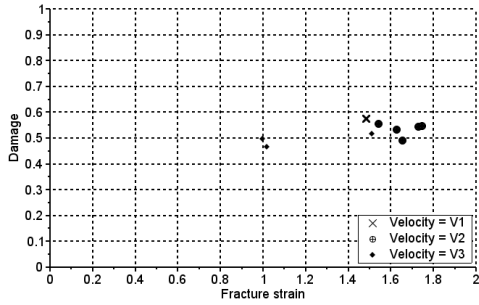
(a) Full, all velocities
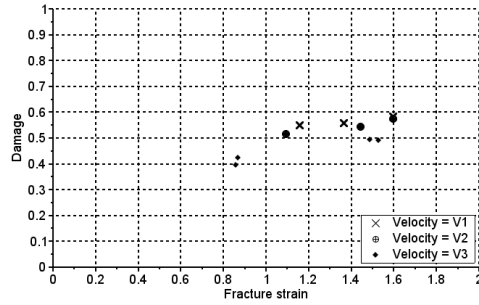
(b) Reduced, all velocities
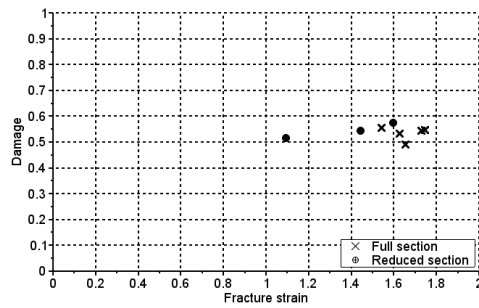
(c) Full vs. reduced, $\dot{\varepsilon}_0 = 10^{-2}s^{-1}$

Figure 3.27: Fracture strain and damage of 3mm uniaxial tensile specimens

The 2mm and 4mm plates, respectively in Figure 3.28 and Figure 3.29, displays a larger scatter in the fracture damage, but less scatter for the fracture strain. For the 2mm, there is a clear trend that the damage at fracture increases with increased velocity. Figure 3.28b) also shows that the specimens with a reduced geometry has a higher damage at fracture than the full specimen. The results from the 4mm thick specimens shows an opposite trend. As the velocity is increased, the damage at fracture decreases, and the specimens with a full cross section has a higher damage at fracture than the specimens with a reduced cross section. No apparent reason for this behavior has been found, but it may be linked to the distribution of particles and the injection molding process.
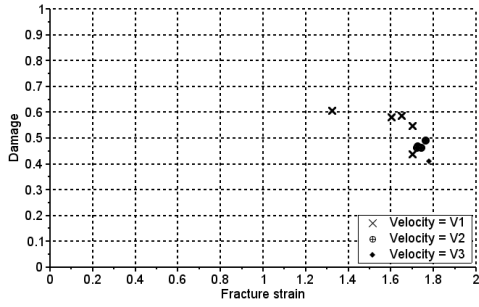
(a) Full, all velocities
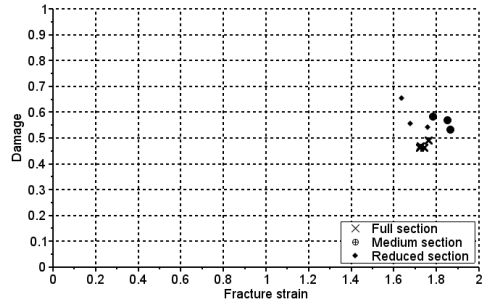
(b) Different reductions, $\dot{\varepsilon}_0 = 10^{-2}s^{-1}$

Figure 3.28: Fracture strain and damage of 2mm uniaxial tensile specimens
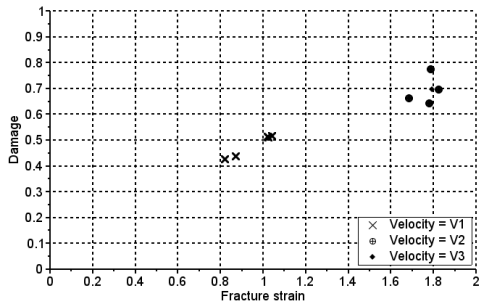
(a) Full, all velocities
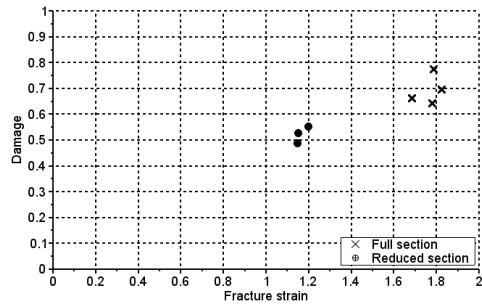
(b) Different reductions, $\dot{\varepsilon}_0 = 10^{-2}s^{-1}$

Figure 3.29: Fracture strain and damage of 4mm uniaxial tensile specimens

Figure 3.30 displays how the specimens damage at fracture varies with different specimen thicknesses. The trend for the specimens with a full cross section is that the damage increases with an increased material thickness, but that the increase from the 3mm plate thickness to 4mm is larger than from 2mm to 3mm. The specimens with a reduced cross section, in Figure 3.30b), is less affected by the increase of the material thickness, which corresponds well with the observations made from Figure 3.26 that the damage is propagating faster for the specimens with a full cross section at different material thicknesses then it does for the specimens with a reduced cross section.

(a) Full specimens (b) Reduced specimens
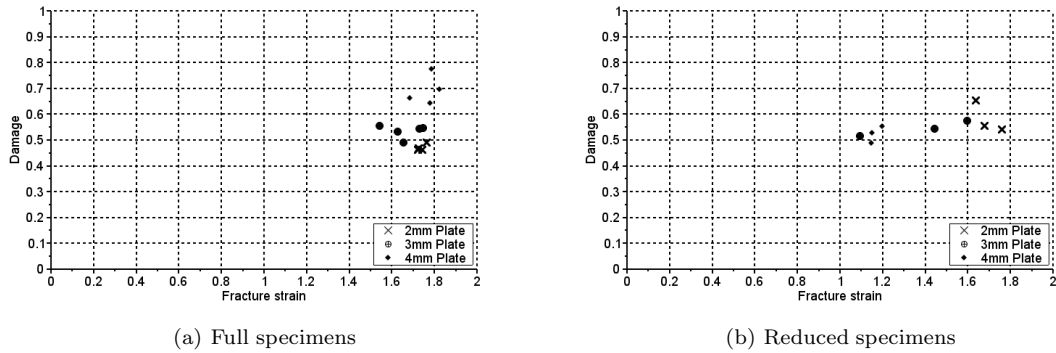
Figure 3.30: Fracture strain and damage for different material thicknesses, $\dot{\varepsilon}_0 = 10^{-2}s^{-1}$

3.1.4 Uniaxial tensile test summary

To summarize the uniaxial tensile tests, a few key findings is listed below:

- No significant temperature increase was observed during the milling of the specimens

- Large scatter in the tests peak force and stress, and the displacement at fracture

- Increasing the test velocity yielded an altered material behavior, which was most likely due to a temperature increase:

  - Peak stress increased
  - General curve shape was the same, but the materials hardening was somewhat lower. Most likely due to an increased damage propagation

- Reducing the specimens' thickness changed the material properties:

  - The specimens with a full thickness has a higher yield stress
  - The shape of the curves are similar, the incompressible stress curves show that the hardening is similar for the full and reduced specimens
  - Damage propagates faster in the reduced specimens
  - All material thicknesses displayed the same behavior

- The full specimens displayed a trend which indicated that the peak stress decreased with an increase in the specimen thickness

  - The damage propagation was also observed to increase with increasing thickness
  - The specimens with a reduced cross section displayed a more constant behavior

- The fracture damage of the 3mm specimens is relatively constant equal to 0.55. Although the the fracture strain varies substantially.

  - The 2mm and 4mm plates displays a significantly larger scatter in its fracture damage

33

- The full specimens displayed an increase in the damage at fracture as the specimens thickness was increased.

  - The reduced specimens did not display the same behavior
  - Corresponds well with the findings of an increased damage propagation at increased material thickness

3.2 Uniaxial compression tests

To determine the materials behavior in compression, a total of 8 tests were performed. The tests were performed using the same geometry, but tested at three different velocities. Compression tests were only performed using specimens milled from the 3mm thick plates, without any thickness reductions.

3.2.1 Test method

The specimens were tested using a hydraulic loading machine, similar to the one used for the uniaxial tensile tests, seen in Figure 3.31a). To perform the uniaxial compression tests, the machine was equipped somewhat differently than it was during the tensile tests, as seen in Figure 3.31b). During the compression tests, only a single CCD camera was used to record the deformation of the specimen. Because the specimens used for the compression tests are so small, DIC analyses will not yield good results. Instead a MatLab script was used to determine the specimens transverse strain history, which will be described in further detail in the post processing section. An Instron controller wired to machines cross head, logged the force and displacement of the specimens as they were deformed.

(a) Test setup

(b) Specimen at loading
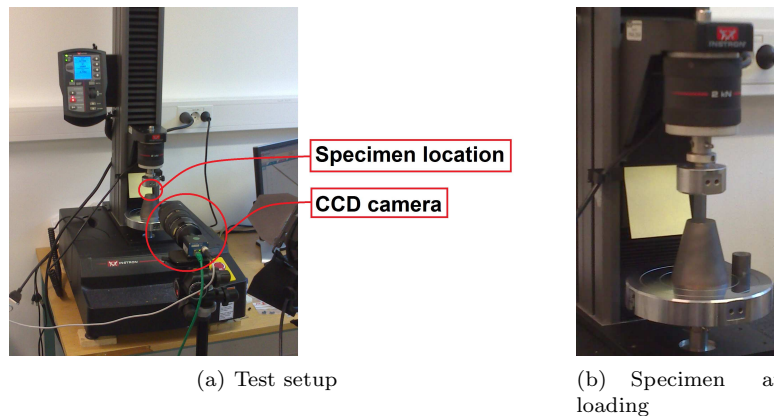
Figure 3.31: Setup of the hydraulic loading machine for uniaxile compression tests

The geometry of the compression specimens is shown in Figure 3.32. The specimens were milled from plates with a full cross section, and the milling was performed perpendicular to the plates largest surface. The tests were labeled in a different way than the uniaxile tensile tests. They were labeled based on: "Material"-"Plate No."- "Test No.". The plate number labeling was used to see if the material behaved differently for each plate.
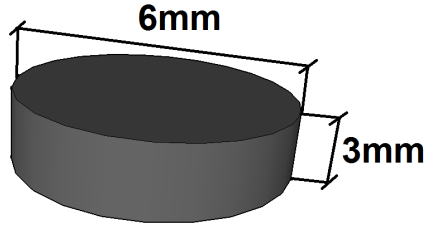
Figure 3.32: Geometry of uniaxial compression specimens

Prior to testing, the specimens contact surfaces were lubricated with oil in order to reduce the friction between the test specimen and the loading machine. The tests were performed at three different initial strain rates, $\dot{\varepsilon}_0$: $10^{-3}s^{-1}$, $10^{-2}s^{-1}$ and $10^{-1}s^{-1}$. During testing, the specimen was deformed with a constant velocity, v, equal to:

$$v = \dot{\varepsilon}_0 H_0 \tag{3.8}$$

Where H_0 is the initial height of the specimen.

3.2.2 Post processing

The force-displacement history of the uniaxial compression tests were taken directly from the Instron controller. The true longitudinal strain history, ε_l, of the tests were obtained by using the displacement history and the following relation:

$$\varepsilon_l = \log\left(\frac{H_0 - d}{H_0}\right) \tag{3.9}$$

Here d, is the cross head displacement at the given time. As previously mentioned, the true transverse strains, ε_t, were obtained using a MatLab script, which is available in Appendix B.2.1. The MatLab script works in the following way:

1. The first picture taken with the CCD camera of the respective test is imported to MatLab.

2. The picture is converted to black and white based on each pixels grey-scale. The black pixels have the value 0, while the white pixels have the value 1.

3. The boundaries of the specimen is located by the following method:

   (a) Left edge is located at the point when all points within a certain step to the left is white and the points within the same step to the right is black

   (b) Right edge is located at the point when all points within a certain step to the right is black and the points within the same step to the right is white

4. This is done at every row to determine the location of the specimen's edges. The median of each side is used to determine the number of pixels in the specimens width. The pixel size is calculated by dividing the initial diameter with the number of pixels.

5. The next image is then imported, and step 2-4 is repeated, except that the pixel size is now not calculated. The new diameter is calculated by multiplying the number of pixels where the specimen has it's largest diameter with the pixel size, which was calculated from the reference image

6. The true transverse strain, ε_t, is then calculated by:

$$\varepsilon_t = \log\left(\frac{D}{D_0}\right)$$

Here D_0 is the initial diameter of the specimen and D is the specimens diameter at the specific time step. The specimens transverse strain history and its diameter history was written to separate files. Figure 3.33 illustrates how the transverse strains of the uniaxial compression specimens is determined.

(a) Step 1   (b) Step 2   (c) Step 4
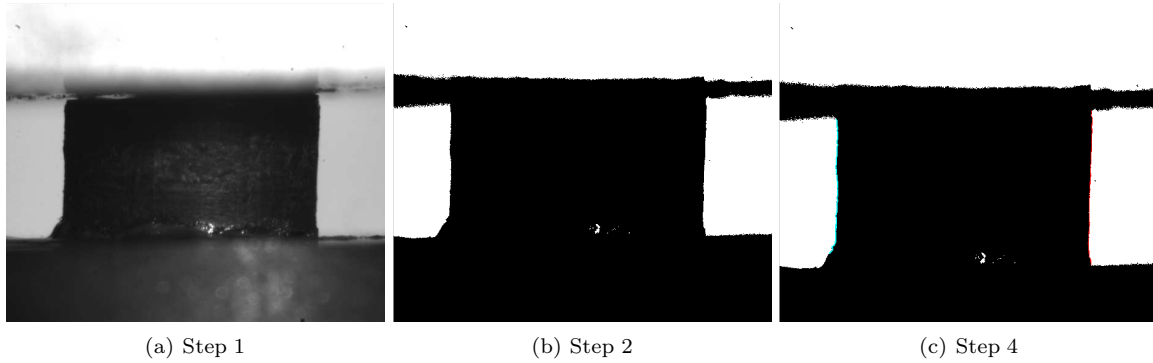
Figure 3.33: Illustration of the method used to determine the transverse strains

To calculate the true stress acting on the specimen, the following relation was used:

$$\sigma = \frac{F}{A} \qquad \text{where;} \quad A = \frac{\pi D^2}{4} \tag{3.10}$$

This relation is true if the specimen is deformed the same way in all directions, and if the specimen did not "barrel". If the specimens barrel, there will no longer be a completely uniaxial stress state. During testing, the specimens did barrel, but the affect on the true stress is not taken into consideration as it is deemed negligible. After testing, the specimens indicated that they had not deformed evenly in all direction. Because cameras can not be placed 360° around the specimen, this is not possible to take into consideration, but will be a possible source of errors for the calculation of the specimen's transverse strains and effective cross section area.

3.2.3   Results

The force-displacement curves from the uniaxial compression tests at varying velocities is shown in Figure 3.34. The force-displacement of all the uniaxile compression tests is found in Appendix A.2 The curves slope in the elastic region is varying significantly. A possible reason for this, is that the sides of the specimens is not perfectly vertical, due to difficulties milling them. As the specimen is loaded the cross head of the machine will then not distribute the load evenly, which may explain why the curve is varying so much in this region. Another possibility is the stiffness of the loading machine itself. As the specimen is loaded in compression, gaps inside of the machine may be pushed together, creating a more gentle slope then what was observed for the tensile tests. When the specimen has reached yielding, the slope of the curves are very similar. It can also be seen from the figure that the force-curves are increasing with an increase in velocity.
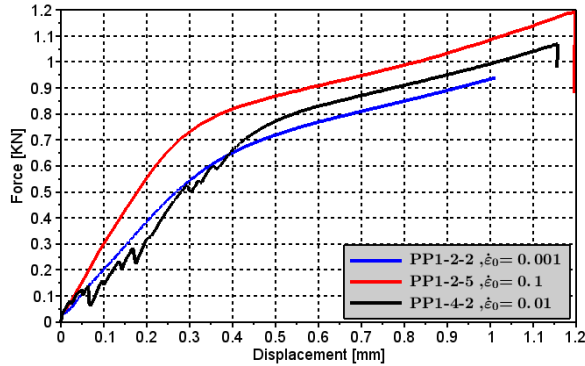
Figure 3.34: Force-displacement history in uniaxial compression

Figure 3.35 shows the stress-strain history of the uniaxile tensile tests at varying velocities. The stress-strain history of all the compression tests can be found in Appendix A.2. Because there were some problems with the pictures of the test specimens, PP1-2-3 and PP1-2-4, it was not possible to calculate the stress-strain history of these tests. The figure indicates a Young's modulus between 160MPa and 230MPa, which is significantly lower than what was observed for the uniaxial tensile tests. As was previously mentioned for the slope of the force-displacement curves in Figure 3.34, the difference in the elastic region is possibly due to irregularities in the specimens' geometry or the stiffness of the hydraulic loading machine, as was described for the force-displacement curves.
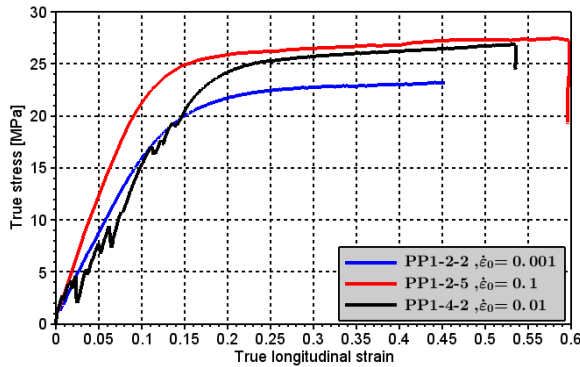
Figure 3.35: True stress-strain history in uniaxial compression

The stress-strain curves in Figure 3.35 does not have the same shape as the uniaxile tensile tests. There is no clearly defined peak stress and the material does not exhibit softening. The force-displacement curves displayed an almost linear relationship between the velocity and force curves. The stress-strain curves does not display the same relation. This is possibly because of a non-uniform deformation of the specimen, which is not captured when calculating the effective cross section area.

37

3.3 Notched tensile tests

Notched tensile tests were performed to validate the material model and it's parameters, especially those linked to fracture. Notched tests are used for validation purposes because they create a more complex loading scenario than the uniaxile tests. When a notched test specimen is loaded in tension, the curve of the notch will create a biaxial loading scenario.

A total of 42 notched tests were performed. The tests were performed using three different geometries, and each geometry was tested at three different velocities. All the notched specimens were milled from 3mm thick plates.

3.3.1 Test method

The notched specimens were tested with the same hydraulic loading machine as the uniaxial tensile and compression tests. The setup of the machine is similar to what was done for the uniaxile tensile tests, and can be seen in Figure 3.36. Two CCD cameras were fixed towards the specimen, one of the cameras took pictures perpendicular to the width while the other recorded the thickness. These images could later be analyzed using DIC to obtain the tests' strain history. An Instron controller was wired to the machine's cross head, and would record the force-displacement history with the same frequency as pictures were taken with the CCD cameras.

(a) Test setup

(b) Clamped notched specimen
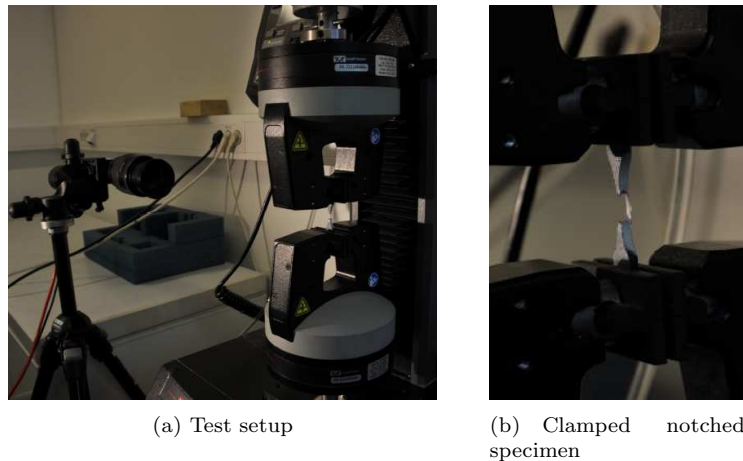
Figure 3.36: Setup of notched tensile tests

For the DIC analyses to work, the specimens had to be given a speckled surface. This procedure has been more thoroughly described in Section 3.1.1 for the uniaxile tensile specimens. The geometry of the notched specimens is visible in Figure 3.37. The radius of the N1 geometry, in Figure 3.37a), is relatively large compared to that of the N2 and N3 geometries, which will most likely create a more biaxial stress state.

(a) N1

(b) N2

(c) N3
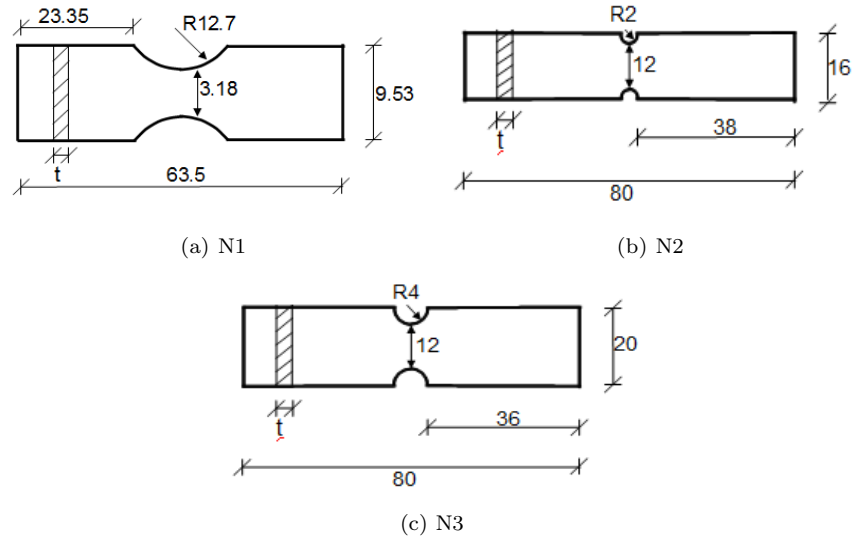
Figure 3.37: Notched geometries

The notched specimens were milled with full section thickness and reduced section thickness. The notched specimens were also milled with their longitudinal direction parallel and perpendicular to the flow direction during molding, as indicated by Figure 3.38. The transverse specimens were only milled with a full cross section, 3mm.
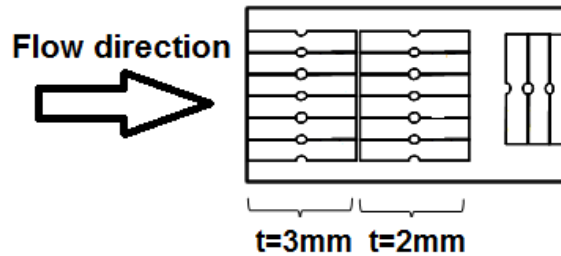
Figure 3.38: Illustration of the notched specimens milling order

The labeling of the notched specimens were performed differently than what was done for the uniaxial tensile and compression tests. The labeling was done based on; "Material"-"Geometry"-"Direction/Reduction"-"Test No.". The material was always TSOP7, which has been abbreviated "PP1", the geometry is either "N1", "N2" or "N3", and the "Direction/Reduction" was either "L", "LR" or "T". Where "L" is a specimen milled parallel to the molding direction with a full cross section, "LR" is milled in the same direction but with a reduced cross section, and "T" is milled perpendicular to the molding flows direction.

During testing, the cross head of the hydraulic loading machine would move with a constant user defined velocity. Each notched geometry was tested at three different velocities. It was attempted to run the notched tests with the same initial strain rates, $\dot{\varepsilon}_0$, as the uniaxial tensile and compression

tests, but due to the specimens geometry, it was very difficult to determine the velocity which would yield initial strain rates similar to those of the uniaxial tests. As a result of this, the three geometries were tested at different velocities, as seen in the table below. The tests have been put into batches; V1, V2 and V3. Where V1 is the highest velocity and V3 is the lowest.

	Velocity group		
Geometry	V1 [mm/s]	V2 [mm/s]	V3 [mm/s]
N1	20.00	2.00	0.20
N2	10.00	1.00	0.10
N3	15.00	1.50	0.15

3.3.2   Post processing

The force-displacement history of the notched tests were obtained directly from the Instron controller, while the strain history was obtained through DIC analyses. The notched specimens main intention was to be used for validation, thus only the force-displacement curve is strictly necessary. Because it was a substantial scatter in the results from the uniaxial tensile tests, DIC was performed for some of the notched tests to determine the fracture damage.

The DIC analyses performed using eCorr has been described in greater detail in the post processing section of the uniaxile tensile tests, see Section 3.1.2. The only difference between the DIC analyses of the notched tests and the uniaxile tensile tests, is that for the N2 and N3 geometries, the mesh was created in Abaqus. Abaqus was used to create the mesh because creating a curved mesh is currently not possible in eCorr, thus the mesh must be created using a different software and then be imported to eCorr, where the mesh can be scaled to fit the geometry in the picture. This was not necessary for the N1 geometry because the curvature is significantly smaller than for the N2 and N3 geometries.

The fracture strain was obtained by using the force-displacement curve, as described in Section 3.1.3 for the uniaxile tensile tests, and the fracture damage was calculated using Eq.(3.7).

3.3.3   Results

The force-displacement relation of the different geometries is shown in Figure 3.39 to Figure 3.41. In the (a) figures, the force-displacement of the longitudinal specimens with a full cross section, longitudinal with reduced cross section and transverse with a full cross section has been plotted. The trend is the same in all figures; the transverse test specimens is located somewhat below the longitudinal specimens, and they also fracture at less displacement. The force-displacement curves of the reduced specimens have about the same shape as the specimens with a full cross section, but the peak force is somewhat less than 2/3 of the full specimen tests, which is good as the cross section area of the reduced specimens is about 2/3 of the full specimens. This correlates very well with what was observed in the results of the uniaxile tensile test specimens in Section 3.1.3.
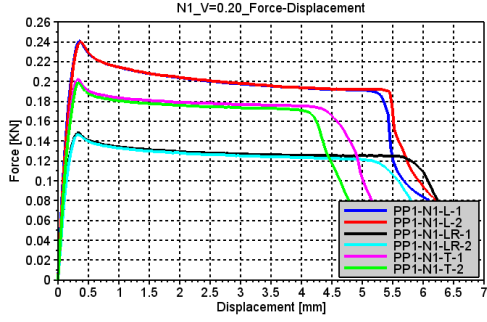
(a) v=0.20 mm/s
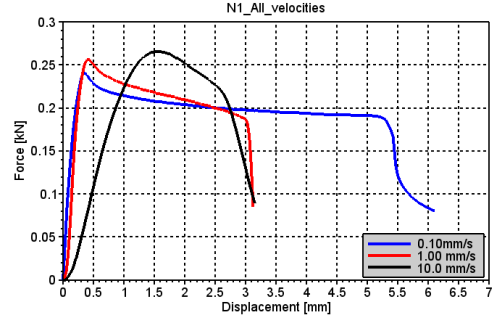
(b) All velocities

Figure 3.39: Force-displacement results from N1 geometry
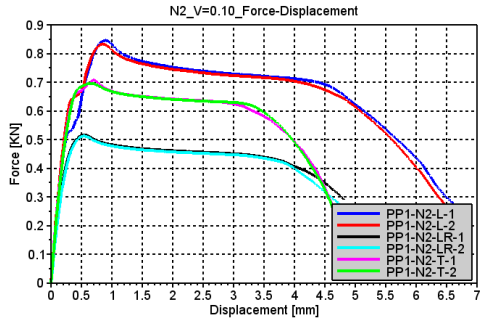
(a) v=0.10 mm/s
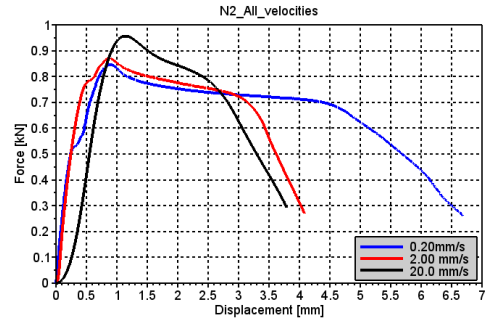
(b) All velocities

Figure 3.40: Force-displacement results from N2 geometry
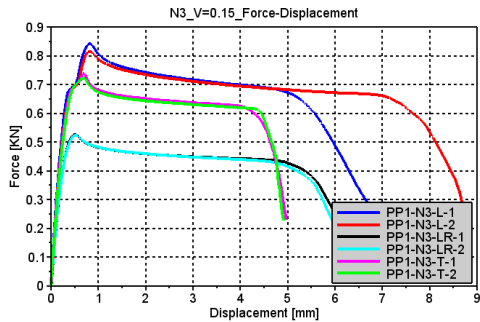
(a) v=0.15 mm/s
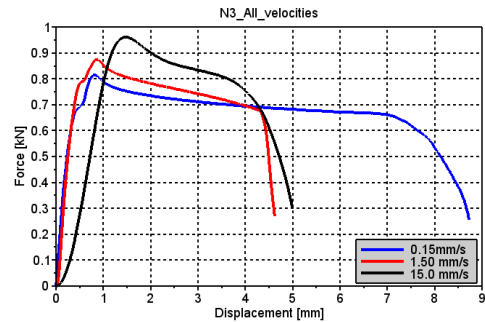
(b) All velocities

Figure 3.41: Force-displacement results from N3 geometry

41
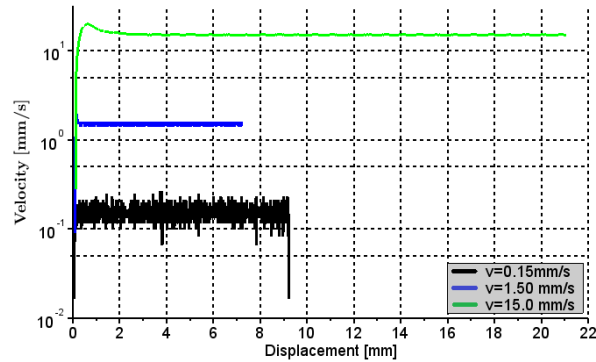
Figure 3.42: Test velocity history for N3 geometry

The (b) figures display how the notched specimens force-displacement relation varies with increasing velocity. The tests at the lowest strain rates behave very similarly to what has previously been observed; the peak force increases linearly with the logarithm of the velocity, while the shape of the curves are the same. For the specimens at the highest velocity, the start of the elastic region has a nonlinear shape which is not consistent with previous observations, and the slope is somewhat lower. This nonlinear shape is most likely due to the acceleration of the cross head which is needed to reach the prescribed constant velocity. Figure 3.42, displays the velocity history of the tests shown in Figure 3.41b). As seen in the figure, the test at the highest velocity does not reach the constant velocity until the specimen has been displaced approximately 1.5mm, which is consistent with the behavior in the elastic region of the test performed at the highest velocity seen in Figure 3.41b). The velocities in Figure 3.42 were calculated using central differences, see Eq. (3.6).

The notched specimens displays significantly less scatter than the uniaxile tensile test specimens. This is possibly because the neck is more localized due to the notched geometry, while the location of the neck for uniaxile test specimens were far less consistent, and thus more affected by the specimen's imperfections.

As previously mentioned, DIC was performed for some of the notched specimens in order to determine the damage at fracture. Unfortunately, it was not possible to perform DIC on the tests performed at the highest velocity, because the frequency needed to save pictures was too great for the computer to handle. Figure 3.43 is thus only displaying the damage at fracture for the tests performed at the two lowest velocities.

(a) Full cross section (b) Reduced cross section
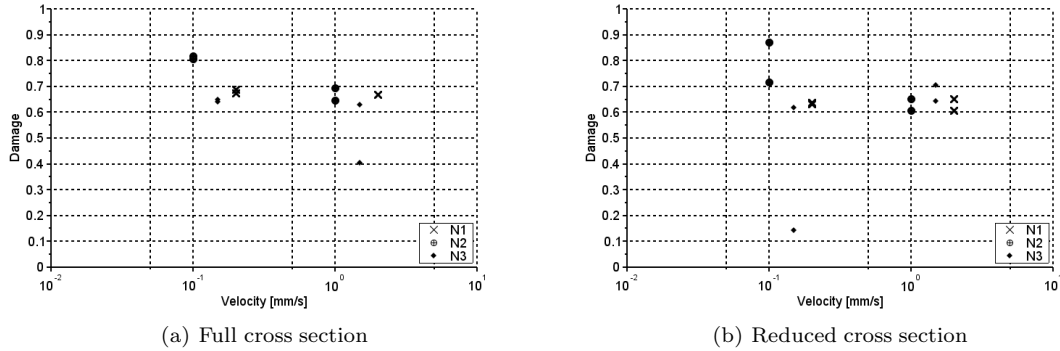
Figure 3.43: Damage at fracture relative to velocity

There is a relatively large scatter in the fracture damage. This is possibly due to the mesh that was used during the DIC analyzes. The figure shows very similar results for the full cross section and the reduced cross section with all geometries and velocities, and it indicates a damage at fracture between 0.60 and 0.65 which is somewhat higher than what was observed for the uniaxial tensile specimens.

3.4 Drop tower tests

In a drop tower test, the material is hit by a steel puncher at a prescribed energy. The drop tower tests creates a very complex loading scenario as it is performed at high velocities, and it creates a triaxial stress state. Thus the purpose of the drop tower tests is not to verify and determine the material parameters, but to validate the accuracy the material model.

3.4.1 Test method

The machine used for the drop tower tests is shown in Figure 3.44. The test specimen was placed on a steel ring which had a hole with a diameter of 80mm. The test specimens used for the drop tower tests were quadratic plates with sides 100mm x 100mm. The drop tower tests where only performed for the first batch of materials, which only included plates with a thickness of 3mm. During testing, only tests with a full section thickness were performed. The puncher hitting the test specimen, was a steel cylinder with a hemisphere at it's end, with a diameter of 20mm. The test specimen was simply placed on top of the plate without any clamps. A safety door was closed to prevent any fragments from the plate making any damage. The desired impact energy was then given as inputs to the machine, and then the steel puncher would drop as the test commenced. The geometry of the some of the elements involved in the drop tower test is shown in the table below.

Part	Geometry	Dimension [mm]	Remark
Test specimen	Quadratic	100X100X3	Simply supported
Steel ring	Ring	80	Diameter of hole
Steel puncher	Cylinder with hemisphere	20	Diameter of hemisphere

43

Figure 3.44: Drop tower testing machine

The impact energy was calculated on the basis of the specimens potential energy, E_p, which was calculated by:

$$E_p = mgh \tag{3.11}$$

m is the mass of the puncher, g is the acceleration of gravity, which is equal to $9.81 m/s^2$, and h is the initial distance between the test specimen and the puncher. Previous tests with the same material showed that the material did not fracture with an impact energy of 55J, but when the energy was increased to 60, fracture occurred [23]. It was expressed a desire from TOYOTA for the drop tower tests to fracture, thus the test was performed at 60J, but also at 120J. The tests at 120J was performed to validate how well the material model would be able to describe the material behavior at high velocities, and also to see how the material would behave at this velocity. When the puncher hits the plate, all the potential energy will be converted to kinetic energy, E_k, if we assume that all the energy is conserved:

$$E_{tot} = E_k + E_p \tag{3.12}$$

The expression for the kinetic energy is:

$$E_k = \frac{1}{2}mv^2 \tag{3.13}$$

Thus the velocity of the puncher, v, can be calculated using:

$$v = \sqrt{\frac{2E_k}{m}} \tag{3.14}$$

If all the energy is conserved, this expression can be used to calculate the velocity of the puncher at impact. The table below shows key data for the tests performed.

Energy [E_{tot}]	Mass puncher [m]	Initial height [h]	Velocity at impact [v]
60 J	5.778 kg	1.059 m	4.56 m/s
120 J	5.778 kg	2.118 m	6.44 m/s

The tests are labeled in the following way; "Material"-"Energy"-"Test No.". The material is TSOP7, which has been abbreviated PP1. The "Energy" is either "D1" or "D2", where "D1" is the drop tower tests performed with an energy of 60J, and "D2" is the tests performed at 120J. The "Test No." is the number of tests performed at the corresponding "Energy".

3.4.2 Post processing

A total of six drop tower tests were executed, three at the lowest energy level and three at the highest. Not much post processing was needed for the drop tower simulations. As previously mentioned, the intention of the drop tower tests are to validate the material model. For the validation, only the global behavior of the tests and simulations will be compared, which can be represented by the force history. The force and time were given as direct outputs, thus the only post processing which were needed was to remove any noise from the outputs.

3.4.3 Results

The force history of the drop tower tests are shown in Figure 3.45. During testing, a CCD camera was recording the deformation of the tests. For the camera to be able to take good pictures, a lamp was directed towards the specimen. This was a high energy lamp, which resulted in an increased temperature of the specimens if it was allowed to light up the specimens for too long. The increased temperature of the specimens was not identified before after the tests at the lowest energy level was performed. This explains why there is a substantial scatter in the results from the tests at the lowest energy level, but not for the tests performed at an energy level of 120J.

(a) 60J (b) 120J
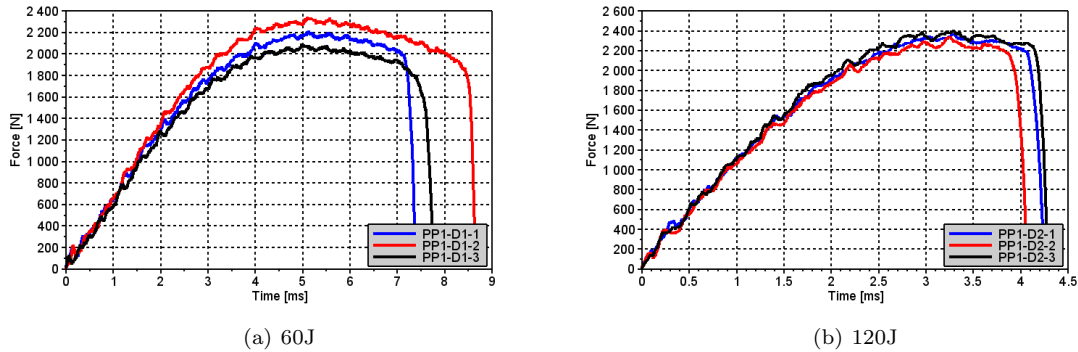
Figure 3.45: Force history of the drop tower tests

As fracture was obtained at both energy levels, there is no substantial difference in the force history, if only the force history of the PP1-D1-2 is considered from the 60J tests. The velocity at impact was measured by a controller wired to the puncher. The results showed that the impact velocity was somewhat less than the intended velocity, which resulted in a lower impact energy. The most probable reason for this reduction in velocity is air resistance and friction between the puncher

and the poles that it was sliding on. The table below displays the true impact velocity and energy. As indicated in the table, the difference between intended energy and the real energy is small.

Intended energy]	Intended velocity	True energy	True velocity
60J	4.56 m/s	57J	4.45 m/s
120J	6.44 m/s	115J	6.30 m/s

3.5 Tests to determine layer thickness

To be able to accurately describe the material's behavior using numerical models, the material's structure needed to be identified. Previous simulations of the same material where performed using numerical models which consisted of a single homogeneous material [23]. These simulations of the material model yielded relatively accurate results, but it was believed that a further study of the skin-core effect could enhance the results. As previously described, multiple articles have been written about the "skin-core" effect that occurs for injection molded polypropylene. In most articles, only the skin and core layers has been discussed, but in an article written by J. Karger-Kocsis and K. Friedrich, five "zones" were identified in the skin layer, but only one in the core [13]. The idea is, that if the "skin-core" layers can be accurately identified, then the numerical models of the material will yield more accurate results.

Multiple methods were applied to determine the thickness and structure of the material's layers. These included optical microscope, hardness tests and scanning electron microscope (SEM). In this section, the test methods and results will be described.

3.5.1 Optical microscope

In the deformed state, the uniaxial tensile test specimens displayed a variation in color in the thickness direction. The part of the material which had been closest to the mold's surface during the molding process, had a darker color than the part of the specimen which was located further away from the mold's surface. The transition in color was very sudden, and could indicate different properties. Figure 3.46 displays a 3mm thick specimen with a full cross section in it's deformed state. Because the outer layer with a darker color is very thin, it is not possible to see it in the figure, but the figure clearly shows that the material has been deformed in layers.

(a) Front view

(b) Top view
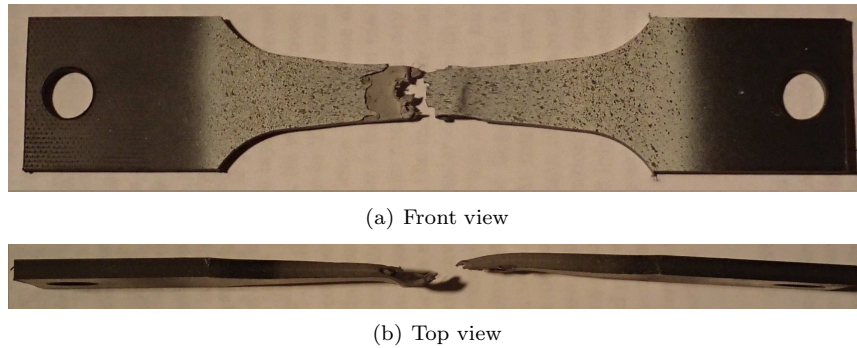
Figure 3.46: Fractured 3mm thick full specimen illustrating material layers

Measuring thickness with optical microscope

To measure the thickness of this color transition, the optical microscope depicted in Figure 3.47 was used. The clamping mechanism where the specimen is placed, is wired to a measuring tool which measures the movement of the clamp. A cross is seen when looking through the optical microscope, which can be used by the viewer to create a reference point. The color variation was clearly visible in the microscope, but unfortunately the microscope was not able to take pictures.
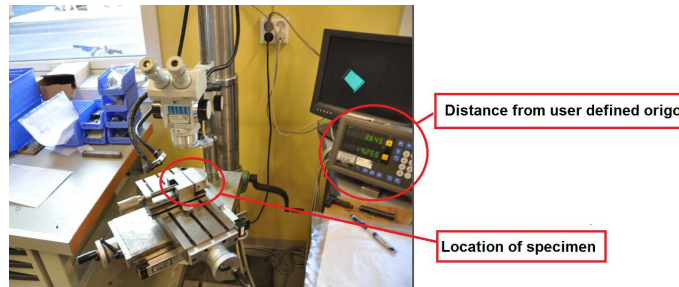
Figure 3.47: Optical microscope used to determine skin thickness

The thickness was measured by placing the center of the optical cross at the edge of the specimen. The measuring tool was zeroed out, and the clamp was moved so that the center of the cross was at the transition between the dark "skin" and the lighter "core". The thickness of the skin could then be read from the measuring tool wired to the clamping mechanism. This was done fore several specimens, and the thickness was very consistently equal to 0.2mm.

In Figure 3.19, the damage propagation at different skin reductions for the 2mm thick specimens is shown. For the 2mm specimens, the section was reduced by 0.25mm and 0.50mm. The increase in damage propagation from a full cross section to a reduction of 0.25mm was much greater than the increase from a reduction of 0.25mm to 0.50mm. This may also indicate that the skin layer is less than 0.25mm, and that 0.20mm is a good approximation.

3.5.2 Scanning electron microscope (SEM)

In a scanning electron microscopy (SEM), the microscope is firing electrons at a specimen and then it processes the reflected electrons to create images of the specimens surface with a very high resolution. A SEM was performed for the specimen with and without a fractured surface to see if it was possible to determine the thickness of the skin and core based on the structure of the specimens surface. The specimens that was viewed in the SEM is shown in Figure 3.48. The SEM was only performed for specimens with a thickness of 3mm, as SEM was only performed for the first batch of tests.

(a) Deformed   (b) Undeformed
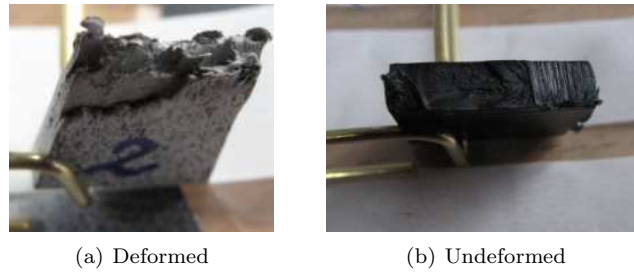
Figure 3.48: Specimens analyzed using SEM

To be able to analyze the cross section of the specimen in an undeformed state, the specimen was first cooled down using liquid nitrogen. After the specimen had stayed in the nitrogen for some time, it was believed that the material would be sufficiently cold so that when it was cut, the fracture would be very brittle, and thus leave the cross section undistorted.

SEM results

Figure 3.49 displays the pictures taken during the SEM of the deformed specimen. From the overview picture in Figure 3.49a) and the pictures in Figure 3.49 b) and c), where a zoom of X1000 is used, there is no apparent difference between the surface of the skin and the core. It is therefore not possible to determine the skin thickness from this analyzes.

(a) Overview

(b) Core X1000   (c) Skin X1000
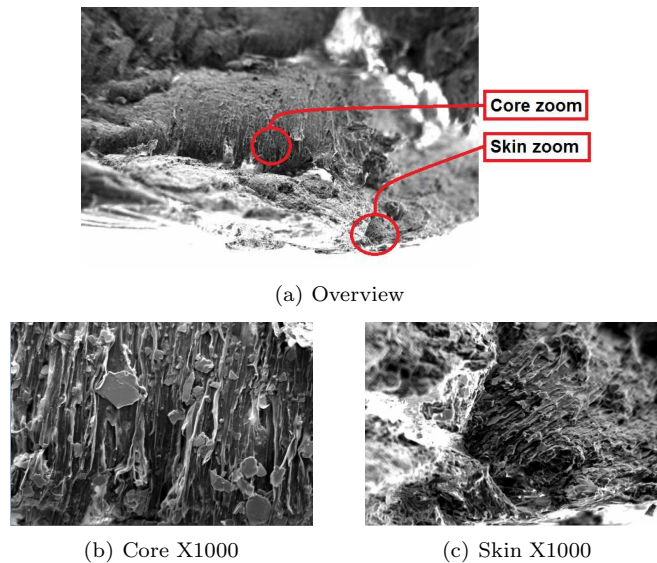
Figure 3.49: Results from SEM analyzes of the deformed specimen

The pictures taken during the SEM of the undeformed section is shown in Figure 3.50. In the middle of the specimen in Figure 3.50a) it can be seen a bright line. This is most likely due to the specimen not having a perfectly leveled surface. For the SEM to work, the electrons must be shot with an angle, if the surface is not completely leveled, then the electrons in these areas will be

reflected with a different angle which creates what we see in the figure. The material structure of the specimen close to the edge and core, seen in Figure 3.50b) and c) respectively, do not display any significant difference. Determining the material layers from the SEM is therefore not possible.

(a) Overview

(b) Core X1000

(c) Skin X1000
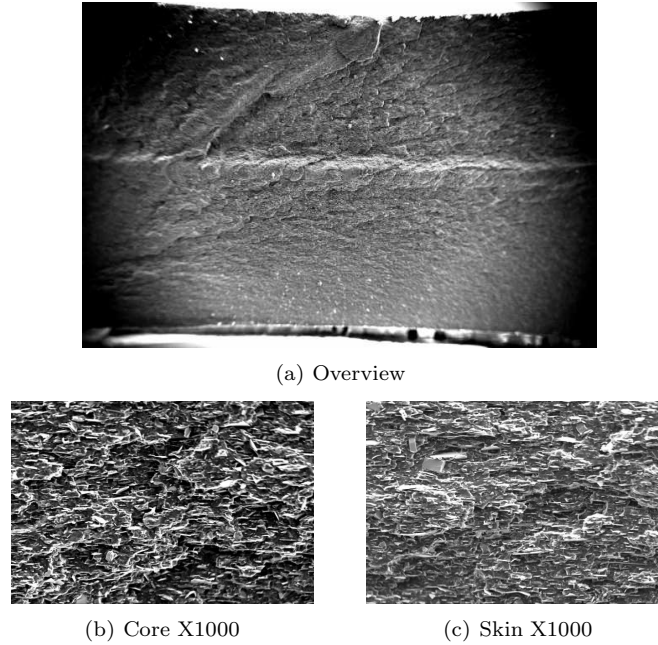
Figure 3.50: Results from SEM analyzes of the undeformed specimen

3.5.3 Hardness tests

An indentation hardness test was performed to measure the material's hardness at different thickness levels. The material's hardness is linked to it's yield stress, thus a higher hardness will give a higher yield stress [3]. The purpose of the hardness test was to determine how the material's hardness would vary across the specimen's cross section. This information would possibly give an indication of how the material's properties were structured; if it was a linear or nonlinear variation from the material's outer edge to it's core, or if the variation would be layered.

The hardness test was performed by SINTEF, which is a research company in Norway. Figure 3.51 shows pictures of the machine used, and the placement of the specimen during one of the hardness tests. Hardness tests were performed without any thickness reductions for all material thicknesses; 2mm, 3mm and 4mm.

(a) Machine

(b) Specimen position
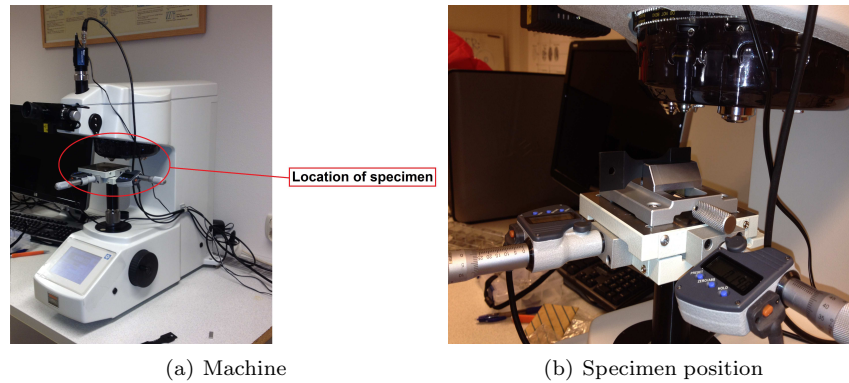
Figure 3.51: Hardness test

Hardness results

The results from the hardness tests of the 2mm and 4mm thick specimens is shown in Figure 3.52. The results from the specimen with a 3mm thickness were similar to that of the 2mm thick specimen. The results in the figure indicate opposite behavior for the 2mm and 4mm specimens. The 4mm thick specimen has a higher hardness at it's core than at it's edges, which is completely opposite to the behavior of the 2mm specimen, which has a higher hardness in the edges than at the core. Because only a few points along the thickness of the specimens were tested, it is not possible to determine how the hardness is varying relative to the thickness. Though it is not possible to determine how the hardness is varying based on the hardness test, it does validate that the material's hardness is different at different locations in it's cross section
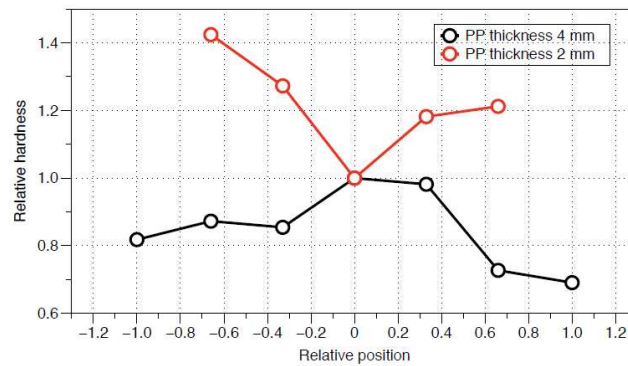
Figure 3.52: Hardness test results for 2mm and 4mm specimens

3.5.4   Material layer summary

The tests performed to determine the thickness of the material's layers were inconclusive. The only test that gave any consistent evidence of the material layers, was the measures performed using the optical microscope. With this microscope, the skin thickness was determined to be 0.2mm thick. This was based on color variation in the specimens' thickness, but unfortunately it was not possible

to take pictures of this variation. The damage propagation results from the uniaxial tensile tests with different reduction performed for the 2mm thick specimens, also indicated a difference occurring after a reduction of 0.25mm. The SEM did not show any apparent structural difference in the specimens core and edge.

The hardness tests did not give any results which could indicate how the material was layered, though it did verify that the material had different hardness at its core relative to its edges. Further testing of the material using hardness tests may give a better understanding of the material layers and material properties, if the tests are performed using more than one specimen at each material thickness and with a shorter distance between each indentation point.

Chapter 4

Calibration procedure

MatPrePost is a software created by SIMLab at NTNU, which has previously been used for calibrating SIMLab's metal model. Currently a feature in this software is under development which allows MatPrePost to also be used to calibrate SIMLab's polymer model. During the calibration procedure in this thesis, MatPrePost was initially used to determine the material parameters, and then inverse modeling was used to optimize these parameters. The calibration methods and results will be described in this chapter.

The calibration of the material model was done on the basis of the test results from the uniaxile tension and compression tests of the 3mm thick specimens. Two material cards were created; one for the material's skin layer and one for the core. The results from Chapter 3 indicated that only the yield stress and damage propagation of the specimens with a full cross section was different from the specimens with a reduced cross section. The material card for the core was thus created using the test results from the reduced cross section specimens, and then a second material card for the skin was created on the basis of this card, where some of the parameters had been altered to better describe the material's skin layer. This procedure will be described in further detail in this chapter.

4.1 MatPrePost

As previously mentioned, the MatPrePost used in this thesis to calibrate the SIMLab polymer model is currently under development. The problems that were experienced and reported during the work of this master thesis has been, or is currently being fixed. The version used for the calibration was a very early beta version, thus some bugs were expected.

In this section the different steps of the MatPrePost calibration procedure for the polymer model will be described, as well as some of the equations and methods used for calibrating the different parameters of the material model.

4.1.1 Material Tests

To be able to accurately determine the parameters of the material model, a selection of tests is required: A uniaxial tensile test, performed at a quasi static strain rate level, two other uniaxile tensile tests performed at different strain rates to determine the materials strain rate dependency,

and a uniaxial compression test to determine the material's tension-compression relation. The tests used for the calibration procedure is listed in the table below.

Test No.	Type	True initial strain rate, $\dot{\varepsilon}_0$
PP1-T3-R-V3-1	Tensile	$10^{-3}\ s^{-1}$
PP1-T3-R-V2-1	Tensile	$10^{-2}\ s^{-1}$
PP1-T3-R-V1-1	Tensile	$10^{-1}\ s^{-1}$
PP1-2-2	Compression	$10^{-3}\ s^{-1}$

Required data for the different tests is shown in the table below. Before the data is uploaded to MatPrePost, all noise from the material testing must be removed, as optimization is used in the calibration procedure. If noise is included, e.g; the sudden drop in force as the material fractures, this may lead to inaccurate material parameters.

	Test type	
Required data	Tensile	Compression
Time	X	X
Engineering stress	X	X
True longitudinal strain	X	X
True transverse strain	X	
Strain rate	X	

4.1.2 Tension-compression ratio, α

As previously mentioned, the material model's relation between tension and compression is controlled by the Raghava parameter, α. This parameter is taken as the material's absolute value of the ratio between yielding in tension, $\sigma_{0,T}$, and compression, $\sigma_{0,C}$:

$$\alpha = \left| \frac{\sigma_{0,C}}{\sigma_{0,T}} \right| \tag{4.1}$$

In MatPrePost, this is done by selecting a compression and a tension test from the tests previously imported. These tests should preferably have been performed at the same strain rate. Figure 4.1 displays the stress strain curves of the uniaxial tension and compression tests, which were tested at an initial strain rate of $10^{-3}s^{-1}$. The user must personally choose the region where he believes that the yield stress is located. The material's yield stress is in SIMLab's material model defined as the point where the material's linear elastic behavior stops. The red dots in the figure indicate the region selected for these tests.
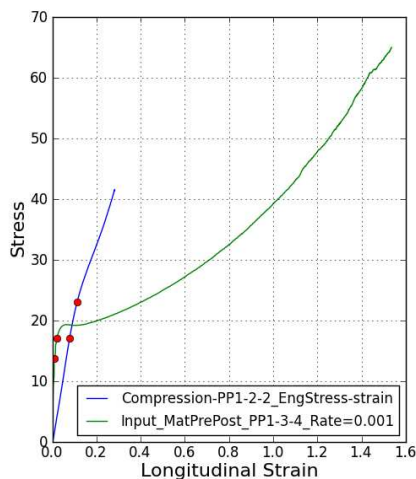
Figure 4.1: Determining the α-parameter using MatPrePost

The selected region yielded an α-value of:

Parameter	Value	Unit
α	1.197	N/A

4.1.3 Material hardening/softening, R

The material hardening/softening in SIMLab's material model consists of three terms, and each of these three terms consists of two parameters, as given in Eq. (2.13). Preferably a test performed at the lowest strain rate should be used to calibrate the hardening/softening parameters in the material model, because the effect of adiabatic heating and strain rate sensitivity is then at its lowest. In Section 3.1.3, it was shown that there was a substantial scatter in the test results for the specimens performed at the lowest strain rate, especially concerning the tests' peak stress, which were varying between 16MPa and 19MPa. It was therefore chosen to use the test performed at the intermediate strain rate for the calibration of the material hardening, as these tests displayed less scatter.

When determining the hardening parameters, the user can choose between parameters calibrated for an incompressible stress-strain relation or a compressible stress-strain relation. Incompressible or compressible parameters should be chosen on the basis of the damage propagation exhibited by the material. If the material exhibits high damage propagation, then the damage should be coupled and the hardening parameters should be calibrated for the incompressible stress-strain relation. If the material does not exhibit a high damage propagation, then the damage does not need to be coupled, and the parameters can be calibrated for a compressible stress-strain relation.

The compressible stress, σ_C, is calculated assuming that the material's volume is changing, $\varepsilon_v \neq 0$. The equation used to calculate the compressible stress in MatPrePost is:

$$\sigma_C = \sigma_e \exp\left(-2\varepsilon_t\right) \tag{4.2}$$

Here σ_e is the engineering stress, and ε_t is the transverse strain. It is in this expression assumed

isotropy, $\varepsilon_2 = \varepsilon_3$. The incompressible stress, σ_I, is calculated by assuming that the volume does not change during the loading, $\varepsilon_v = 0$. If isotropy is still assumed, then the following expression is valid:

$$\varepsilon_v = \varepsilon_1 + \varepsilon_2 + \varepsilon_3 = 0 \quad \Rightarrow \quad \varepsilon_2 = -\frac{\varepsilon_1}{2} \tag{4.3}$$

The incompressible stress can then be written as:

$$\sigma_I = \sigma_e \exp(\varepsilon_1) \tag{4.4}$$

The test results showed that the material exhibited a significant increase in volume as it was deformed. The material model was therefore calibrated to fit the incompressible stress-strain relation, as damage propagation would be included in the material model.

To determine the parameters in MatPrePost, the relevant test is selected and the user clicks on the stress-strain curve where he believes that the yield stress is situated, as indicated by a red dot in Figure 4.2. The hardening parameters is then optimized using a RALG solver [19]. Ralg is a free non-linear problem solver written in the programming languages Python and NumPy. The solver will determine the material parameters based on the non-linear hardening function given in Eq. (2.13), and the constraints which the tensile test's stress-strain relation represents.
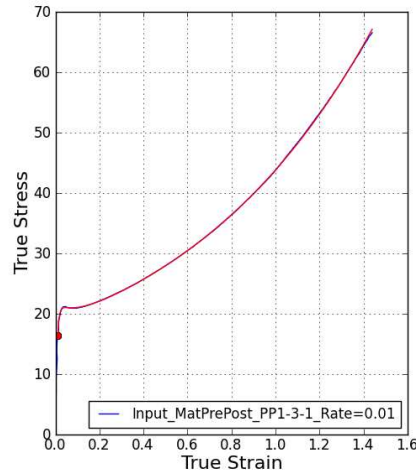
Figure 4.2: Calibrating the hardening/softening parameters in MatPrePost

The red curve in Figure 4.2 is created in MatPrePost and illustrates how well the material parameters fit the stress-strain relation of the selected test. The hardening/softening parameters optimized by MatPrePost and the yield stress, selected by the user, is given in the table below.

Parameter	Value	Unit
σ_0	16.40	MPa
θ_{R1}	682.39	MPa
Q_{R1}	5.14	MPa
θ_{R2}	13.89	MPa
Q_{R2}	-12.62	MPa
θ_{R3}	-34.00	MPa
Q_{R3}	-2.61	MPa

4.1.4 Plastic dilatation, β

The plastic dilatation parameter, β, is calculated in MatPrePost by assuming a constant retraction ratio:

$$R = -\left(\frac{\varepsilon_{long}}{\varepsilon_{trans}}\right) = \text{Constant} \tag{4.5}$$

The equations derived to determine the dilatation parameter is based on the master thesis of Martin Hovden [9]. The material's volumetric strain is controlled by the equation for the plastic flow potential, g, given in Eq. (2.15). The gradient of the flow potential can be written as [21]:

$$\frac{\delta g}{\delta \sigma_{\mathbf{eq}}} = \frac{\delta g}{\delta I_1}\frac{\delta I_1}{\delta \sigma} + \frac{\delta g}{\delta J_2}\frac{\delta J_2}{\delta \sigma} = f_1 + f_2 \tag{4.6}$$

The partial derivatives $\delta g/\delta I_1$ and $\delta g/\delta J_2$ can be written as:

$$\frac{\delta g}{\delta I_1} = \frac{1}{2\beta}\left[(\beta - 1) + \frac{(\beta - 1)^2 I_1}{\sqrt{(\beta - 1)^2 I_1^2 + 12 J_2 \beta}}\right] \tag{4.7}$$

$$\frac{\delta g}{\delta J_2} = \frac{3}{\sqrt{(\beta - 1)^2 I_1^2 + 12 J_2 \beta}} \tag{4.8}$$

For a uniaxial tensile test, the stress invariants I_1 and J_2 becomes:

$$I_1 = \sigma \qquad \text{and} \qquad J_2 = \frac{1}{3}\sigma^2 \tag{4.9}$$

The derivatives of the stress invariants can be expressed by:

$$\frac{\delta I_1}{\delta \sigma} = \begin{bmatrix} 1 & 0 & 0 \\ 0 & 1 & 0 \\ 0 & 0 & 1 \end{bmatrix} \qquad \text{and} \qquad \frac{\delta J_2}{\delta \sigma} = \frac{\sigma}{3}\begin{bmatrix} 2 & 0 & 0 \\ 0 & -1 & 0 \\ 0 & 0 & -1 \end{bmatrix} \tag{4.10}$$

The material tests showed that the material exhibited large deformations before the material fractured. It has therefore been assumed that the elastic deformations are negligible relative to the plastic deformations in the calculations performed in this section. By inserting the values of the stress invariants for a uniaxile tensile case, Eq. (4.9), into Eq. (4.7) and Eq. (4.8). The functions f_1 and f_2 in Eq. (4.6) can be written as:

$$f_1 = \frac{\delta g}{\delta I_1}\frac{\delta I_1}{\delta \sigma} = \frac{1}{2\beta}\left[(\beta-1) + \frac{(\beta-1)^2\sigma}{\sqrt{(\beta-1)^2\sigma^2 + 4\sigma^2\beta}}\right]\begin{bmatrix} 1 & 0 & 0 \\ 0 & 1 & 0 \\ 0 & 0 & 1 \end{bmatrix} = \frac{(\beta-1)}{(\beta+1)}\begin{bmatrix} 1 & 0 & 0 \\ 0 & 1 & 0 \\ 0 & 0 & 1 \end{bmatrix} \qquad (4.11a)$$

$$f_2 = \frac{\delta g}{\delta J_2}\frac{\delta J_2}{\delta \sigma} = \frac{\sigma}{\sqrt{(\beta-1)^2\sigma^2 + 4\sigma^2\beta}}\begin{bmatrix} 2 & 0 & 0 \\ 0 & -1 & 0 \\ 0 & 0 & -1 \end{bmatrix} = \frac{1}{(\beta+1)}\begin{bmatrix} 2 & 0 & 0 \\ 0 & -1 & 0 \\ 0 & 0 & -1 \end{bmatrix} \qquad (4.11b)$$

The materials plastic flow, $\hat{D}^p$, is given in Eq. (2.14). The $\dot{\lambda}$ in Eq. (2.14) will for a uniaxial tensile test always be equal to the plastic strain rate; e.g $\dot{\lambda} = \dot{\varepsilon}^p$. If the relation between the longitudinal and transverse strains are assumed to be constant, then the materials plastic flow can be expressed as:

$$\hat{D}^p = \begin{bmatrix} \dot{\varepsilon}_1^p & 0 & 0 \\ 0 & \dot{\varepsilon}_2^p & 0 \\ 0 & 0 & \dot{\varepsilon}_3^p \end{bmatrix} = \dot{\varepsilon}_1^p\begin{bmatrix} 1 & 0 & 0 \\ 0 & -R & 0 \\ 0 & 0 & -R \end{bmatrix} \qquad (4.12)$$

Setting the plastic flow in Eq. (4.12) equal to Eq. (2.14), and using the expression derived for the gradient of the plastic flow in Eq. (4.6), the following relation is obtained:

$$\dot{\varepsilon}_1^p\begin{bmatrix} 1 & 0 & 0 \\ 0 & -R & 0 \\ 0 & 0 & -R \end{bmatrix} = \dot{\lambda}\frac{(\beta-1)}{(\beta+1)}\begin{bmatrix} 1 & 0 & 0 \\ 0 & 1 & 0 \\ 0 & 0 & 1 \end{bmatrix} + \dot{\lambda}\frac{1}{(\beta+1)}\begin{bmatrix} 2 & 0 & 0 \\ 0 & -1 & 0 \\ 0 & 0 & -1 \end{bmatrix} \qquad (4.13)$$

Solving the equations in Eq. (4.13) yields the relation between β and R:

$$R = \frac{2-\beta}{\beta+1} \qquad \Leftrightarrow \qquad \beta = \frac{2-R}{R+1} \qquad (4.14)$$

Figure 4.3 displays the procedure to determine the dilatation parameter, β, in MatPrePost. The figure shows the retraction ratio of the relevant tensile test. The user selects two points on the graph, illustrated with the red dots in the figure, from which the dilatation parameter will be calculated. The dilatation parameter is calculated by taking the mean retraction ratio in the selected region, and then applying Eq. (4.14).
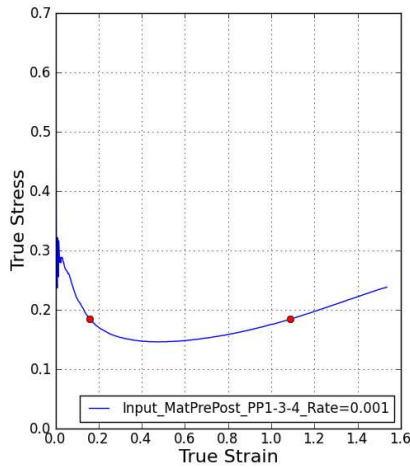
Figure 4.3: Calibrating the plastic dilatation parameter, β, in MatPrePost

The calibrated dilatation parameter from MatPrePost with the selected region and test was:

Parameter	Value	Unit
β	1.591	N/A

4.1.5   Strain rate dependency

Because the data available for the elastic region is very limited, only the visco-plastic material parameters were calibrated. The material's visco-plastic parameters is the C, which is the material's strain rate dependency, and the material's reference strain rate, $\dot{p}_0$. In previous calibration procedures, the parameter C was optimized by linear regression, while $\dot{p}_0$ was set as the plastic strain rate at the onset of necking. In MatPrePost, these variables are determined by first activating tensile tests at multiple strain rates, preferably more than two. A well recognizable point is selected on each of the curves, as indicated by red dots in Figure 4.4. For the calibration to give the best result, the points selected should have the same plastic strain. In this thesis, the peak stress is a very recognizable point on the curves, and was therefore chosen. The parameters, C and $\dot{p}_0$, is determined by optimization using the RALG solver, which was described in Section 4.1.3. The expression for the material's strain rate dependency, given in Eq. (2.17), the points selected by the user and the tests' stress-strain relation, is the constraining inputs to MatPrePost which is used to optimize the materials strain rate dependancy.
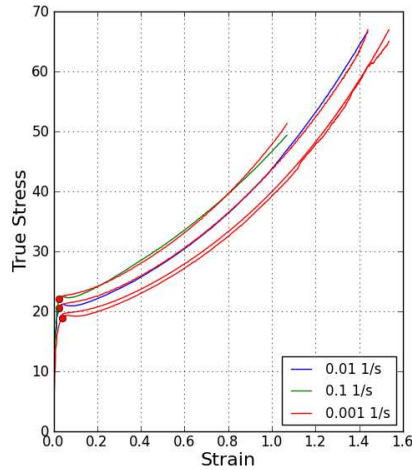
Figure 4.4: Determining visco-plastic parameters using MatPrePost

The red curves in Figure 4.4 is generated by MatPrePost to illustrate how well the calibrated visco-plastic material parameters fit. The parameters in the table below displays the strain rate dependent parameters calibrated by MatPrePost.

Parameter	Value	Unit
C	5.79E-4	N/A
$\dot{p}_0$	3.79E-2	s^{-1}

4.1.6   User defined parameters

MatPrePost does not calibrate all the material parameters, some must be given by the user as inputs. These include:

- Density, ρ

- Young's modulus, E

- Poisson's ratio, ν

- (Yield stress, σ_0)

The yield stress is given as an output by MatPrePost, but the user must personally select the point where he believes the material yields. It has therefore not been considered calibrated by Mat-PrePost, and is written in parenthesis.

The material's density was provided by TOYOTA, the Young's modulus was set at 1000MPa and the Poisson's ratio at 0.4, as this is the normal values for polypropylene [3].

4.1.7 Result

The material parameters given as outputs by MatPrePost is shown in the table below.

Table 4.1: Material parameters from MatPrePost

ρ [kg/mm^3]	E [MPa]	ν	K [MPa]	G [MPa]	σ_0 [MPa]	α	β
1180E-9	1000	0.4	1667	357	14.48	1.20	1.59

θ_{R1} [MPa]	Q$_{R1}$ [MPa]	θ_{R2} [MPa]	Q$_{R2}$ [MPa]	θ_{R3} [MPa]	Q$_{R3}$ [MPa]
682	5.14	13.89	-12.62	-34.00	-2.61

C	$\dot{p}_0$ [s^{-1}]	
3.79E-2	5.79E-4	

To verify the material parameters calibrated by MatPrePost, a numerical simulation for the uniaxial tensile test with a reduced cross section, using the material parameters determined by Mat-PrePost, was performed. The geometry and boundary conditions of the numerical simulations will be described more thoroughly in Chapter 5, where the numerical simulations are described. The results from the numerical simulations is shown in Figure 4.5.

(a) Force-displacement

(b) Stress-strain

(c) Retraction ratio

(d) Strain rate dependency
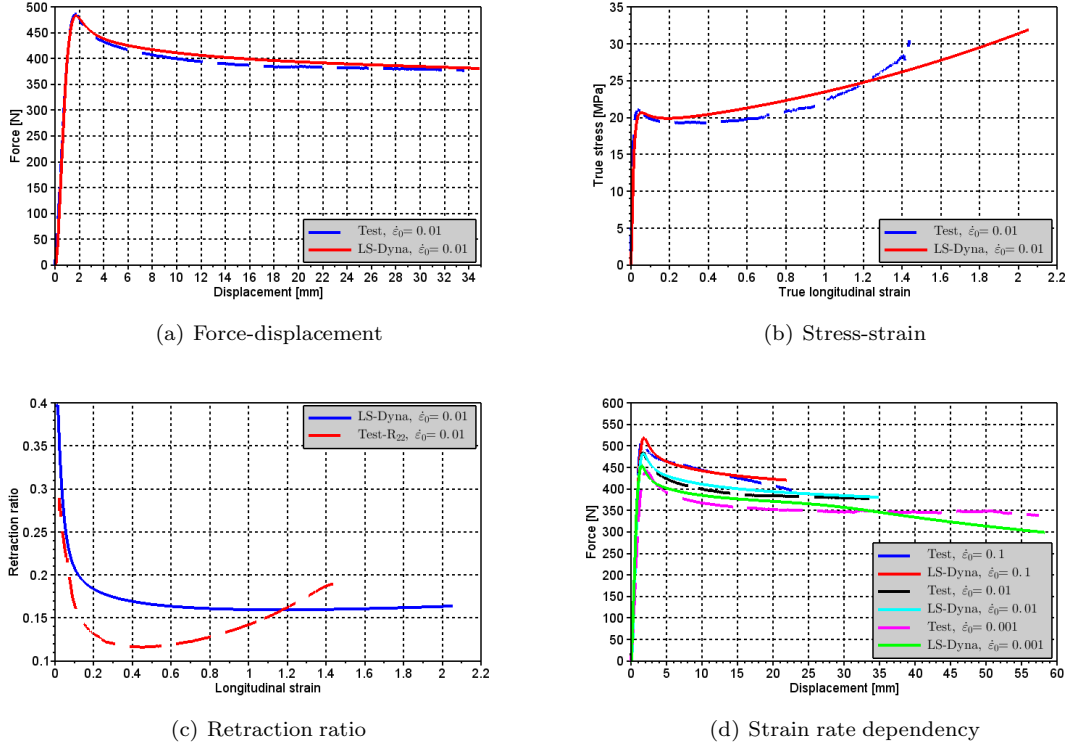
Figure 4.5: Simulation results using direct outputs from MatPrePost

The figure shows that the material parameters describe the force-displacement relation very well, but that the stress-strain relation after necking is described with less accuracy. The simulation's retraction ratio gives an ok result, though it is difficult to say how well it fits in the material's elastic region as the number of data points from the tests is very scarce in this region. The material's strain rate dependent parameters is also well calibrated, but they do not describe the material behavior perfectly.

The calibration performed using MatPrePost gives good results, the global behavior, which is given by the force displacement, correlates well with the tests, but the local behavior, e.g the stress-strain, does not. In this thesis, the main focus has been to fit the stress-strain, because if the stress-strain and material's strain history fit, then the global behavior will also match well. It was therefore believed that the results could be improved by altering some of the parameters which is linked to the material hardening/softening, and the strain rate dependency.

4.2 Inverse modeling

Depending on the intended usage of the material model and the necessary accuracy, the material parameters from MatPrePost can be used as they are, or they can be improved, either with new calibration procedures, or by inverse modeling. Inverse modeling was used in this thesis to optimize the material parameters from MatPrePost. In inverse modeling, the material parameters are opti-

mized by altering only one or a few parameters, then rerun the analyses and see how well the new values fit the test. The method is not very scientific and should be used with care.

Figure 4.5b) showed that the current calibration of the material hardening could be greatly improved. When performing inversed modeling it is important to understand how altering the different parameters will affect the material behavior, and how sensitive the material is to differences in the specific material parameters. Figure 4.6 display how the different hardening terms affect the material hardening with the signs as given by MatPrePost.
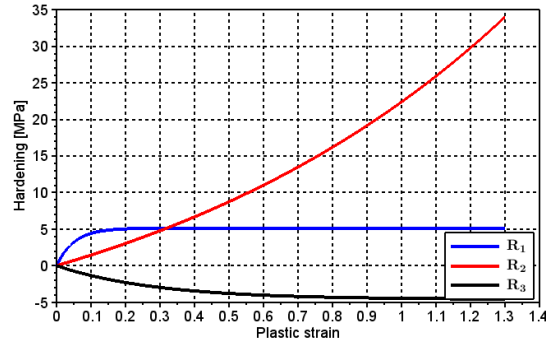
Figure 4.6: Hardening terms affect on the material hardening

The result in Figure 4.5b) indicated that the material exhibited more softening than the current parameters yield, and that the material's re-hardening is in the test occurring with a different slope. Thus the material parameters concerning the material's re-hardening and softening was re-calibrated using inversed modeling.

Figure 4.5d) shows that the simulation is somewhat overestimating the material's peak force at the strain rates that is not performed at the reference strain rate of $10^{-2}s^{-1}$. The material model's visco-plastic stress is given in Eq. (2.17). The materials peak force is affected by the yield stress, σ_0, the rate sensitivity of the flow stress, C, and the R_1 hardening part given by the parameters Q_{R1} and θ_{R1}. To make the material model better fit the material's strain rate sensitivity, these parameters had to be optimized.

Final material card for the core

The optimized material parameters are displayed in the table below. The table shows that not only the parameters linked to the materials hardening and strain rate dependency is altered, but that some of the other parameters has also been somewhat changed. The difference in the other parameters is very small and were only changed because Figure 4.5 gave a small indication that a change in one of the parameters may give the material model a better fit.

63

Table 4.2: Final material parameters for core part

ρ [kg/mm³]	E [MPa]	ν	K [MPa]	G [MPa]	σ₀ [MPa]	α	β
1180E-9	950	0.35	1222	407	15.80	1.18	1.59

θ_{R1} [MPa]	Q_{R1} [MPa]	θ_{R2} [MPa]	Q_{R2} [MPa]	θ_{R3} [MPa]	Q_{R3} [MPa]
700	4.07	7.00	-3.40	-7.53	-2.39

C	$\dot{p}_0$ [s⁻¹]	
4.74E-2	5.97E-4	

4.3 Determining skin parameters

The material testing showed that the specimens with a full cross section had different material properties than the specimens with a reduced cross section. It was therefore decided to model the material specimens using two parts, where each part had a different material card. The results from the uniaxial tensile tests presented in Section 3.1.3 indicated that the main difference between the specimens with a full cross section and the specimens with a reduced cross section was the yield stress and the damage propagation, as seen in Figure 3.13 and Figure 3.14. Thus the main difference between the material card of the skin and core was the yield stress, σ_0, and the plastic dilatation parameter, β.

Calculating skin yield stress, $\sigma_{0,s}$

The yield stress of the skin was calculated by assuming that the total force acting through the specimen of the uniaxial tensile tests consisted of one skin part and one core part:

$$F_{tot} = F_c + F_s \quad \Leftrightarrow \quad wt_{tot}\sigma_F = wt_s\sigma_s + wt_c\sigma_c \quad \Rightarrow \quad t_{tot}\sigma_F = t_s\sigma_s + t_c\sigma_c \quad (4.15)$$

Where the different parameters are;

Abbreviation	Description
w	Width
t_{tot}	Total thickness
σ_F	Total mean stress
t_c	Core thickness
σ_c	Core stress
t_s	Skin thickness
σ_s	Skin stress

Determining the yield stress on the curves is somewhat difficult, thus the peak force was used as a reference point for the specimens with a full and reduced cross section. The stress at the peak force is mainly affected by the yield stress, σ_0, the material hardening, R, and the materials strain rate sensitivity, C. The materials stress after yielding, given in Eq. (2.17), can be divided into two parts; a non viscous and a viscous:

$$\sigma = (\sigma_0 + R) \overbrace{\left[1 + C \ln\left(1 + \frac{\dot{p}}{\dot{p}_0}\right)\right]}^{\text{Viscous}} \tag{4.16}$$

The material testing gives no indication of the viscous part not being the same for the full and reduced specimens, thus this has been assumed to be the same for both the skin and the core. The test results showed that there were no difference in the material hardening of the specimens with a full and reduced cross section. In Section 3.1.3, it was found that the average peak stress, $\sigma_{P,R}$, of the specimens with a reduced cross section tested at an initial strain rate of $10^{-2}s^{-1}$, was 20.54MPa. If only the yield stress is different for the skin and the core, then the difference between the peak stress and yield stress of the specimens with a reduced cross section will be the same for the specimens with a full cross section:

$$\sigma_{P,R} = \sigma_{0,R} + \sigma_{diff} \qquad \text{and} \qquad \sigma_{P,F} = \sigma_{0,F} + \sigma_{diff} \tag{4.17}$$

At the peak stress, the stress difference, σ_{diff}, between the peak stress of the reduced cross section, which is assumed only consists of core material, and the yield stress is:

$$\sigma_{diff} = \sigma_{P,R} - \sigma_{0,c} \qquad \text{where} \qquad \sigma_{0,R} = \sigma_{0,c} \tag{4.18}$$

By applying Eq. (4.18) and Eq. (4.17) to Eq. (4.15), the yield stress of the skin layer can be calculated by:

$$\sigma_{0,s} = \left[\frac{(t_{tot}\sigma_{P,F}) - (t_c\sigma_{P,R})}{t_s}\right] - (\sigma_{P,R} - \sigma_{0,c}) \tag{4.19}$$

The material testing using an optical microscope, in Section 3.5.1, was the only test that gave an indication of the materials skin thickness. The skin thickness was therefore set to 0.2mm when calculating the the yield stress of the skin. During the material testing, the thickness of the specimens was measured prior to each test. These measures indicated that the thickness of the specimens with a full cross section was about 3.1mm. The yield stress of the skin, $\sigma_{0,s}$, was calculated to:

Parameter	Value	Unit
$\sigma_{0,s}$	19.83	MPa

Determining the skin's plastic dilatation parameter, β_s

The plastic dilatation parameter of the skin, β_s, was calculated by assuming that the total retraction ratio of the specimen with a full cross section, R_F, given by Eq. (4.5), consisted of one core part and one skin part:

$$R_F = r_s R_s + r_c R_c \qquad \Rightarrow \qquad R_s = \frac{R_F - r_c R_c}{r_s} \tag{4.20}$$

r_s is the skin to thickness ratio, (t_s/t_{tot}), and r_c is the core to thickness ratio, (t_c/t_{tot}), while R_s and R_c is the retraction ratio of the skin and core, respectively. The retraction ratio of the reduced

and full specimens is shown in Figure 4.7. The figure indicates that the specimens with a full cross section has a slightly higher retraction ratio.
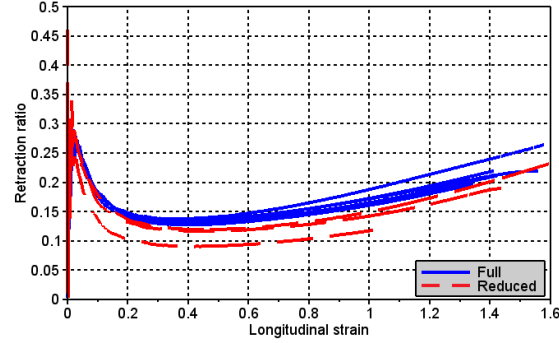
Figure 4.7: Retraction ratio of 3mm full and reduced specimens tested at $\dot{\varepsilon}_0 = 10^{-2}s^{-1}$

The plastic dilatation parameter was then calculated by inserting Eq. (4.20) to Eq. (4.14):

$$\beta_s = \frac{2 - R_s}{1 + R_s} = \frac{2r_s - R_F - r_c R_c}{r_s + R_F - r_c R_c} \tag{4.21}$$

The β-value determined for the core by MatPrePost yielded a retraction ratio R_c equal to 0.16, the mean retraction ratio of the specimens with a full cross section, R_F, was determined from Figure 4.7 to be approximately 0.20. Thus the skin's plastic dilatation parameter was calculated to:

Parameter	Value	Unit
β_s	1.49	N/A

Material card for the skin

The material parameters determined for the material's skin part is shown in the table below. The material tests suggested that the specimens with a full cross section had a somewhat lower slope than the core, the Young's modulus of the skin is therefore decreased.

Table 4.3: Material parameters for the skin part

ρ [kg/mm^3]	E [MPa]	ν	K [MPa]	G [MPa]	σ_0 [MPa]	α	β
1180E-9	550	0.40	917	196	19.83	1.18	1.49

θ_{R1} [MPa]	Q_{R1} [MPa]	θ_{R2} [MPa]	Q_{R2} [MPa]	θ_{R3} [MPa]	Q_{R3} [MPa]
700	4.07	7.00	-3.40	-7.53	-2.39

C	$\dot{p}_0$ [s^{-1}]				
4.74E-2	5.97E-4				

Chapter 5

Numerical simulations

Numerical simulations were performed in order to verify that the material parameters determined in Chapter 4 were correct, and to control the material model's ability to accurately describe the material's behavior.

The simulations were primarily done using LS-DYNA, which is an implicit/explicit finite-element software, apart from the simulations of the drop-tower tests, for which Abaqus was used. The simulations were performed using an explicit non-linear dynamic solver. An explicit solver was chosen because the relevant problem is dynamic and involves small time steps, which makes an explicit method most suitable [15].

5.1 Uniaxile tensile test simulation

Uniaxile tensile tests were performed using specimens milled at three different initial plate thicknesses. The specimens have the same geometry, the only difference is the initial plate thickness. The description of the numerical modeling in this section, will describe the modeling in general, as this was the same for all thicknesses. The figures showing the numerical models will primarily be of the specimens milled from the 3mm thick plates, unless something else is noted. The 3mm plate was the plate thickness that was primarily used to determine the skin thickness and also the parameters for the material model. The simulations of the 3mm plate will therefore be most thoroughly analyzed. The simulations of the 2mm and 4mm specimens were done to determine the material model's capability to describe the material behavior if it was molded with a different thickness.

The 3mm specimens were most thoroughly tested, with tests performed at three initial strain rates using specimens with a full section thickness and specimens whose section thickness were reduced. The 2mm and 4mm specimens were also tested at three initial strain rates, but only using a full cross section. Specimens with a reduced cross section was only performed at a single strain rate. Because the 2mm and 4mm plates were intended for validation, only simulations using a full cross section were performed.

The dog-bone tests had a significant fracture variation, and the numerical simulations of the uniaxial dog-bone specimens do therefore not include a fracture formulation in their material card. The primary focus of these simulations has instead been to verify the material model's remaining parameters and their ability to accurately describe the materials behavior. The material card used

for the numerical models' core was presented in Table 4.2, and the material parameters used for the numerical models' skin part was presented in Table 4.3.

5.1.1   Modeling

The modeling was done in two steps. The first step was to create a model of the cross section with a reduced thickness, and the second step was to model the full cross section. It was assumed that the reduced cross section consisted of only the core, while the full cross section consisted of both the core and the skin. The specimens had three symmetry planes; one in the thickness direction, one in the width, and one at the center in the gauge length direction. Because necking did not always occur in the middle of the specimen, the symmetry plane at the center in the gauge length direction was not used. The applied symmetry planes are depicted in Figure 5.1.
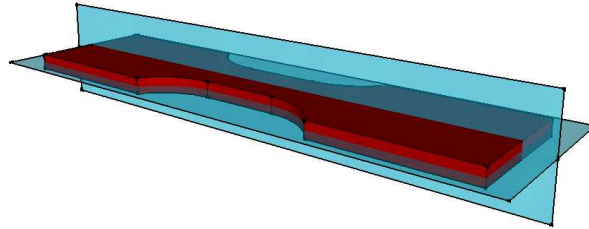
Figure 5.1: Symmetry planes used for modeling

During testing, the specimens were clamped in both ends, as depicted in Figure 3.1. One of the clamped ends would move with a constant velocity, while the other would be kept still throughout the test. The clamped areas of the specimen were not subjected to any deformations, thus the numerical model, shown in Figure 5.2, only consists of the parts that were free to deform. The fixed clamp was modeled by constraining displacements in the x and y direction for the nodes in the left end of the specimen, see Figure 5.2. The constant velocity, inflicted by one of the clamps, was modeled by prescribing the right end nodes a constant velocity. The symmetry plane normal to the Y-axis was modeled by constraining displacements in the Y direction, similarly was the symmetry plane normal to the Z-axis modeled by constraining displacements in the Z direction.

(a) Plane view

(b) Section view

(c) Through thickness view
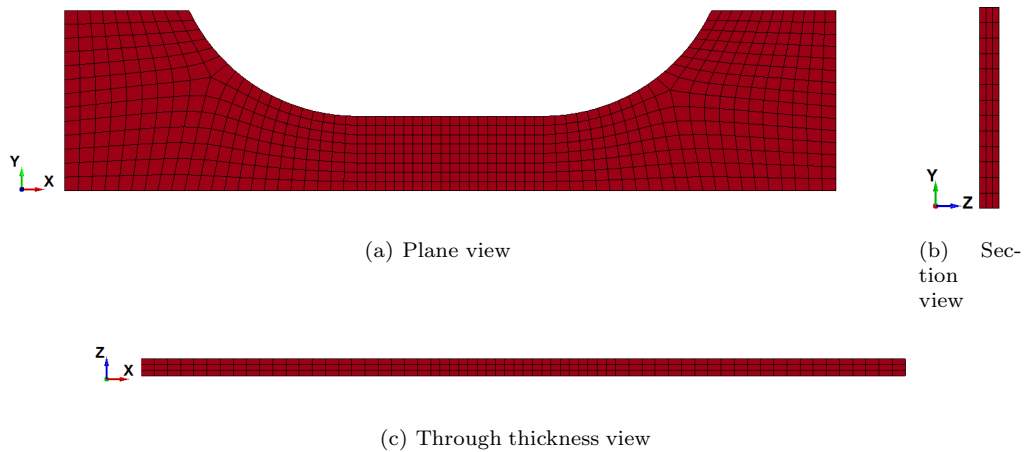
Figure 5.2: Discretization of the Dog-Bone specimens with reduced cross section

The central part of the specimen has been given an element size that allows the model to have three elements in the thickness direction and eight in the width direction. This enabled the gauge length part of the specimen to have relatively cubic elements. Three elements in the thickness direction was considered to be enough to accurately describe the material's neck propagation at an acceptable CPU cost.

The model of the full cross section specimens consists of two parts, one part for the core and one part for the skin. The core part was made by using the mesh and geometry of the reduced cross section model, and then the skin was added as a second part. In order for the mesh of the skin and the core to match, the element size of the skin in the longitudinal direction and in the width direction had to be the same as for the core. The skin thickness was determined in Section 3.5 to be 0.2mm, and two elements were used in the thickness direction of the skin. The skin-core model was given the same boundary conditions as the core model.

(a) Plane view

(b) Section view

(c) Through thickness view
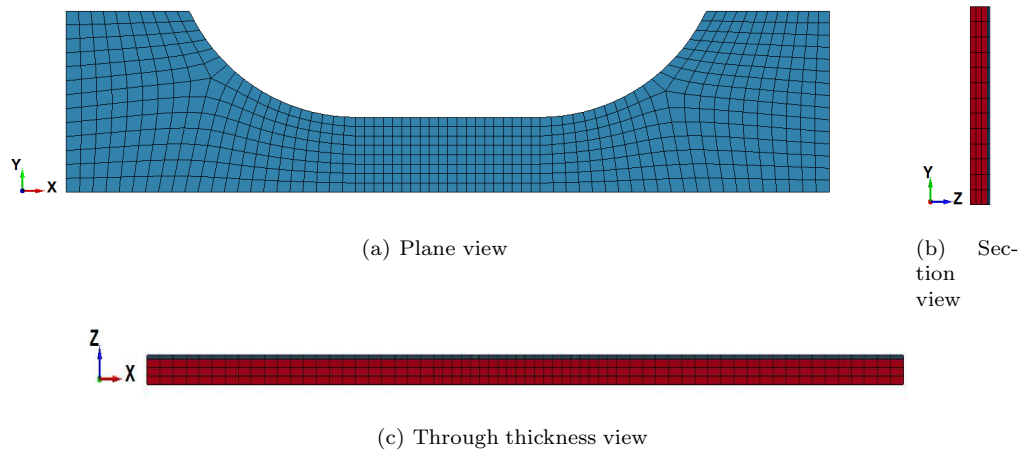
Figure 5.3: Discretization of the Dog-Bone specimens with full cross section

69

Table 5.1 gives key data for the core and skin-core models. Because creating and meshing curved geometry is somewhat difficult in LS-PrePost, the geometry and mesh of each part was made separately in Abaqus, which is a software very similar to LS-Dyna. The nodal coordinates and the elements from the Abaqus input file was converted to an LS-Dyna compatible k-file using a MatLab script. The MatLab script is available in Appendix B.2.3. The two parts was then imported to LS-PrePost where the nodes between the skin and core was merged in order to make the two parts interact.

Table 5.1: Key data for uniaxial tensile tests

Part/Model	Element type	Nodes	Elements
Core	Solid	2940	1944
Skin	Solid	1470	1296
Skin-core	Solid	4410	3240

The numerical integration formulation used for the uniaxial tensile tests in LS-Dyna is element formulation 1. Element formulation 1 is an under-integrated constant-stress formulation [22]. A constant-stress formulation will work very well, as the specimen is deformed uniaxialy and a more or less constant stress state will develop.

The numerical model used for simulating the uniaxile dog-bone specimens with a thickness of 2mm is pictured in Figure 5.4. Because this model has the same element size as the 3mm plate in the longitudinal direction and the same number in the thickness direction, it will have a somewhat poorer aspect ratio. But this has been deemed acceptable.

(a) Plane view

(b) Section view

(c) Through-thickness view
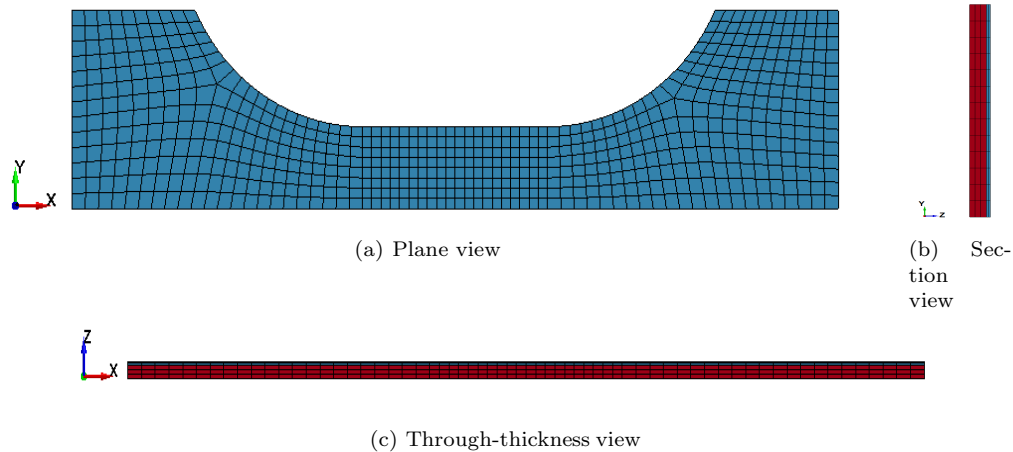
Figure 5.4: Discretization of the Dog-Bone specimens with 2mm thickness

Figure 5.5 displays the numerical model used for simulating the 4mm uniaxial dog-bone specimen. This model has the same number of elements in the thickness direction and the same longitudinal element size as the 2mm and 3mm numerical models.

70

(a) Plane view

(b) Section view

(c) Through-thickness view
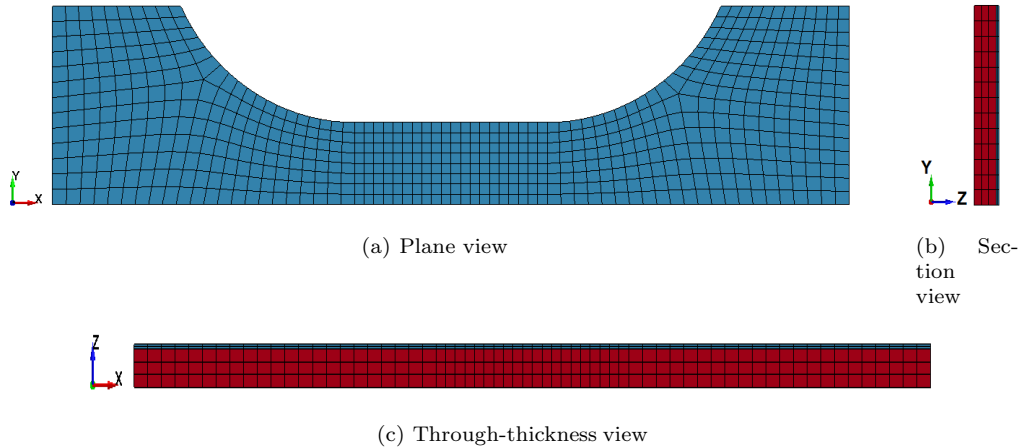
Figure 5.5: Discretization of the Dog-Bone specimens with 4mm thickness

5.1.2 3mm reduced cross section simulations

In this section the results from the numerical simulations using the 3mm thick reduced cross section model will be described. The tests at an intermediate strain rate has been studied most thoroughly. The reason for this is, as described in more detail in Chapter 4, that the tests at the lowest strain rate has a much larger scatter in their results which resulted in the tests at the intermediate strain rate was used as a baseline for the calibration. The tests used for comparing the simulations and the tests, are listed in the table below.

Table 5.2: Tests used to compare LS-Dyna simulations with reduced uniaxile tensile tests

Test	Initial strain rate, $\dot{\varepsilon}_0$ $[s^{-1}]$	Remarks
PP1-T3-R-V1-1	10^{-1}	
PP1-T3-R-V2-1	10^{-2}	Baseline test
PP1-T3-R-V3-1	10^{-3}	

Stress-strain relation

The correlation between the stress-strain curves of the numerical model and the test can be seen in Figure 5.6. The stresses and strains from LS-Dyna is taken as the average from where the neck first occurs, which is similar to what was done during the post-processing of the experimental material tests. The figure shows that the stress-strain of the test and the LS-Dyna simulation is almost identical. The curves behave very similarly in the elastic region, they have the same peak stress, and the softening/hardening region is identical.
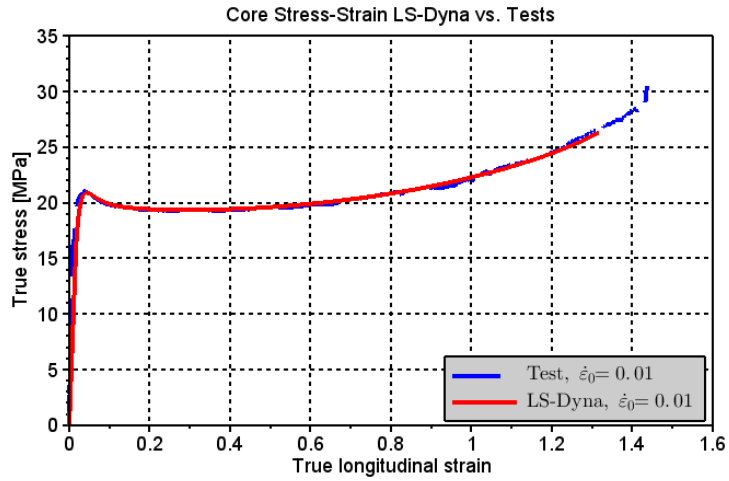
Figure 5.6: True stress-strain uniaxial test specimen, LS-Dyna vs. test

Figure 5.6 confirmes that the material parameters in Table 4.2 is able to describe the material's stress-strain behavior very well, and that the calibration procedure in Chapter 4 is able to accurately determine the material parameters.

Force-displacement relation

Figure 5.7 displays the correlation between the force-displacement from the tests and the LS-Dyna simulations. We see from the figure that the force-displacement from the test and the LS-Dyna simulation does not correlate as well as the stress-strain. They have a very good match up to the maximum force, which is identical, but after this point the two curves start to differ. The LS-Dyna simulation has a somewhat steeper drop in force from the maximum force, which is the onset of necking, until the force stabilizes. The shape of the curves is also different in the area where the forces has stabilized. The LS-Dyna simulation has a slight increase in force, while the test is slightly decreasing.
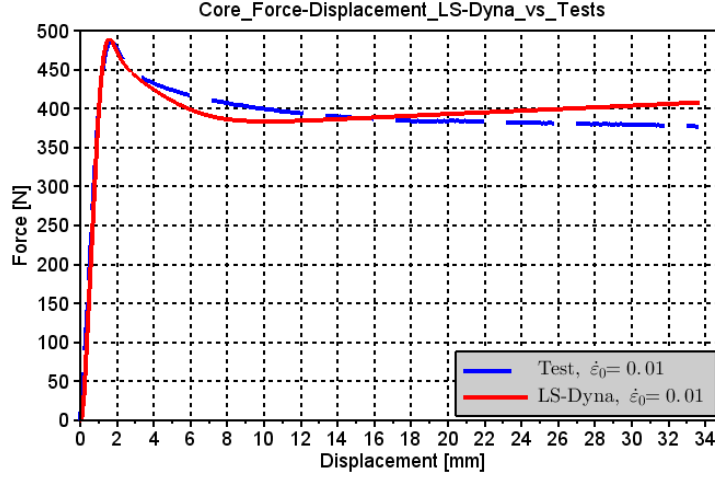
Figure 5.7: Force-displacement uniaxial test specimen, LS-Dyna vs. test

Because the stress-strain correlated very well, the misfit in the force-displacement must be due to the specimens' volumetric change, as the specimens cross section area is directly linked to the material's volumetric strain.

Dilatation relation

It is evident that the misfit for the force-displacement curves is due to a mismatch between the transverse strains of the simulation and the tests. Figure 5.8 displays a comparison of the volumetric strain of the LS-Dyna simulation and the test. Figure 5.9 compares the retraction ratios. As previously mentioned, the retraction ratio is the ratio between the transverse and longitudinal strain:

$$R = -\frac{\varepsilon_{transverse}}{\varepsilon_{longitudinal}} \tag{5.1}$$

The ratio, R_{22}, in Figure 5.9 is the transverse strain in the width direction divided by the longitudinal strain, while the R_{33} ratio is the transverse strain in the thickness direction divided by the longitudinal strain.

73
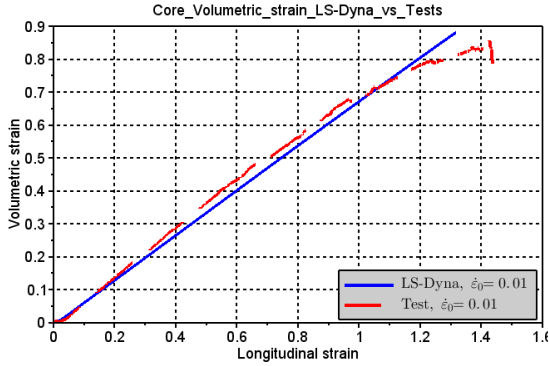
Figure 5.8: Volumetric strain, ε_V
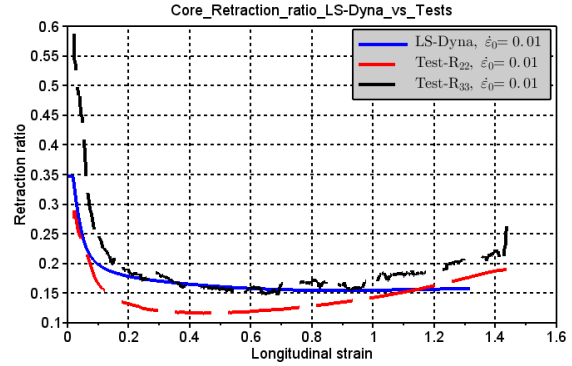
Figure 5.9: Retraction ratio, R

In Figure 5.9 the shape of the retraction ratio of the simulation and the test is similar until a longitudinal strain of about 0.4 to 0.5. After this point the tests have an increase in their retraction ratio, while the simulation is decreasing steadily. The dilatation parameter, β, was calibrated for the retraction ratio in the width direction, R_{22}, but the retraction ratio of the simulation has a better fit for the retraction ratio in the thickness direction, R_{33}. This difference is possibly because β was calculated based on a mean value of R_{22}, which Figure 5.9 indicates was too high.

The flow rule used for the material model is described in Eq. 2.15. This flow rule does not allow for an increase in the retraction ratio for a uniaxial tensile test as the deformation of the specimen progresses. In Section 2.1.1 the deformation of polypropylene is described. After necking, the weak Van der Waals bonds between the molecular chains are broken, and the material is stretched. These bindings are a lot easier to break than the covalent bonds holding the molecular chains together. It is therefore natural that the retraction ratio will start to decrease as more and more of the Van der Waals bonds are broken and we are left with the covalent bonds. The physical interpretation of the retraction ratio in the material model is that when only the covalent bonds remain, the retraction of the material will be very small. A possible explanation for the increase in the retraction ratio is the onset of fracture occurring in the center of the specimen, which creates more space for the other molecular chains.

Figure 5.9 displays that the LS-Dyna simulation is overestimating the retraction ratio from a longitudinal strain of about 0.1 until a longitudinal strain of about 1.0. The retraction ratio of the LS-Dyna simulation is in this area closer to the R_{33} than R_{22}. A higher retraction ratio means that the specimen's cross section area is decreasing more rapidly, which explains why the force is dropping faster after necking for the simulation than for the test. At a longitudinal strain of about 1.0, the simulation underestimates the retraction of the cross section, which explains why the force is larger for the simulation at larger displacements than for the test.

In Section 3.1.3, the material was discovered to be anisotropic, but due to a limited amount of time and number of tests, it has not been possible to perform a more accurate study of the anisotropic behavior of the material. As previously mentioned, the material model used in this thesis is isotropic, thus having different retraction ratios in the width and thickness direction of the numerical model has therefore not been possible. Figure 5.9 indicates that the difference between the two retraction

74

ratios is small, which reduces the error of assuming an isotropic material behavior.

Strain rate dependency relation

The results from the numerical simulations at an initial strain rate of $10^{-3}s^{-1}$ compared to a test at the same initial strain rate is shown in Figure 5.10 and Figure 5.11. Figure 5.10 displays the stress-strain while Figure 5.11 displays the relation between the force-displacement.
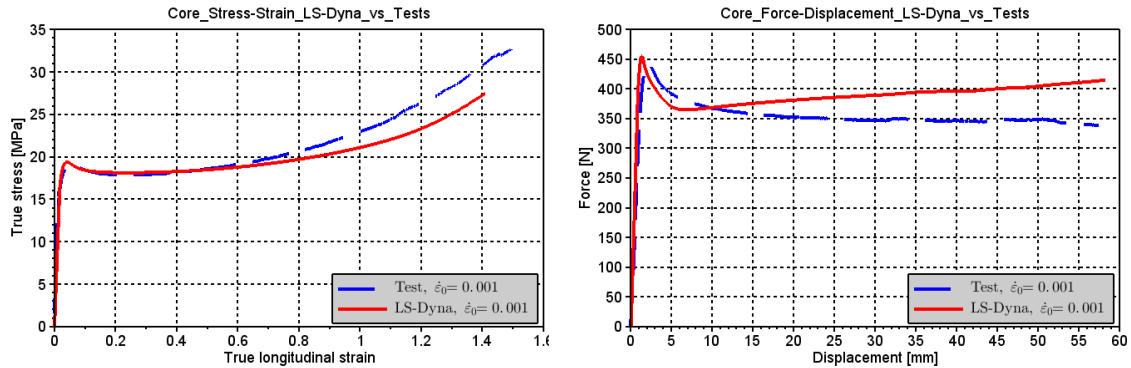
Figure 5.10: True stress-strain, $\dot{\varepsilon}_0 = 10^{-3}s^{-1}$ Figure 5.11: Force-displacement, $\dot{\varepsilon}_0 = 10^{-3}s^{-1}$

We see in Figure 5.10 that the maximum stress of the test and the simulation is identical. The shape of the two curves is also very good for the elastic region and the softening part of the plastic region. In the plastic hardening region, the two curves differs. As the re-hardening of the test is steeper than the LS-Dyna model, this difference could be due to adiabatic heating, as mentioned in Section 3.1.3, or due to scatter in the test results. The force-displacement curves in Figure 5.11 displays a larger deviation. The peak force is well captured, but similarly to what occurred at the intermediate strain rate, the LS-Dyna model predicts a higher force at large displacements, even though the stress from the test was higher than the simulation at large strains. This is most likely due to a large increase in the test's contraction ratio at higher strains.

Figure 5.12 and Figure 5.13 display the stress-strain and force-displacement, respectively, of the numerical simulation and test performed at an initial strain rate of $10^{-1}s^{-1}$. The peak stress of the simulation in Figure 5.12 is somewhat overestimated, while the general shape of the curve has a relatively good fit. For large strains, the LS-Dyna model is overestimating the stress, which is in accordance with previous observations. The force-displacement curve in Figure 5.13 displays an expected behavior.
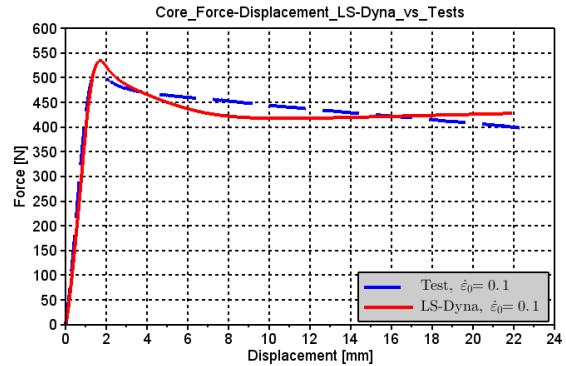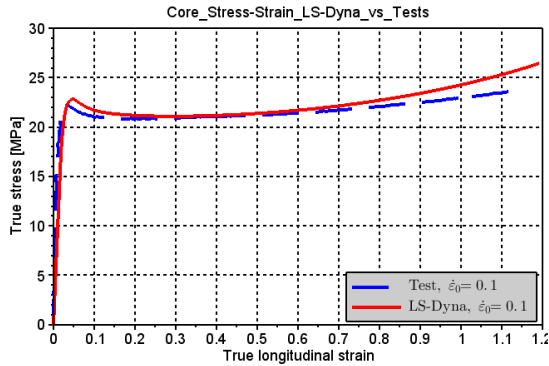
Figure 5.12: True stress-strain, $\dot{\varepsilon}_0 = 10^{-1}s^{-1}$ Figure 5.13: Force-displacement, $\dot{\varepsilon}_0 = 10^{-1}s^{-1}$

The material model is able to capture the strain rate dependency of the material relatively well. It gives a good prediction of the peak force, but either because the material is not logarithmically linear to the strain rate or due to scatter in the test results, it does not fit perfectly. The material does not take adiabatic heating into consideration. It is therefore not able to predict a lower stress hardening for simulations at higher strain rates, or higher stress hardening for simulations at lower strain rates. The misfit in the force-displacement curve at high displacements, seems to be in accordance with what was observed and described in the previous section concerning the dilatation relation of the simulation at the intermediate strain rate.

5.1.3   3mm full cross section simulations

In this section, the results from the 3mm thick full cross section model will be presented. The geometry and mesh of the specimens with a full cross section was shown in Figure 5.3. The material card used for the core part is the same as was used for the model with a reduced cross section, and it's material parameters is available in Table 4.2. The material parameters of the skin part, which was determined in Section 4.3 based on the difference in the test results of the uniaxile tensile tests with a full and reduced cross section, was shown in Table 4.3.

Similar to the model with a reduced section thickness, the simulation at the intermediate strain rate has been studied most thoroughly. This is because it was the tests at this strain rate that was primarily used for the calibration. The simulation results from the two other velocities will primarily be used to determine the material model's ability to describe the material's strain rate sensitivity.

The tests which has been used to compare the simulation results with the tests, is listed in the table below.

Table 5.3: Tests used to compare LS-Dyna simulations with full uniaxile tensile tests

Test	Initial strain rate, $\dot{\varepsilon}_0$ $[s^{-1}]$	Remarks
PP1-T3-F-V1-1	10^{-1}	
PP1-T3-F-V2-1	10^{-2}	Baseline test
PP1-T3-F-V3-3	10^{-3}	

Stress-strain relation

How well the model is able to capture the stress-strain behavior of tests, gives a very good indication of the accuracy of the calibration method and the material model. The average value of the stresses and strains at the location where the neck first formed in the simulation, has been compared with the true stress-strain history of the test's corresponding location in Figure 5.14.
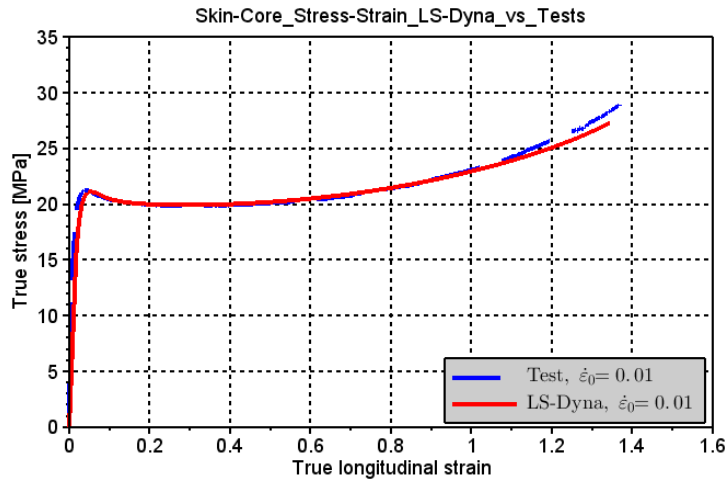
Figure 5.14: True stress-strain of full uniaxial test specimen, LS-Dyna vs. test

The two curves match very well. The slope in the elastic region is the same, the peak stress is identical, and the simulation has the same hardening/softening as the test. For very high strains, the test hardens somewhat quicker than the simulation, though it is very possible that this difference is due to test variation. In Section 3.1.3 it was noted that the tests had a substantial scatter in the hardening region.

Force-displacement relation

The force-displacement curve from the simulation and the corresponding test is shown in Figure 5.15. Similar to the force-displacement of the reduced cross section simulation in Figure 5.7, the force-displacement does not fit as good as the stress-strain. The elastic region and peak force match well, but the shape of the simulation's force-displacement curve from the peak force until fracture is very different.
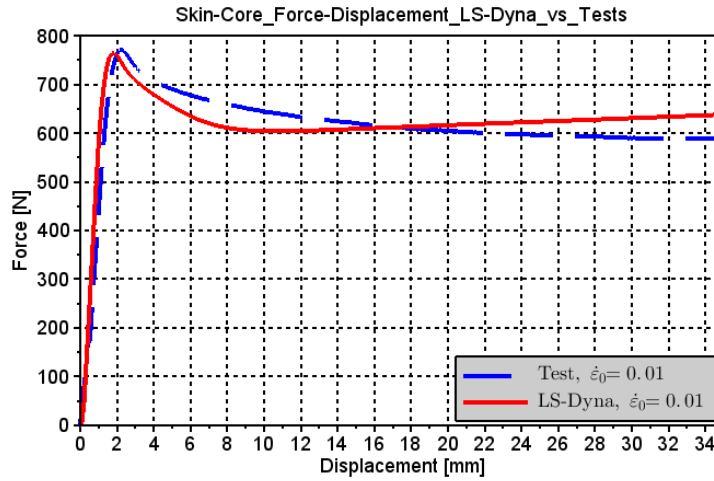
Figure 5.15: Force-displacement of full uniaxial test specimen, LS-Dyna vs. test

The difference between the force-displacement curvatures in Figure 5.15 is most likely due to a difference in the material's volumetric strain, which is in accordance with what was observed for the simulation of the specimen with a reduced section thickness in Section 5.1.2.

Dilatation parameters

The retraction ratio of the numerical model with a full cross section compared with the retraction ratio of the equivalent test, is shown in Figure 5.16. As the dilatation parameter, β, of the skin was determined using the same method as for the core, the correlation between the simulation and the experimental tests should be similar to what was observed for the simulation of the specimen with a reduced section thickness, in Figure 5.9.
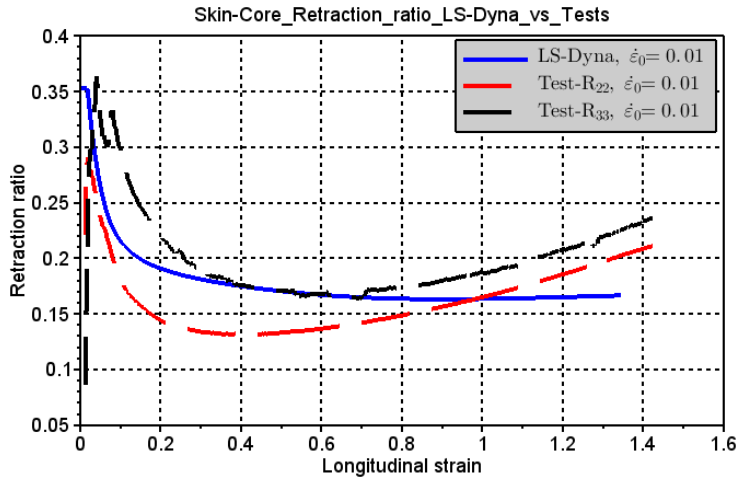
Figure 5.16: Retraction ratio of full uniaxial test specimen, LS-Dyna vs. test

Figure 5.16 gives a good indication of why the numerical model is not able to capture the tests' force-displacement. Almost identical to the result for the model with a reduced cross section, depicted in Figure 5.9, the model overestimates the retraction ratio from a strain of about 0.2 until about 0.8. As previously mentioned, overestimating the retraction ratio will result in an underestimate of the models cross section area. An underestimate of the cross section area will underestimate the force, if the stress-strain curves are equal. After a strain of about 0.8, the retraction ratio of the test surpasses the simulation's retraction ratio, which results in the model overestimating the force at large displacements.

The material model will not be able to accurately describe the material's force-displacement relation unless the material's retraction ratio is more accurately described. Further studies of the material's anisotropy may help improve this, as the material model then will have different transverse strains in the width and thickness direction, which will be more similar to what has been observed in the tests. The increase that occurs after a certain point in the material's retraction ratio will not be possible to reproduce, but the gap between the test and simulation may be minimized if the transverse strains in the width and thickness direction is not equal. Further tests on the material's skin thickness and number of layers, may give a better understanding of the material's fracture propagation, which may help understand why the material exhibits this increase in its retraction ratio.

Strain rate dependency relation

Simulations were run at initial strain rates of $10^{-1}s^{-1}$ and $10^{-3}s^{-1}$ in order to determine the the model's ability to describe the material's strain rate dependency. Figure 5.17 and Figure 5.18 displays a comparison of the model's and the test's stress-strain and force-displacement behavior, respectively, at an initial strain rate of $10^{-1}s^{-1}$.

Contrary to the stress-strain curve of the numerical model with a reduced cross section at the equivalent initial strain rates, depicted in Figure 5.12, the numerical model of the specimen with a

79

full cross section in Figure 5.17 is able to more accurately determine the peak stress. The model is also able to capture the shape of the experimental test's stress-strain curve well, but somewhat overestimates the stress at high strains. As previously mentioned, this is likely due to adiabatic heating which is not captured by the material model. The force-displacement is in accordance with previous observations.

Figure 5.17: Stress-strain, $\dot{\varepsilon}_0 = 10^{-1}s^{-1}$
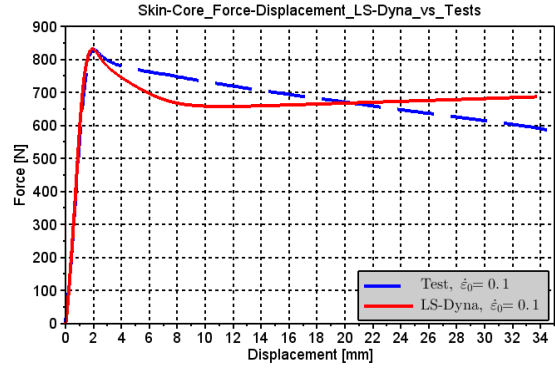
Figure 5.18: Force-displacement, $\dot{\varepsilon}_0 = 10^{-1}s^{-1}$

The stress-strain and force-displacement of the numerical model run at an initial strain rate of $10^{-3}s^{-1}$, and compared to a corresponding test, is depicted in Figure 5.19 and Figure 5.20, respectively. The simulation result of the stress-strain curve follows the shape of the corresponding experimental test very well, and it gives a good indication of the peak stress. The misfit in the peak force of the test and the simulation is most likely due to some variation in the tests' geometries, as some of the tests had a slight deviation in their geometrical measures. Apart from this, the fit between the force-displacement curvature of the simulation and the test is according to what has been observed and described previously.

Figure 5.19: Stress-strain, $\dot{\varepsilon}_0 = 10^{-3}s^{-1}$
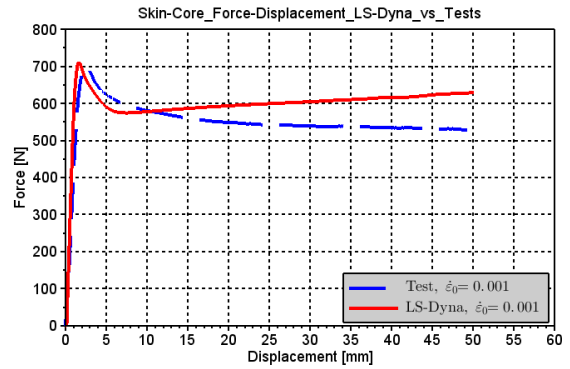
Figure 5.20: Force-displacement, $\dot{\varepsilon}_0 = 10^{-3}s^{-1}$

In Section 5.1.2, it was observed that the material model overestimated the peak stress for the simulation with a reduced cross section run at an initial strain rate of $10^{-1}s^{-1}$, while the simulation

using a full cross section was able to better determine this point. This is peculiar, as the tests using a reduced cross section were used to determine the material's strain rate dependency. The most probable reason for this is test variation. Considering that the material has exhibited an extensive test variation, the material model's ability to describe the material's strain rate dependency is good. To further improve the model's accuracy of describing the materials strain rate dependency, adiabatic heating should be included to better describe softening when the material is deformed at high strain rates.

5.1.4   2mm full cross section simulations

In this section, the results from the simulations using the numerical model of the 2mm uniaxile dog-bone specimen with a full cross section will be described. Because the majority of the material parameters are calibrated based on the tests performed with the 3mm specimen at an initial strain rate of $10^{-2}s^{-1}$, the simulation performed at this velocity will be studied most thoroughly. Simulations performed at two other velocities will serve to validate the material model's ability to accurately describe the strain rate sensitivity at different initial plate thicknesses.

The table below displays the tests which has been compared with the simulation at the corresponding strain rate. The material cards used for the simulations' skin and core, seen in Table 4.3 and Table 4.2 respectively, is the same as where used for the 3mm thick simulations.

Table 5.4: Tests used to compare LS-Dyna simulations with 2mm thick full uniaxile tensile tests

Test	Initial strain rate, $\dot{\varepsilon}_0$ $[s^{-1}]$	Remarks
PP1-T2-F-V1-2	10^{-1}	
PP1-T2-F-V2-4	10^{-2}	Baseline test
PP1-T2-F-V3-1	10^{-3}	

Stress-strain and force-displacement relation

How well the numerical model of the 2mm specimen is able to reproduce the stress-strain behavior of a corresponding test is shown in Figure 5.21. The figure shows that the model is able to very accurately describe the test's behavior until the material starts to re-harden. At this point, the test hardens much faster than the simulation. Figure 5.22 displays the correlation between the force-displacement of the LS-Dyna simulation and the test. The simulation gives a good estimate until the curves reaches its peak force. From this point the simulation is overestimating the force.

It was in Section 3.1.3 observed that the material damage increased with an increase in the materials molding thickness, as seen in Figure 3.26. As the material parameters are calibrated for the test specimens with a plate thickness of 3mm, the overestimate of the material stress curve in Figure 5.21, is in accordance with the observations made of the uniaxile tensile tests. As the damage propagation is overestimated for the simulations of the 2mm plates, the simulation's re-hardening will not be as steep as the tests'.
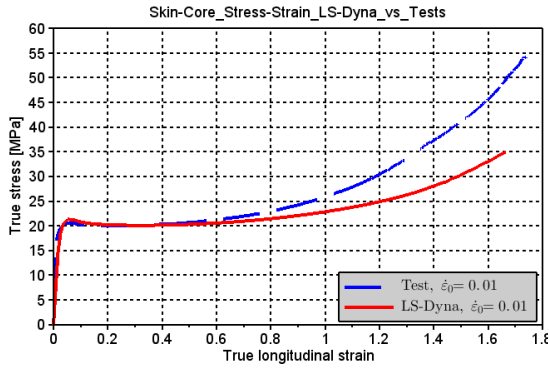
Figure 5.21: True stress-strain, 2mm plate
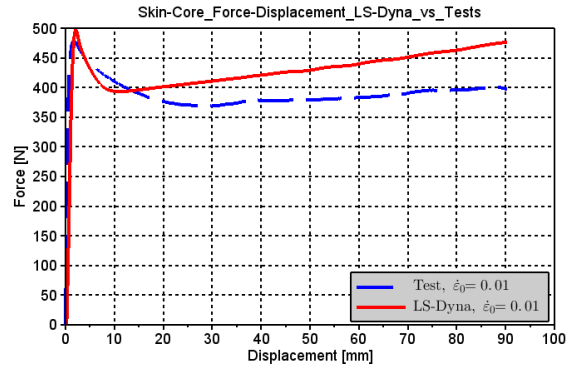
Figure 5.22: Force-displacement, 2mm plate

Although the simulation is underestimating the re-hardening of the 2mm thick material tests, it still overestimates the end of the force-displacement curve in Figure 5.22. This is most likely because the damage's effect on the stress-strain relation is lower than the effect of the difference between the simulation's and tests' volumetric strain, which can be seen in Figure 5.23.
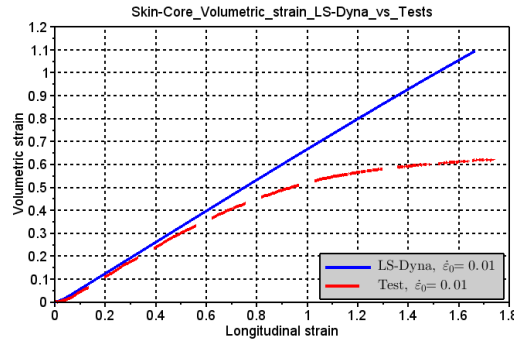
Figure 5.23: Volumetric strain of 2mm plate

The misfit of the force-displacement curves in Figure 5.22 is most likely due to a combination of an overestimated volumetric strain, which will also overestimate the cross section area, and due to the model's inability to accurately describe the transverse strains, which creates the curved shape of the volumetric strain curve. The material model's inability to reproduce the material's transverse strains was also observed for the 3mm plate simulation, in Figure 5.16 and has been further discussed in that section. Figure 5.24 is included to visualize that this is also a problem for the 2mm plate.

82
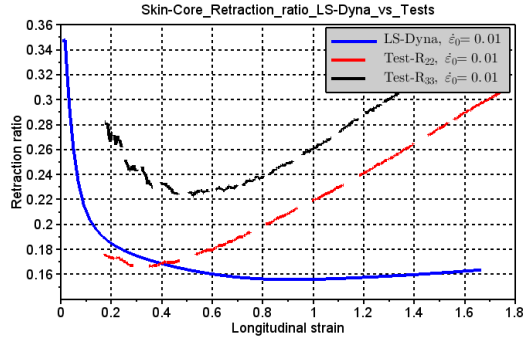
Figure 5.24: Retraction ratio of 2mm plate

Strain rate dependency

Figure 5.25 and Figure 5.26 displays the stress-strain and force-displacement curves, respectively, of the simulation and the test of a 2mm thick specimen with an initial strain rate of $10^{-3}s^{-1}$. Both figures shows the same behavior and fit between the simulation and test, as was observed at the intermediate strain rate of $10^{-2}s^{-1}$ in Figure 5.21 and Figure 5.22.
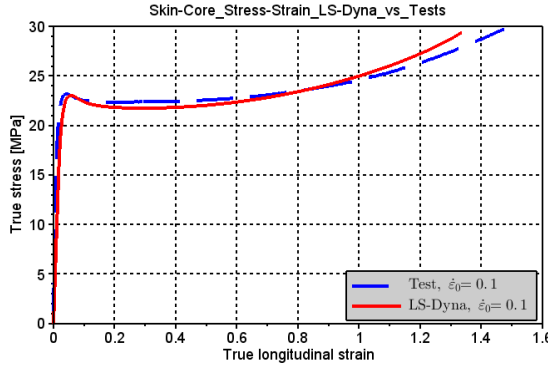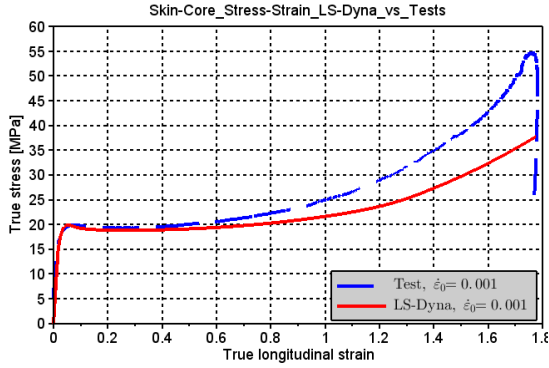

Figure 5.25: Stress-strain, $\dot{\varepsilon}_0 = 10^{-3}s^{-1}$
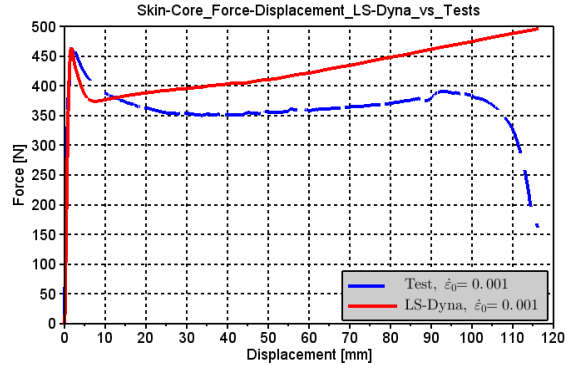
Figure 5.26: Force-displacement, $\dot{\varepsilon}_0 = 10^{-3}s^{-1}$

The material model's ability to describe the material with a thickness of 2mm and an initial strain rate of $10^{-1}s^{-1}$ is shown in Figure 5.27 and Figure 5.28. Figure 5.27 displays a comparison of the test's and simulation's stress-strain, while in Figure 5.28 the force-displacement curves are compared. In Figure 5.27, the gap between the stress-strain curves is smaller than what was observed at the two lower strain rates. This decreased gap is most likely due to adiabatic heating, which occurs at higher strain rates and decreases the material hardening. As previously mentioned, adiabatic heating is not taken into account in the material model, which explains the decreased gap.
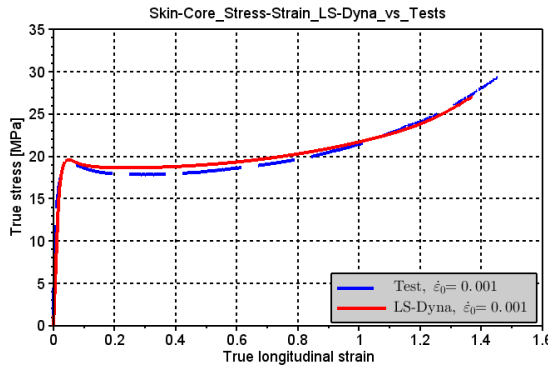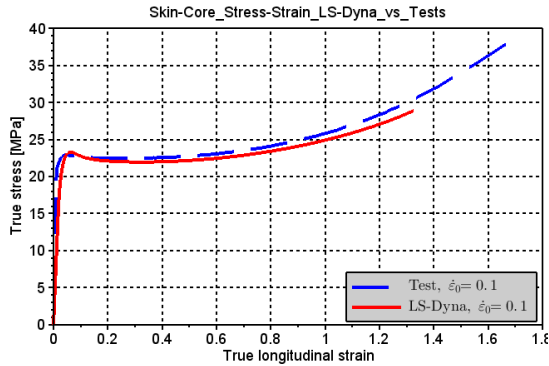
Figure 5.27: Stress-strain, $\dot{\varepsilon}_0 = 10^{-1}s^{-1}$ Figure 5.28: Force-displacement, $\dot{\varepsilon}_0 = 10^{-1}s^{-1}$
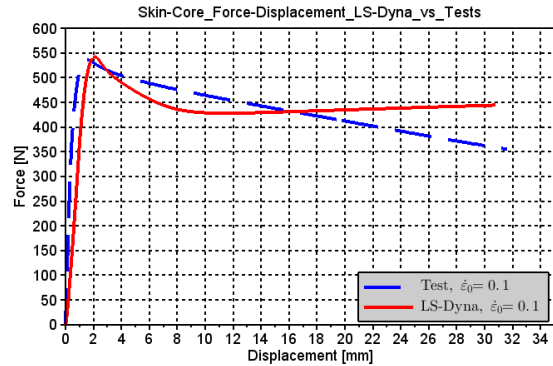
The results from the numerical simulations at various strain rates suggests that the material model is able to quite accurately capture the strain rate dependency of the material, also at an initial material thickness of 2mm. The material model is almost spot on when describing the material's stress-strain state, until the point of re-hardening. Because adiabatic heating is not taken into account in the material model, the model is not able to capture the lower hardening that occurs at higher strain rates.

5.1.5   4mm full cross section simmulations

The results from the numerical simulations of uniaxile tensile dog-bone specimens with an initial plate thickness of 4mm, will be described and discussed in this section. Because the material model was mainly calibrated using specimens with a thickness of 3mm at an initial strain rate of $10^{-2}s^{-1}$, the simulation at this strain rate will be most thoroughly examined. Simulations were also performed at initial strain rates of $10^{-1}s^{-1}$ and $10^{-3}s^{-1}$ in order to determine the material model's ability to describe the material's strain rate dependency when the material had a different initial thickness.

The table below displays the tests which has been compared with the simulation at the corresponding strain rate. The material cards used for the 4mm thick simulations skin and core were the same as those used for the simulations of the 2mm and 3mm thick simulations. The material parameters for the core is shown in Table 4.2 and material parameters for the skin in Table 4.3.

Table 5.5: Tests used to compare LS-Dyna simulations with 4mm thick full uniaxile tensile tests

Test	Initial strain rate, $\dot{\varepsilon}_0$ [s^{-1}]	Remarks
PP1-T4-F-V1-3	10^{-1}	
PP1-T4-F-V2-3	10^{-2}	Baseline test
PP1-T4-F-V3-1	10^{-3}	

84

Stress-strain relation

The material model's ability to recreate the materials stress-strain is shown in Figure 5.29. The simulation does not match the test very well, it overestimates the peak stress and it has a very different shape. The results from the material tests, see Figure 3.25, showed that the average peak stress decreased with an increase in the material's plate thickness. As the material cards used for the simulations of the 4mm thick specimens are calibrated based on test results from the 3mm thick specimens, it is expected that the simulation overestimates the peak stress.
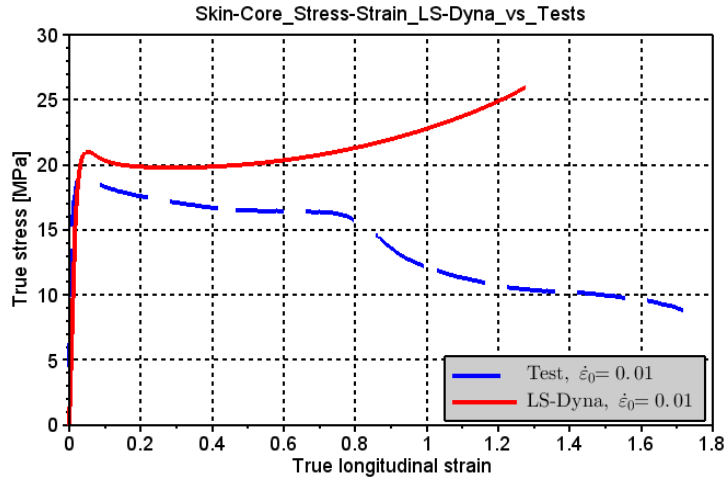
Figure 5.29: True stress-strain of 4mm thick specimen, LS-Dyna simulation compared with test

Figure 5.29 displays a severe misfit between the stress-strain relation of the simulation and the test. The test never re-hardens and at a longitudinal strain of about 0.8, it exhibit a sudden drop before it continues to soften. The sudden drop in the stress has been described in Section 3.1.3, and is due to the onset of fracture in the test specimen's core which was not possible to capture when calculating the effective cross section area. If the true stress of the 4mm test specimens were calculated, then it is very possible that the slope of the tests' hardening curves would be lower than that of the simulation, as the damage propagated faster for the 4mm thick specimens than the specimens that were 3mm thick, as seen in Figure 3.26.

Force-displacement relation

The force-displacement curve of the simulation and test for a 4mm thick specimen is shown in Figure 5.30. The drop in the test's force is due to the onset of fracture in the test specimen's core, which then spreads to the test specimen's skin. The misfit between the force-displacement curvatures are primarily due to the material model's inability to accurately describe the material's stress-strain relation, as the stress is overestimated, and because fracture is not included.
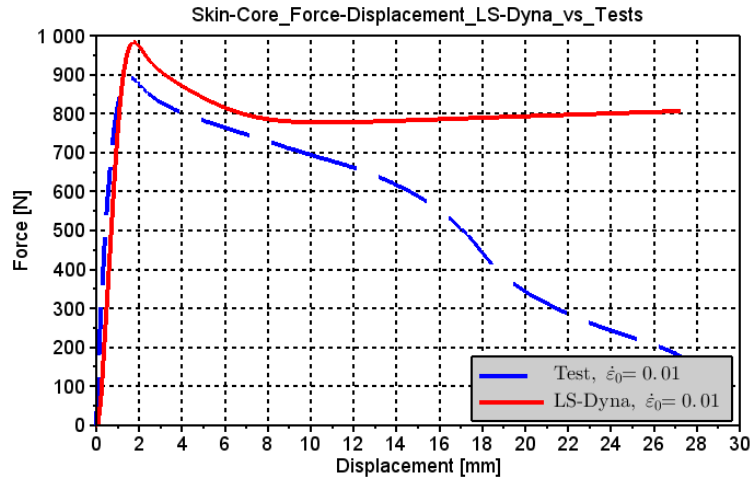
Figure 5.30: Force-displacement of 4mm thick specimen, LS-Dyna simulation compared with test

Strain rate dependency

The stress-strain curves of the simulations and tests at the initial strain rates of $10^{-1}s^{-1}$ and $10^{-3}s^{-1}$ is shown in Figure 5.31 and Figure 5.32, respectively. The test at the highest strain rate, Figure 5.31, differs from the other strain rates by not having a sudden drop, which is due to fracture. Because such a drop is not present, the numerical model is more able to describe the stress-strain relation at this strain rate, even though it overestimates the peak stress and hardening. The overestimate of the peak stress, is most likely due to the same reasons as for the simulation performed at a strain rate of $10^{-2}s^{-1}$, and the lower hardening is due to adiabatic heating not included in the model. In Figure 5.32, the test behaves very different from the simulation. The numerical model does not capture the softening and fracture, which occurs in the test.
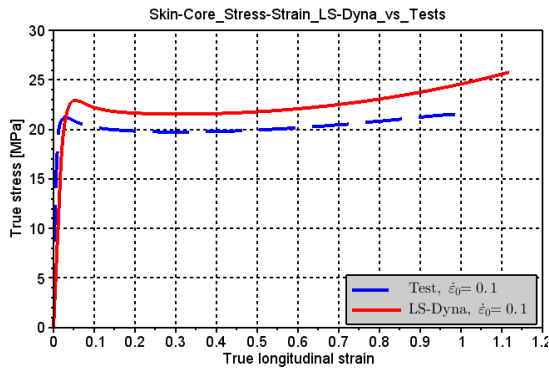
Figure 5.31: Stress-strain, $\dot{\varepsilon}_0 = 10^{-1}s^{-1}$
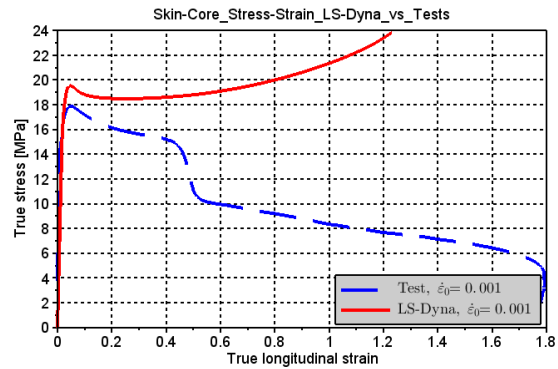
Figure 5.32: Stress-strain, $\dot{\varepsilon}_0 = 10^{-3}s^{-1}$

The distance between the peak stress of the simulation and the tests is approximately 2MPa

for all strain rates with the 4mm thick specimens. In Figure 5.33, the stress curve of the LS-Dyna simulations are reduced by 2MPa. The figure helps to illustrate that the strain rate sensitive parameters, $\dot{p}_0$ and C, have been calibrated correctly to enable the material model to accurately determine the increase/decrease in the material's yield stress due to the strain rate also if the material has been molded with a 4mm thickness. Because adiabatic heating is not taken into account in the material model, the hardening will not be reduced at higher strain rates. This correlates well with the observations made in Section 3.1.3, that the main difference between the material properties of the specimens with different molding thickness, is the yield stress and the damage propagation.
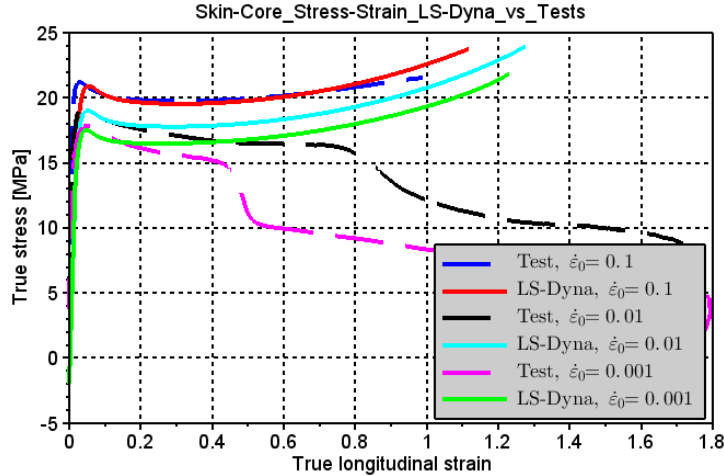
Figure 5.33: Stress-strain, 4mm simulations vs. tests where LS-Dyna stress is reduced by 2MPa

5.1.6   Stability of numerical model

In order to determine the robustness of the numerical model, a sensitivity analysis was performed. The analysis was performed using the geometry of the 3mm specimen with reduced cross section. In the sensitivity analysis the element formulation, mass scaling and mesh size was analyzed. As previously mentioned, a reduced element formulation was used in the simulations of the uniaxial test specimens. The reduced integration formulation is fast, but hourglass modes may occur [14]. The other possible numerical integration formulations are full and full with selective reduced integration. The full integration formulation is very accurate, but it is more time consuming. A full selective reduced integration formulation does not exhibit hourglass deformation modes, but it may display shear locking because it is overly stiff [22]. Figure 5.34 shows the effect of changing the element formulation..

Element formulation	ELFORM No. in LS-Dyna	CPU time
Full integration	3	5h 36min 17s
Full-SR integration	2	2h 22min 32s
Reduced integration (*Reference model*)	1	0h 23min 4s
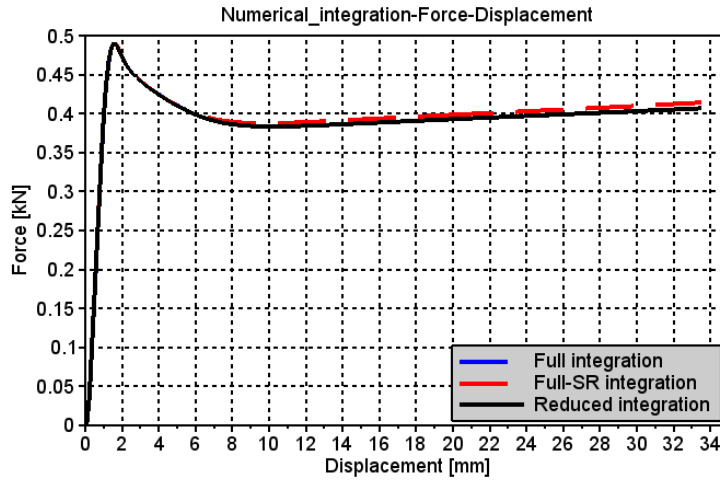
Figure 5.34: Sensitivity analyses of the numerical integration formulation of the uniaxial tensile test

As expected, Figure 5.34 shows that as the neck forms, there is a small difference between the reduced integration, and the full and selective reduced integration schemes. This is because of the triaxiality of the stresses as the neck forms, which the reduced integration does not capture. The figure indicates that this effect is very small, thus the reduced integration scheme gives an accurate enough representation at a much lower CPU cost.

Refining the mesh will in most cases increase the accuracy, but at a certain point the increase in accuracy will be very small compared to the increase in CPU cost. Mass scaling can be done in order to increase the time step. If mass scaling does not affect the result, then it can be done safely to reduce the CPU time. An analysis where every element was split into eight elements, and the mass scaling was reduced by a factor of 10^2, was performed in order to verify that the model had reached convergence. Figure 5.35 displays that the affect of mass scaling and mesh refinement is negligible. The table below shows the CPU cost from mesh refining and reduced mass scaling.

	Mass scaling	Number of elements	CPU time
Refined mesh	10^4	15552	4h 38min 1s
Reduced mass scaling	10^2	1944	4h 30min 13s
Reference model	10^4	1944	0h 23min 4s
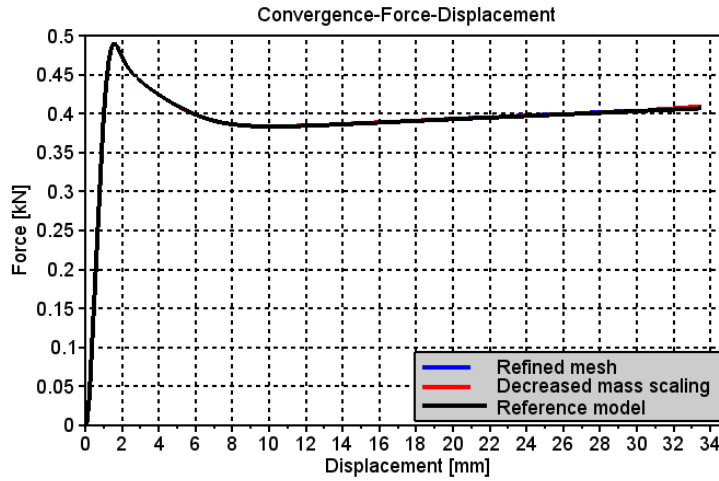
Figure 5.35: Sensitivity analyses of the convergence of the uniaxial tensile test

5.1.7 Remarks

A few summarizing remarks from the uniaxile tensile simulations has been listed below.

- The material cards were calibrated based on the test results from the 3mm thick specimens

- The simulations performed fit the tests with a plate thickness of 3mm well. It recreates the local behavior, given by the stress-strain curve, almost perfectly, but is unable to recreate the global behavior, which can be seen from the force-displacement curves, with similar accuracy due to an inability to describe the retraction ratio precisely.

  - This inability is also valid for the 2mm and 4mm test specimens
  - Calibrating the material model for the anisotropic behavior may help to increase the accuracy to describe the transverse strains

- The strain rate sensitive parameters, $\dot{p}_0$ and C, are calibrated so that they are able to fit the strain rate sensitivity of the material well for all material thicknesses.

  - The material model is not able to reproduce increased softening at higher strain rates because adiabatic heating is not included in the material model.

- The material testing showed that the damage propagation increased with an increased specimen thickness, which explains the mismatch in the stress-strain relation of the simulation and test for the 2mm thick specimens, as the material cards are calibrated based on the test results from the 3mm thick specimens.

  - If the true stress history of the 4mm test specimens was correctly calculated, then the comparison of the simulation and the tests would most likely have shown a steeper re-hardening slope in the simulation than in the test

- The uniaxial tensile test results in Section 3.1.3 indicated that the yield stress decreased with increasing molding thickness, which explains why the simulation does not accurately determines the peak stress of the 4mm thick tests.

5.2 Uniaxile compression test simulations

Compression test simulations were performed in order to verify that the Raghava parameter, α, had been correctly calibrated and that the material model was able to accurately describe the material in compression.

Compression tests were only performed for the 3mm plate, and the tests were performed at three different initial strain rates. The numerical model of the uniaxial compression specimens consisted of a skin part and a core part, similar to the uniaxial tensile tests. The material parameters used for the skin and the core is shown Table 4.3 and Table 4.2, respectively.

5.2.1 Modeling

Similar to the uniaxile tensile tests, the compression tests had three symmetry planes. Two of these symmetry planes were used when modeling the specimen. The symmetry planes used when modeling can be seen in Figure 5.36.
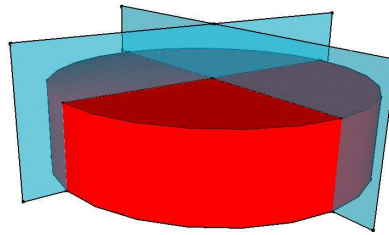
Figure 5.36: Symmetry planes used for modeling uniaxial compression specimen

The skin-core of the cylinder was modeled using the same method as described for the uniaxile tensile specimens. Two parts were created, one for the core layer and one for the skin layer. The thickness of each of these layers were corresponding to what was observed and determined in Section 3.5. The geometry and mesh of the cylinder parts were created in Abaqus and then transformed to an LS-Dyna compatible k-file using a MatLab script, which is available in Appendix B.2.3. The two parts were then imported to LS-Dyna where the adjacent nodes of the two parts were merged. The resulting geometry and mesh of the material cylinder can be seen in Figure 5.37. The number of elements and the element type of each part is listed in the table below.

Table 5.6: Key data for uniaxial compression models

Part	Element type	No. of Elements
Core	Solid	2808
Skin	Solid	864
Model total	Solid	3672

(a) Front

(b) Back

(c) Top
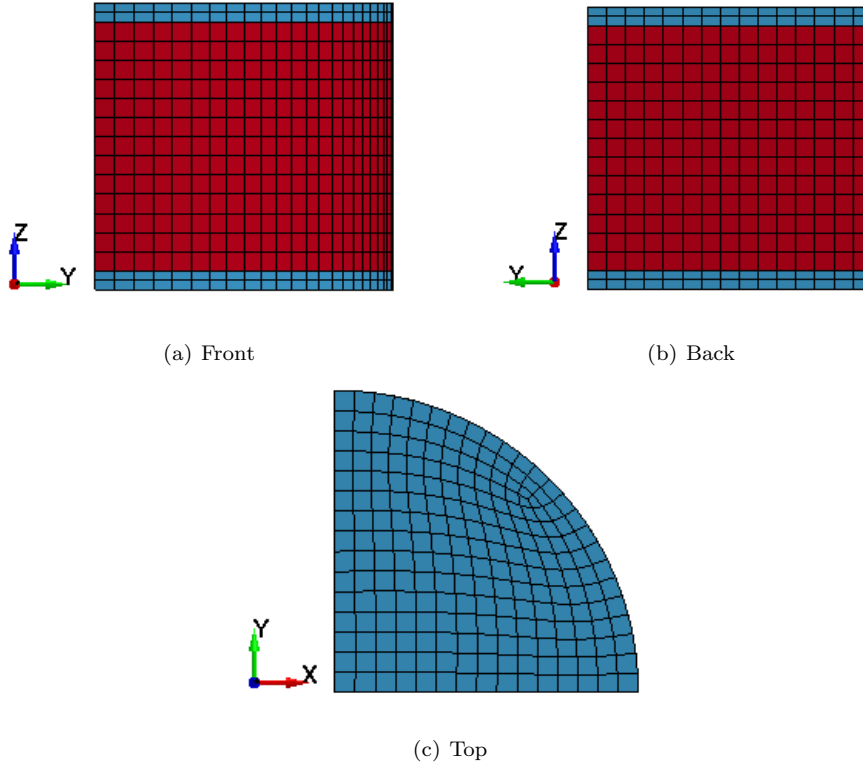
Figure 5.37: Discretization of the cylinder used for uniaxial compression test simulation

The contact between the loading machine and the specimen was modeled by including two rigid solid elements to represent the contact surface between the top and bottom of the material and the loading machine. This can be seen in Figure 5.38. Prior to testing, the top and bottom of the specimen was lubricated with grease in order to reduce the friction between the loading machine and the test specimen. Even though this was done, there was still some friction present, as the specimen barreled during testing. Previous experience with similar lubricant suggests a friction number of 0.05 [25]. The symmetry axes normal to the X-direction was modeled by restraining displacements and rotations in the X-direction. Similarly was the symmetry plane normal to the Y-axes modeled by restraining rotations and displacements in the Y-direction. The compression process itself was modeled by prescribing the top rigid element with a constant velocity in the Z-direction, equal to the constant velocity of it's corresponding test.
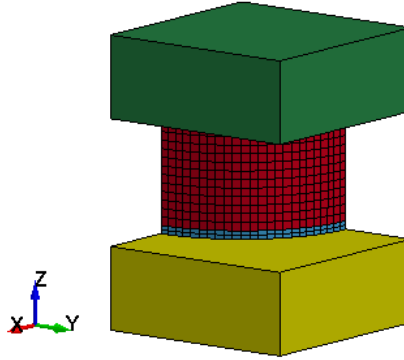
Figure 5.38: Numerical model of uniaxile compression specimen including contact surface

The numerical integration formulation used for the uniaxial compression analysis was a full selective reduced integration scheme. A full selective reduced integration scheme was chosen due to the barreling of the specimen, which would result in a non-uniform stress state.

5.2.2 Simulation results

In this section the results from the numerical simulations will be presented and discussed. The simulations were performed at initial strain rates of $10^{-3}s^{-1}$, $10^{-2}s^{-1}$ and $10^{-1}s^{-1}$. The tests used for comparison is listed in the table below.

Table 5.7: Uniaxial compression tests used to compare with the LS-Dyna simulation results

Test	Initial strain rate, $\dot{\varepsilon}_0$
PP1-2-2	$10^{-3}s^{-1}$
PP1-4-2	$10^{-2}s^{-1}$
PP1-2-5	$10^{-1}s^{-1}$

Result from simulation with $\dot{\varepsilon}_0 = 10^{-3}\text{s}^{-1}$

Figure 5.39 and Figure 5.40 displays the stress-strain and the force-displacement, respectively of the LS-Dyna simulation and a test performed at a corresponding strain rate. From Figure 5.39 it is evident that the material model is able to capture the material's local behavior well in compression, but that the global behavior, represented by the force-displacement curve in Figure 5.40, is less accurately represented.

92
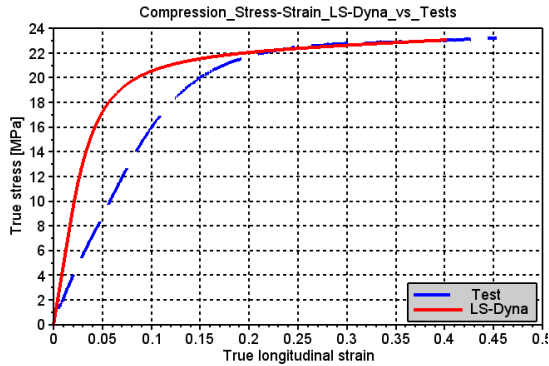
Figure 5.39: Compression stress-strain
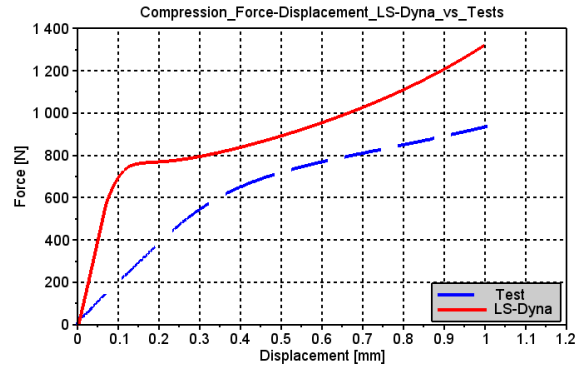
Figure 5.40: Compression force-displacement

Figure 5.39 shows that the elastic slope of the test is significantly lower than the simulation's. It was also observed in the results for the uniaxial compression tests is Section 3.2.3 that the compression tests had a significantly lower slope in the elastic region than the uniaxile tensile tests. As previously mentioned, possible reasons for this is a not completely leveled contact surface, which results in a lower slope, or it may be due to cavities in the loading machine which closes, thus affecting the stiffness, when the machine is used in compression.

Apart from the elastic region, the material model is able to describe the material's behavior in compression relatively well. A misfit between the numerical simulation and the tests were expected, as the model is calibrated for a uniaxial tensile stress state. The material model will have the same stress-strain curve in compression and in tension, the only difference is the Raghava parameter, α, which sets the yield surface to be a certain ratio higher in compression than in tension. Unless the material behaves exactly the same in compression and in tension, the model will not be able to describe a uniaxial compression state with the same accuracy.

Results from simulations at $\dot{\varepsilon}_0 = 10^{-2}\text{s}^{-1}$ and $\dot{\varepsilon}_0 = 10^{-1}\text{s}^{-1}$

The simulation results from the uniaxial compression tests performed at initial strain rates of $10^{-2}s^{-1}$ and $10^{-1}s^{-1}$ is shown in Figure 5.41 and Figure 5.42 , respectively.

93

(a) Stress-strain (b) Force-displacement
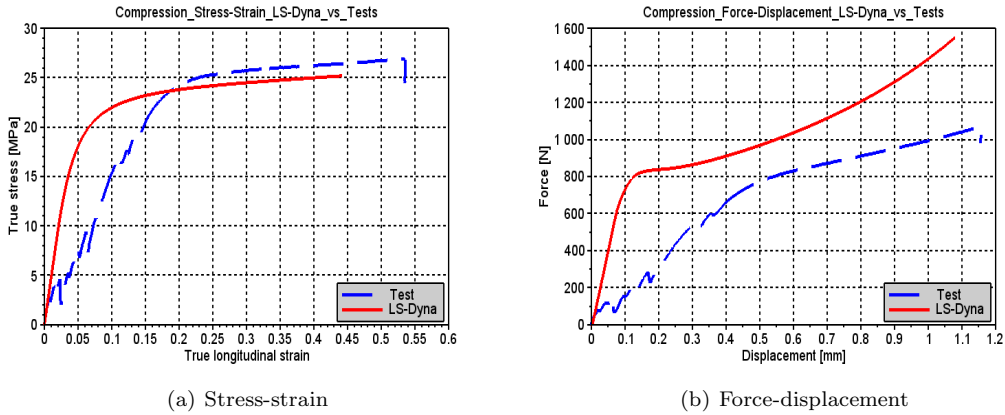
Figure 5.41: Simulation results from uniaxial compression, $\dot{\varepsilon}_0 = 10^{-2}s^{-1}$

(a) Stress-strain (b) Force-displacement
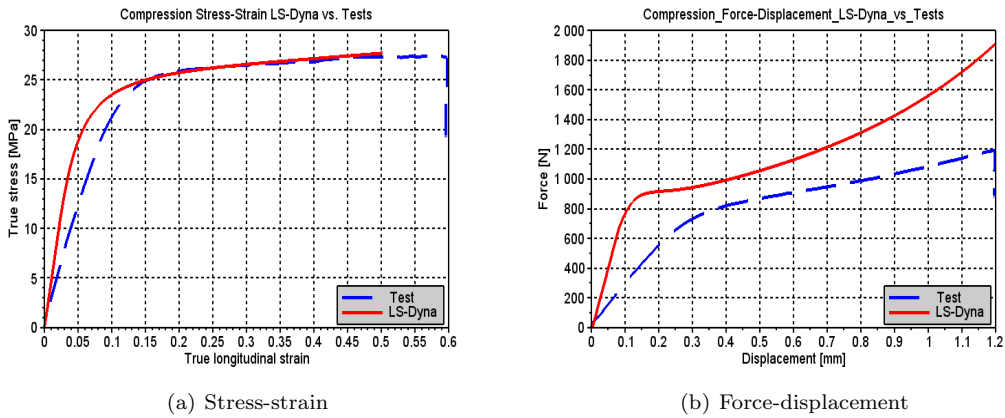
Figure 5.42: Simulation results from uniaxial compression, $\dot{\varepsilon}_0 = 10^{-1}s^{-1}$

Figure 5.41 and Figure 5.42 indicates that the strain rate dependent parameters, $\dot{p}_0$ and C, is well calibrated to also fit the variation in the material's yield stress at different velocities when the material is loaded in compression. Because the compression tests were stopped after a displacement of 1mm, the simulations did not deviate from the tests due to adiabatic heating at higher velocities, which occurred for the uniaxile tensile simulations.

Volumetric strain relation

The volumetric strain of the tests and the simulations are shown in Figure 5.43. The numerical simulation predicts a slight decrease in the material volume in the elastic region, due to a 3D Hooke's law with Poisson ratio less than 0.5, and it predicts an increased material volume in the plastic region. The majority of the tests indicate incompressibility or a slight decrease in the material's volume. As the simulation overestimates the volumetric strain, it will overestimate the global response of

the material, which explains the deviation in the force-displacement behavior of the tests and the simulations.
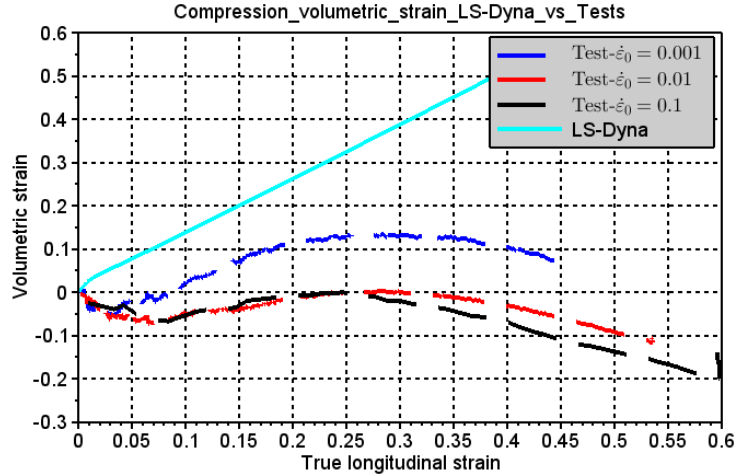
Figure 5.43: Volumetric strain for uniaxile compression

The mismatch of the volumetric strain of the tests and simulations is partly due to the flow potential used in the material model. The flow potential, defined in Eq. 2.15, which is based on the Raghava yield surface, will always yield a positive volumetric strain. The flow potential has the same shape as the Raghava yield surface in Figure 2.5. The direction of the plastic flow will always be perpendicular to the yield surface, and the horizontal part of this will of course be positive for all stress states [8]. Because the total stress invariant, $\mathbf{I}_1$, is positive for all stress states, the material model will always exhibit a positive volumetric strain.

5.2.3   Remarks

Some of the key findings from the numerical simulations of the uniaxile compression tests have been listed below.

- The material model describes the local behavior of the material well.
  - Has a very different slope in the elastic region, but this is most likely due to irregularities in the machine or test specimen
  - The Raghava parameter, α has been correctly calibrated
  - The general shape fits well, and it estimates the yield plateau accurately
  - The strain rate dependency fits well
- The global behavior is less accurately described.
  - Overestimates the force
  - Most likely due to an inability to describe the material's volumetric strain

- The volumetric strain does not fit well because of the plastic flow potential used in the material model.

  - The material model predicts a positive plastic volumetric strain for all stress states

5.3   Notched specimen simulation

The notched specimens are intended to be used for validation, in particular of the material model's fracture formulation. The results from the notched specimen simulations will indicate how accurate the material model is at determining the material's fracture, but also how well it is able to reproduce a more complex loading scenario than the uniaxial tests represent. As previously mentioned, the calibration of the fracture was performed by PhD. David Morin. In this section, the results from the numerical simulations performed for the notched specimens will be presented and compared with the test results.

The material cards for the notched specimens skin and core is seen in Table 4.3 and Table 4.2, respectively. In addition to this, the material cards of the notched specimens also included material fracture parameters, seen in Table 5.8. These parameters were the same for both the skin and core.

Table 5.8: Material cards' fracture parameters

Parameter	Abbreviation	Value	Unit
Initial damage	D_I	0.00	N/A
Critical damage	D_c	0.60	N/A

Notched specimens were milled using three different geometries, and they were tested with and without a reduced cross section at three different velocities. Tests were only performed using specimens milled from 3mm thick plates.

5.3.1   Modeling

The numerical models were created by PhD. David Morin, who is currently a researcher at NTNU. The models' geometry and boundary conditions will in this section be described briefly. Three different geometries were used during testing, and numerical simulations for each of these three geometries were created. The geometrical measures of each geometry is seen in Figure 3.37. The boundary conditions used for each of these geometries are the same, and will be described in general. The images will primarily be of the N3 geometry, unless otherwise is noted.

Two symmetry planes were used when modeling the notched specimens. One symmetry plane normal to the Z-axis and one plane normal to the X-axis, as seen in Figure 5.44. To represent the symmetry plane normal to the Z-axis, displacement in the Z-direction was restrained, similarly was the displacement in the X-direction restrained in order to represent the symmetry plane normal to the X-axis.
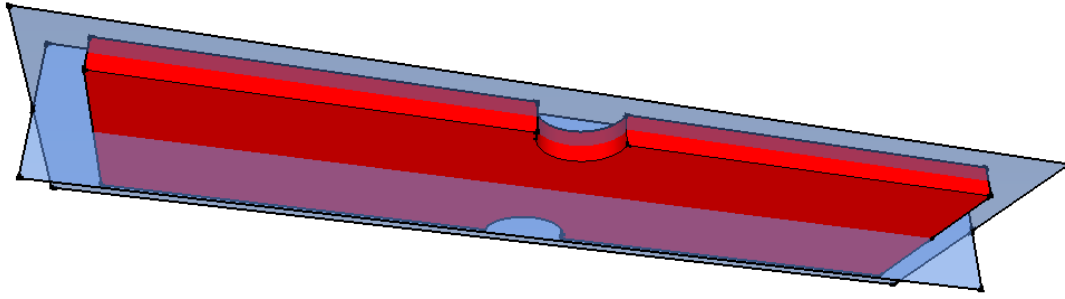
Figure 5.44: Symmetry planes used for notched specimen simulations

The ends of the specimens were clamped during testing, this restrained the specimens' ability to deform in this region. This was included in the model by omitting the clamped regions of the specimen in the model. The transition from where the clamp stopped to the point where the test specimen begins, is modeled by restraining each end of the specimen from displacements in the X- and Z-direction. During testing one clamp was held still while the other moved with a constant velocity. This is modeled by restraining displacements in the Y-direction for the left end, and prescribing the right end a constant velocity in the Y-direction.

The numerical integration scheme used for the simulations was the reduced integration, which is element formulation 1 in LS-Dyna. The reduced integration allows the numerical model to deform smoothly.

Numerical models with reduced cross section

The geometry and mesh of the numerical models with a reduced cross section, used for the simulations is shown in Figure 5.45 to Figure 5.47.

(a) Plane view   (b) Section view   (c) Through thickness view
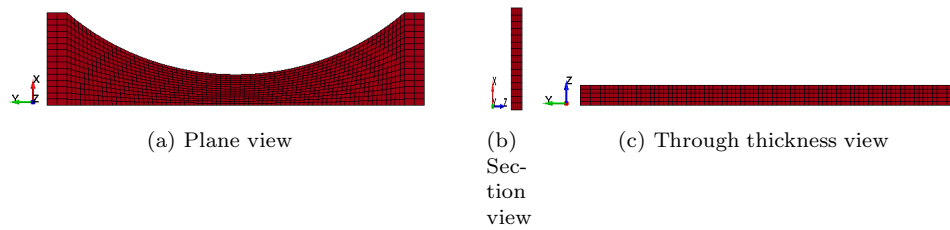
Figure 5.45: Numerical model of reduced N1 geometry

(a) Plane view   (b) Section view   (c) Through thickness view
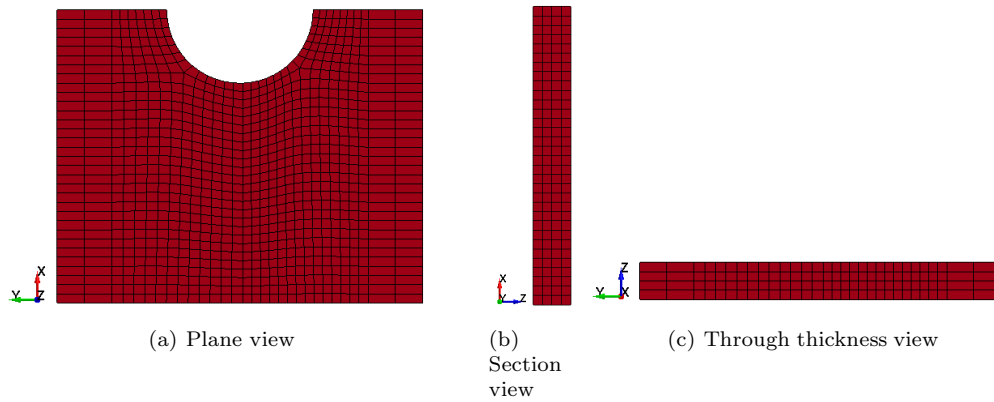
Figure 5.46: Numerical model of reduced N2 geometry

(a) Plane view   (b) Section view   (c) Through thickness view
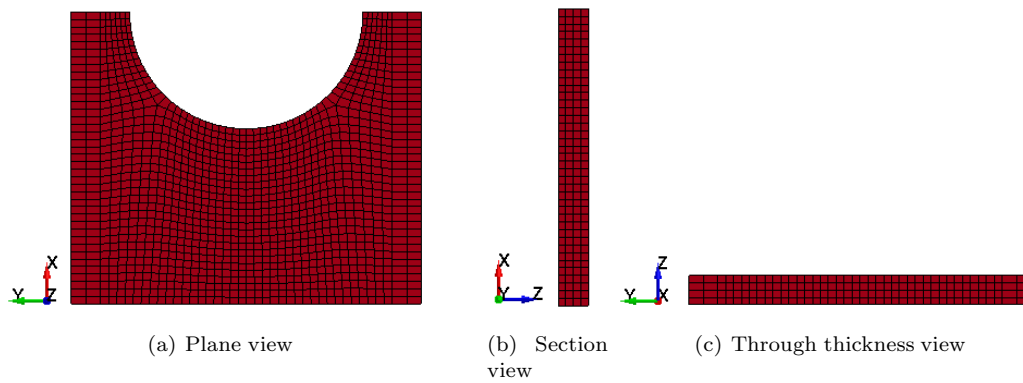
Figure 5.47: Numerical model of reduced N3 geometry

Numerical models with full cross section

The geometry and mesh of the numerical models with a full cross section, used for the simulations is shown in Figure 5.48 to Figure 5.50.

(a) Plane view   (b) Section view   (c) Through thickness view
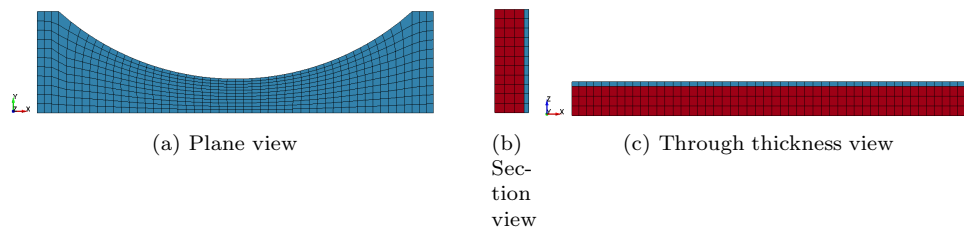
Figure 5.48: Numerical model of full N1 geometry

(a) Plane view
(b) Section view
(c) Through thickness view
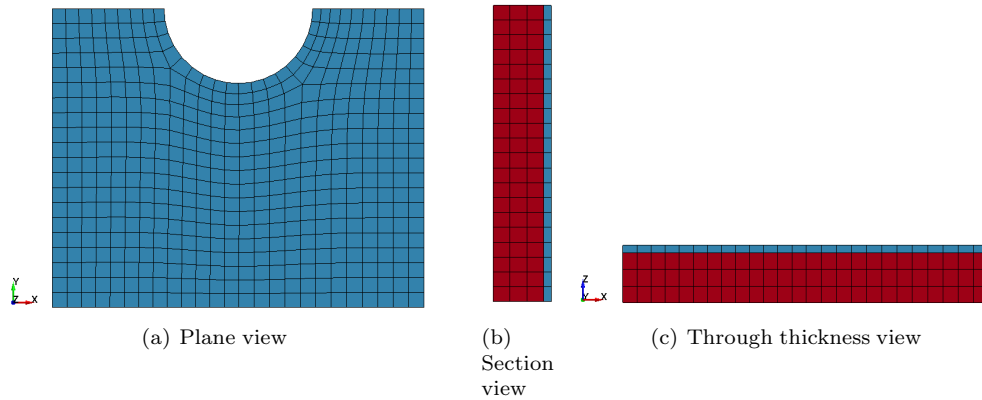
Figure 5.49: Numerical model of full N2 geometry

(a) Plane view
(b) Section view
(c) Through thickness view
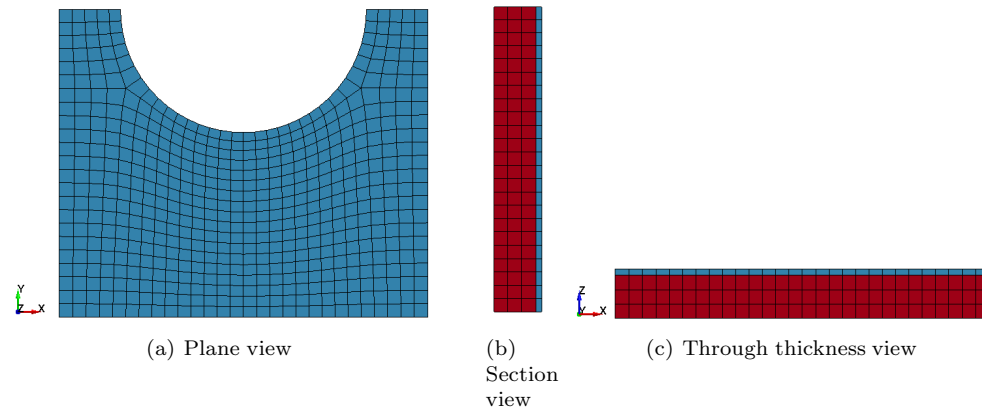
Figure 5.50: Numerical model of full N3 geometry

5.3.2 Reduced cross section simulation results

The numerical models ability to describe the behavior of the material, in particular the fracture, will be described in this section. The accuracy of the numerical simulations is based on it's ability to recreate the force-displacement relation of the experimental tests.

Simulation results from N1-geometry

The results from the numerical simulations using the N1-geometry is shown in Figure 5.51. Simulations were run using velocities of 0.2mm/s, 2.0mm/s and 20.0mm/s. The misfit in the elastic region between the test and the simulation at the highest velocity, Figure 5.51 c), is very possibly due to the acceleration of the loading machine. The duration and shape of the loading machine's acceleration, in Figure 3.42, match the non-linear shape in the elastic region well. The simulation gives a good estimate of the tests' peak force, and the model's ability to recreate the shape of the tests' force-displacement curves is in accordance with what was observed in Section 5.1 for the uniaxial tensile specimens.

The material model fail to predict the fracture of the N1-geometry accurately. It overestimates the fracture at all velocities, and it differs more from the tests at increasing velocities. As the velocities increase, the tests' displacement at fracture becomes lower, the material model fails to capture this effect.

(a) v=0.20 mm/s

(b) v=2.00 mm/s

(c) v=20.00 mm/s
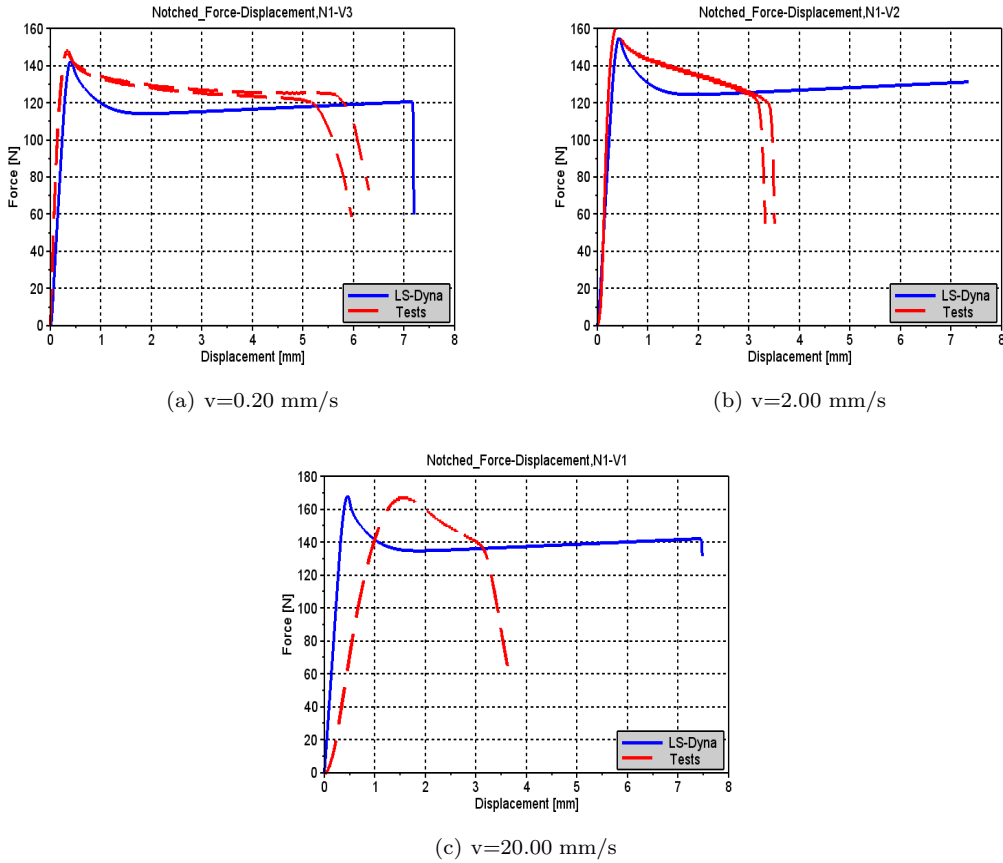
Figure 5.51: Notched simulation results using N1 geometry with reduced cross section

Simulation results from N2- and N3-geometry

Figure 5.52 and Figure 5.53 displays the results from the N2- and N3-geometry respectively. The N2 simulations in Figure 5.52 were done at velocities of 0.1mm/s, 1.0mm/s and 10.0mm/s, and the N3 simulations were done at velocities of 0.15mm/s, 1.50mm/s and 15.0mm/s. The model gives a good estimation of the fracture for all velocities using both geometries, which indicates that the material model can accurately predict the fracture of the material.

The simulations describe the shape of the force-displacement curves well. The elastic region of the simulation differs from the tests at the highest velocity, which is most likely due to the acceleration of the loading machine during the tests. The simulation was able to very accurately predict the

peak force of the N1-geometry. This geometry does not have a very strong curvature, which yields less triaxiality, than for the N2 and N3 geometries, which have stronger curvature. The smaller the radius of the notch is, the larger is the triaxiality [18]. The misfit of the peak force may be due to an incorrectly determined Raghava parameter, α. The triaxiality of the N2 and N3 geometry will make these specimens more affected by the material model's compression sensitivity.
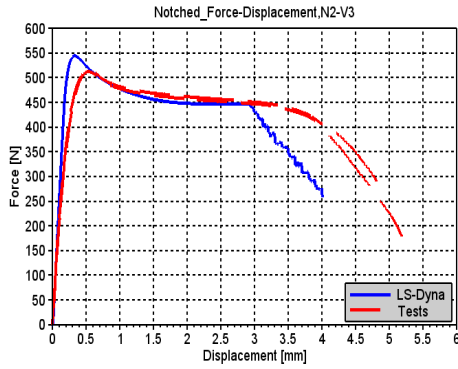
(a) v=0.10 mm/s
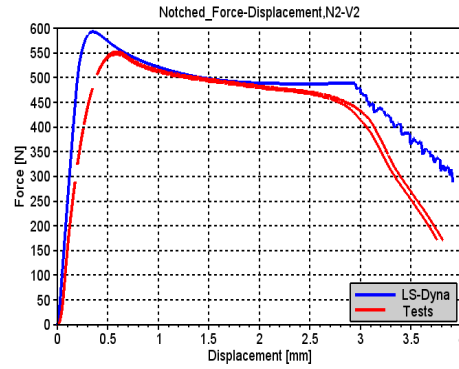
(b) v=1.00 mm/s
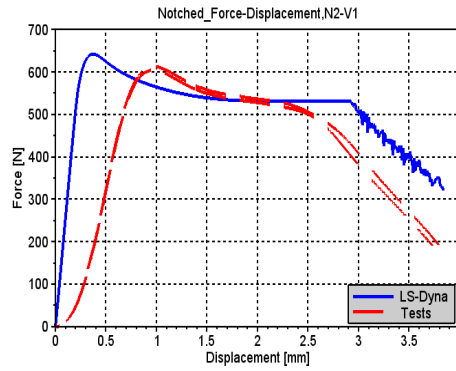
(c) v=10.00 mm/s

Figure 5.52: Notched simulation results using N2 geometry with reduced cross section

(a) v=0.15 mm/s

(b) v=1.50 mm/s

(c) v=15.00 mm/s
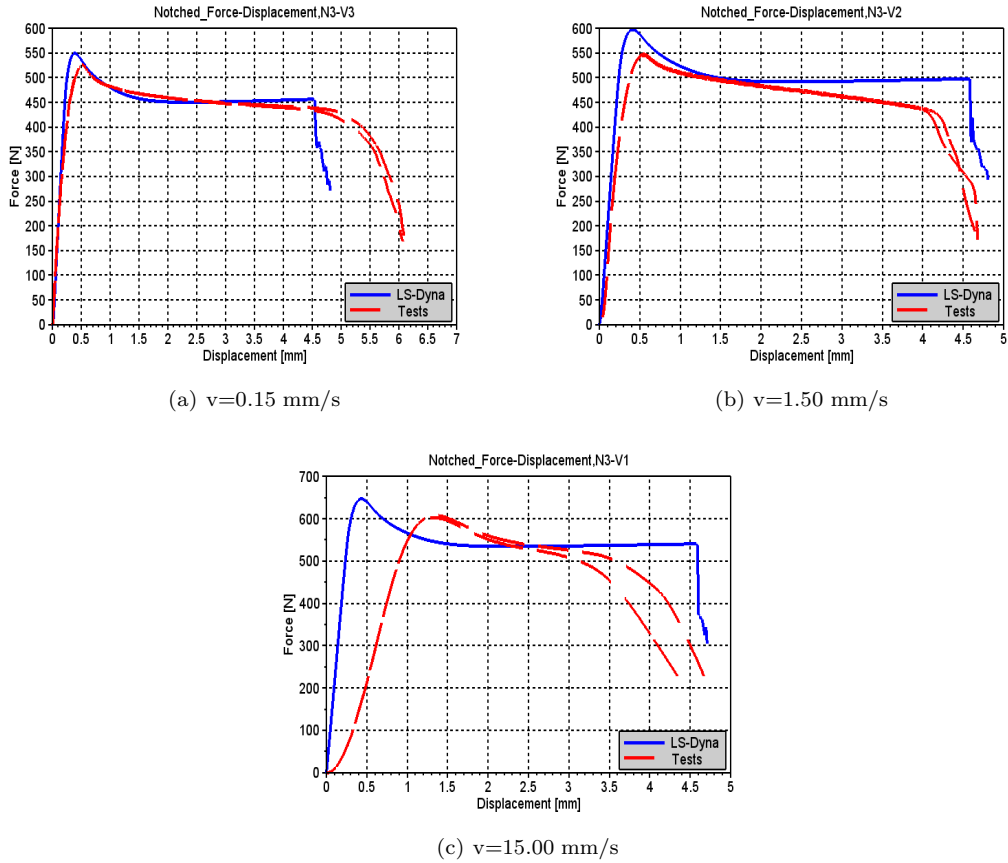
Figure 5.53: Notched simulation results using N3 geometry with reduced cross section

The results from the material tests in Chapter 3, suggested that the damage increased with increasing strain rates. The material's temperature increase due to strain rate has not been included in the material model, and as a result, the material's damage do not vary with the material's strain rate. If this was included, then an increased strain rate would lead to an increase in temperature, which would lead to an increased damage propagation. As the material's fracture is determined by when the material reaches a certain damage level, D_c, the material will fracture earlier with an increased strain rate, which corresponds better with what has been observed in the material tests.

The numerical model determined the fracture well for the geometries with the small notch radiuses, N2 and N3, but it was more inaccurate when determining the fracture of the N1, which has a much larger notch radius. The reason for this is possibly because the N1 geometry forms a large neck before fracturing, and the fracture will be very sensitive to any deformations or irregularities in this region [16]. The N2 and N3 geometries will have a much more localized fracture due to a smaller notch radius, and will therefore be less sensitive to material irregularities.

5.3.3 Full cross section simulation results

Simulation results from N1-geometry

The results from the numerical simulations of the N1 geometry with a full cross section is shown in Figure 5.54. The results from the numerical simulation with the full cross section is similar to what was obtained with the simulations of the reduced cross section in Section 5.3.2; the simulation gives a good estimation of the peak force at all velocities, at the lowest velocity the fracture location is well predicted, but because adiabatic heating is not included in the material model, the reduction in displacement at fracture with an increased velocity is not captured. Because this geometry has a very large radius, the effect of triaxiality is small, and as seen in the figure, the simulations ability to capture the shape of the force-displacement curve is very similar to that observed from the uniaxial tensile simulations at high strain rates.

(a) v=0.20 mm/s

(b) v=2.00 mm/s

(c) v=20.00 mm/s
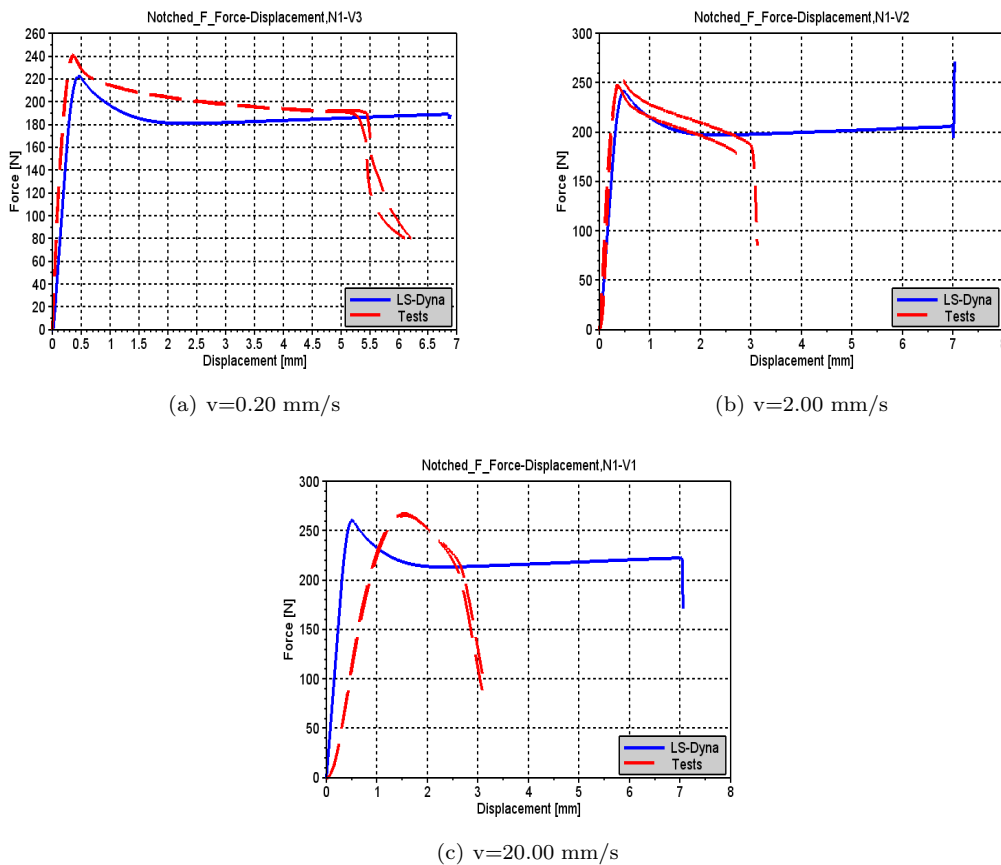
Figure 5.54: Notched simulation results using N1 geometry with full cross section

Simulation results from N2- and N3-geometry

Figure 5.55 and Figure 5.56, is depicting the simulation results of the N2 and N3 geometry, respectively. The figures shows that the simulations ability to estimate the fracture is similar to what

was observed for the simulations with a similar geometry, but with a reduced cross section, seen in Figure 5.52 and Figure 5.53. The fracture estimation of the notched geometries N2 and N3 is better than for the N1 geometry. As previously mentioned, this is possibly due to the forming of the neck. For the N2 and N3 geometries, the neck is much more localized than for the N1 geometry where the neck is larger and the fracture is more prone to imperfections in the specimen. It is also possible that the critical damage parameter, D_c, and the Raghava parameter, α, is too high. If the critical damage was decreased, then fracture would occur earlier, which would correlate better with the results of the N1 geometry. A decrease in the α-parameter would increase the displacement at fracture, as the equivalent stress in the biaxial stress state would be lower, which would have a larger effect on simulation results of the N2 and N3 geometries.

(a) v=0.10 mm/s

(b) v=1.00 mm/s

(c) v=10.00 mm/s
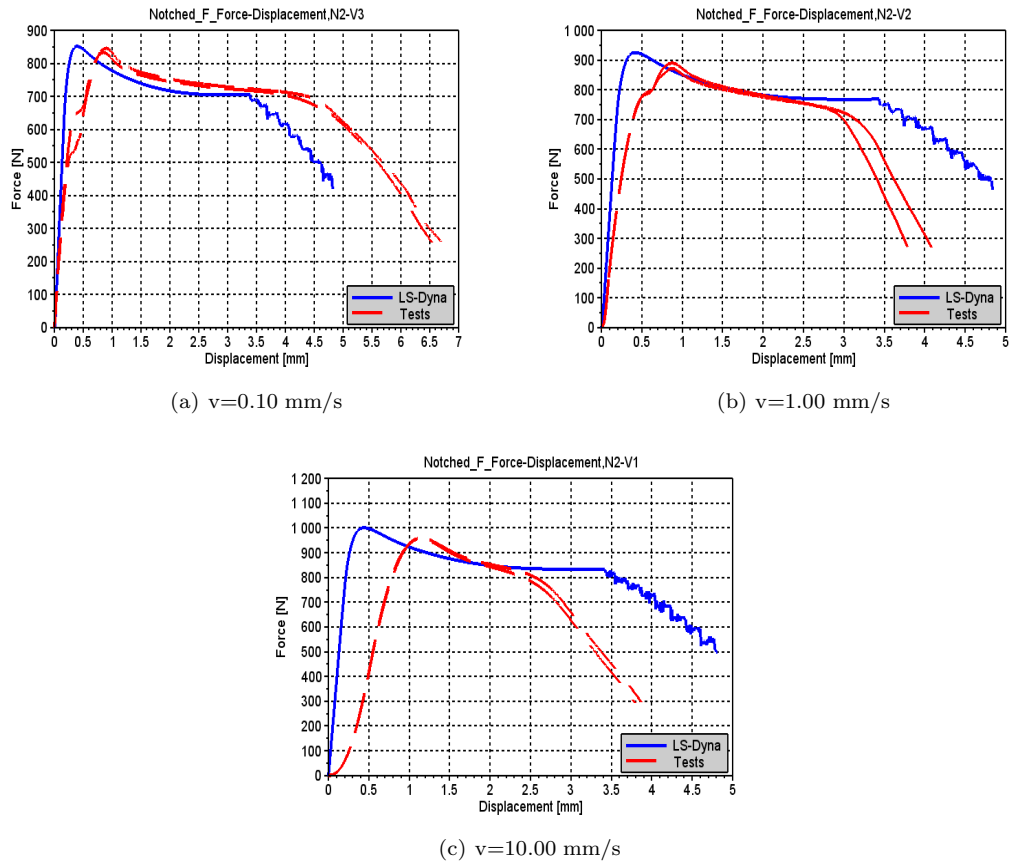
Figure 5.55: Notched simulation results using N2 geometry with full cross section

104

(a) v=0.15 mm/s

(b) v=1.50 mm/s

(c) v=15.00 mm/s
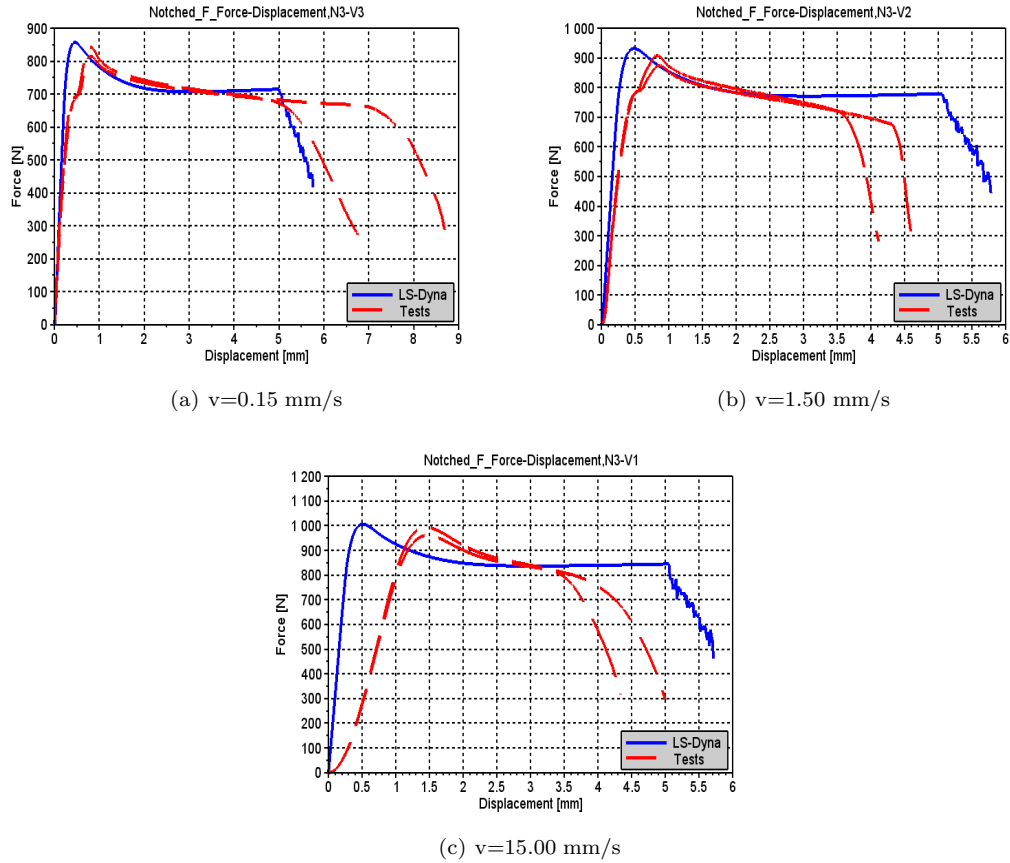
Figure 5.56: Notched simulation results using N3 geometry with full cross section

The simulations with a reduced geometry tended to overestimate the peak force, but the peak force of the simulations of the N2 and N3 geometries with a full cross section gives a very good match with the tests. This is possibly because the $\alpha-$value was determined using a plate without any thickness reductions. In section 3.1.3 it was observed that the specimens with a reduced cross section had a higher damage propagation than the full specimen, which may be due to the amount of particles. Thus, the $\alpha-$value of the skin may be different from that of the core, and the $\alpha-$value chosen gives the best approximation for specimens with a full cross section.

The fit of the force-displacement curves is in accordance with what has been previously observed, and is relatively good. The tests at the two lowest strain rates have a small notch in the curve prior to the peak force. It is uncertain why this occurs for these tests, as it was not observed for the specimens with a reduced cross section. It may be linked to the difference in the yield stress of the materials skin and core, but in Figure 5.55a), it is seen that it occurs at a force of about 500N, while the peak force is about 850N, a difference that is much larger than the calibrated difference in yield stress. It is therefore hard to make any conclusions on this point.

5.3.4 Notched simulations' sensitivity to α

The value of the α-parameter will affect the result of the notched geometries much more than the uniaxial tensile tests, as the specimens notch will create a biaxial stress state. The value of the α-parameter will therefore affect the simulations behavior, and it's influence on the simulation results will increase with a decrease in the specimens notch radius, as the effect of triaxiality increases as the radius decreases. The affect of varying the α-parameter with ± 0.1 for the simulation of the N2 geometry is seen in Figure 5.57.
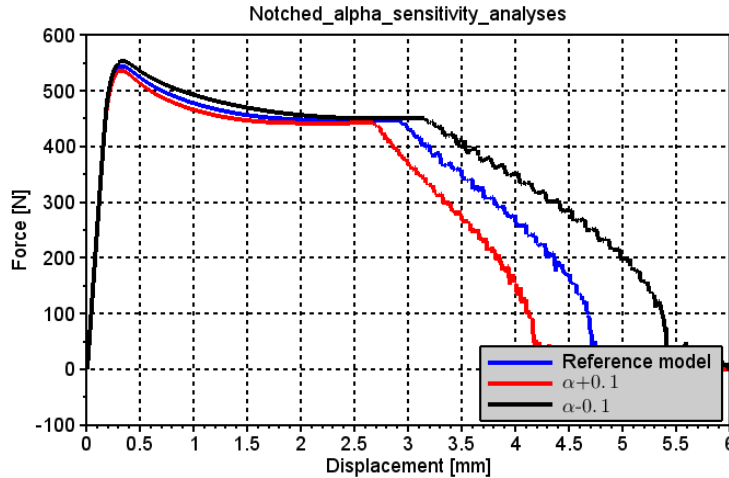
Figure 5.57: Notched geometry N2's sensitivity to α

Figure 5.57 indicate that the α-parameter does not have a significant influence on the peak force of the simulation results with notched geometry but an increased α-value will increase the triaxial stresses, which will increase the material's damage. Thus the simulation results may be improved by lowering the value of both the D_c- and the α-parameter.

5.3.5 Remarks

Some key findings from the simulations of the notched specimens is listed below.

- The shape and fracture of the simulated notched geometries N2 and N3 fit the tests well
  - Somewhat inaccurate determining the peak force for the reduced cross section, which may be linked to the $\alpha-$value
- Overestimates the displacement at fracture for the N1-geometry
  - The larger radius of the N1 notch enables the material to have a larger neck. A possibility for the inaccuracy to determine fracture is that the larger neck makes this geometry more sensitive to material an geometrical irregularities.
  - A decrease in the value of the D_c parameter will yield a better correlation

– If the D_c is lowered, the α-parameter must also be decreased to increase the displacement at fracture for the notched specimens which are more affected by triaxiality

- The inability to recreate the force-displacement curves of the tests with the N1 geometry is maybe due to the material softening that occurs at higher strain rates

  – Adiabatic heating is not included in the material model, thus this effect will not be captured
  – Similar observations were made for the uniaxial tensile tests

- The peak force of the notch specimens is not very sensitive to variations in the α-parameter, but the fracture is.

- Reduced displacement at fracture with increasing velocities is not captured by the material model.

  – This is most likely due to adiabatic heating not being included in the material model

5.4 Drop tower simulation

The purpose of the drop tower simulation is to be a final validation of the material models ability to accurately describe a complex loading scenario. The problem with the simulation was that it required a contact description of the contact between the puncher and the test specimen, as well as between the test specimen and the steel ring, that the specimen was placed upon. As will later be presented in the simulation results, the simulation results are very sensitive to the friction ratio in the contact regions. An LS-Dyna simulation of the tests presented in Section 3.4 was performed, but the results were not good. The poor results were possibly linked to the complexity of the boundary conditions that two contact surfaces represented, and because the specimen was simply supported. It was therefore decided to use the data from previous drop tower tests using the same material. In these tests the test specimen was clamped, which greatly reduced the complexity of the boundary conditions.

5.4.1 Test setup

The data used for comparison was provided by Prof. Arild Clausen, while the specifics of the test setup was from the master thesis of Kjetil Vange [3, 23]. The previous drop tower simulations had a somewhat different setup than the tests presented in Section 3.4. The main difference was that the test specimen was clamped, and that the light opening of the clamped region had a diameter of 70mm. The light opening is what controls how much of the test specimen is allowed to deform. Figure 5.58 displays where the test specimen was placed during testing. Before the test commenced, the lower ring in the figure was moved up, so that the test specimen was clamped between the ring and the plate.
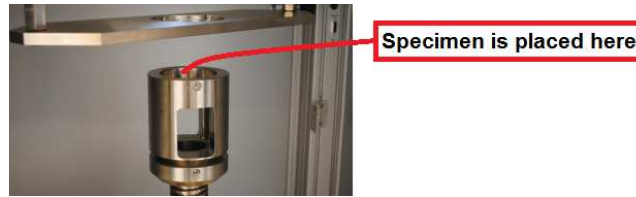
Figure 5.58: Location of specimen during drop tower testing [23]

The geometry of some of the key parts involved in the test is shown in the table below.

Part	Geometry	Dimension [mm]	Remark
Test specimen	Quadratic	100X100X3	
Light opening	circular	70	Diameter of the opening
Steel puncher	Cylinder with hemisphere	20	Diameter of hemisphere

The table below shows the mass, m, impact velocity, v, and kinetic energy at impact, E_k of the puncher during the tests.

Mass, m	Velocity, v	Kinetic energy, E_k
5.045 kg	4.41 m/s	49J
5.045 kg	4.77 m/s	57J

5.4.2 Modeling

A numerical model was initially created in LS-Dyna, but possible due to contact problems, the simulation results were very noisy. The results displayed a physically incorrect behavior, as the force peaked at the moment the puncher hit the plate. Abaqus, which is a finite element analysis software very similar to LS-Dyna, was therefor used for the numerical simulation and modeling.

The numerical model was created by Ph.D. David Morin at NTNU [16]. In this section the model and it's boundary conditions will be described.

Test specimen

Two symmetry planes were used for the numerical model of the test specimen, as indicated by Figure 5.59. Because only the part of the test specimen that was located in the light opening had the possibility to deform, this was the only part of the specimen that was modeled, as indicated in the figure by part that has a solid dark color.
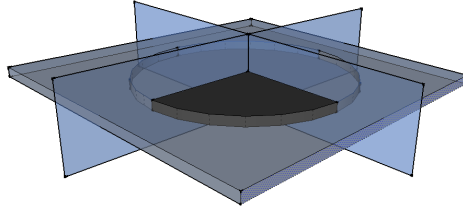
Figure 5.59: Illustration of the test specimen modeled

To ensure that the simulation was allowed to deform in a proper manner, boundary conditions were introduced. The curved rim of the specimen was fixed during testing, thus the nodal displacements and rotations in this region were restrained. The model's symmetry plane perpendicular to the x-direction was modeled by restraining the displacements in the x-direction and the rotations in the y- and z-direction. Similarly was the symmetry plane perpendicular to the z-direction modeled by restraining displacements in the z-direction and the rotations in the x- and y-direction.

The specimen's skin and core was modeled by separating the plate into sets, one set for the core and one for the skin. In Figure 5.60 the boundaries of these sets are indicated. The figure also displays the mesh of the numerical model. The region of the plate that was impacted by the puncher had a much finer mesh than the remaining plate. This was done to allow the impacted region to deform in the most natural manner, and to reduce the CPU time by not meshing the whole plate with the same mesh size.

(a) Top view

(b) Symmetry plane view

(c) Rim view
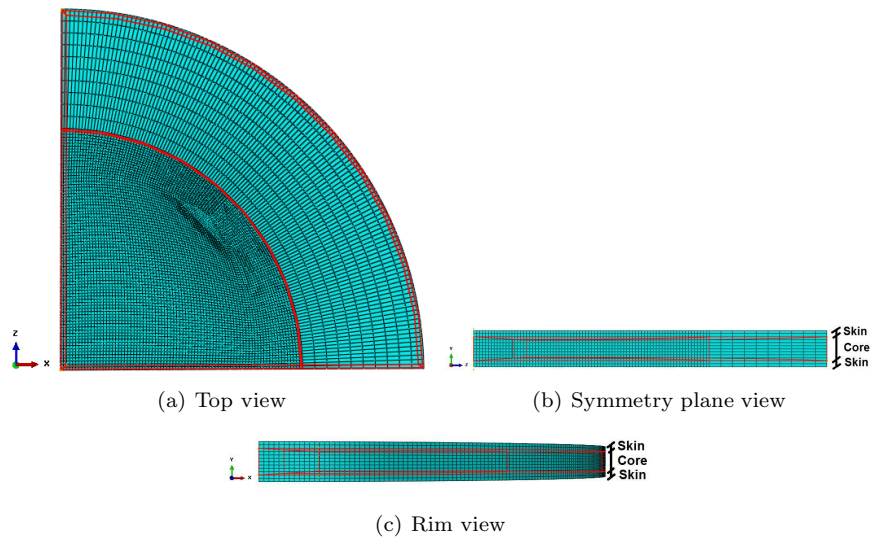
Figure 5.60: Geometry and mesh of the drop tower test specimen part

The elements used for the plate is in Abaqus called C3D8R. C3D8 means that the elements are eight noded cubic 3D elements, and the R means that the numerical integration is solved using a

reduced integration scheme.

Puncher

The puncher was created as a rigid shell. No symmetry planes were used when modeling the puncher, but only the hemisphere and 20mm of the cylinder was modeled. The geometry of the puncher is shown in Figure 5.61. Because the puncher is rigid, meshing was not necessary.

(a) Side view   (b) Bottom view
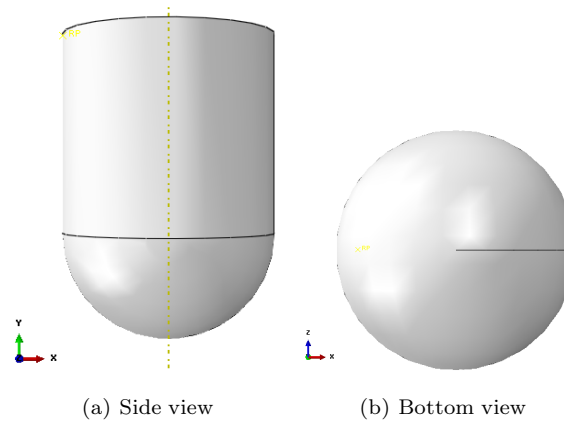
Figure 5.61: Geometry of the drop tower puncher part

To model that the puncher's displacement was only perpendicular to the test specimen, the puncher's displacements in the x- and z-direction and the rotations in all directions were constrained. The impact energy was modeled by only applying a quarter of the puncher's mass to the puncher in the numerical model, as only a quarter of the test specimen was modeled, and to prescribe the puncher with an initial velocity that was equal to what was observed in the tests.

Assembled model

The puncher and plate part was assembled to the final model seen in Figure 5.62. The tangential contact between the plate and the puncher was friction formulated with a penalty value. In the master thesis of Kjetil Vange, he suggested that a friction coefficient of 0.2-0.3 yielded good results for the drop tower simulations performed with the same material, thus the friction coefficient is set to 0.3 in the simulations [23]. The normal contact was formulated as "hard".
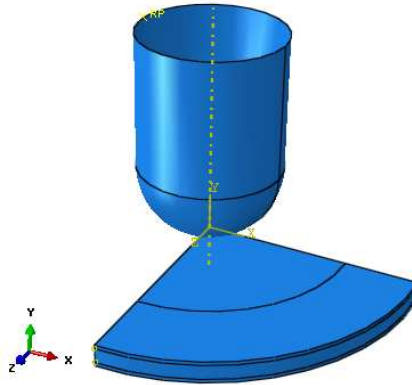
Figure 5.62: Assembled drop tower model

The simulations are solved using what is in Abaqus called a "Dynamic Explicit" integration technique. The dynamic explicit technique solves the equations of motion in time using a forward Euler algorithm [10]. In the forward Euler algorithm, the unknown values in the next time step is solved using the values in the current time step [2].

5.4.3 Simulation results

The results from the numerical simulations are shown in Figure 5.63 and Figure 5.64. Figure 5.63 displays the results from the simulation performed with an impact velocity of 4.41 m/s. At this velocity the simulation failed, but the test did not. The simulation describes the drop tower test well, the peak force and the general shape of the simulation and test display a good correlation. The main difference between the test and the simulation is that the experimental test results are stiffer than the simulation, which is seen from the difference it the two curves' slope.

(a) Force-displacement

(b) Force-time
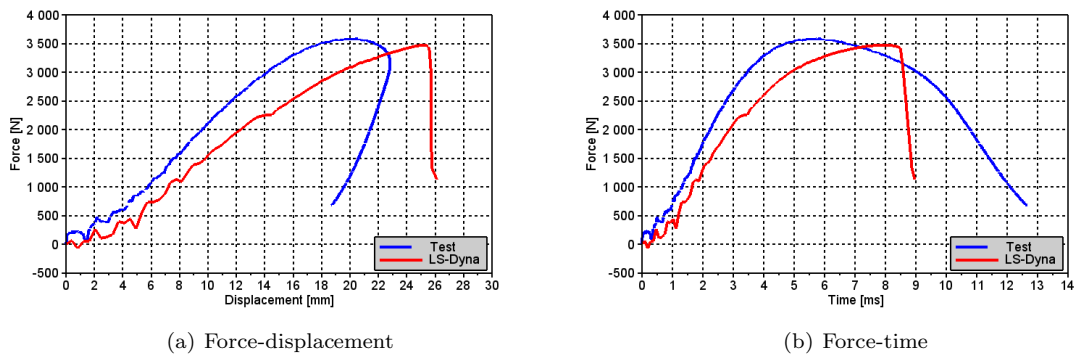
Figure 5.63: Drop tower simulation performed with an impact velocity of 4.41 m/s

Figure 5.64 displays the results of the drop tower simulation performed with an impact velocity of 4.77 m/s. At this velocity the simulation fractured, while the test results indicate that fracture was not obtained. It is seen in the figure, that the difference between the peak force of the simulation

and the test is larger in Figure 5.64 than in Figure 5.63. This increased difference may be due to the fracture, it is very possible that if the simulation was allowed to deform further, it would have reached approximately the same peak force as the test. The correlation between the slope of the force-displacement curves at this impact velocity is very similar to that of the simulation performed at a lower velocity, in Figure 5.63.

(a) Force-displacement

(b) Force-time
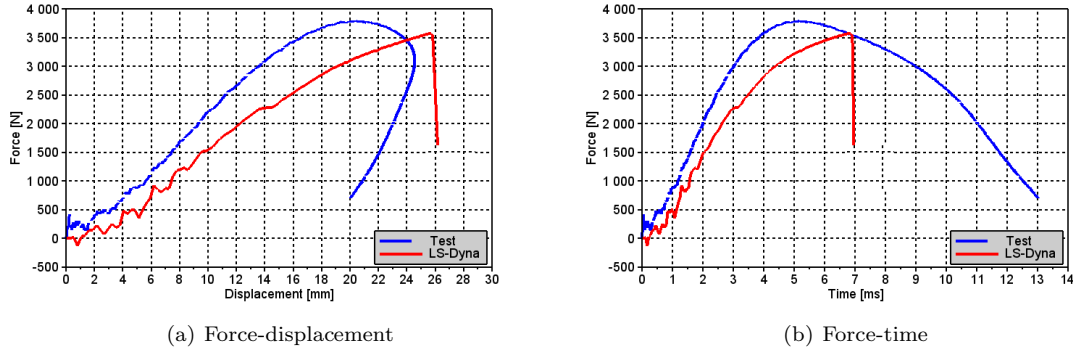
Figure 5.64: Drop tower simulation performed with an impact velocity of 4.77 m/s^2

Evaluation

As previously mentioned, the test results in Kjetil Vange's master thesis showed that the material fractured at an impact energy of 60J, but not at 55J, which means that the material's capacity, with this particular material thickness and test setup, is somewhere between 55J and 60J. The simulations was in this thesis performed with an impact energy of 49J and 57J, the peak force of the simulation performed with an impact energy of 49J was very close to that of the test, which could indicate that the fracture energy of the simulations, with the specific parameters, are very close to 49J. Due to a limited amount time, it was not performed a sensitivity analyses to determine the fracture energy of the simulations. The increase in the peak force of the simulation performed at a velocity of 4.41 m/s to a velocity of 4.71 m/s is very small, which is because fracture occurred for both simulations. It was shown in Figure 5.57 in Section 5.3.4, that the material model's fracture in a biaxial stress state is very sensitive to variations in the α-parameter. The drop tower tests creates a very triaxial stress state, thus a slight decrease in the α-parameter may yield a better correlation between the simulation and the test, as fracture will occur at a later time.

The difference in the slope of the simulation and the test is possibly because the value of the material model's Young modulus is too low. In the current material parameters, the Young modulus of the skin layer is 550MPa while it is 950MPa for the core. An increase in the Young modulus of the skin layer would decrease the difference in the slope of the drop tower tests and simulations. Visco-elasticity is not included in the material model. Although it is very uncertain how strain rate dependent the material is in the elastic region, as no tests were performed to measure this effect, it is very possible that including visco-elasticity in the material model will give a better correlation between the simulations and the tests, due to the high strain rates imposed to the test specimen in the drop tower tests.

As previously mentioned, the effect of the friction coefficient, μ, between the test specimen and

112

the puncher at impact is significant, but the value of this coefficient is very uncertain. The value of the friction coefficient is not determined analytically nor through testing, but to the value which has previously proven to give a good fit [23]. Figure 5.65 displays how the simulation results are varying with different values of the friction coefficient for the simulation performed with an impact energy of 59J. The figure shows that the deformation and peak force depends highly on the value of the friction coefficient.
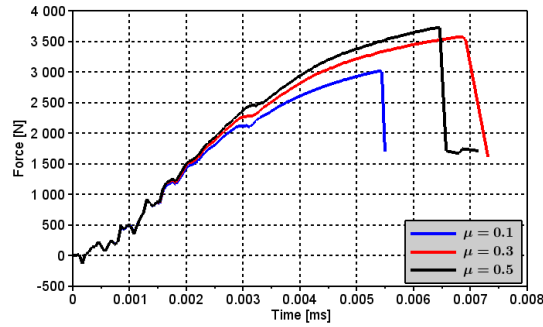
Figure 5.65: Effect of the friction coefficient, μ, on the simulation results

Though there are rooms for improvement, the material model and the calibrated material parameters have proven to be able to reproduce the complex load case of the drop tower test quite accurately. Small adjustments of the material parameters and including a viscoelastic behavior, would most likely make the simulations correlate better with the tests.

Chapter 6

Conclusions

The results from the uniaxial tensile tests showed a very complex material behavior. The material was strain rate dependent, anisotropic, displayed a non-linear plastic hardening/softening behavior and a large scatter in it's results. In addition to this, the material displayed different material properties through it's thickness. Even though the material is very complex, the material model and the suggested method for separating the numerical models into a skin part and a core part has proved to give quite accurate results.

Reducing the cross section of some of the specimens provided some very interesting results. By comparing the incompressible stress-strain history of the specimens with a full and a reduced cross section, it was seen that the shape of the curves was very similar, but that the curve of the specimens with a full cross section was situated somewhat higher than the specimens with a reduced cross section. The incompressible stress-strain curve omits any effects that may be due to damage, thus this relation indicated that the only difference between the specimens with a full cross section and with a reduced cross section was the yield stress, and also possibly the damage propagation. The specimens damage history showed that the reduced specimens had a higher damage propagation than the specimens with a full cross section, thus the main difference in the material's properties at different layers was the damage propagation and the yield stress. This difference is possibly linked to the amount of particles present in the different material layers, and/or the material's temperature gradient during molding.

The test specimens milled from different plate thicknesses showed that the material's yield stress decreased as the specimens' thickness increased for the specimens with a full cross section, while the same thing was not observed for the specimens with a reduced cross section. This correlated very well with the observations made for the tests damage history, which showed that the specimens with a full cross section had a much larger increase in it's damage propagation at increasing plate thicknesses than the specimens with a reduced cross section. One possibility for the decrease in the yield stress of the specimens with a full cross section is the amount of particles present in the skin layer. An increased amount of particles present in the skin layer will create an initial damage that reduces the yield stress and increases the damage propagation.

Multiple methods were applied to determine the thickness of the material's layers. The only method that gave any consistency was using an optical microscope, where a sudden color transition from the materials surface to it's core in the materials deformed state was measured to approximately 0.2

mm. Neither the hardness tests nor the SEM gave any indication of the thickness of the material layers, but the hardness test did confirm that the material's hardness varied through the thickness.

MatPrePost is an easy to use calibration tool which yields well calibrated material parameters if used properly. The main problem with the current MatPrePost is that it is user dependent. The user must personally choose the location of the material's yield stress, which highly influences the calibration of the material parameters. The material parameters linked to the material's hardening/softening were not well calibrated and required further optimization to ensure a good fit between the material model and the tests.

It has in this thesis been suggested a method to calibrate a second material card for the materials skin layer, that mainly affects the yield stress and plastic dilatation of the material. This second material card requires tests to be performed with and without a reduction in the material specimens thickness. The methods are simple and easy to use, and gave a good correlation between the numerical simulations and the tests.

The plastic potential function used in the material model is not able to reproduce the increase in the material's retraction ratio at large strains, which results in an overestimation of the force. The function is also not able to describe the plastic volumetric strains in compression, as it describes an increase in the specimens volume, while the material tests indicates incompressibility or a small decrease in volume when the material is loaded in compression.

The simulation results showed that there was a substantial difference between the results from the simulations, which consisted of material cards calibrated based on the test results from the 3mm thick specimens, and the material tests with a molding thickness of 2mm and 4mm. This difference was, as also indicated by the test results, linked to the material's damage propagation and yield stress at different molding thicknesses. Thus material cards should be calibrated for every molding thickness.

The simulation results of the drop tower tests and notched specimens shows that the material model and it's parameters can describe the material behavior very well, as it captured the general shape of these tests' force history quite accurately. The simulation results of the notched specimens suggested that a decrease in the current value of the material parameters α and D_c, would yield a better correlation between the simulations and the experimental tests. This was again indicated by the simulation results of the drop tower tests, which fractured even though the tests did not. Including more mechanical effects, such as adiabatic heating and visco-elasticity will also most likely improve the accuracy of the material model.

Recommendations for further work:

To better understand how the material properties are varying at different material layers, material tests with multiple reductions should be performed. These tests would give a good indication of whether the material properties are varying linearly, non-linearly, or by layers. Thus it will be possible to create a more accurate representation of the material behavior.

If the material properties does prove to be varying by layers, the thickness of these layers should be further investigated. Multiple hardness tests, testing the material's hardness along it's thickness with very small steps will possibly give a good indication of the thickness of these layers. To be able to create an accurate numerical model, the number of layers, and it's thickness must be known.

The accuracy of the material model would be further increased if adiabatic heating and visco-elasticity were included. To account for adiabatic heating, the temperature should be measured during the material testing. Creep and relaxation tests should also be performed in order to determine the material's visco-elastic dependency.

More information regarding the material molding process should be obtained. Currently the information provided concerning the molding process is very limited. It is very likely that the material properties is highly dependent on the molding process, thus information regarding the amount of particles in the material, injection rate, number of nozzles and injection points, and the molds surface temperature should be provided. This would enable the creation of a simulation of the molding process, which may give a better understanding of the material's temperature gradient during molding, and the distribution of particles.

The current plastic potential function is not able to reproduce the material's retraction ratio and the material's plastic volumetric strain in compression. A plastic potential function that is able to reproduce the material's longitudinal and transverse strain history, would greatly increase the accuracy of the material model.

Chapter 7

Bibliography

[1] Lexan 940. Polymer additives and mechanical properties, December 2003.

[2] Jan B. Aarseth. Compendium: TKT4140: Numerical Methods with Computer Laboratorium, 2012.

[3] Prof. Arild Holm Clausen. Professor, NTNU. Personal correspondence.

[4] Hamid Daiyan. *Experimental and Numerical Investigation of the Mechanical Response of Injection Moulded Polypropylene Materials.* PhD thesis, University of Oslo, 2011.

[5] PhD. Egil Fagerholt. Postdoctoral fellow, NTNU.

[6] Mitsuyoshi Fujiyama and Tetsuo Wakino. Structure of skin layer in injection-molded polypropylene. *Journal of applied polymer science*, pages 29–49, 1988.

[7] Tokyo Institute of Technology H. Ito. Injection molded semicrystalline polymers: Structure development and modeling. *Concise encyclopedia of the mechanical properties of materials*, pages 229–235, 2007.

[8] Odd Sture Hopperstad and Tore Boervik. Compendium: TKT4135: Material Mechanics, 2013.

[9] Martin Thuve Hovden. Tests and numerical simulations of polymer components. Master thesis, Norwegian University of Science and Technology, NTNU, June 2010.

[10] Abaqus Inc. Overview of abaqus/explicit. Presentation, 2005.

[11] M. Bäker J. Rösler, H. Harders. *Mechanical Behaviour of Engineering Materials: Metals, Ceramics, Polymers, and Composites.* Springer-Verlag Berlin Heidelberg, 2001.

[12] M.R. Kantz, H.D. Newman Jr., and F.H. Stigale. The Skin-Core Morphology and Structure-Property Relationships in Injection-Molded Polypropylene. *JOURNAL OF APPLIED POLYMER SCIENCE*, 16:1249–1260, 1972.

[13] J. Karger-Kocsis and K. Friedrich. Effect of skin-core morphology on fatigue crack propagation in injection moulded polyprpylene homopolymer. *Int J Fatigue*, 3:161–168, 1989.

[14] Kjell Magne Mathisen. Lecture 11: Numerical integration. Lecture in TKT4197 Non-Linear Finite Element Method, 2012.

[15] Kjell Magne Mathisen. Lecture 7: Solution of the dynamic equilibrium equations by explicit direct integration. Lecture in TKT4197 Non-Linear Finite Element Method, 2012.

[16] PhD. David Morin. Personal correspondence, 2014.

[17] M.Sc. Yann Claude Ngueveu. Graduate, TOYOTA-Europe.

[18] Anne Serine Ognedal. *Large-Deformation Behavior of Thermoplastics at Various Stress States.* PhD thesis, NTNU, 2012.

[19] OpenOpt. http://openopt.org/ralg, January 2014.

[20] Ram Raghava, Robert M. Caddell, and Gregory S.Y. Yeh. The macroscopic yield behaviour of polymers. *Journal of Materials Science*, 8:225–232, 1973.

[21] SIMLab, NTNU. Theory manual: SIMLab Polymers Model, 2013.

[22] DYNAMORE Tobias Erhart. Review of solid element formulations in ls-dyna: Properties, limits, advantages, disadvanteges, 2011.

[23] Kjetil Vange. Validation of material model for polypropylene (PP). Master thesis, Norwegian University of Science and Technology, NTNU, June 2012.

[24] Wikipedia. Injection molding, January 2014.

[25] Olve Winjum and Heine H. Roestum. Project assignment: Mechanical response of thermoplastics, 2013.

Chapter 8

Appendix

Appendix A

Material tests

In this chapter, images and the load history of the experimental tests will be presented. For the uniaxile tensile and compression tests, both the force-displacement history and the stress-strain history will be presented. For the remaining tests, only the force history will be presented.

A.1   Uniaxial tensile tests

A.1.1   PP1-T2-F-V1-1

	Value	Unit
Initial thickness [t]	2.05	mm
Initial width [w]	11.94	mm
Velocity [v]	1.500	mm/s
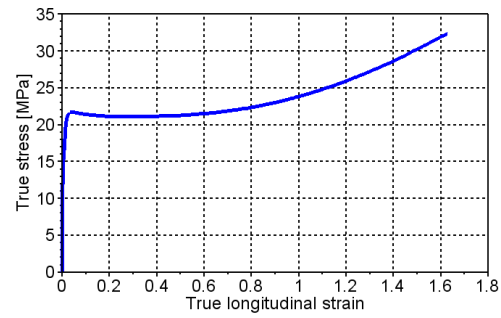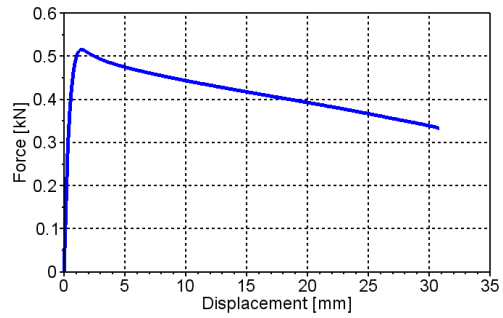
Figure A.1: Test specimen

(a) True stress-strain

(b) Force-displacement

Figure A.2: Stress-strain

A.1.2 PP1-T2-F-V1-2

	Value	Unit
Initial thickness [t]	2.03	mm
Initial width [w]	11.92	mm
Velocity [v]	1.500	mm/s

Figure A.3: Test specimen
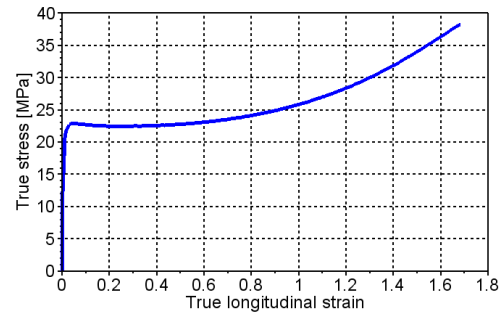
(a) True stress-strain
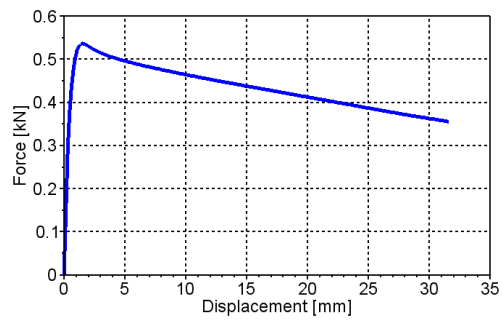
(b) Force-displacement

Figure A.4: Load history

A.1.3 PP1-T2-F-V1-3

	Value	Unit
Initial thickness [t]	2.05	mm
Initial width [w]	11.92	mm
Velocity [v]	1.500	mm/s

Figure A.5: Test specimen
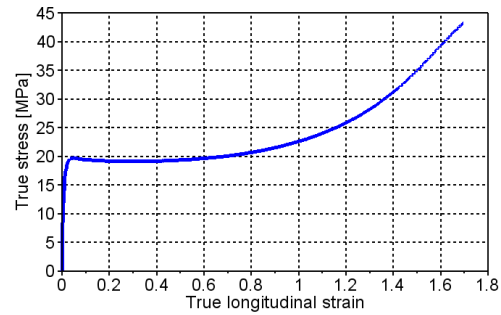
(a) True stress-strain
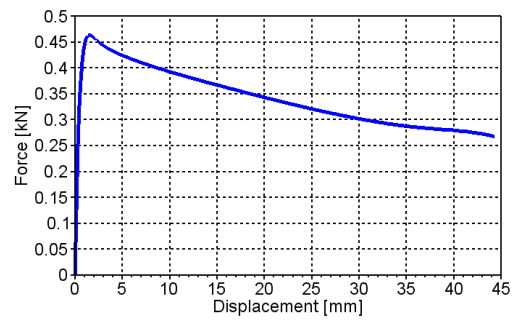
(b) Force-displacement

Figure A.6: Load history

A.1.4 PP1-T2-F-V1-4

	Value	Unit
Initial thickness [t]	2.04	mm
Initial width [w]	12.08	mm
Velocity [v]	1.500	mm/s

Figure A.7: Test specimen
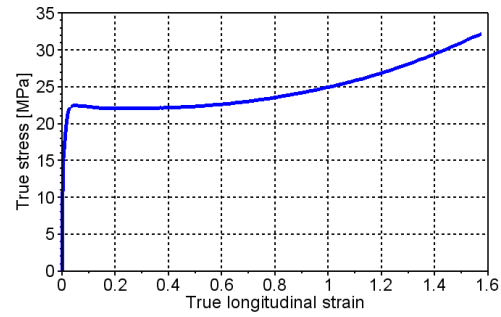
(a) True stress-strain
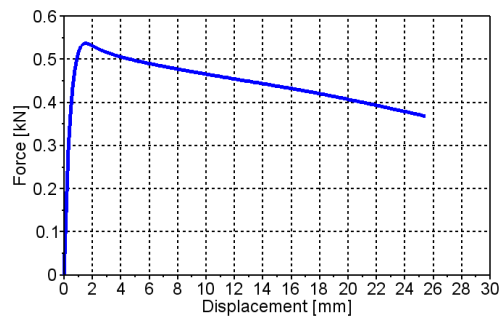
(b) Force-displacement

Figure A.8: Load history

A.1.5 PP1-T2-F-V1-5

	Value	Unit
Initial thickness [t]	2.04	mm
Initial width [w]	12.07	mm
Velocity [v]	1.500	mm/s

Figure A.9: Test specimen
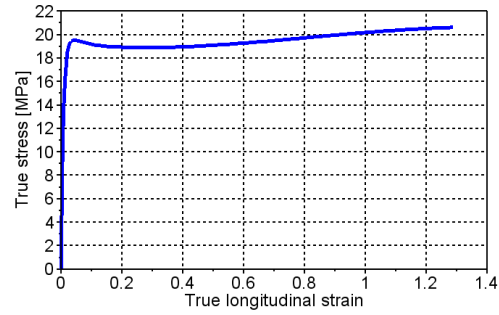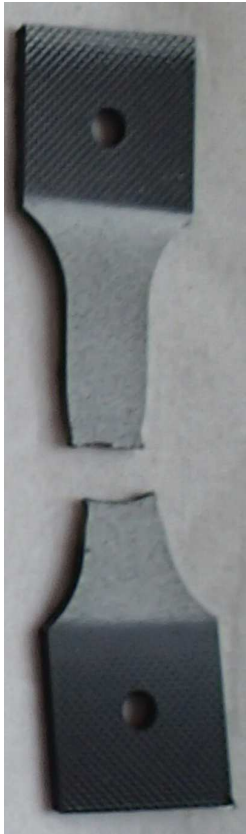
(a) True stress-strain
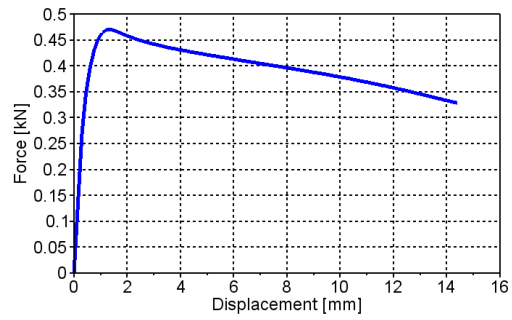
(b) Force-displacement

Figure A.10: Load history

A.1.6   PP1-T2-F-V2-1

	Value	Unit
Initial thickness [t]	2.06	mm
Initial width [w]	11.95	mm
Velocity [v]	0.150	mm/s

Figure A.11: Test specimen
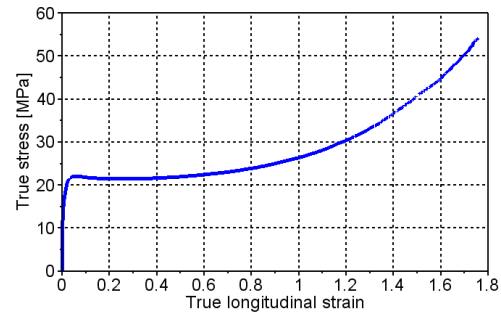
(a) True stress-strain
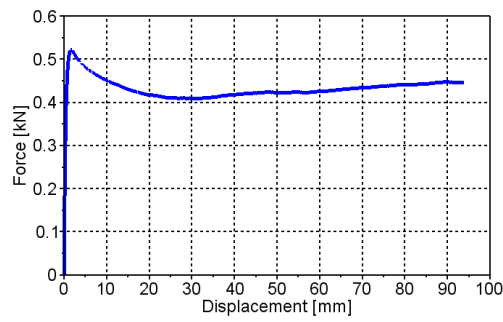
(b) Force-displacement

Figure A.12: Load history

A.1.7 PP1-T2-F-V2-3

	Value	Unit
Initial thickness [t]	2.10	mm
Initial width [w]	11.97	mm
Velocity [v]	0.150	mm/s
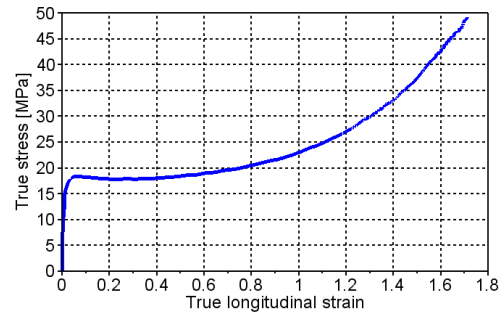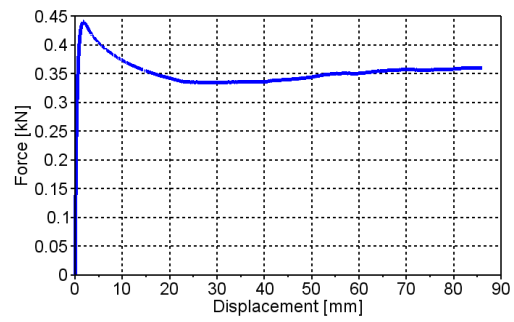
Figure A.13: Test specimen

(a) True stress-strain

(b) Force-displacement

Figure A.14: Load history

A.1.8 PP1-T2-F-V2-4

	Value	Unit
Initial thickness [t]	2.04	mm
Initial width [w]	11.94	mm
Velocity [v]	0.150	mm/s
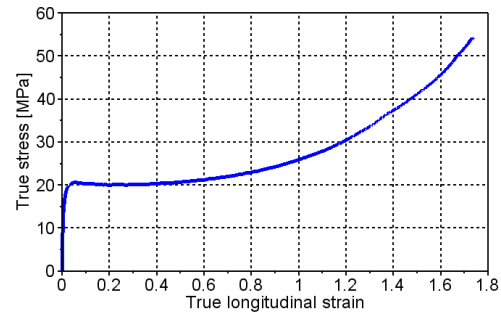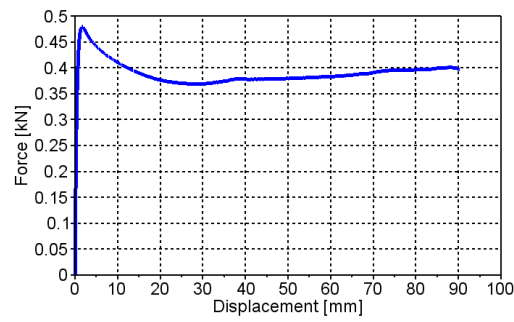
Figure A.15: Test specimen

(a) True stress-strain

(b) Force-displacement

Figure A.16: Load history

A.1.9　PP1-T2-M-V2-1

	Value	Unit
Initial thickness [t]	1.54	mm
Initial width [w]	11.95	mm
Velocity [v]	0.150	mm/s

Figure A.17: Test specimen
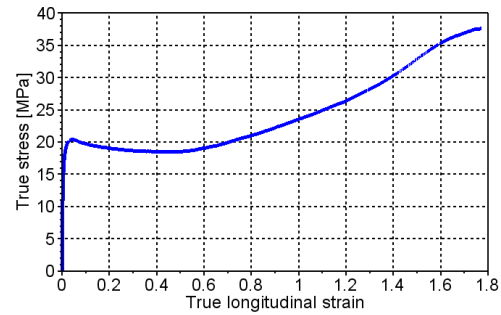
(a) True stress-strain
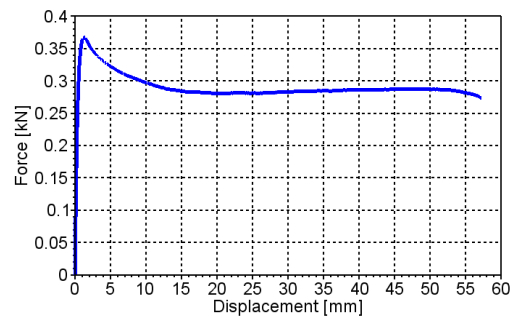
(b) Force-displacement

Figure A.18: Load history

A.1.10   PP1-T2-M-V2-2

	Value	Unit
Initial thickness [t]	1.56	mm
Initial width [w]	11.95	mm
Velocity [v]	0.150	mm/s
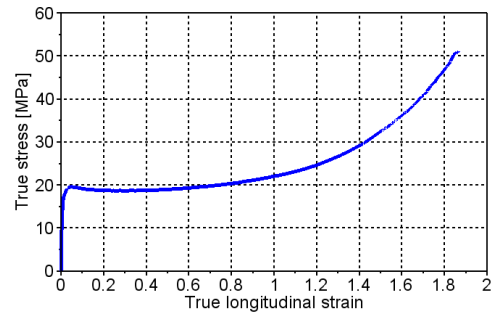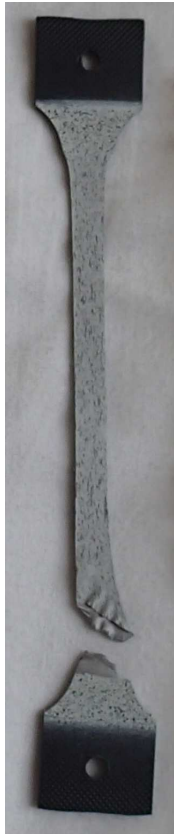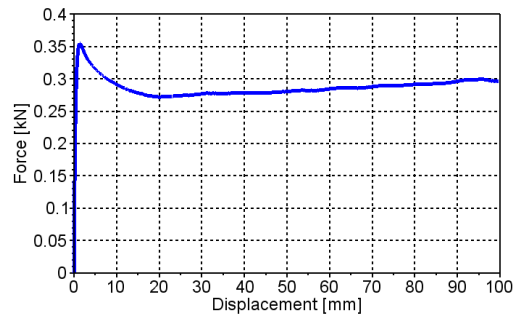
Figure A.19: Test specimen

(a) True stress-strain

(b) Force-displacement

Figure A.20: Load history

A.1.11 PP1-T2-M-V2-3

	Value	Unit
Initial thickness [t]	1.60	mm
Initial width [w]	11.96	mm
Velocity [v]	0.150	mm/s
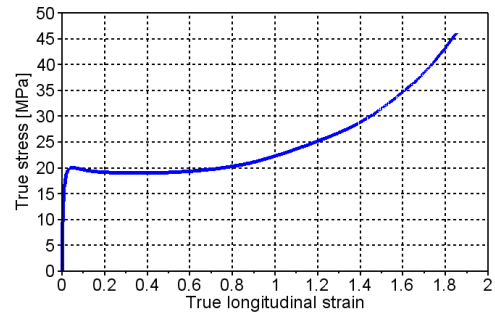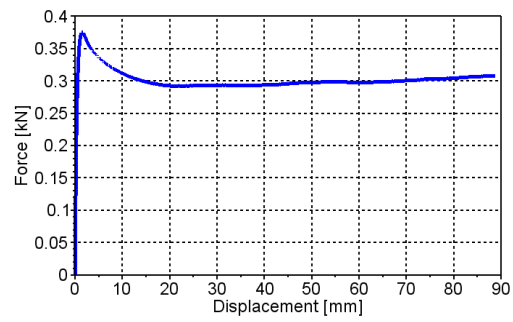
Figure A.21: Test specimen

(a) True stress-strain

(b) Force-displacement

Figure A.22: Load history

A.1.12 PP1-T2-R-V2-1

	Value	Unit
Initial thickness [t]	1.00	mm
Initial width [w]	11.94	mm
Velocity [v]	0.150	mm/s
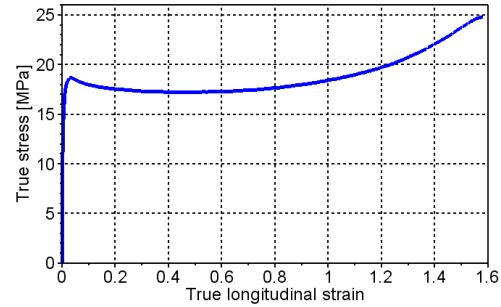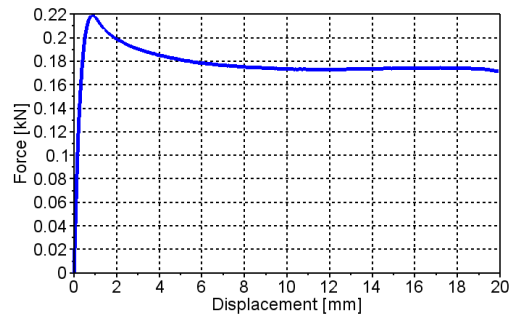
Figure A.23: Test specimen

(a) True stress-strain

(b) Force-displacement

Figure A.24: Load history

A.1.13   PP1-T2-R-V2-2

	Value	Unit
Initial thickness [t]	1.05	mm
Initial width [w]	11.93	mm
Velocity [v]	0.150	mm/s
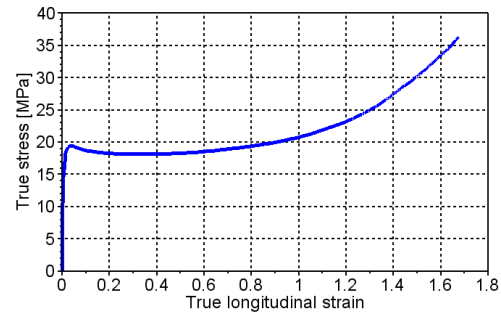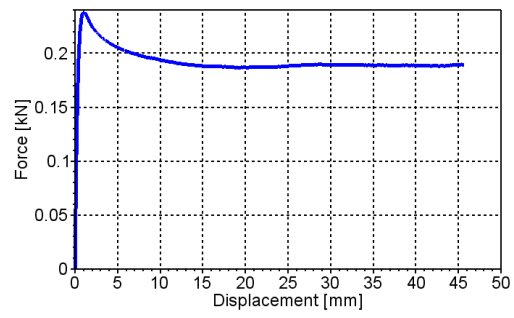
Figure A.25: Test specimen

(a) True stress-strain

(b) Force-displacement

Figure A.26: Load history

A.1.14   PP1-T2-R-V2-3

	Value	Unit
Initial thickness [t]	1.03	mm
Initial width [w]	11.95	mm
Velocity [v]	0.150	mm/s
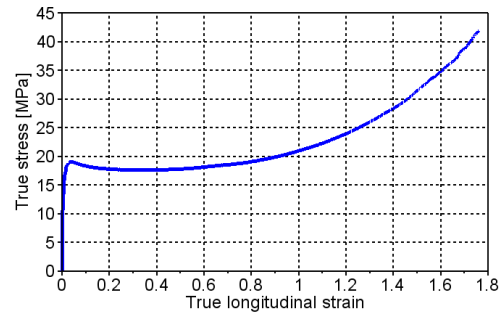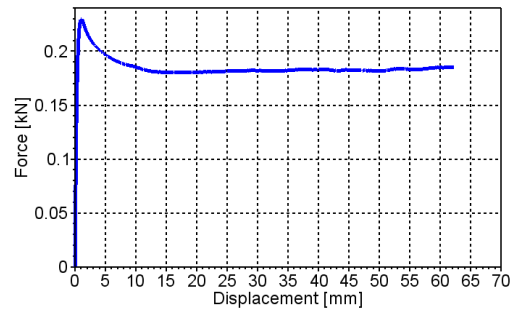
Figure A.27: Test specimen

(a) True stress-strain

(b) Force-displacement

Figure A.28: Load history

A.1.15   PP1-T2-F-V3-1

	Value	Unit
Initial thickness [t]	2.05	mm
Initial width [w]	11.93	mm
Velocity [v]	0.015	mm/s

Figure A.29: Test specimen
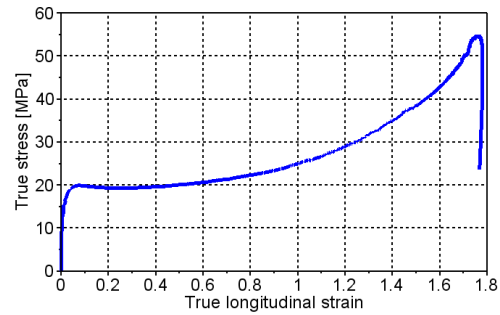
(a) True stress-strain
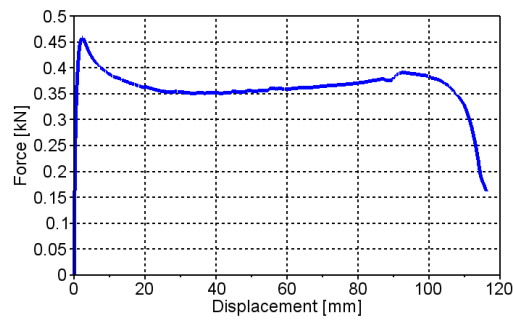
(b) Force-displacement

Figure A.30: Load history

A.1.16 PP1T-T2-F-V1-1

	Value	Unit
Initial thickness [t]	1.00	mm
Initial width [w]	11.99	mm
Velocity [v]	1.500	mm/s

Figure A.31: Test specimen

(a) True stress-strain

(b) Force-displacement

Figure A.32: Load history

A.1.17   PP1T-T2-F-V2-1

	Value	Unit
Initial thickness [t]	1.99	mm
Initial width [w]	11.94	mm
Velocity [v]	0.150	mm/s

Figure A.33: Test specimen

(a) True stress-strain

(b) Force-displacement

Figure A.34: Load history

A.1.18 PP1T-T2-F-V2-2

	Value	Unit
Initial thickness [t]	2.01	mm
Initial width [w]	12.03	mm
Velocity [v]	0.150	mm/s

Figure A.35: Test specimen
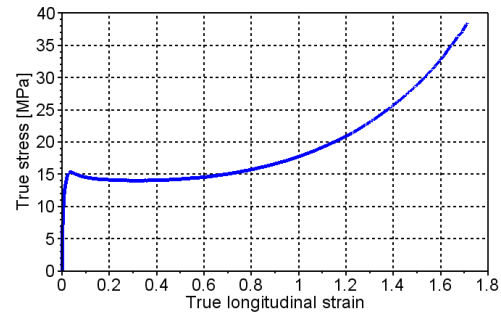
(a) True stress-strain
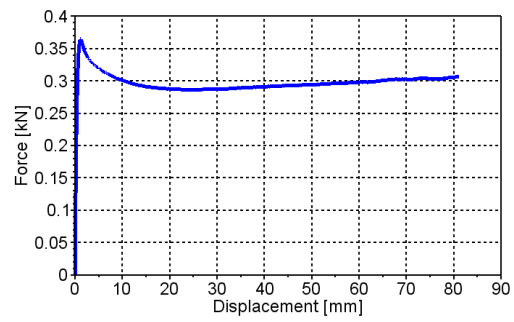
(b) Force-displacement

Figure A.36: Load history

A.1.19 PP1-T3-F-V1-1

	Value	Unit
Initial thickness [t]	3.10	mm
Initial width [w]	11.87	mm
Velocity [v]	1.500	mm/s

Figure A.37: Test specimen
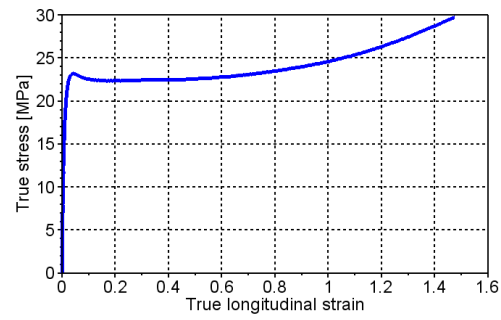
(a) True stress-strain
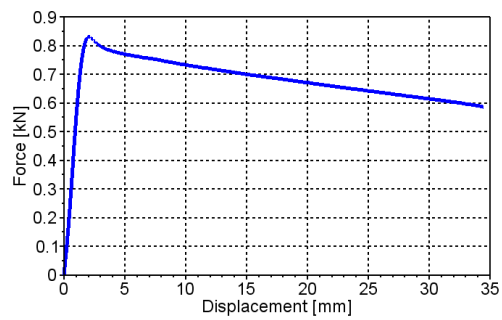
(b) Force-displacement

Figure A.38: Load history

A.1.20 PP1-T3-R-V1-1

	Value	Unit
Initial thickness [t]	1.97	mm
Initial width [w]	12.05	mm
Velocity [v]	1.500	mm/s

Figure A.39: Test specimen
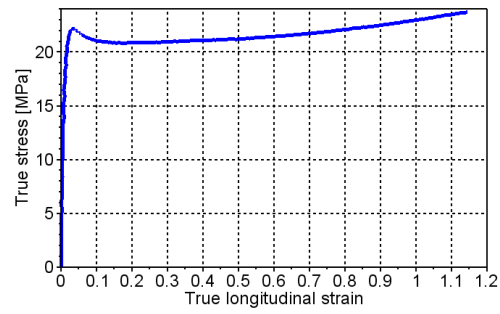
(a) True stress-strain

(b) Force-displacement

Figure A.40: Load history

A.1.21   PP1-T3-R-V1-2

	Value	Unit
Initial thickness [t]	1.99	mm
Initial width [w]	12.05	mm
Velocity [v]	1.500	mm/s

Figure A.41: Test specimen
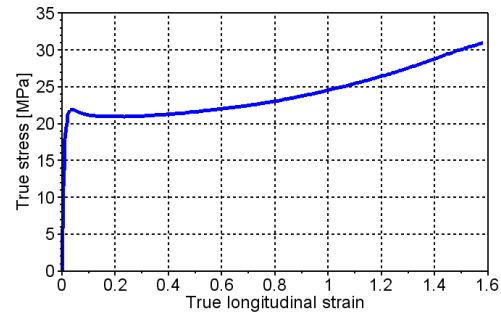
(a) True stress-strain

(b) Force-displacement

Figure A.42: Load history

A.1.22 PP1-T3-R-V1-3

	Value	Unit
Initial thickness [t]	1.99	mm
Initial width [w]	12.11	mm
Velocity [v]	1.500	mm/s

Figure A.43: Test specimen
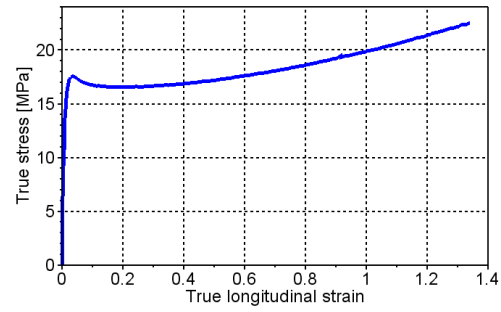
(a) True stress-strain
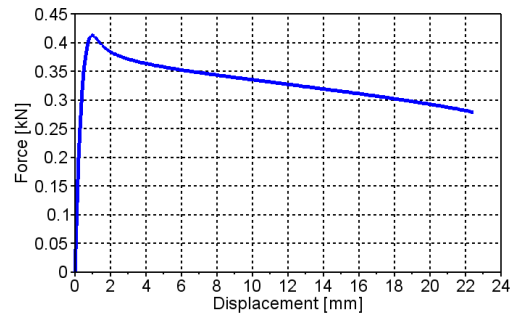
(b) Force-displacement

Figure A.44: Load history

A.1.23 PP1-T3-F-V2-1

	Value	Unit
Initial thickness [t]	3.11	mm
Initial width [w]	11.97	mm
Velocity [v]	0.150	mm/s

Figure A.45: Test specimen
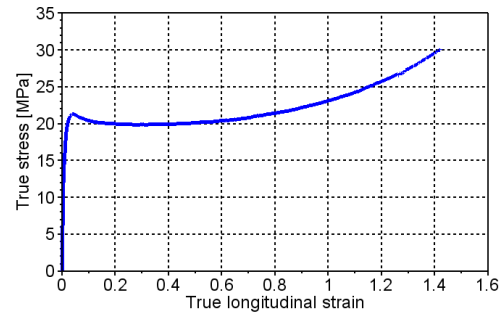
(a) True stress-strain
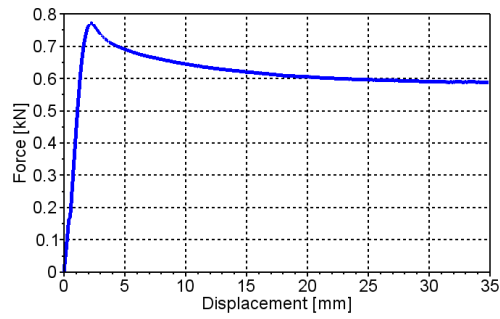
(b) Force-displacement

Figure A.46: Load history

146

A.1.24 PP1-T3-F-V2-2

	Value	Unit
Initial thickness [t]	3.11	mm
Initial width [w]	11.91	mm
Velocity [v]	0.150	mm/s

Figure A.47: Test specimen
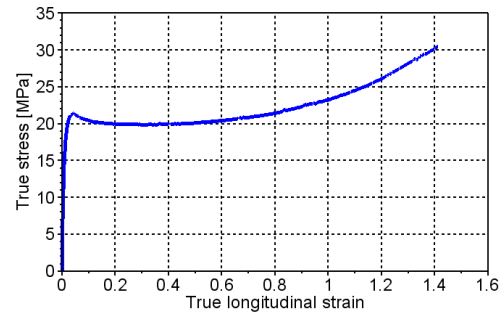
(a) True stress-strain
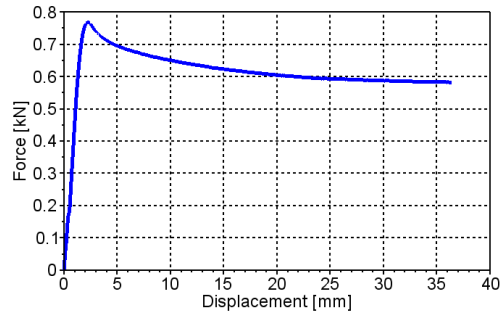
(b) Force-displacement

Figure A.48: Load history

A.1.25 PP1-T3-F-V2-3

	Value	Unit
Initial thickness [t]	3.12	mm
Initial width [w]	11.92	mm
Velocity [v]	0.150	mm/s

Figure A.49: Test specimen
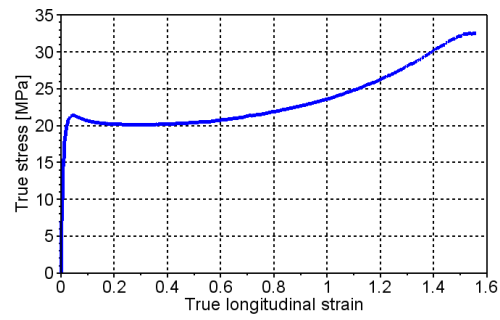
(a) True stress-strain
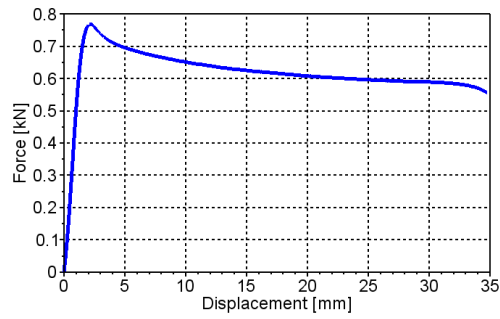
(b) Force-displacement

Figure A.50: Load history

A.1.26   PP1-T3-F-V2-4

	Value	Unit
Initial thickness [t]	3.12	mm
Initial width [w]	11.93	mm
Velocity [v]	0.150	mm/s

Figure A.51: Test specimen
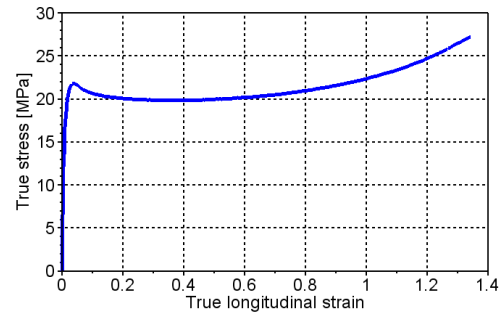
(a) True stress-strain
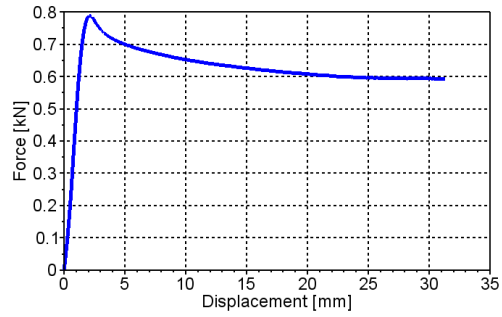
(b) Force-displacement

Figure A.52: Load history

A.1.27   PP1-T3-F-V2-5

	Value	Unit
Initial thickness [t]	3.13	mm
Initial width [w]	12.15	mm
Velocity [v]	0.150	mm/s

Figure A.53: Test specimen
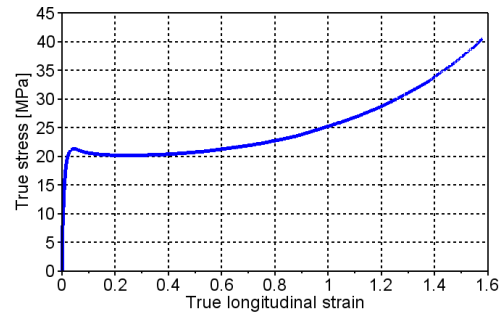
(a) True stress-strain
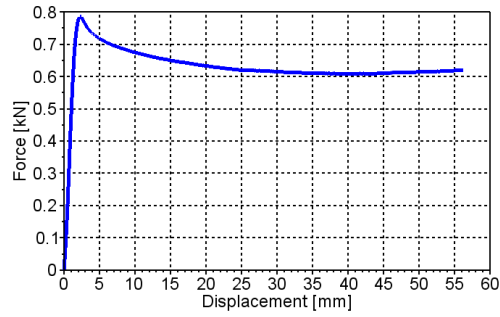
(b) Force-displacement

Figure A.54: Load history

A.1.28 PP1-T3-R-V2-1

	Value	Unit
Initial thickness [t]	2.00	mm
Initial width [w]	11.92	mm
Velocity [v]	0.150	mm/s

Figure A.55: Test specimen
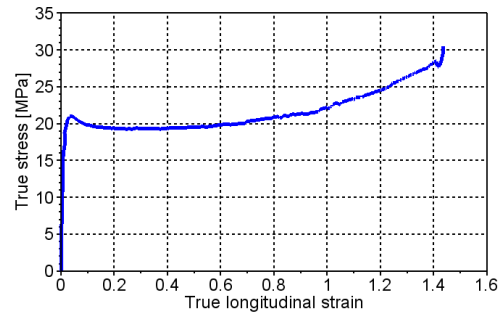
(a) True stress-strain
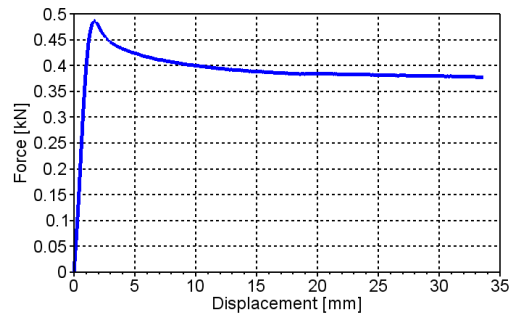
(b) Force-displacement

Figure A.56: Load history

151

A.1.29 PP1-T3-R-V2-2

	Value	Unit
Initial thickness [t]	1.98	mm
Initial width [w]	12.17	mm
Velocity [v]	0.150	mm/s

Figure A.57: Test specimen
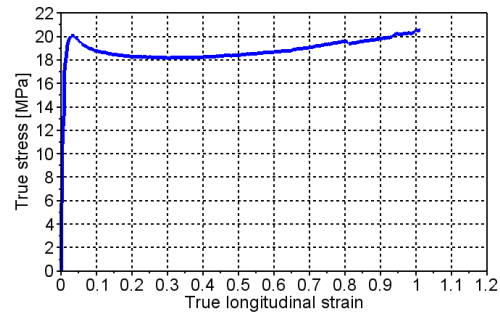
(a) True stress-strain
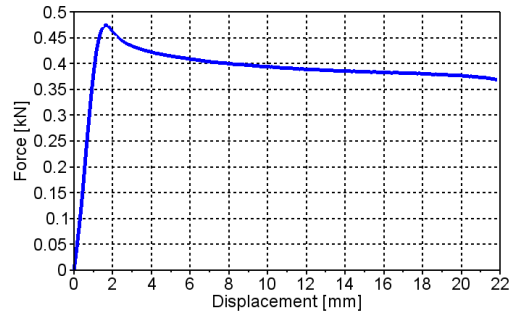
(b) Force-displacement

Figure A.58: Load history

A.1.30 PP1-T3-R-V2-3

	Value	Unit
Initial thickness [t]	1.99	mm
Initial width [w]	11.90	mm
Velocity [v]	0.150	mm/s

Figure A.59: Test specimen
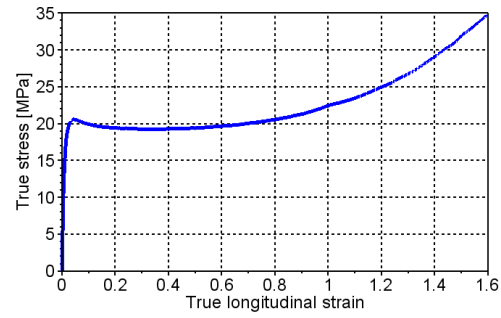
(a) True stress-strain
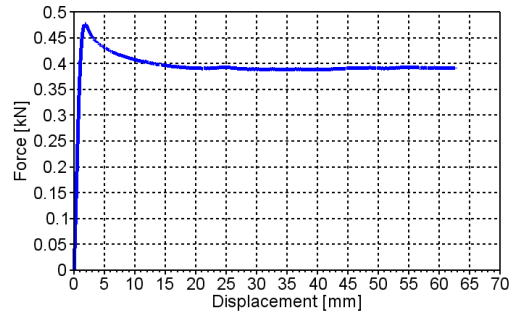
(b) Force-displacement

Figure A.60: Load history

A.1.31   PP1-T3-F-V3-1

	Value	Unit
Initial thickness [t]	3.10	mm
Initial width [w]	11.87	mm
Velocity [v]	0.015	mm/s

Figure A.61: Test specimen
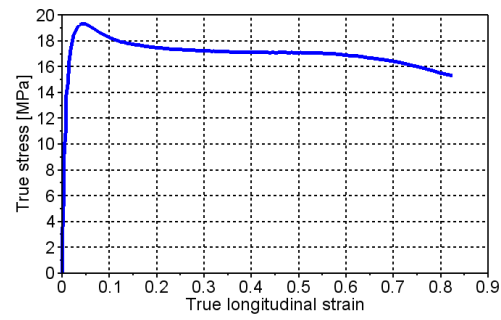
(a) True stress-strain
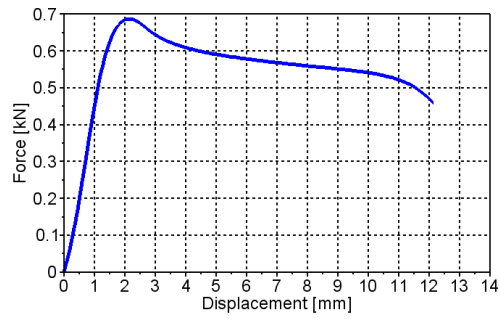
(b) Force-displacement

Figure A.62: Load history

A.1.32 PP1-T3-F-V3-2

	Value	Unit
Initial thickness [t]	3.10	mm
Initial width [w]	11.92	mm
Velocity [v]	0.015	mm/s

Figure A.63: Test specimen
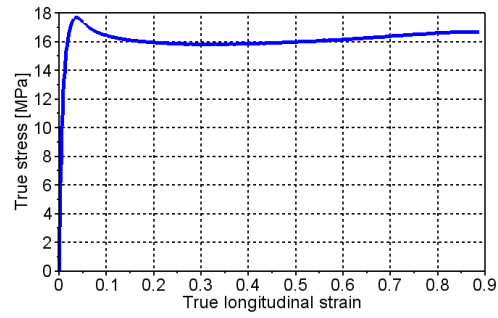
(a) True stress-strain
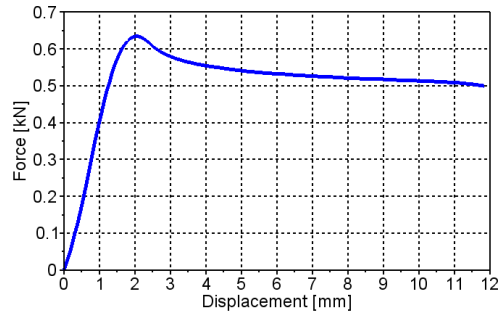
(b) Force-displacement

Figure A.64: Load history

A.1.33 PP1-T3-F-V3-3

	Value	Unit
Initial thickness [t]	3.15	mm
Initial width [w]	12.12	mm
Velocity [v]	0.015	mm/s

Figure A.65: Test specimen
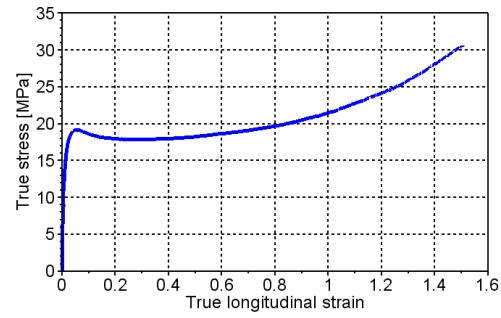
(a) True stress-strain
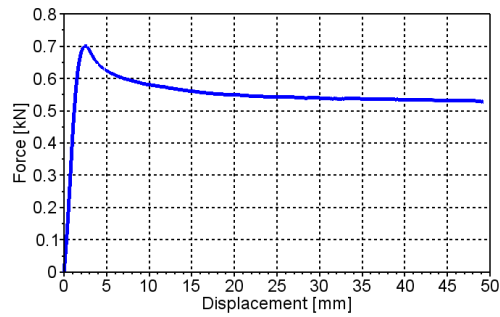
(b) Force-displacement

Figure A.66: Load history

A.1.34 PP1-T3-R-V3-1

	Value	Unit
Initial thickness [t]	1.99	mm
Initial width [w]	12.15	mm
Velocity [v]	0.015	mm/s

Figure A.67: Test specimen
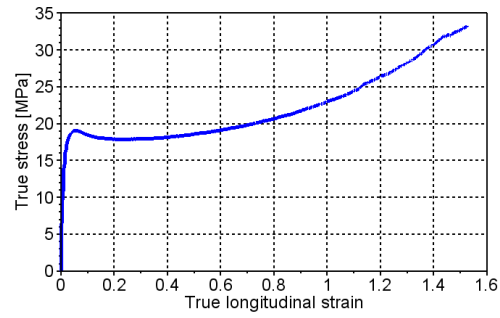
(a) True stress-strain
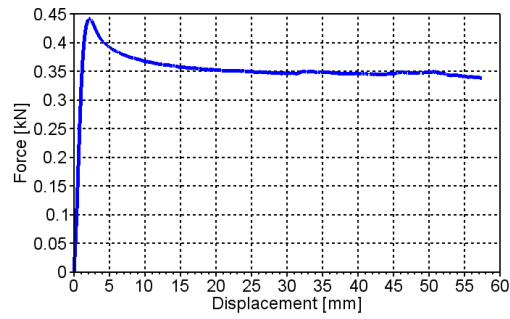
(b) Force-displacement

Figure A.68: Load history

157

A.1.35 PP1-T3-R-V3-2

	Value	Unit
Initial thickness [t]	1.99	mm
Initial width [w]	12.02	mm
Velocity [v]	0.015	mm/s

Figure A.69: Test specimen
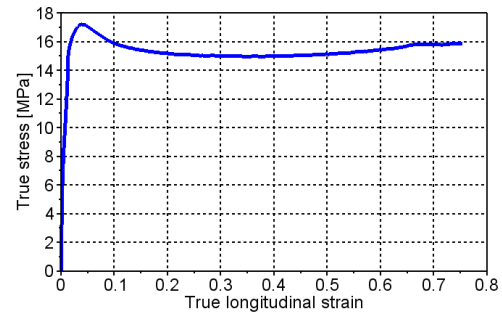
(a) True stress-strain
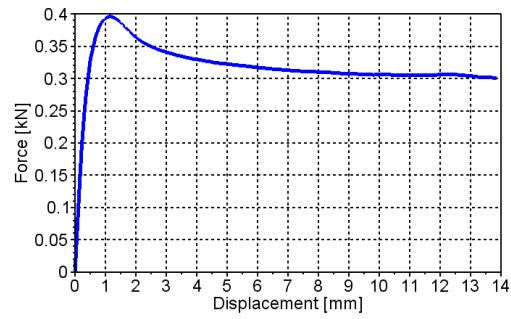
(b) Force-displacement

Figure A.70: Load history

A.1.36 PP1-T3-R-V3-3

	Value	Unit
Initial thickness [t]	2.00	mm
Initial width [w]	12.17	mm
Velocity [v]	0.015	mm/s

Figure A.71: Test specimen
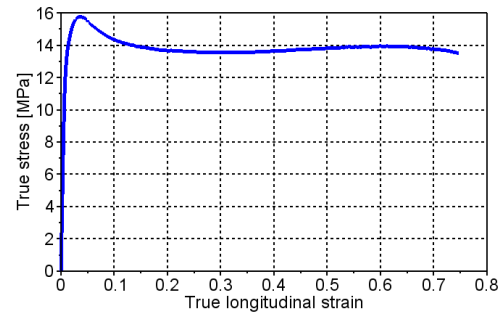
(a) True stress-strain
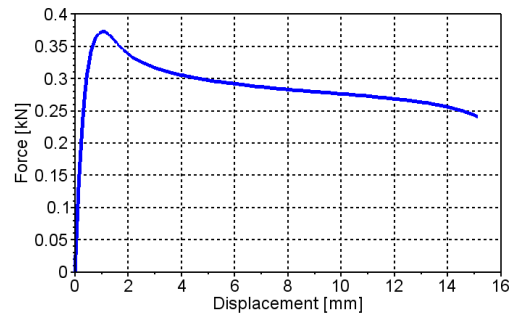
(b) Force-displacement

Figure A.72: Load history

159

A.1.37 PP1-T3-R-V3-4

	Value	Unit
Initial thickness [t]	1.96	mm
Initial width [w]	11.87	mm
Velocity [v]	0.015	mm/s

Figure A.73: Test specimen
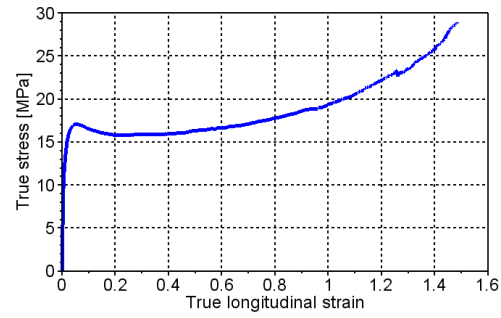
(a) True stress-strain
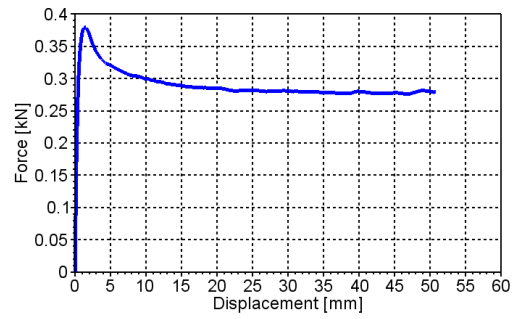
(b) Force-displacement

Figure A.74: Load history

A.1.38 PP1T-T3-F-V1-1

	Value	Unit
Initial thickness [t]	3.18	mm
Initial width [w]	12.16	mm
Velocity [v]	1.500	mm/s

Figure A.75: Test specimen
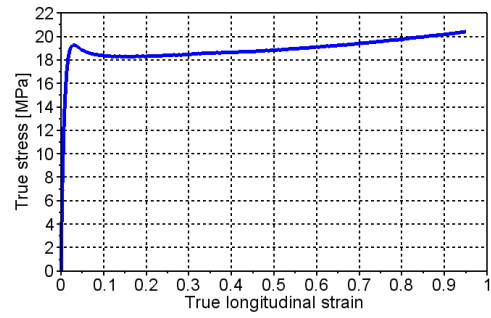
(a) True stress-strain
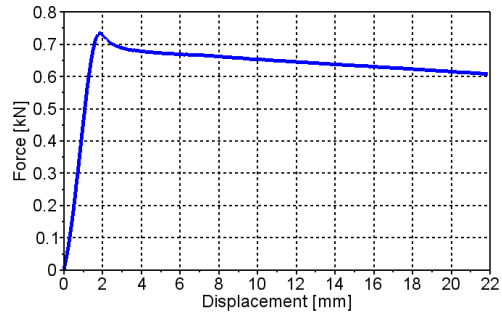
(b) Force-displacement

Figure A.76: Load history

A.1.39 PP1T-T3-R-V1-1

	Value	Unit
Initial thickness [t]	1.93	mm
Initial width [w]	11.88	mm
Velocity [v]	1.500	mm/s

Figure A.77: Test specimen
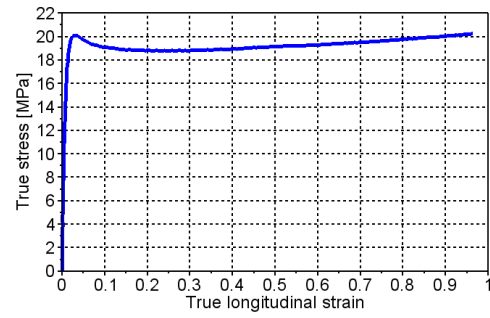
(a) True stress-strain
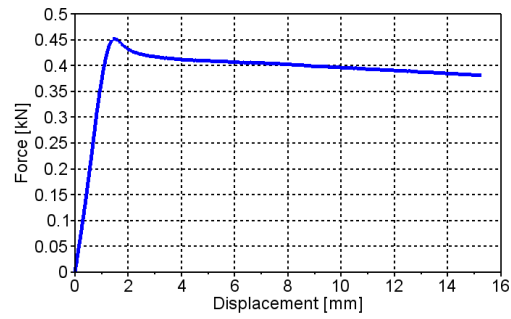
(b) Force-displacement

Figure A.78: Load history

A.1.40 PP1T-T3-F-V2-1

	Value	Unit
Initial thickness [t]	3.16	mm
Initial width [w]	12.28	mm
Velocity [v]	0.150	mm/s

Figure A.79: Test specimen
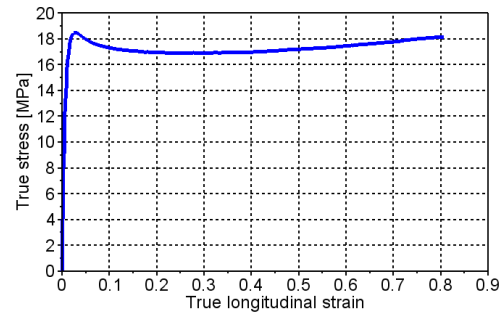
(a) True stress-strain
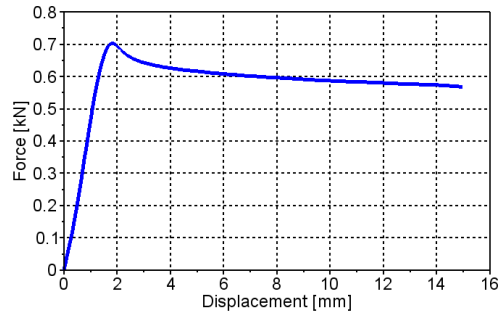
(b) Force-displacement

Figure A.80: Load history

A.1.41 PP1T-T3-F-V2-2

	Value	Unit
Initial thickness [t]	3.14	mm
Initial width [w]	12.02	mm
Velocity [v]	0.150	mm/s

Figure A.81: Test specimen
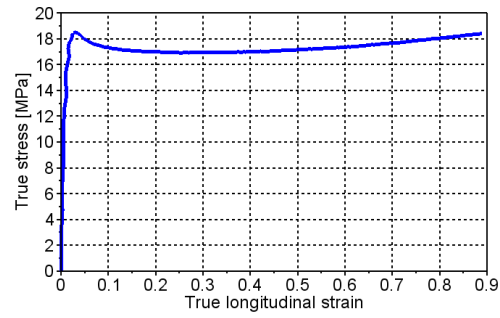
(a) True stress-strain
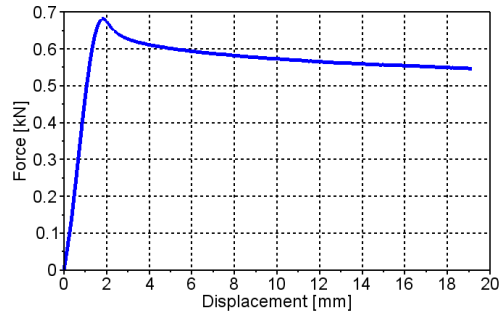
(b) Force-displacement

Figure A.82: Load history

A.1.42 PP1T-T3-R-V2-1

	Value	Unit
Initial thickness [t]	1.94	mm
Initial width [w]	11.91	mm
Velocity [v]	0.150	mm/s

Figure A.83: Test specimen
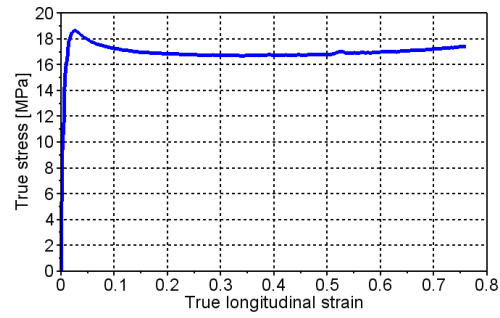
(a) True stress-strain
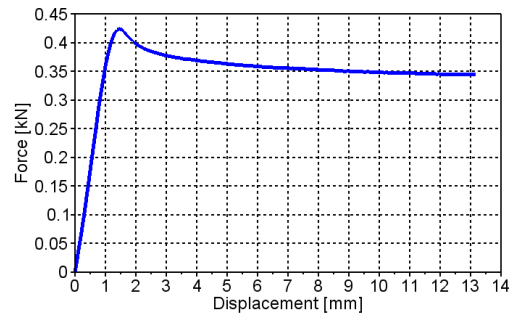
(b) Force-displacement

Figure A.84: Load history

A.1.43 PP1T-T3-R-V2-2

	Value	Unit
Initial thickness [t]	1.97	mm
Initial width [w]	11.88	mm
Velocity [v]	0.150	mm/s
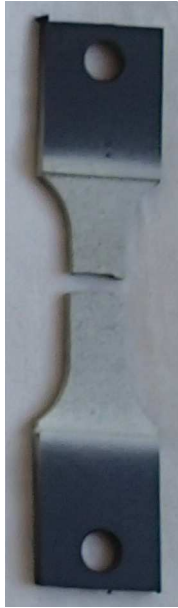
Figure A.85: Test specimen
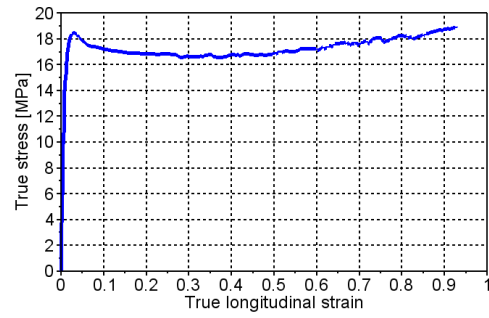
(a) True stress-strain
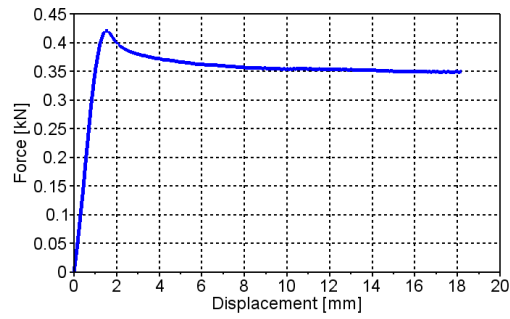
(b) Force-displacement

Figure A.86: Load history

166

A.1.44 PP1-T4-F-V1-2

	Value	Unit
Initial thickness [t]	3.94	mm
Initial width [w]	11.95	mm
Velocity [v]	1.500	mm/s

Figure A.87: Test specimen
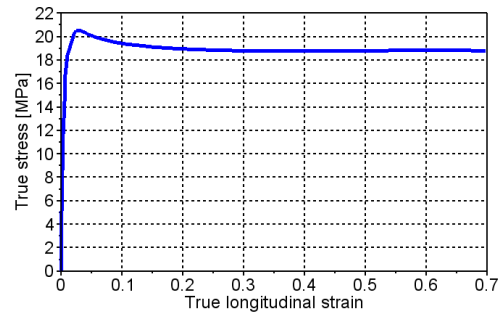
(a) True stress-strain
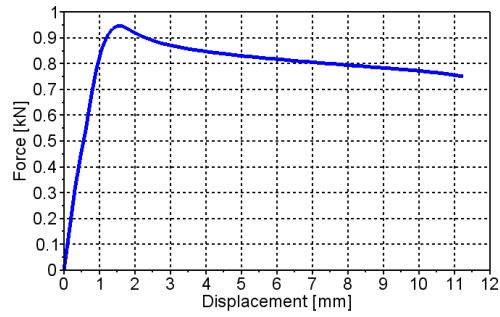
(b) Force-displacement

Figure A.88: Load history

A.1.45 PP1-T4-F-V1-3

	Value	Unit
Initial thickness [t]	3.97	mm
Initial width [w]	11.94	mm
Velocity [v]	1.500	mm/s

Figure A.89: Test specimen
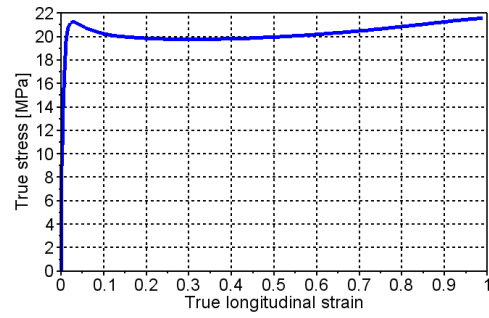
(a) True stress-strain
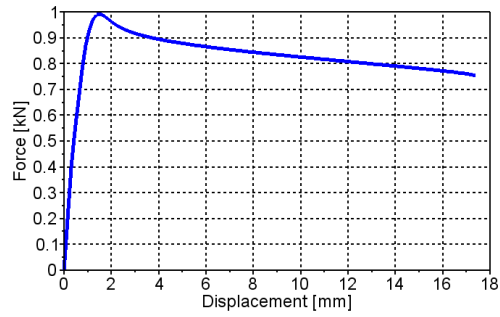
(b) Force-displacement

Figure A.90: Load history

A.1.46 PP1-T4-F-V1-4

	Value	Unit
Initial thickness [t]	3.98	mm
Initial width [w]	11.94	mm
Velocity [v]	1.500	mm/s
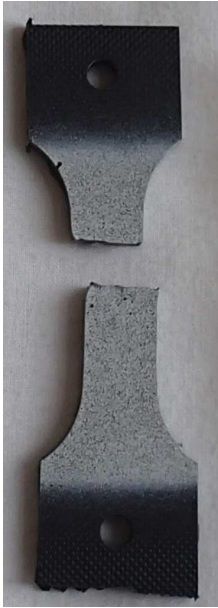
Figure A.91: Test specimen
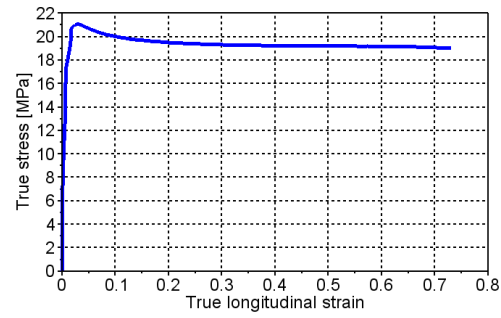
(a) True stress-strain
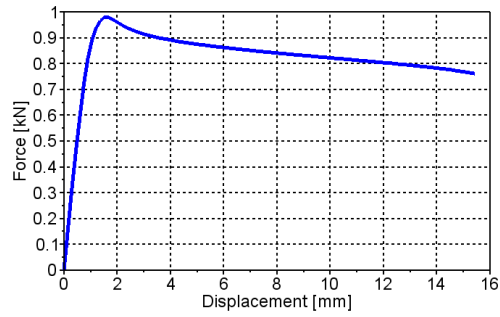
(b) Force-displacement

Figure A.92: Load history

169

A.1.47   PP1-T4-F-V1-5

	Value	Unit
Initial thickness [t]	3.97	mm
Initial width [w]	11.95	mm
Velocity [v]	1.500	mm/s

Figure A.93: Test specimen
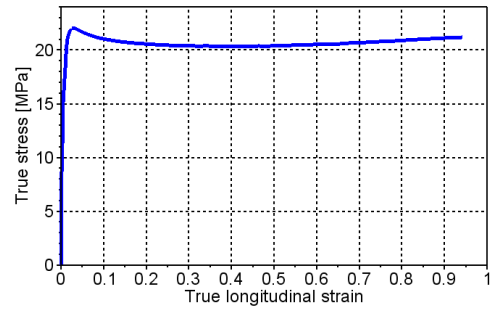
(a) True stress-strain
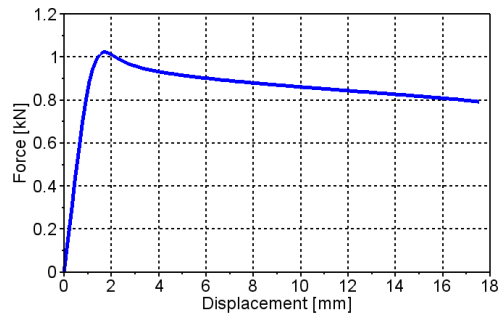
(b) Force-displacement

Figure A.94: Load history

A.1.48   PP1-T4-F-V2-1

	Value	Unit
Initial thickness [t]	3.98	mm
Initial width [w]	11.97	mm
Velocity [v]	0.150	mm/s

Figure A.95: Test specimen
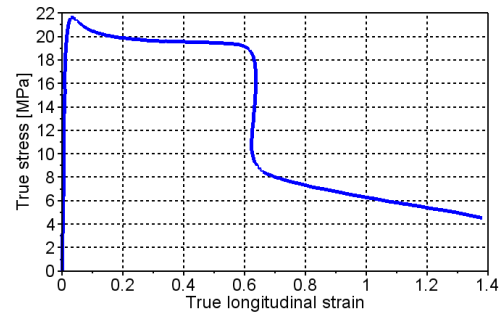
(a) True stress-strain
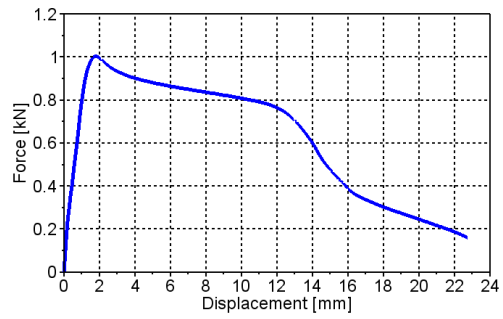
(b) Force-displacement

Figure A.96: Load history

171

A.1.49   PP1-T4-F-V2-2

	Value	Unit
Initial thickness [t]	3.97	mm
Initial width [w]	11.94	mm
Velocity [v]	0.150	mm/s

Figure A.97: Test specimen
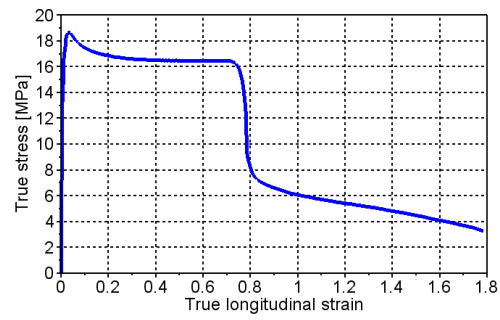
(a) True stress-strain
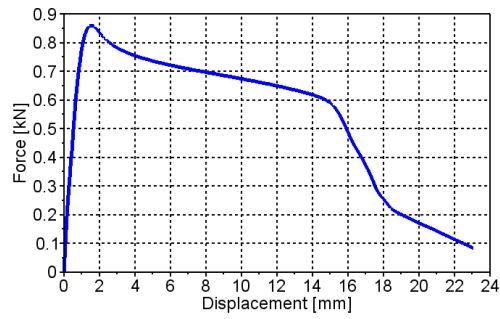
(b) Force-displacement

Figure A.98: Load history

A.1.50   PP1-T4-F-V2-3

	Value	Unit
Initial thickness [t]	3.98	mm
Initial width [w]	11.98	mm
Velocity [v]	0.150	mm/s

Figure A.99: Test specimen
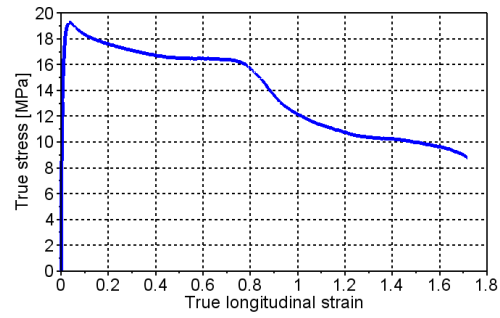
(a) True stress-strain
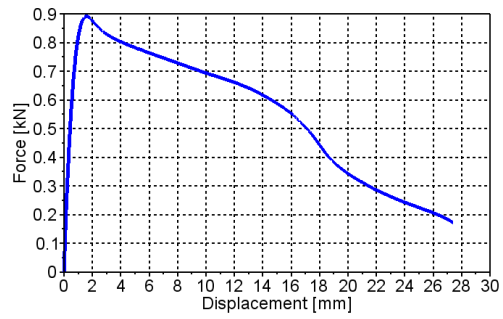
(b) Force-displacement

Figure A.100: Load history

A.1.51 PP1-T4-F-V2-4

	Value	Unit
Initial thickness [t]	3.94	mm
Initial width [w]	11.94	mm
Velocity [v]	0.150	mm/s
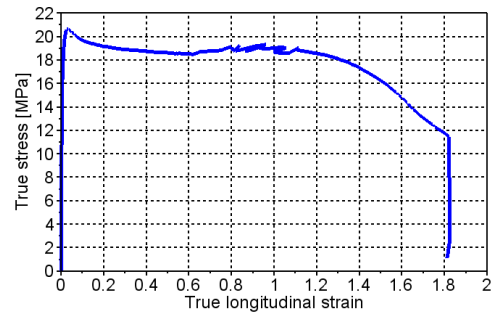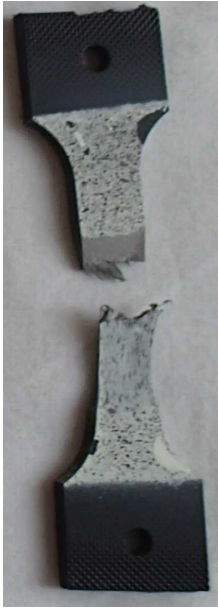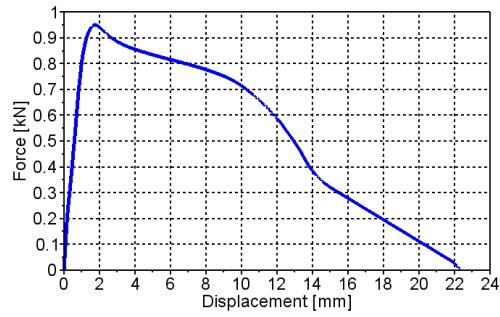
Figure A.101: Test specimen

(a) True stress-strain

(b) Force-displacement

Figure A.102: Load history

A.1.52 PP1-T4-R-V2-1

	Value	Unit
Initial thickness [t]	2.99	mm
Initial width [w]	11.94	mm
Velocity [v]	0.150	mm/s

Figure A.103: Test specimen
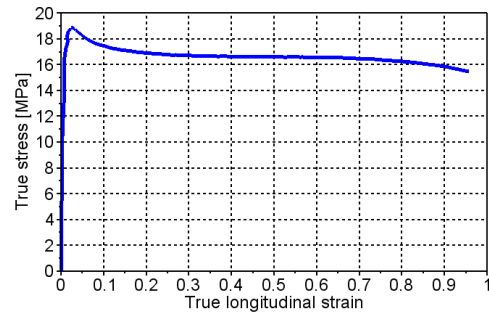
(a) True stress-strain
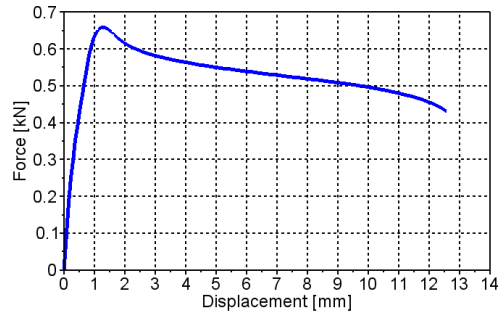
(b) Force-displacement

Figure A.104: Load history

175

A.1.53 PP1-T4-R-V2-2

	Value	Unit
Initial thickness [t]	2.99	mm
Initial width [w]	11.95	mm
Velocity [v]	0.150	mm/s
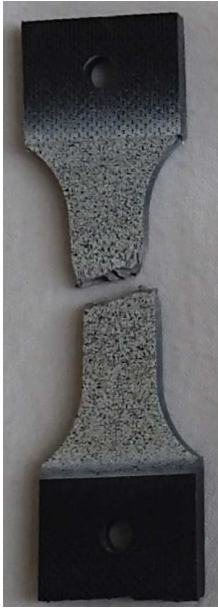
Figure A.105: Test specimen
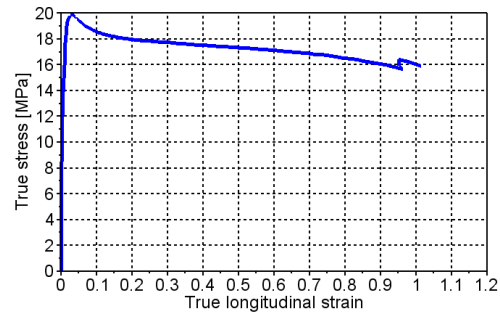
(a) True stress-strain
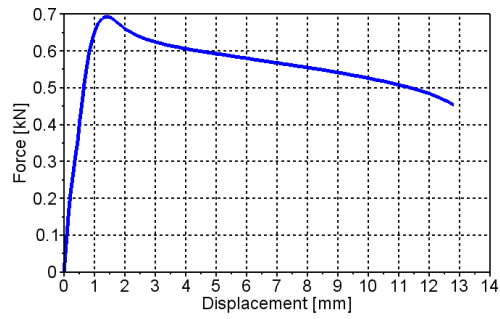
(b) Force-displacement

Figure A.106: Load history

A.1.54   PP1-T4-R-V2-3

	Value	Unit
Initial thickness [t]	2.97	mm
Initial width [w]	11.95	mm
Velocity [v]	0.150	mm/s

Figure A.107: Test specimen
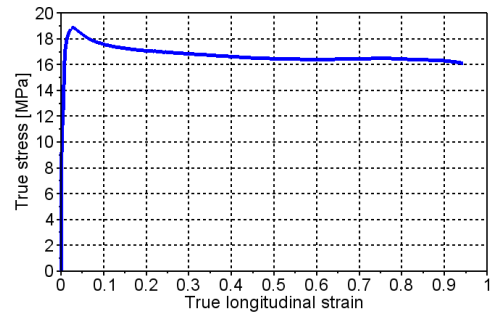
(a) True stress-strain
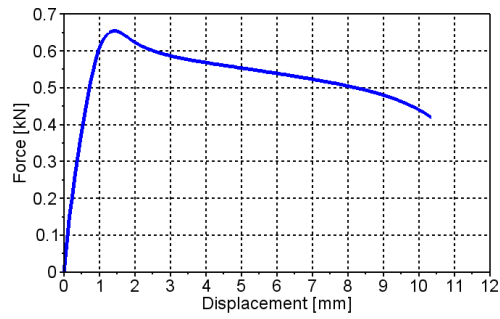
(b) Force-displacement

Figure A.108: Load history

A.1.55 PP1-T4-F-V3-1

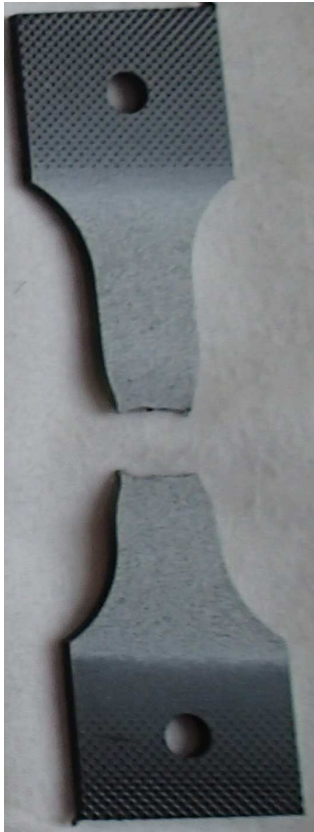|	Value	Unit
Initial thickness [t]	3.97	mm
Initial width [w]	11.96	mm
Velocity [v]	0.015	mm/s

Figure A.109: Test specimen
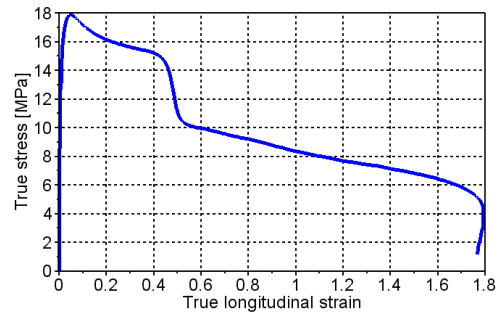
(a) True stress-strain
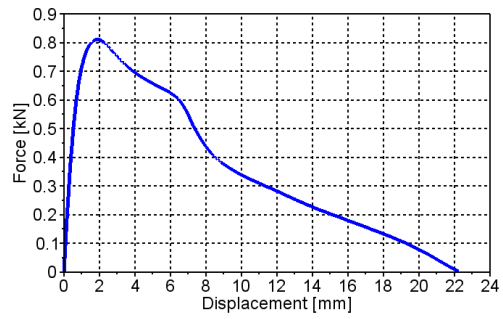
(b) Force-displacement

Figure A.110: Load history

A.1.56   PP1T-T4-F-V1-1

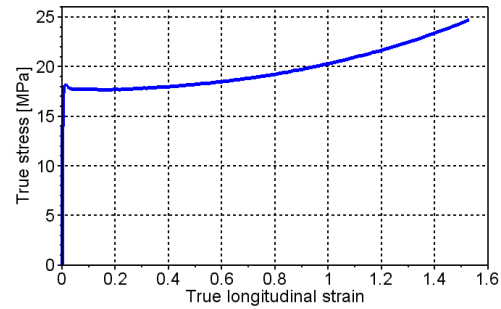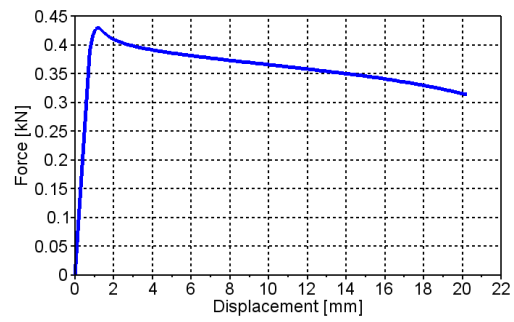|	Value	Unit
Initial thickness [t]	3.98	mm
Initial width [w]	11.94	mm
Velocity [v]	1.500	mm/s

Figure A.111: Test specimen
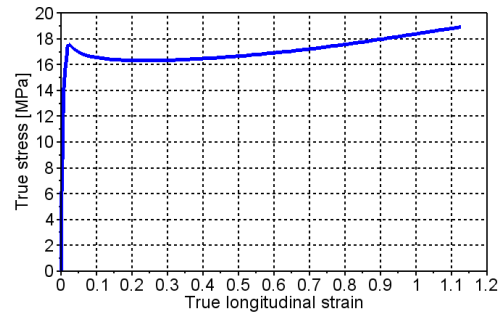
(a) True stress-strain
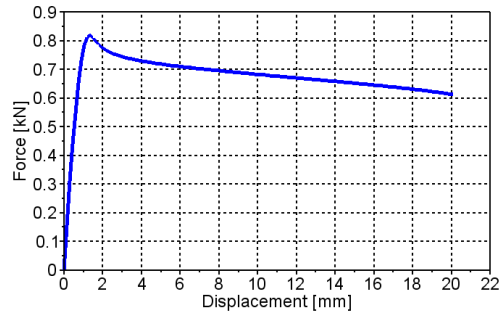
(b) Force-displacement

Figure A.112: Load history

A.1.57   PP1T-T4-F-V2-1

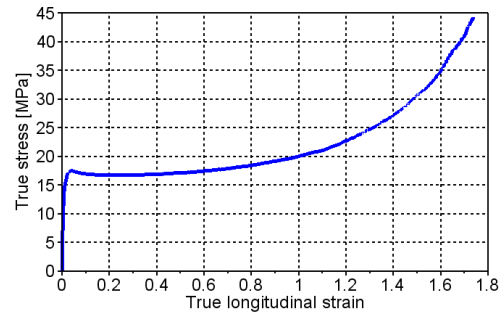|	Value	Unit
Initial thickness [t]	3.96	mm
Initial width [w]	11.97	mm
Velocity [v]	0.150	mm/s

Figure A.113: Test specimen
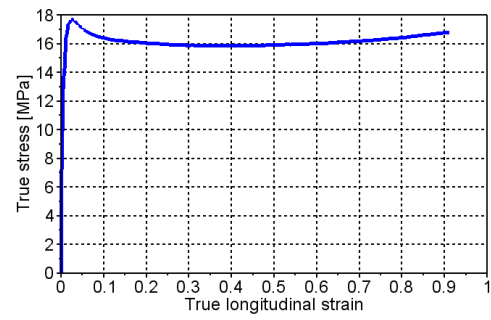
(a) True stress-strain
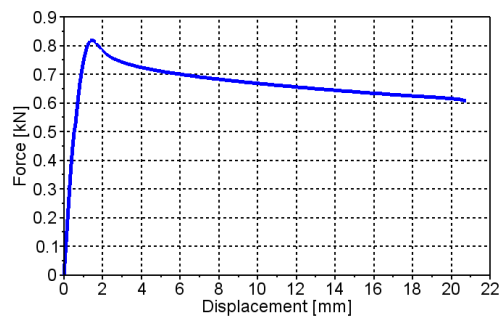
(b) Force-displacement

Figure A.114: Load history

A.1.58 PP1T-T4-F-V2-2

	Value	Unit
Initial thickness [t]	3.99	mm
Initial width [w]	11.96	mm
Velocity [v]	0.150	mm/s

Figure A.115: Test specimen
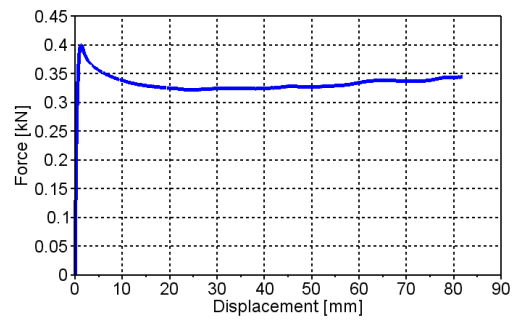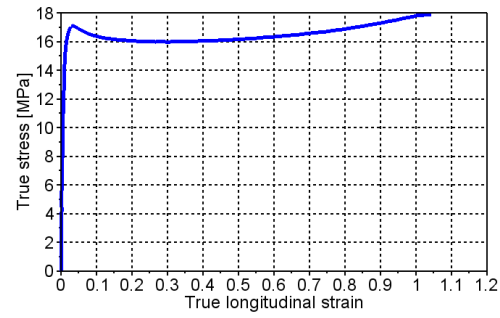

(a) True stress-strain
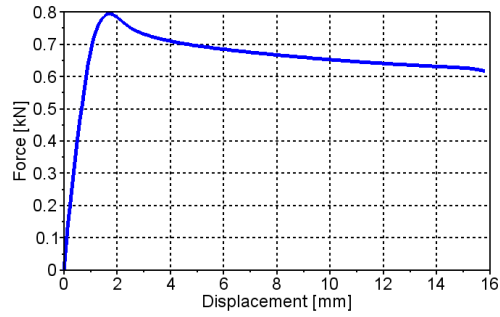
(b) Force-displacement

Figure A.116: Load history

A.2 Uniaxial compression tests

A.2.1 PP1-2-2

	Value	Unit
Initial height [h]	3.05	mm
Initial diameter [D]	6.17	mm
Velocity [v]	0.003	mm/s

Figure A.117: Test specimen
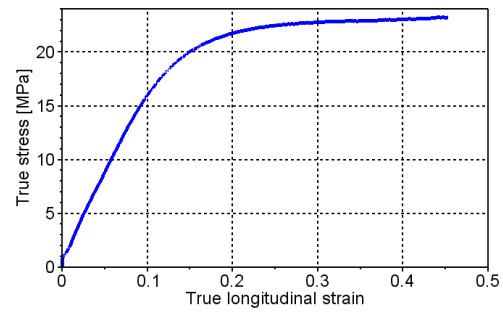
(a) True stress-strain
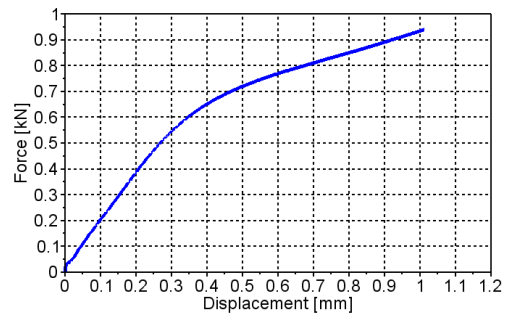
(b) Force-displacement

Figure A.118: Load history

A.2.2   PP1-2-3

	Value	Unit
Initial height [h]	3.05	mm
Initial diameter [D]	6.11	mm
Velocity [v]	0.030	mm/s

Figure A.119: Test specimen
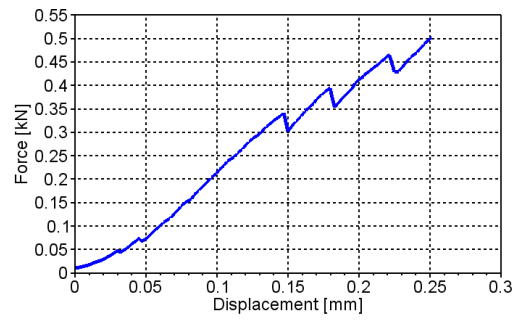
Figure A.120: Force-displacement

A.2.3 PP1-2-4

	Value	Unit
Initial height [h]	3.06	mm
Initial diameter [D]	6.16	mm
Velocity [v]	0.030	mm/s

Figure A.121: Test specimen
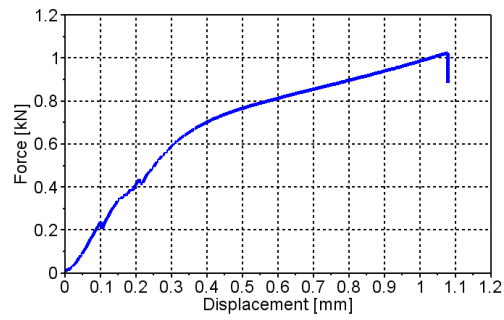
Figure A.122: Force-displacement

A.2.4 PP1-4-2

	Value	Unit
Initial height [h]	3.06	mm
Initial diameter [D]	6.20	mm
Velocity [v]	0.030	mm/s

Figure A.123: Test specimen
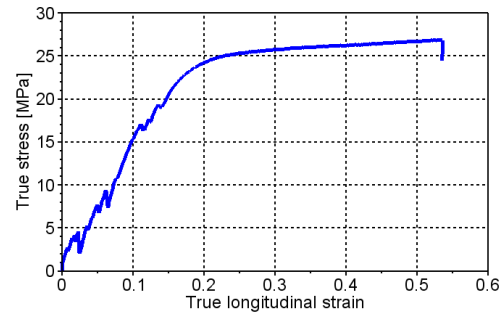
(a) True stress-strain
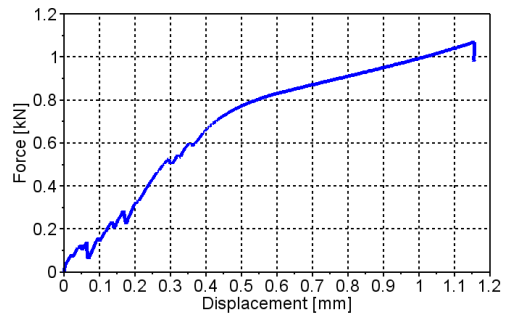
(b) Force-displacement

Figure A.124: Load history

A.2.5   PP1-2-5

	Value	Unit
Initial height [h]	3.06	mm
Initial diameter [D]	6.17	mm
Velocity [v]	0.300	mm/s

Figure A.125: Test specimen
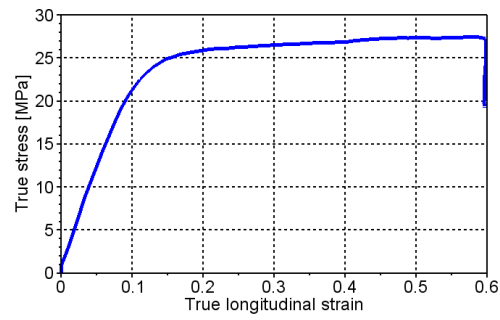
(a) True stress-strain
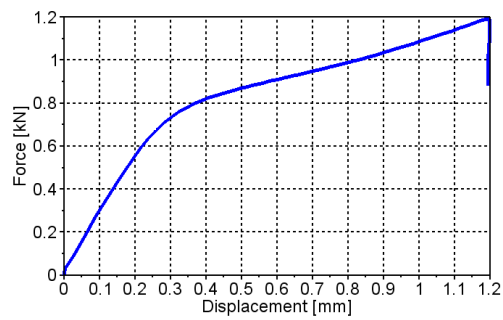
(b) Force-displacement

Figure A.126: Load history

186

A.2.6 PP1-2-6

	Value	Unit
Initial height [h]	3.04	mm
Initial diameter [D]	6.18	mm
Velocity [v]	0.300	mm/s

Figure A.127: Test specimen
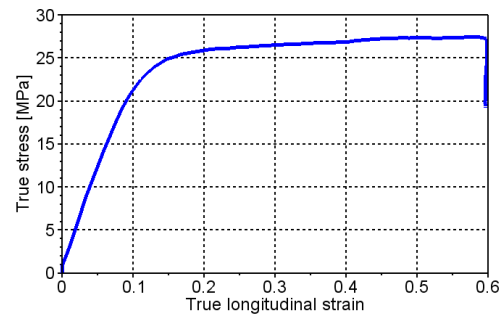
(a) True stress-strain
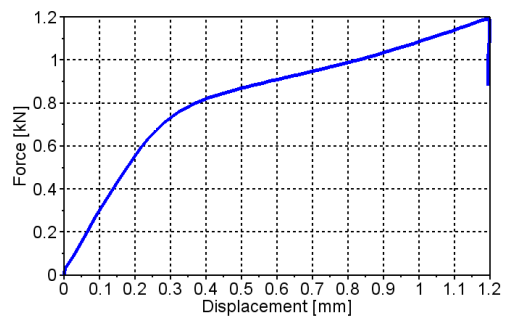
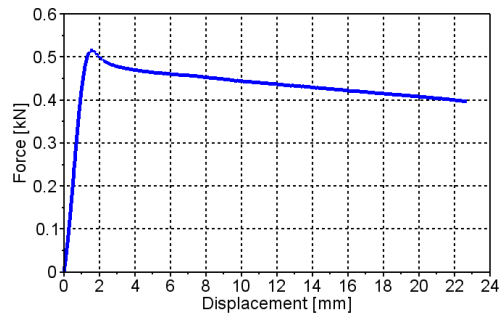(b) Force-displacement

Figure A.128: Load history

A.2.7 PP1-4-1

	Value	Unit
Initial height [h]	3.03	mm
Initial diameter [D]	6.20	mm
Velocity [v]	0.300	mm/s

Figure A.129: Test specimen
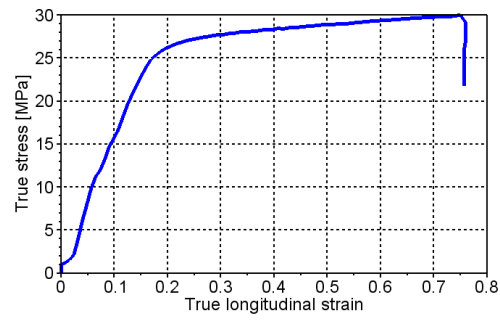
(a) True stress-strain

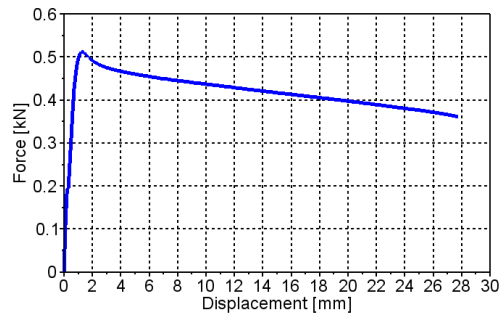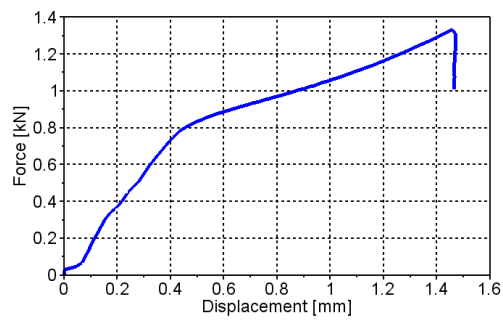
(b) Force-displacement

Figure A.130: Load history

A.3 Notched specimen tests

A.3.1 PP1-N1-L-1

	Value	Unit
Initial thickness [t]	3.17	mm
Initial width [w]	3.12	mm
Velocity [v]	0.20	mm/s

Figure A.131: Test specimen
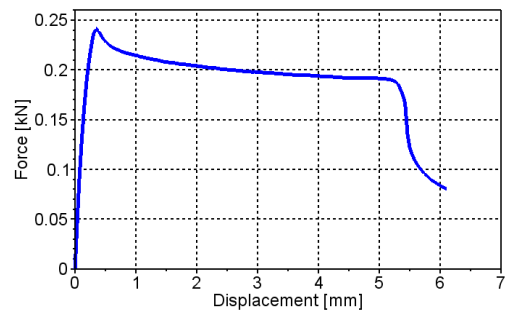
Figure A.132: Force-displacement

A.3.2 PP1-N1-L-2

	Value	Unit
Initial thickness [t]	3.10	mm
Initial width [w]	3.17	mm
Velocity [v]	0.20	mm/s

Figure A.134: Force-displacement

Figure A.133: Test specimen

A.3.3 PP1-N1-T-1

	Value	Unit
Initial thickness [t]	3.13	mm
Initial width [w]	3.19	mm
Velocity [v]	0.20	mm/s

Figure A.135: Test specimen
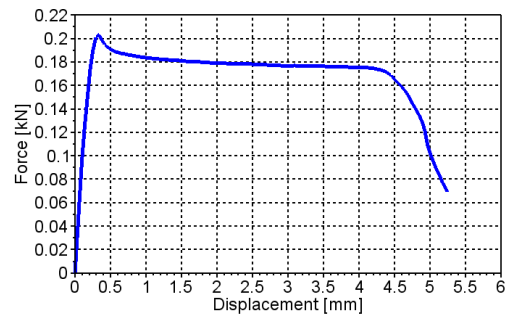
Figure A.136: Force-displacement

A.3.4 PP1-N1-T-2

	Value	Unit
Initial thickness [t]	3.19	mm
Initial width [w]	3.18	mm
Velocity [v]	0.20	mm/s

Figure A.137: Test specimen
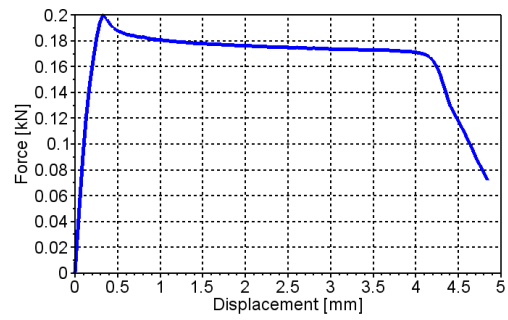
Figure A.138: Force-displacement

A.3.5   PP1-N1-LR-1

	Value	Unit
Initial thickness [t]	2.00	mm
Initial width [w]	3.18	mm
Velocity [v]	0.20	mm/s

Figure A.140: Force-displacement

Figure A.139: Test specimen

A.3.6 PP1-N1-LR-2

	Value	Unit
Initial thickness [t]	2.00	mm
Initial width [w]	3.18	mm
Velocity [v]	0.20	mm/s

Figure A.142: Force-displacement

Figure A.141: Test specimen

A.3.7 PP1-N1-L-4

	Value	Unit
Initial thickness [t]	3.12	mm
Initial width [w]	3.20	mm
Velocity [v]	2.00	mm/s

Figure A.143: Test specimen
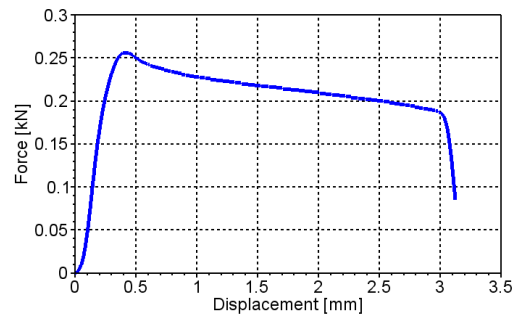
Figure A.144: Force-displacement

A.3.8 PP1-N1-LR-3

	Value	Unit
Initial thickness [t]	1.97	mm
Initial width [w]	3.16	mm
Velocity [v]	2.00	mm/s

Figure A.145: Test specimen
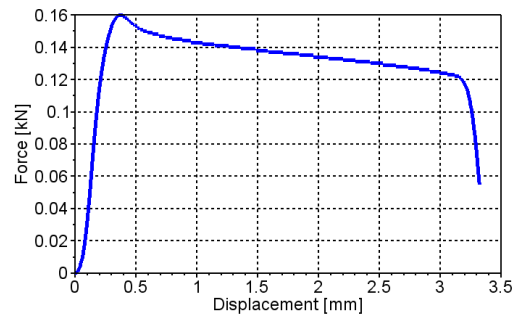
Figure A.146: Force-displacement

A.3.9 PP1-N1-LR-4

	Value	Unit
Initial thickness [t]	1.98	mm
Initial width [w]	3.18	mm
Velocity [v]	2.00	mm/s

Figure A.148: Force-displacement

Figure A.147: Test specimen

A.3.10   PP1-N1-L-5

	Value	Unit
Initial thickness [t]	3.12	mm
Initial width [w]	3.16	mm
Velocity [v]	20.00	mm/s

Figure A.150: Force-displacement

Figure A.149: Test specimen

A.3.11 PP1-N1-L-6

	Value	Unit
Initial thickness [t]	3.11	mm
Initial width [w]	3.18	mm
Velocity [v]	20.00	mm/s

Figure A.151: Test specimen
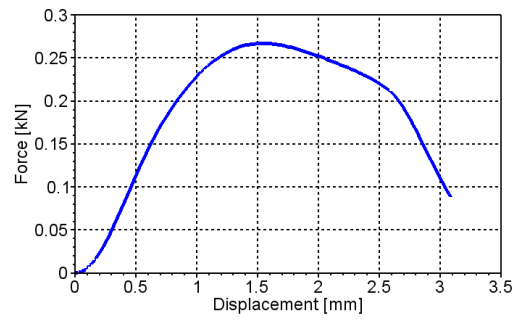
Figure A.152: Force-displacement

A.3.12   PP1-N1-LR-5

	Value	Unit
Initial thickness [t]	1.98	mm
Initial width [w]	3.16	mm
Velocity [v]	20.00	mm/s

Figure A.154: Force-displacement

Figure A.153: Test specimen

A.3.13 PP1-N1-LR-6

	Value	Unit
Initial thickness [t]	1.98	mm
Initial width [w]	3.16	mm
Velocity [v]	20.00	mm/s

Figure A.156: Force-displacement

Figure A.155: Test specimen

A.3.14   PP1-N2-L-1

	Value	Unit
Initial thickness [t]	3.18	mm
Initial width [w]	12.05	mm
Velocity [v]	0.10	mm/s
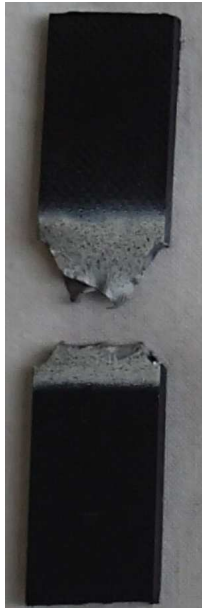
Figure A.157: Test specimen
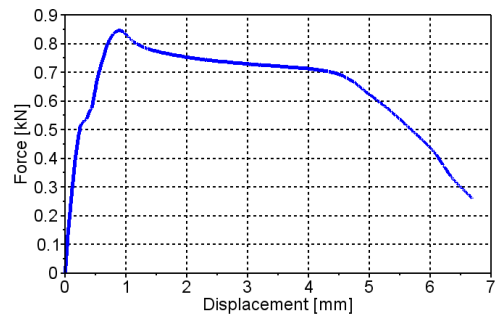
Figure A.158: Force-displacement

A.3.15   PP1-N2-L-2

	Value	Unit
Initial thickness [t]	3.12	mm
Initial width [w]	12.08	mm
Velocity [v]	0.10	mm/s
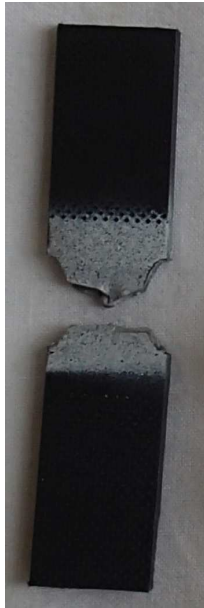
Figure A.159: Test specimen
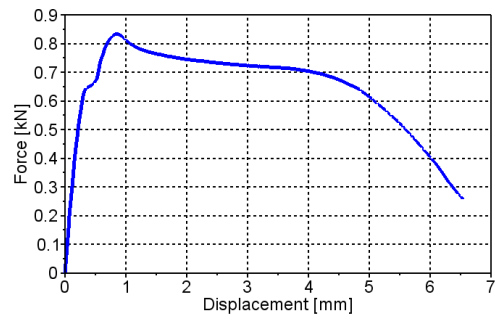
Figure A.160: Force-displacement

A.3.16   PP1-N2-T-1

	Value	Unit
Initial thickness [t]	3.14	mm
Initial width [w]	12.04	mm
Velocity [v]	0.10	mm/s

Figure A.161: Test specimen
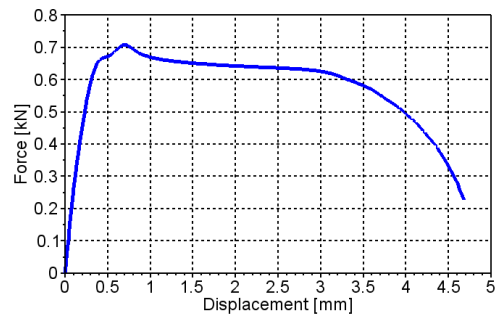
Figure A.162: Force-displacement

A.3.17 PP1-N2-T-2

	Value	Unit
Initial thickness [t]	3.15	mm
Initial width [w]	12.04	mm
Velocity [v]	0.10	mm/s

Figure A.164: Force-displacement

Figure A.163: Test specimen

A.3.18   PP1-N2-LR-1

	Value	Unit
Initial thickness [t]	2.03	mm
Initial width [w]	12.03	mm
Velocity [v]	0.10	mm/s

Figure A.165: Test specimen
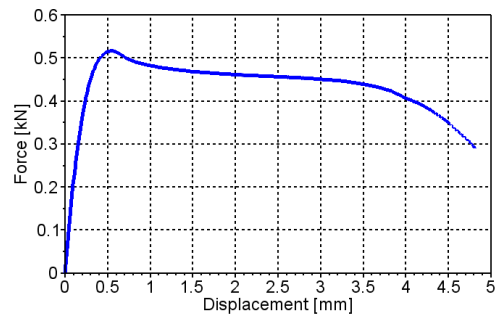
Figure A.166: Force-displacement

A.3.19   PP1-N2-LR-2

	Value	Unit
Initial thickness [t]	2.02	mm
Initial width [w]	12.04	mm
Velocity [v]	0.10	mm/s

Figure A.168: Force-displacement

Figure A.167: Test specimen

A.3.20   PP1-N2-L-3

	Value	Unit
Initial thickness [t]	3.15	mm
Initial width [w]	12.05	mm
Velocity [v]	1.00	mm/s

Figure A.170: Force-displacement

Figure A.169: Test specimen

A.3.21 PP1-N2-L-4

	Value	Unit
Initial thickness [t]	3.13	mm
Initial width [w]	12.06	mm
Velocity [v]	1.00	mm/s

Figure A.172: Force-displacement

Figure A.171: Test specimen

A.3.22 PP1-N2-LR-3

	Value	Unit
Initial thickness [t]	2.03	mm
Initial width [w]	12.04	mm
Velocity [v]	1.00	mm/s

Figure A.174: Force-displacement

Figure A.173: Test specimen

A.3.23   PP1-N2-LR-4

	Value	Unit
Initial thickness [t]	2.03	mm
Initial width [w]	12.06	mm
Velocity [v]	1.00	mm/s

Figure A.176: Force-displacement

Figure A.175: Test specimen

A.3.24   PP1-N2-L-5

	Value	Unit
Initial thickness [t]	3.12	mm
Initial width [w]	12.08	mm
Velocity [v]	10.00	mm/s
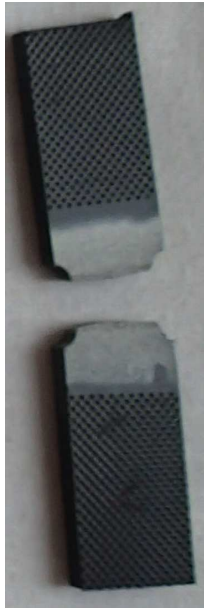
Figure A.177: Test specimen
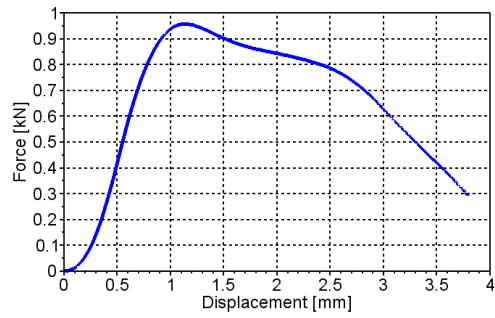
Figure A.178: Force-displacement

A.3.25 PP1-N2-L-6

	Value	Unit
Initial thickness [t]	3.14	mm
Initial width [w]	12.04	mm
Velocity [v]	10.00	mm/s

Figure A.180: Force-displacement

Figure A.179: Test specimen

A.3.26   PP1-N2-LR-5

	Value	Unit
Initial thickness [t]	2.02	mm
Initial width [w]	12.05	mm
Velocity [v]	10.00	mm/s

Figure A.182: Force-displacement

Figure A.181: Test specimen

A.3.27   PP1-N2-LR-6

	Value	Unit
Initial thickness [t]	2.03	mm
Initial width [w]	12.04	mm
Velocity [v]	10.00	mm/s

Figure A.184: Force-displacement

Figure A.183: Test specimen

A.3.28 PP1-N3-L-1

	Value	Unit
Initial thickness [t]	3.10	mm
Initial width [w]	12.02	mm
Velocity [v]	0.15	mm/s

Figure A.186: Force-displacement

Figure A.185: Test specimen

A.3.29   PP1-N3-L-2

	Value	Unit
Initial thickness [t]	3.12	mm
Initial width [w]	12.07	mm
Velocity [v]	0.15	mm/s
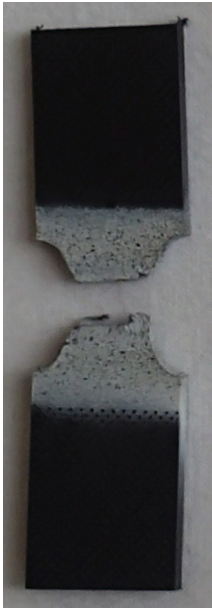
Figure A.187: Test specimen
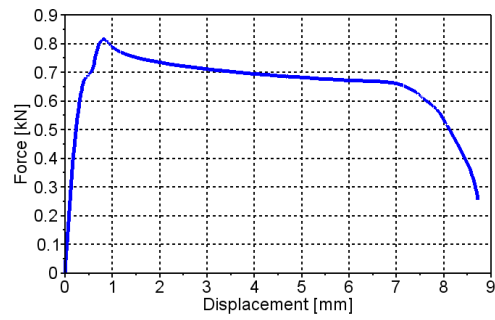
Figure A.188: Force-displacement

A.3.30   PP1-N3-T-1

	Value	Unit
Initial thickness [t]	3.16	mm
Initial width [w]	12.05	mm
Velocity [v]	0.15	mm/s

Figure A.189: Test specimen
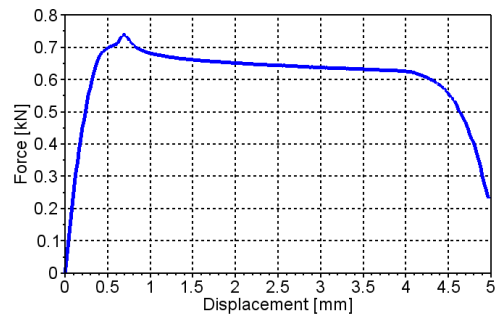
Figure A.190: Force-displacement

A.3.31   PP1-N3-T-2

	Value	Unit
Initial thickness [t]	3.16	mm
Initial width [w]	12.04	mm
Velocity [v]	0.15	mm/s

Figure A.191: Test specimen
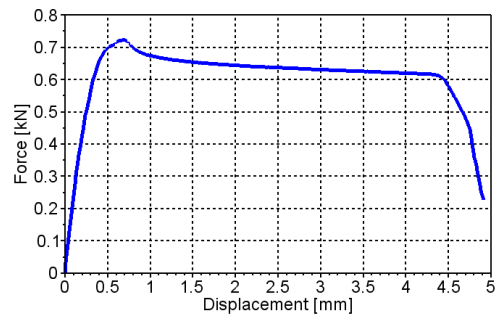
Figure A.192: Force-displacement

A.3.32   PP1-N3-LR-1

	Value	Unit
Initial thickness [t]	2.01	mm
Initial width [w]	12.02	mm
Velocity [v]	0.15	mm/s
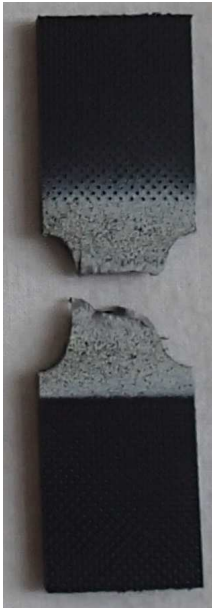
Figure A.193: Test specimen
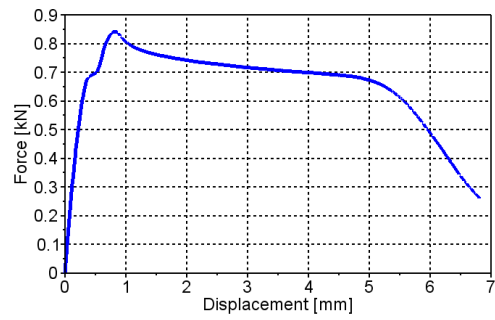
Figure A.194: Force-displacement

A.3.33 PP1-N3-LR-2

	Value	Unit
Initial thickness [t]	2.01	mm
Initial width [w]	12.01	mm
Velocity [v]	0.15	mm/s
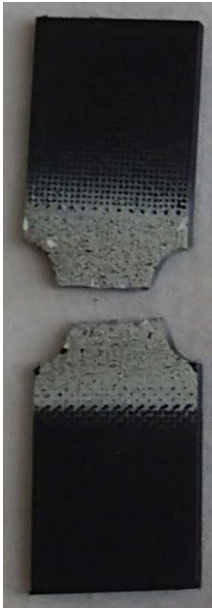
Figure A.195: Test specimen
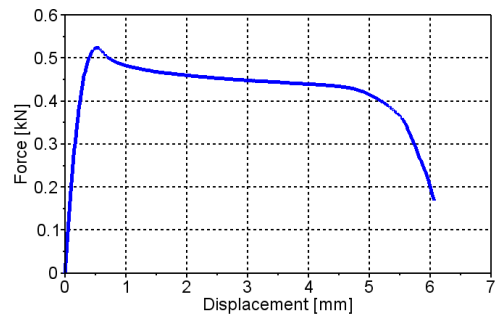
Figure A.196: Force-displacement

A.3.34   PP1-N3-L-3

	Value	Unit
Initial thickness [t]	3.11	mm
Initial width [w]	12.02	mm
Velocity [v]	1.50	mm/s

Figure A.197: Test specimen
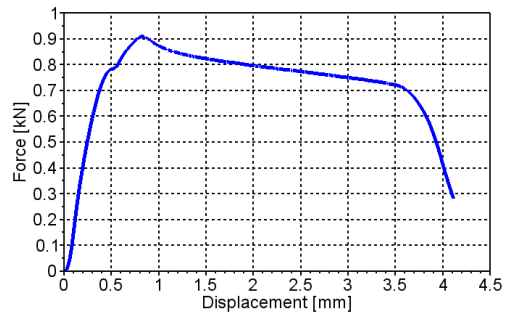
Figure A.198: Force-displacement

A.3.35   PP1-N3-L-4

	Value	Unit
Initial thickness [t]	3.12	mm
Initial width [w]	12.09	mm
Velocity [v]	1.50	mm/s

Figure A.199: Test specimen
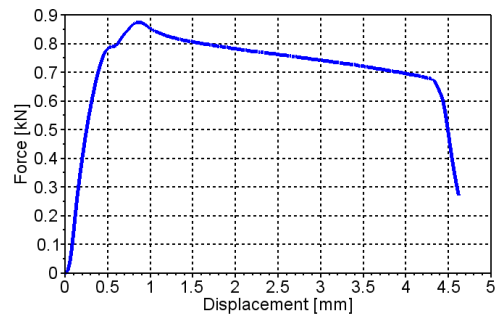
Figure A.200: Force-displacement

A.3.36   PP1-N3-LR-3

	Value	Unit
Initial thickness [t]	2.01	mm
Initial width [w]	12.03	mm
Velocity [v]	1.50	mm/s

Figure A.202: Force-displacement

Figure A.201: Test specimen

A.3.37 PP1-N3-LR-4

	Value	Unit
Initial thickness [t]	2.00	mm
Initial width [w]	12.04	mm
Velocity [v]	1.50	mm/s

Figure A.204: Force-displacement

Figure A.203: Test specimen

A.3.38   PP1-N3-L-5

	Value	Unit
Initial thickness [t]	3.13	mm
Initial width [w]	12.05	mm
Velocity [v]	15.00	mm/s

Figure A.205: Test specimen
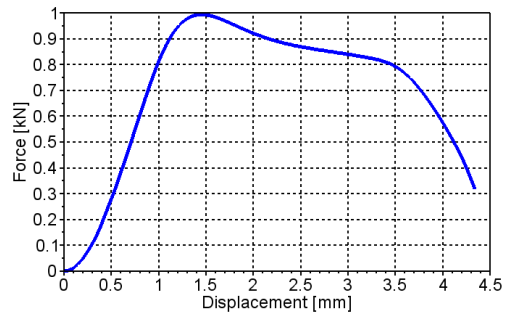
Figure A.206: Force-displacement

A.3.39   PP1-N3-L-6

	Value	Unit
Initial thickness [t]	3.12	mm
Initial width [w]	12.05	mm
Velocity [v]	15.00	mm/s
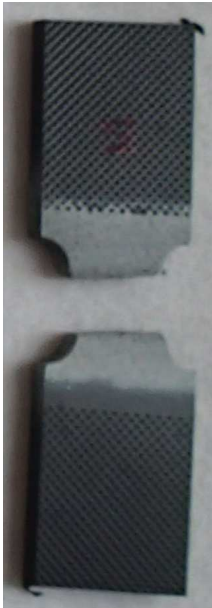
Figure A.207: Test specimen
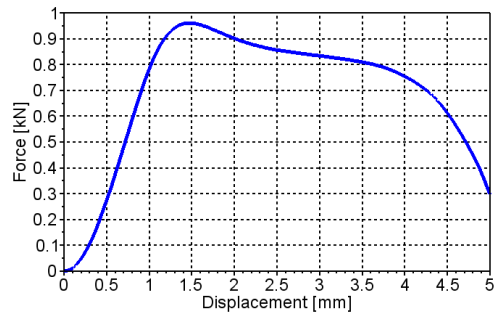
Figure A.208: Force-displacement

A.3.40   PP1-N3-LR-5

	Value	Unit
Initial thickness [t]	2.00	mm
Initial width [w]	12.11	mm
Velocity [v]	15.00	mm/s

Figure A.210: Force-displacement

Figure A.209: Test specimen

A.4 Drop tower tests

A.4.1 PP1-D1-1

	Value	Unit
Mass puncher	5.778	kg
Diameter light opening	80.0	mm
Impact velocity	4.45	m/s
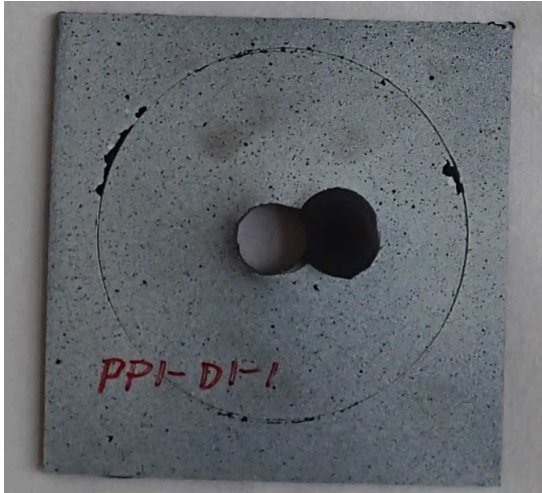
Figure A.211: Test specimen
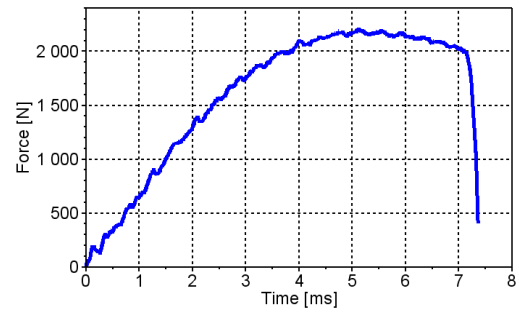
Figure A.212: Force history

A.4.2 PP1-D1-2

	Value	Unit
Mass puncher	5.778	kg
Diameter light opening	80.0	mm
Impact velocity	4.45	m/s

Figure A.213: Test specimen
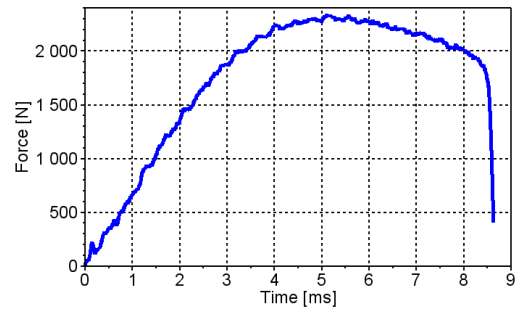
Figure A.214: Force history

A.4.3 PP1-D1-3

	Value	Unit
Mass puncher	5.778	kg
Diameter light opening	80.0	mm
Impact velocity	4.45	m/s

Figure A.215: Test specimen
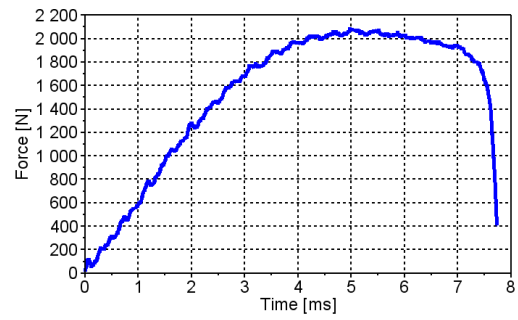
Figure A.216: Force history

A.4.4 PP1-D2-1

	Value	Unit
Mass puncher	5.778	kg
Diameter light opening	80.0	mm
Impact velocity	6.44	m/s

Figure A.217: Test specimen
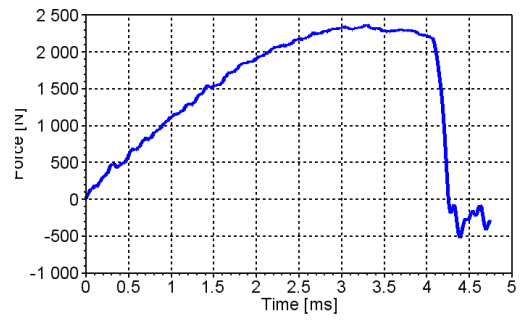
Figure A.218: Force history

A.4.5   PP1-D2-2

	Value	Unit
Mass puncher	5.778	kg
Diameter light opening	80.0	mm
Impact velocity	6.44	m/s
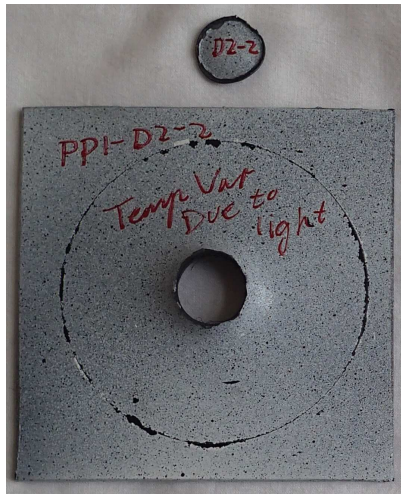
Figure A.219: Test specimen
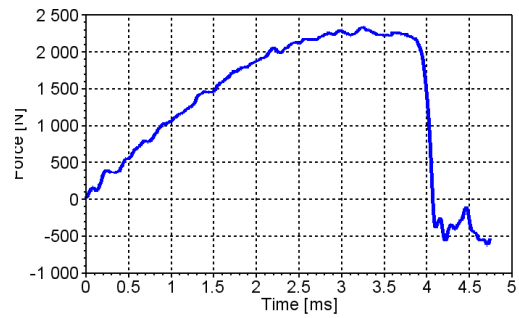
Figure A.220: Force history

A.4.6 PP1-D2-3

	Value	Unit
Mass puncher	5.778	kg
Diameter light opening	80.0	mm
Impact velocity	6.44	m/s
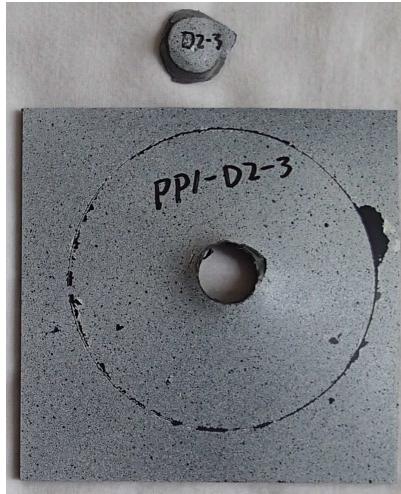
Figure A.221: Test specimen
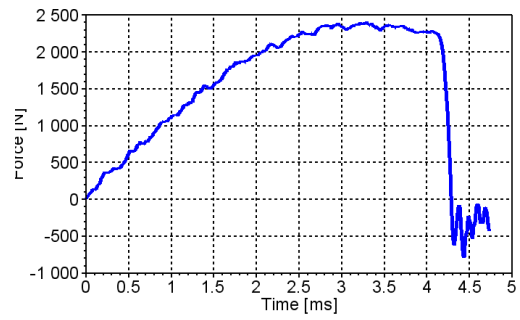
Figure A.222: Force history

Appendix B

Mathematical programming scripts

Mathematical programming scripts were created to perform calculations. These scripts were used to perform the post-processing of the experimental tests, determine key data points and for image processing. The majority of the scripts were created in the mathematical programming language SCILAB, as this is the language mainly used by TOYOTA, but MATLAB was also used.

B.1 SCILAB scripts

B.1.1 Post processing uniaxial tensile

This script removes noise, calculates the true stress, and creates the input file for MatPrePost from the uniaxial tensile tests.

The script:

```
clear; clc;
exec('C:\Users\Heine\Documents\SCILAB files\figurePlot.sci');clc;

saveForce='C:\Users\Heine\Documents\Masteroppgave\Tension_Tests\Force\'
saveFigF='C:\Users\Heine\Documents\Masteroppgave\Tension_Tests\Figures\PP1\Force\'
dirForce='C:\Users\Heine\Documents\Masteroppgave\Tension_Tests\PP1-Test_data\'
n=dir(strcat([dirForce '*_Log.txt'])); nF=size(n(2),1); dirForce=n(2)

dirEps='C:\Users\Heine\Documents\Masteroppgave\Tension_Tests\Strains\Epsilon\'
saveStress='C:\Users\Heine\Documents\Masteroppgave\Tension_Tests\Stress\'

dirInf1='C:\Users\Heine\Documents\Masteroppgave\Tension_Tests...
\Tensile_Test_Description.txt'
dirInf2='C:\Users\Heine\Documents\Masteroppgave\Tension_Tests...
\Tensile_Test_Description-variousThickness.txt'
Information=[dirInf1,dirInf2]
for p=1:size(Information,2)
Inf=mgetl(Information(p))
for i=2:size(Inf,1)
    TID=strsplit(Inf(i),',')
    if p==2 then
        TestName=strcat([TID(1) '-' TID(2) '-' TID(3) '-' TID(4) '-' TID(5)])
    elseif p==1 & TID(4)~='0.67'
        TName=TID(9) //strsplit(TID(9),{'PP1-','PP1T-'}); TName=TName(2)...
 //Given new abbreviations
        TestName=strcat([TID(1) '-' TID(2) '-' TID(3)])
    end
    if TID(1)=='PP1' | TID(1)=='PP1T'  & TID(4)~='0.67' | TID(5)=='T' then
        for j=1:nF
            Test=strsplit(dirForce(j),{'\','-','_'})
            n=size(Test,1)
            if p==1 then
                TestName2=strcat([Test(n-5) '-' Test(n-4) '-' Test(n-3)])
            elseif p==2
                TestName2=strcat([Test(n-7) '-' Test(n-6) '-' Test(n-5) '-' Test(n-4) '-
            end
            if TestName==TestName2 then
                //Writing the Force
                w0=strtod(TID(7))         //Initial width
```

```
                        t0=strtod(TID(6))         //Initial thickness
                        FD=mgetl(dirForce(j))
                        ForceDisplacement=[]
                        Time=[]
                        for k=6:size(FD,1)
                            dataL=strsplit(FD(k),'/\t/')
                            //Setup: [Displacement, Force]
                            if size(dataL,1)>1 then
                                Time=[Time, strtod(dataL(2))]
                                ForceDisplacement=[ForceDisplacement; [dataL(5),dataL(4)]]
                            end
                        end
                        //Writing the stress
                        Eps11=['0']; Eps22=['0']; Eps33=['0']
                        Eps11=[Eps11; mgetl(strcat([dirEps TestName '-Epsilon_11.txt']))]
                        Eps22=[Eps22; mgetl(strcat([dirEps TestName '-Epsilon_22.txt']))]
                        Eps33=[Eps33; mgetl(strcat([dirEps TestName '-Epsilon_33.txt']))]
                        if size(Eps22,1)~=size(Eps33,1) then
                            Eps33=Eps22
                        end
                        StressStrain=[]
                        if size(Eps11,1)>=size(ForceDisplacement,1) then
                            N=size(ForceDisplacement,1)
                        elseif size(Eps11,1)<size(ForceDisplacement,1)
                            N=size(Eps11,1)
                        end
                        //[Time, Epsilon_11, Epsilon_22, Epsilon_33, Sigma_e, Sigma_t]
                        for k=1:N
                            w=w0*%e^strtod(Eps22(k))
                            t=t0*%e^strtod(Eps33(k))
                            sigma_t=(strtod(ForceDisplacement(k,2))*1000)/(w*t)
//True stress
                            sigma_e=(strtod(ForceDisplacement(k,2))*1000)/(w0*t0)
//Engineering stress
                            StressStrain=[StressStrain; [Time(k),strtod(Eps11(k)),...
strtod(Eps22(k)),strtod(Eps33(k)),sigma_e,sigma_t]]
                        end
                        n=size(StressStrain,1)
                        Info=[strtod(ForceDisplacement(1:n,:)),StressStrain]
//Info=[Displacement, Force, Time, Eps11, Eps22, Eps33, Sigma_e, Sigma_t]
                        Output=[]
                        for k=1:size(Info,1)
                            if Info(k,2)>0 then       //Positive force
                                Output=[Output; Info(k,:)]
                            end
                        end
                        if p==1 then
                            fracFrame=strtod(strsplit(mgetl(strcat...
```

```
([ 'C:\Users\Heine\Documents\Masteroppgave\Tension_Tests\Strains\FractureFrameNumber\' Tl
        elseif p==2
            fracFrame=strtod(strsplit(mgetl(strcat ...
([ 'C:\Users\Heine\Documents\Masteroppgave\Tension_Tests\Strains\FractureFrameNumber\' Tl
        end
        yieldStrain=Eps11(fracFrame(1))
        initial_frac=Eps11(fracFrame(2))
        fracture=Eps11(fracFrame(3))
        output=[]
        for k=1:size(Output,1)
            if Output(k,4)<strtod(fracture) then
                output=[output; Output(k,:)]
            end
        end

        Output=[]
        a=output
        no=size(output,1)
        [m2,n2]=max(output(floor(no*0.94):no,size(output,2)))
        n2=floor(no*0.94)+n2
        for k=1:size(output,1)
            if k<n2 then
                Output=[Output; output(k,:)]
            end
        end
        output=Output
        b=output
        Output=[]
        output0=[output(1,:)]
        for k=1:size(output,1)
            Output=[Output; output(k,:)-output0]
        end
        output=[]
        for k=1:size(Output,1)
            if Output(k,(1:2))>0 then
                output=[output; Output(k,:)]
            end
        end
        Output=[]
        for k=1:size(output,1)
            if k==1 then
                Output=[Output; [zeros(1,size(output,2))]]
            elseif k>1 & output(k,(1:2))>0 & output(k,4)>0 &...
output(k,size(output,2))>0
                Output=[Output; output(k,:)]
            end
        end
        for k=1:size(Output,1)
```

238

```
            end

            ForceDisplacement=[Output(:,(1:2))]
            StressStrain=[Output(:,(3:size(Output,2)))]
            if p==1 then
                TestName=TName
            end
            destFile=strcat([saveForce 'Force-Displacement_' TestName '.txt'])
            csvWrite(ForceDisplacement,destFile)

            destFile=strcat([saveStress 'Stress-Strain_' TestName '.txt'])
            csvWrite(StressStrain,destFile)
        end
      end
    end
end
end
```

B.1.2 Post processing notched tests

This script removes noise from the experimental results for the notched tests.

The script:

```
clear; clc;
exec('C:\Users\Heine\Documents\SCILAB files\figurePlot.sci'); clc;

saveForce='C:\Users\Heine\Documents\Masteroppgave\Tension_Tests\Force\Notched\'
dirForce='C:\Users\Heine\Documents\Masteroppgave\Tension_Tests\PP1-Test_data\Notched\'

dirEps='C:\Users\Heine\Documents\Masteroppgave\Tension_Tests\Strains\Epsilon\Notched\'
saveStress='C:\Users\Heine\Documents\Masteroppgave\Tension_Tests\Stress\Notched\'

dirInf='C:\Users\Heine\Documents\Masteroppgave\Tension_Tests\Notched_Test_Description.tx

Inf=mgetl(dirInf)
for i=2:size(Inf,1)
    TID=strsplit(Inf(i),','); Tname=TID(1);
    TestData=mgetl(strcat([dirForce Tname '_Log.txt']))
    w0=strtod(TID(4))
    t0=strtod(TID(3))

    ForceDisplacement=[]
    Time=[]
    for k=1:size(TestData,1)
      dataL=strsplit(TestData(k),',')
      //Setup: [Displacement, Force]
      if size(dataL,1)>1 then
          Time=[Time, strtod(dataL(2))]
          ForceDisplacement=[ForceDisplacement; [dataL(4),dataL(3)]]
      end
    end
    FD=strtod(ForceDisplacement)
    [Max, n]=max(FD(:,2))
    fd=[]
    for j=1:size(FD,1)
        if j<(0.4*n) then
            fd=[fd; [FD(j,1),FD(j,2)]]
        elseif j>=(0.4*n) & FD(j,2)>(0.3*Max)
            fd=[fd; [FD(j,1),FD(j,2)]]
        end
    end
    fd0=fd(1,:)
    FD=[]
    for j=1:size(fd,1)
```

```
        if  fd(j,1)-fd0(1)>=0 & fd(j,2)-fd0(2)>=0  then
            FD=[FD;  fd(j,:)-fd0]
        end
    end
//Writing the stress
nEps=dir(strcat([dirEps  'DIC-' Tname '*'])); nEps=size(nEps(2),1);
if nEps==3 then
    Eps11=[]; Eps22=[]; Eps33=[]
    Eps11=[Eps11; mgetl(strcat([dirEps  'DIC-' Tname '-Epsilon_11.txt']))]
    Eps22=[Eps22; mgetl(strcat([dirEps  'DIC-' Tname '-Epsilon_22.txt']))]
    Eps33=[Eps33; mgetl(strcat([dirEps  'DIC-' Tname '-Epsilon_33.txt']))]
    if  size(Eps22,1)~=size(Eps33,1)  then
            Eps33=Eps22
    end
elseif nEps==2
    Eps11=[]; Eps22=[];
    Eps11=[Eps11; mgetl(strcat([dirEps  'DIC-' Tname '-Epsilon_11.txt']))]
    Eps22=[Eps22; mgetl(strcat([dirEps  'DIC-' Tname '-Epsilon_22.txt']))]
    Eps33=Eps22;
end
    StressStrain =[]
    if  size(Eps11,1)>=size(ForceDisplacement,1)  then
          N=size(ForceDisplacement,1)
    elseif  size(Eps11,1)<size(ForceDisplacement,1)
          N=size(Eps11,1)
    end
    //[Time, Epsilon_11, Epsilon_22, Epsilon_33, Sigma_e, Sigma_t]
    for k=1:N
        w=w0*%e^strtod(Eps22(k))
        t=t0*%e^strtod(Eps33(k))
        sigma_t=(strtod(ForceDisplacement(k,2))*1000)/(w*t)      //True stress
        sigma_e=(strtod(ForceDisplacement(k,2))*1000)/(w0*t0)   //Engineering stress
        StressStrain =[StressStrain ; [Time(k),strtod(Eps11(k)),strtod(Eps22(k)),strtod(E
    end
    n=size(StressStrain,1)
    Info=[strtod(ForceDisplacement(1:n,:)),StressStrain]
//Info=[Displacement, Force, Time, Eps11, Eps22, Eps33, Sigma_e, Sigma_t]
    Output =[]
    for k=1:size(Info,1)
        if Info(k,2)>0 then      //Positive force
            Output=[Output; Info(k,:)]
        end
    end
    fracFrame=strtod(strsplit(mgetl(strcat(['C:\Users\Heine\Documents\Masteroppgave\Ten
    if fracFrame(3)>N then
        fracture=Eps11(floor(0.95*N))
    else
        yieldStrain=Eps11(fracFrame(1))
```

241

```
    initial_frac=Eps11(fracFrame(2))
    fracture=Eps11(fracFrame(3))
end

output=[]
for k=1:size(Output,1)
    if Output(k,4)<strtod(fracture) then
        output=[output; Output(k,:)]
    end
end
Output=[]
a=output
no=size(output,1)
[m2,n2]=max(output(floor(no*0.94):no,size(output,2)))
n2=floor(no*0.94)+n2
for k=1:size(output,1)
    if k<n2 then
        Output=[Output; output(k,:)]
    end
end
output=Output
b=output
Output=[]
output0=[output(1,:)]
for k=1:size(output,1)
    Output=[Output; output(k,:)-output0]
end
output=[]
for k=1:size(Output,1)
    if Output(k,(1:2))>0 then
        output=[output; Output(k,:)]
    end
end
Output=[]
for k=1:size(output,1)
    if k==1 then
        Output=[Output; [zeros(1,size(output,2))]]
    elseif k>1 & output(k,(1:2))>0 & output(k,4)>0 & output(k,size(output,2))>0
        Output=[Output; output(k,:)]
    end
end
for k=1:size(Output,1)

end

ForceDisplacement=[Output(:,(1:2))]
StressStrain=[Output(:,(3:size(Output,2)))]
destFile=strcat([saveForce 'Force-Displacement_' Tname '_V=' TID(2) '.txt'])
```

```
csvWrite (FD, destFile )

destFile=strcat ([ saveStress  'Stress-Strain_' Tname '_V=' TID(2)  '. txt '])
csvWrite ( StressStrain , destFile )
end
```

B.1.3   Determining fracture damage

This script determines the fracture damage for the uniaxile tensile tests and the notched tests.

The script:

```
clear; clc;

folderFracStrains='C:\Users\Heine\Documents\Masteroppgave\Tension_Tests\Strains...
\FractureStrains\Notched\'
folderStrains='C:\Users\Heine\Documents\Masteroppgave\Tension_Tests\...
Stress\Notched\'
dirSave='C:\Users\Heine\Documents\Masteroppgave\Tension_Tests\Strains\...
FractureStrains\Notched\Fracture damage\'

Tests=dir(strcat([folderFracStrains '*.txt'])); Tests=Tests(2);

for t=1:size(Tests,1)
    TData=mgetl(Tests(t))
    for d=1:size(TData,1)
        Test=strsplit(TData(d),',')
        Tname=Test(1); Initial_fracture=Test(3); Fracture=Test(4);
        FoldStrains=dir(strcat([folderStrains '*.txt']))
        FoldStrains=FoldStrains(2)
        for i=1:size(FoldStrains,1)
            Strain=strsplit(FoldStrains(i),'_')
            if Strain(3)==Tname then
                V=strsplit(Strain(4),{'.t','='}); V=V(2)
                Strains=mgetl(FoldStrains(i))
                if V=='0.10' | V=='0.15' | V=='0.20' then
                    Velocity='V3'
                elseif V=='1.00' | V=='1.50' | V=='2.00'
                    Velocity='V2'
                elseif V=='10.00' | V=='15.00' | V=='20.00'
                    Velocity='V1'
                end
            end
        end
//Strains=mgetl(strcat([folderStrains 'Stress-Strain_' Tname '.txt'])) //Dog-Bone
        D_Initial=0; D_Fracture=0;
        Initial_input=[]; Fracture_input=[];
        for i=1:size(Strains,1)
            DataL=strsplit(Strains(i),',')
            if DataL(2)==Initial_fracture then
                Eps_V=strtod(DataL(2))+strtod(DataL(3))+strtod(DataL(4))
                D_Initial=1-(1/(%e^Eps_V))
            elseif DataL(2)==Fracture
```

244

```
                Eps_V=strtod(DataL(2))+strtod(DataL(3))+strtod(DataL(4))
                D_Fracture=1-(1/(%e^Eps_V))
            elseif i==size(Strains,1) & D_Fracture==0
                Eps_V=strtod(DataL(2))+strtod(DataL(3))+strtod(DataL(4))
                D_Fracture=1-(1/(%e^Eps_V))
            end
        end
        if D_Initial>0 then
            Initial_input=[Initial_fracture, string(D_Initial)]
            destFile=strcat([dirSave 'Initial_Damage_' Tname...
             '-' Velocity '.txt'])
            csvWrite(Initial_fracture,destFile)
        end
        if D_Fracture>0 then
            Fracture_input=[Fracture, string(D_Fracture)]
            destFile=strcat([dirSave 'Fracture_Damage_' Tname '_' V '.txt'])
            csvWrite(Fracture_input,destFile)
        end
    end
end
```

B.1.4 Uniaxial tensile, LS-Dyna vs. experimental tests

This script compares the results from the uniaxial tensile LS-Dyna simulations with the results from the experimental tests.

The script:

```
clear; clc;
exec('C:\Users\Heine\Documents\SCILAB files\figurePlot.sci'); clc;

DirLSDyna='C:\Users\Heine\Documents\Masteroppgave\Numerical Simulations...
\Varying velocity\Results MatPrePost Output\'
DirFD='C:\Users\Heine\Documents\Masteroppgave\Tension_Tests\Figures\PP1...
\Force\InputFig\'
DirSS='C:\Users\Heine\Documents\Masteroppgave\Tension_Tests\Figures\PP1...
\True stress\InputFig\'
dirSave='C:\Users\Heine\Documents\Masteroppgave\Numerical Simulations...
\Varying velocity\Results MatPrePost Output\Figures\'

CS='R'

//T1='PP1-T2-F-V1-2'; T2='PP1-T2-F-V2-4'; T3='PP1-T2-F-V3-1' //2mm Full specimens
//T1='PP1-T3-F-V1-1'; T2='PP1-T3-F-V2-1'; T3='PP1-T3-F-V3-3' //3mm Full specimens
T1='PP1-T3-R-V1-1'; T2='PP1-T3-R-V2-1'; T3='PP1-T3-R-V3-1' //3mm Reduced-Core
//T1='PP1-T4-F-V1-3'; T2='PP1-T4-F-V2-3'; T3='PP1-T4-F-V3-1' //4mm Full specimens

Tests=[T2]
S1='0.1'; S2='0.01'; S3='0.001';
Strains=[S2]

Legendinfo_1=[]; Legendinfo_2=[]
for v=1:size(Strains,2)
    DynaF=mgetl(strcat([DirLSDyna 'Force-PP1-' Strains(v) '-' CS '-L.txt']))
    DynaD=mgetl(strcat([DirLSDyna 'Displacement-PP1-' Strains(v) '-' CS '-L.txt']))
    TestFD=mgetl(strcat([DirFD 'Force-Displacement_' Tests(v) '.txt']))

    //comparing force-displacement
    figure(1)

    Title='Skin-Core_Force-Displacement_LS-Dyna_vs_Tests'
    Xlabel='Displacement [mm]'
    Ylabel='Force [N]'

    TForce=[]
    TDisplacement=[]
    nFD=size(TestFD,1)
    for i=1:nFD
        DataRow=strsplit(TestFD(i),',')      //[Displacement,Force]
```

```
        TForce=[TForce, strtod(DataRow(2))*1000]
        TDisplacement=[TDisplacement, strtod(DataRow(1))]
    end
    Legendinfo_1=[Legendinfo_1, strcat(['$\text{Test, }\dot{\varepsilon}_0...
    \text{=' Strains(v) '}$'])]
    figurePlot(TDisplacement,TForce,Title,Xlabel,Ylabel,Legendinfo_1,...
    dirSave,'--',4)

    Time=[]
    Displacement=[]
    Force=[]
    if size(DynaF,1)>size(DynaD,1) then
        nDyna=size(DynaD,1)
    else
        nDyna=size(DynaF,1)
    end
    for i=1:nDyna
        DynaForce=4*strtod(DynaF(i))
        DynaDisplacement=strtod(DynaD(i))

        Displacement=[Displacement, DynaDisplacement]
        Force=[Force, DynaForce]
    end
    Legendinfo_1=[Legendinfo_1, strcat(['$\text{LS-Dyna, }...
    \dot{\varepsilon}_0\text{=' Strains(v) '}$'])]

    figurePlot(Displacement,Force,Title,Xlabel,Ylabel,Legendinfo_1,dirSave,'-',4)

    //Comparing stress-strain
    DynaStrain=mgetl(strcat([DirLSDyna 'Strain-PP1-' Strains(v) '-' CS '-L.txt']))
    DynaStress=mgetl(strcat([DirLSDyna 'X-stress-PP1-' Strains(v) '-' CS '-L.txt']))
    TestSS=mgetl(strcat([DirSS 'Stress-Strain_' Tests(v) '.txt']))

    figure(2)
    Xlabel=['True longitudinal strain']
    Ylabel=['True stress [MPa]']
    Title='Skin-Core_Stress-Strain_LS-Dyna_vs_Tests'

    //Strain rate=0.1
    TStrain=[];
    TStress=[];
    for i=1:size(TestSS,1)
        TestData=strsplit(TestSS(i),',')
        if strtod(TestData(1))>0 then
            TStrain=[TStrain; strtod(TestData(1))]
            TStress=[TStress; strtod(TestData(4))]
        end
    end
```

247

```
Legendinfo_2=[Legendinfo_2 , strcat(['$\text{Test, }\dot{\varepsilon}_0 ...
\text{=' Strains(v) '}$'])]

figurePlot(TStrain , TStress , Title , Xlabel , Ylabel , Legendinfo_2 , dirSave ,'−−',4)

//XX−strain , YY−strain , ZZ−strain , volume−strain
LSStrainXX =[]; LSStrainYY =[]; LSStrainZZ=[]; LSStrainV =[]
LSStress =[]
for i=1:size(DynaStrain ,1)
    StrainData=strtod(strsplit(DynaStrain(i),','))
    Vstrain=StrainData(1)+StrainData(2)+StrainData(3)
    LSStrainXX =[LSStrainXX ; StrainData(1)]
    LSStrainYY =[LSStrainYY ; StrainData(2)]
    LSStrainZZ=[LSStrainZZ; StrainData(3)]
    LSStrainV =[LSStrainV ; Vstrain ]
    LSStress =[LSStress ; strtod(DynaStress(i))]
end
Legendinfo_2=[Legendinfo_2 , strcat(['$\text{LS−Dyna, }\dot{\varepsilon}_0 ...
\text{=' Strains(v) '}$'])]
figurePlot(LSStrainXX , LSStress , Title , Xlabel , Ylabel , Legendinfo_2 , dirSave ,'−',4)

if Strains(v)=='0.01' then
    //comparing volumetric strains
    figure(3)

    Legendinfo_3 =[]
    Xlabel='Longitudinal strain '
    Ylabel='Volumetric strain '
    Title='Skin−Core_Volumetric_strain_LS−Dyna_vs_Tests '
    Legendinfo_3=[Legendinfo_3 , strcat(['$\text{LS−Dyna, }...
    \dot{\varepsilon}_0\text{=' Strains(v) '}$'])]
    figurePlot(LSStrainXX , LSStrainV , Title , Xlabel , Ylabel , Legendinfo_3 , dirSave ,'−',4)

    Txstrain =[]
    Tystrain =[]
    Tzstrain =[]
    TVstrain =[]

    dataLoc=strcat([DirSS 'Stress−Strain_' Tests(v) '.txt '])
    data=mgetl(dataLoc)
    for i=1:size(data ,1)
        dataL=strsplit(data(i),',')
        Txstrain=[Txstrain; strtod(dataL(1))]
        Tystrain=[Tystrain; strtod(dataL(2))]
        Tzstrain =[Tzstrain ; strtod(dataL(3))]
    end

    for i=1:size(Txstrain ,1)
```

```
        TVstrain=[TVstrain; [Txstrain(i)+Tystrain(i)+Tzstrain(i)]]
    end

    Legendinfo_3=[Legendinfo_3,strcat(['$\text{Test, }...
    \dot{\varepsilon}_0\text{=' Strains(v) '}$'])]
    figurePlot(Txstrain,TVstrain,Title,Xlabel,Ylabel,Legendinfo_3,dirSave,'--',4)

    //Comparing retraction ratios
    figure(4)
    Legendinfo_4=[]
    Xlabel='Longitudinal strain'
    Ylabel='Retraction ratio'
    Title='Skin-Core_Retraction_ratio_LS-Dyna_vs_Tests'

    R22=[]; R33=[];
    nDyna=size(LSStrainXX,1)
    for i=2:nDyna
        R22=[R22; -(LSStrainYY(i)/LSStrainXX(i))]
        R33=[R33; -(LSStrainZZ(i)/LSStrainXX(i))]
    end

    Legendinfo_4=[Legendinfo_4,strcat(['$\text{LS-Dyna, }...
    \dot{\varepsilon}_0\text{=' Strains(v) '}$'])]
    figurePlot(LSStrainXX(2:nDyna),R22,Title,Xlabel,Ylabel,Legendinfo_4,dirSave,'-'
    //Legendinfo_4=[Legendinfo_4,strcat(['$\text{LS-Dyna, }R_{33}\text{ }...
    \dot{\varepsilon}_0\text{=' Strains(v) '}$'])]
    //figurePlot(LSStrainXX(2:nDyna),R33,Title,Xlabel,Ylabel,Legendinfo_4,...
    dirSave,'-',1)
    R=[]
    nTest=size(Txstrain,1)
    nstart=round(0.05*nTest)
    for i=nstart:nTest
        R=[R;(-Tystrain(i)/Txstrain(i))]
    end

    Legendinfo_4=[Legendinfo_4,strcat(['$\text{Test-R}_{22}\text{, }...
    \dot{\varepsilon}_0\text{=' Strains(v) '}$'])]
    figurePlot(Txstrain(nstart:nTest),R,Title,Xlabel,Ylabel,Legendinfo_4,dirSave,'-

    R=[]
    nTest=size(Txstrain,1)
    for i=nstart:nTest
        R=[R;(-Tzstrain(i)/Txstrain(i))]
    end

    //Legendinfo_4=[Legendinfo_4,strcat(['$\text{Test-R}_{33}\text{, }\dot{\varepsil
    //figurePlot(Txstrain(nstart:nTest),R,Title,Xlabel,Ylabel,Legendinfo_4,dirSave,'
end
```

end

B.1.5 Uniaxial compression, LS-Dyna vs. experimental tests

This script compares the results from the uniaxial compression LS-Dyna simulations with the results from the experimental tests.

The script:

```
clear; clc;
exec('C:\Users\Heine\Documents\SCILAB files\figurePlot.sci'); clc;

DirLSDyna='C:\Users\Heine\Documents\Masteroppgave\Numerical Simulations\...
LS-Dyna_Results\Compression\'
DirFD='C:\Users\Heine\Documents\Masteroppgave\Compression Tests\Force\'
DirSS='C:\Users\Heine\Documents\Masteroppgave\Compression Tests\Stress...
 Strain Data\True stress\'
dirSave='C:\Users\Heine\Documents\Masteroppgave\Compression Tests\Figures...
\Test vs LS-Dyna\'

S3='0.001'; S2='0.01'; S1='0.1'
T3='PP1-2-2'; T2='PP1-4-2'; T1='PP1-2-5'

strains=[S3,S2,S1]
tests=[T3,T2,T1]
Legend1=[]

for t=1:size(strains,2)
    DynaFv=mgetl(strcat([DirLSDyna 'Force-Compression_dEps=' strains(t) '.txt']))
    DynaDv=mgetl(strcat([DirLSDyna 'Displacement-Compression_dEps=' strains(t) '.txt']))
    TestFDv=mgetl(strcat([DirFD tests(t) '.txt']))
    //%%%%%%%%%% Comparing Force-Displacement %%%%%%%%%%
    figure(1)
    Legend=[]
    Title='Compression_Force-Displacement_LS-Dyna_vs_Tests'
    Xlabel='Displacement [mm]'
    Ylabel='Force [N]'

    Test_Force=[]
    Test_Displacement=[]
    nT=size(TestFDv,1)
    for i=1:nT
        dataL=strtod(strsplit(TestFDv(i),','))
        Test_Force=[Test_Force; abs(dataL(3))*1000]
        Test_Displacement=[Test_Displacement; abs(dataL(4))]
    end
    Legend=[Legend,'Test']
    figurePlot(Test_Displacement,Test_Force,Title,Xlabel,Ylabel,Legend,dirSave,'--',4)

    Dyna_Force=abs(strtod(DynaFv)*4)
```

```
Dyna_Displacement=abs(strtod(DynaDv))
Legend=[Legend , 'LS−Dyna']
figurePlot(Dyna_Displacement , Dyna_Force , Title , Xlabel , Ylabel , Legend , dirSave ,'−',4)

//%%%%%%%% Comparing Stress−Strain %%%%%%%%%
DynaStrain=mgetl(strcat([DirLSDyna 'Strain−Compression_dEps=' strains(t) '.txt']))
DynaStress=mgetl(strcat([DirLSDyna 'X−stress −Compression_dEps=' strains(t) '.txt']))
TestSS=mgetl(strcat([DirSS 'Compression−' tests(t) '_stress−strain.txt']))

figure(2)
Legend=[]

Xlabel=['True longitudinal strain']
Ylabel=['True stress [MPa]']
Title='Compression_Stress−Strain_LS−Dyna_vs_Tests'

Test_strain =[]; Test_stress =[]; Test_R =[]; Test_V =[];
for i=3:size(TestSS,1)
    dataL=strtod(strsplit(TestSS(i),','))
    Test_strain =[Test_strain; dataL(1)]
    Test_stress=[Test_stress; dataL(2)]
    Test_R =[Test_R; [dataL(1),dataL(3)]]
  Eps_V=−dataL(1)+(2*dataL(3))
  Test_V =[Test_V; [dataL(1), Eps_V]]
end
Legend=[Legend , 'Test']
figurePlot(Test_strain , Test_stress , Title , Xlabel , Ylabel , Legend , dirSave ,'−−',4)
Dyna_strain =[0]; Dyna_R =[]; Dyna_V =[];
for i=2:size(DynaStrain,1)
    dataL=abs(strtod(strsplit(DynaStrain(i),',')))
    Dyna_strain =[Dyna_strain; dataL(3)]
  R=log(dataL(2)/dataL(3))
    Dyna_R=[Dyna_R; [dataL(3), R]]
  Eps_V=−dataL(1)+dataL(2)+dataL(3)
  Dyna_V=[Dyna_V; [dataL(1), Eps_V]]
end
Dyna_stress=abs(strtod(DynaStress))
Legend=[Legend , 'LS−Dyna']
figurePlot(Dyna_strain , Dyna_stress , Title , Xlabel , Ylabel , Legend , dirSave ,'−',4)

//%%%%%%%%% Comparing Retraction−Ratio %%%%%%%%%
figure(3)
Legend=[]

Xlabel=['True longitudinal strain']
Ylabel=['Retraction ratio ']
Title='Compression_Retraction_ratio LS−Dyna vs. Tests'
R=[]
```

```
    for i=1:size(Test_R,1)
        if Test_R(i,1)>0.05 then
            R=[R; Test_R(i,:)]
        end
    end

    //Legend=[Legend, 'Test']
    //figurePlot(R(:,1),R(:,2),Title,Xlabel,Ylabel,Legend,dirSave,'--',4)

    //R=[]
    //for i=1:size(Dyna_R,1)
    //    if Test_R(i,1)>0.05 then
    //        R=[R; abs(Dyna_R(i,:))]
    //    end
    //end

    //Legend=[Legend, 'LS-Dyna']
    //figurePlot(R(:,1),R(:,2),Title,Xlabel,Ylabel,Legend,dirSave,'--',4)

    //%%%%%%%%%% Comparing Volumetric strain %%%%%%%%%%
    figure(4)
    Legend=[]

    Xlabel=['True longitudinal strain']
    Ylabel=['Volumetric strain ']
    Title='Compression_volumetric_strain_LS-Dyna_vs_Tests'

    Legend1=[Legend1, strcat(['$\text{Test-}\dot{\varepsilon}_0=' strains(t) '$'])]
    figurePlot(Test_V(:,1),Test_V(:,2),Title,Xlabel,Ylabel,Legend1,dirSave,'--',1)

    if size(Legend1,2)>=3 then
        Legend1=[Legend1, 'LS-Dyna']
        figurePlot(Dyna_V(:,1),Dyna_V(:,2),Title,Xlabel,Ylabel,Legend1,dirSave,'-',1)
    end
end
```

B.1.6 Notched, LS-Dyna vs. experimental tests

This script compares the results from the notched LS-Dyna simulations with the results from the experimental tests.

The script:

```
clear; clc;
exec('C:\Users\Heine\Documents\SCILAB files\figurePlot.sci'); clc;

LSDyna_Folder='C:\Users\Heine\Documents\Masteroppgave\Numerical Simulations\...
Notch_full\Simulations\Results\'
Folder_tests='C:\Users\Heine\Documents\Masteroppgave\Tension_Tests\Force\Notched\'
DirSave=strcat([LSDyna_Folder 'Figures\'])
Geometry='N3'
Velocity=['V3','V2','V1']

//%%%%%%% TESTS %%%%%%%%%
N1_v3='0.20'; N1_v2='2.00'; N1_v1='20.00';
N2_v3='0.10'; N2_v2='1.00'; N2_v1='10.00'
N3_v3='0.15'; N3_v2='1.50'; N3_v1='15.00'

Test=strcat(['PP1-' Geometry '-L-'])
Tests_v=[N3_v3, N3_v2, N3_v1]

for v=1:size(Velocity,2)
    Dyna_Displacement=strtod(mgetl(strcat([LSDyna_Folder 'Displacement-'...
     Geometry '-' Velocity(v) '.txt'])))
    TNR2=string(v*2);
    if v==1 then
        TNR1='1'
    elseif v==2
        TNR1='3'
    elseif v==3
        TNR1='5'
    end

    Dyna_Force=strtod(mgetl(strcat([LSDyna_Folder 'Force-' Geometry...
     '-' Velocity(v) '.txt'])))*4
    Test1=mgetl(strcat([Folder_tests 'Force-Displacement_' Test TNR1...
     '_V=' Tests_v(v) '.txt']))
    Test2=mgetl(strcat([Folder_tests 'Force-Displacement_' Test TNR2...
     '_V=' Tests_v(v) '.txt']))
    Test_Displacement1=[]; Test_Displacement2=[];
    Test_Force1=[]; Test_Force2=[]
    L=size(Dyna_Force,1)
    [Dyna_Max, n]=max(Dyna_Force(1:(L*0.5)))
    Dyna_Result=[]
```

```
i =1;  b=0
while  b==0
    if  i<=n  then
        Dyna_Result=[Dyna_Result;  [Dyna_Displacement(i),  Dyna_Force(i)]]
    elseif  i>n & Dyna_Force(i)>=(0.2*Dyna_Max)
        Dyna_Result=[Dyna_Result;  [Dyna_Displacement(i),  Dyna_Force(i)]]
    end
    if  i>n & Dyna_Force(i)<(0.5*Dyna_Max)  then
        b=1
    elseif  i==size(Dyna_Force,1)
        b=1
    end
    i=i+1
end
for  i =1:size(Test1,1)
    TestL=strtod(strsplit(Test1(i),','))
    Test_Displacement1=[Test_Displacement1;  TestL(1)]
    Test_Force1=[Test_Force1;  TestL(2)*1000]
end
for  i =1:size(Test2,1)
    TestL=strtod(strsplit(Test2(i),','))
    Test_Displacement2=[Test_Displacement2;  TestL(1)]
    Test_Force2=[Test_Force2;  TestL(2)*1000]
end
figure(v)
Title=strcat(['Notched_F_Force-Displacement,'  Geometry  '-'  Velocity(v)])
Xlabel='Displacement  [mm]'
Ylabel='Force  [N]'
Legend='LS-Dyna'
figurePlot(Dyna_Result(:,1),Dyna_Result(:,2),Title,Xlabel,Ylabel,...
Legend,DirSave,'-',4)
Legend=[Legend,  'Tests']
figurePlot(Test_Displacement1,Test_Force1,Title,Xlabel,Ylabel,Legend,...
DirSave,'--',4)
figurePlot(Test_Displacement2,Test_Force2,Title,Xlabel,Ylabel,Legend,...
DirSave,'--',4)
end
```

B.1.7 Updating nodal coordinates in k-files

This script can be used to change the nodal coordinates of a k-file.

The script:

```
clear; clc;

change='C:\Users\Heine\Documents\Masteroppgave\Numerical Simulations ...
\Drop-Tower_Node.txt'
data=mgetl(change)
output=[]
for i=1:size(data,1)
    dataL=strsplit(data(i),{' ',',','})
    DataL=[]
    for j=1:size(dataL,1)
        if length(dataL(j))>=1 then
            DataL=[DataL, [strtod(dataL(j));j]]
        end
    end
    zPos=DataL(1,4)
    yPos=DataL(1,3)
    updatedYPos=yPos-0
    updatedZPos=zPos+3.5
    DataL(1,3)=updatedYPos
    DataL(1,4)=updatedZPos
    output=[output; DataL(1,:)]
end
csvWrite(output,change)
```

B.1.8 Figure plot

This function was used when plotting most of the graphs.

The script:

```
function figurePlot(xvalue,yvalue,ftitle,fxlabel,fylabel,flegend,savedir,...
    Style,Location)
    colors=['b','r','k','c','m','g','k','y']
    f=gcf()
    f.background=8
    f.figure_size=[800,600]
    a=gca()
    a.font_size=4
    a.x_label.font_size=4
    a.y_label.font_size=4
    a.title.font_size=4
    n=size(flegend,2)
    if n>size(colors,2) & n<2*size(colors,2) then
        n=size(flegend,2)-size(colors,2)
    elseif n>2*size(colors,2)
        n=size(flegend,2)-(2*size(colors,2))
    end
    xgrid(1)
    b=plot(xvalue,yvalue, strcat([colors(n) Style]))
    a=gca();
    a.thickness = 1.5;
    a.children // list the children of the axes : here it is an Compound...
     child composed of 2 entities
    poly1= a.children.children; //store polyline handle into poly1
    poly1.thickness = 4;  // ...and the tickness of a curve.
    xlabel(fxlabel)
    ylabel(fylabel)
    title(ftitle)
    legend(flegend,loc=Location)
    saveName=strcat([savedir ftitle '.png'])
    xs2png(f,saveName)
endfunction
```

B.2 MatLab scripts

B.2.1 Determining compression diameter

This script was used to determine the diameter history of the uniaxial compression tests based on the images taken of the compression specimens with the CCD camera.

The script:

```matlab
close all; fclose all; clear all; clc;

for i=1:1
dataValues = importdata('C:\Users\Heine\Documents\Masteroppgave...
\Compression Tests\fileInformation.txt','_');
date=dataValues.data(i,1);
time=dataValues.data(i,2);
testnr=dataValues.textdata(i,2);
dirN=['_' num2str(date) '_' num2str(time)];

%Location of the various files%
dirF = strjoin(['C:\Users\Heine\Documents\Masteroppgave\...
    Compression Tests\Raw Data\' testnr(1) '.txt'],'');
dirP = strjoin(['C:\Users\Heine\Documents\Masteroppgave\...
    Compression Tests\Pictures\' testnr '\Cam1\'],'');
dird = 'C:\Users\Heine\Documents\Masteroppgave\...
Compression Tests\Diameter\';
picnm = strjoin(['Cam1_' testnr],'');
nopic = length(dir([dirP '*.bmp']));

saveName=strjoin(['Diameter-',testnr],'');

testpic = imread([dirP picnm dirN '0001.bmp']);
testbw = im2bw(testpic,0.65);

[h,b] = size(testbw);

D0=6.2; %Initial diameter of specimen%

is = 0;
a = 1;

%White is has the value 1 and black is the value 0%
while is == 0
    if sum(testbw(a,1:floor(0.03*b))) >= 0.03*0.95*b && a>(0.1*h)
        is = a;
    end
    a = a + 1;
end
```

```matlab
istart = floor(is+0.10*h);

iend = h - 0.15*b;
di = floor(0.005*h);
jstart = floor(0.045*b);
area = floor(0.044*b);
l = 1;
r = 1;

for i = istart:di:iend
    for j = jstart:b-jstart
        if max(testbw(i,j:j+area)) == 0 && min(testbw(i,j-area:j-1)) == 1
            L(l,:) = [i,j];
            l = l + 1;
        elseif min(testbw(i,j:j+area)) == 1 &&...
                max(testbw(i,j-area:j-1)) == 0
            R(r,:) = [i,j];
            r = r + 1;
        end
    end
end
figure(1)
imshow(testbw)
figure(2)
hold on
plot(L(:,2),L(:,1),'c')
plot(R(:,2),R(:,1),'r')
hold off
drawnow

Lmedian = floor(median(L(:,2)));
Rmedian = floor(median(R(:,2)));
pixelSize = D0/(Rmedian-Lmedian);
%The size of each pixel based on initial values%

di = 1;
iend = h - 0.10*b;
dpic = 1;
ant = nopic/dpic;
zer = '0000';

Diameter=zeros(nopic/dpic,1); %creates the diameter matrix%

for p = dpic:nopic
    n = ceil(log10(p+1));

    nr = [zer(1:4-n) num2str(p)];
```

```
pic = imread([dirP picnm dirN nr '.bmp']);
pbw =(im2bw(pic,0.65));

is = 0;
a = 1;
while is == 0
    if sum(testbw(a,1:floor(0.03*b))) >= 0.03*0.95*b && a>(0.1*h)
        is = a;
    end
    a = a + 1;
end
istart = max(istart,floor(is+0.100*h));

Lm = floor(median(L(:,2)));
Rm = floor(median(R(:,2)));

Diameter(p) = (Rm-Lm)*pixelSize;

clear R L

Db = floor(0.02*b);
db = floor(0.015*b);
l = 1;
r = 1;

for i = istart:di:iend
    for jl = Lm-Db:Lm+Db
        if max(pbw(i,jl:jl+db)) == 0 &&...
                sum(pbw(i,jl-db:jl-1)) >= 0.90*db
            L(l,:) = [i,jl];
            l = l + 1;
        end
    end
    for jr = Rm-Db:Rm+Db
        if min(pbw(i,jr:jr+db)) == 1 && max(pbw(i,jr-db:jr-1)) == 0
            R(r,:) = [i,jr];
            r = r + 1;
        end
    end
end

imshow(pbw)
hold on
plot(L(:,2),L(:,1),'c')
plot(R(:,2),R(:,1),'r')
hold off
drawnow
```

```
end
save ( [ 'C:\Users\Heine\Documents\Masteroppgave\Compression  Tests\Diameter\ '...
    saveName  '.txt'] ,  'Diameter',' − ASCII');
clear  L R
end
```

B.2.2 Determining fracture strain

This script determines the longitudinal fracture strain based on the specimens force history.

The script:

```
close all; fclose all; clear all; clc;

dirForce='C:\Users\Heine\Documents\Masteroppgave\Tension_Tests ...
\PP1-Test_data\';
dirSave='C:\Users\Heine\Documents\Masteroppgave\Tension_Tests\...
Strains\FractureFrameNumber\';
Information=importdata('C:\Users\Heine\Documents\Masteroppgave\...
Tension_Tests\Tensile_Test_Description-variousThickness.txt');
Tests=dir(strcat([dirForce '*_Log.txt']));
FractureLoc=[];
Output=[];
for t=5:5%size(Tests,1)
    TID=strsplit(Tests(t).name,{'-','_'});

    if strcmp(TID(1),'PP1')==1 || strcmp(TID(1),'PP1T')==1....
    %&& strcmp(TID(2),'N1')~=1 && strcmp(TID(2),'N2')~=1...
 && strcmp(TID(2),'N3')~=1
        test=strcat([dirForce Tests(t).name]);
        if length(char(TID(2)))==2
            if strcmp(TID(2),'N1')==1 || strcmp(TID(2),'N2')==1 ||...
                    strcmp(TID(2),'N3')==1
                Tname=char(strjoin([TID(1) '-' TID(2) '-' TID(3) '-'...
                    TID(4)],''));
            else
                Tname=char(strjoin([TID(1) '-' TID(2) '-' TID(3) '-'...
                    TID(4) '-' TID(5)],''));
            end
        elseif length(char(TID(2)))==1
            for i=1:size(Information,1)
                INF=strsplit(strjoin(Information(i),''),',');
                if strcmp(TID(1),INF(1))==1 && strcmp(TID(2),INF(2))==1...
                    && strcmp(TID(3),INF(3))==1
                    if strcmp(INF(4),'0.67')~=1
                        Tname=char(INF(9));
                    elseif strcmp(INF(4),'0.67')==1
                        Tname='DONT_INCLUDE';
                    end
                end
            end
        end
        dF=[];
        ddF=[];
```

```
Force =[];
data=importdata(test ,'\t',5);
if  size(data.data,1)>10
     data=data.data; nD=size(data,1);
     for  i=6:nD
          Force=[Force;  [data(i,1),  data(i,4)]];
     end
%elseif  size(data,1)<10
%     data=importdata(test ,',');
%     nD=size(data,1);
%     for  i=6:nD
%          dataL=str2double(strsplit(char(data(i)),'\t'));
%          Force=[Force;  [dataL(1),  dataL(4)]];
%     end
end
nF=size(Force,1);
for  i=(1+2):(nF-2)
     dF=[dF;[i,  (-Force(i+2,2)+(8*Force(i+1,2))-(8*Force(i-1,2))...
          +Force(i-2,2))/(12*(Force(i,1)-Force(i-1,1)))]];
     ddF=[ddF;[Force(i,1),  ((-Force(i+2,2))+(16*Force(i+1,2))...
          -(30*Force(i,2))+(16*Force(i-1,2))-(Force(i-2,2)))...
          /(12*((Force(i,1)-Force(i-1,1))^2))]];
end
figure(1)
dF2=smooth(dF(:,2));
if  nF>1000
     dF2=smooth(dF2);
     dF2=smooth(smooth(smooth(dF2)));
end
plotyy(Force(:,1),Force(:,2),dF(:,1),dF2)
xlabel('Frame  number')
ylabel('Force  [kN]')
grid  on

dirSaveF ='C:\Users\Heine\Documents\My PCTeX  Files\Tests\fracture \';
legend('Force  (F)','dF')
saveNameF =[dirSaveF  'determining_Fracture.png'];
saveas(1,saveNameF);
nF=size(Force,1);
if  nF<1000
     [pks,  loc] = findpeaks(-dF2(:),'MINPEAKHEIGHT',...
          0.0025,'MINPEAKDISTANCE',ceil(0.05*nF));
     [max,  Loc] = findpeaks(dF2(:),'MINPEAKHEIGHT',...
          0.012,'MINPEAKDISTANCE',ceil(0.05*nF));
else
     [pks,  loc] = findpeaks(-dF2(:),'MINPEAKHEIGHT',...
          2e-04,'MINPEAKDISTANCE',ceil(0.05*nF));
     [max,  Loc] = findpeaks(dF2(:),'MINPEAKHEIGHT',...
```

```matlab
            0.012,'MINPEAKDISTANCE',ceil(0.05*nF));
    end
    if size(loc,1)>0
        Necking=num2str(loc(1));
    elseif size(loc,1)==0
        Necking=num2str(Loc(1));
    end
    n=size(loc,1);

    if n>1 && n<=2 && (loc(n-1)/loc(n))>0.8
        Initial_Fracture=num2str(loc(n-1));
        Fracture=num2str(loc(n));
    elseif n>1 && n<=2
        Fracture=num2str(loc(2));
        for i=floor(0.6*str2double(Fracture)):str2double(Fracture)
            if dF(i,2)<-0.0025
                Initial_Fracture=num2str(dF(i,1));
                break
            end
        end
    elseif n>2 && (loc(2)/loc(3))>0.8
        Initial_Fracture=num2str(loc(2));
        Fracture=num2str(loc(n));
    elseif n>2
        Fracture=num2str(loc(n));
        Initial_Fracture=num2str(loc(2));
    else
        nD=size(dF,1);
        for i=floor(0.6*nD):nD
            if dF(i,2)<-0.0025
                Initial_Fracture=num2str(dF(i,1));
                break
            end
        end
        Fracture=num2str(Force(nF,1)-floor(0.1*nF));
    end
    if str2double(Initial_Fracture)>=str2double(Fracture)
        Initial_Fracture=Fracture;
    end

    input=strjoin({Necking,Initial_Fracture,Fracture},',');
    if strcmp(Tname,'DONT_INCLUDE')~=1
        filename = strjoin({dirSave Tname '.txt'},'');
        fid = fopen(filename, 'w');
        fprintf(fid, input);
        fclose(fid);
    end
end
```

end

B.2.3 Converting from Abaqus to LS-Dyna

This script converts the geometry and mesh of an Abaqus input file, to an LS-Dyna compatible k-file.

The script:

```
clc
clear all

node=csvread('Drop-Tower_Node.txt');% text file containing ...
the node of the part
nnode=size(node);
element=csvread('Drop-Tower_Element.txt');% text file containing ...
the element of the part
nelement=size(element);
partid1 = 1; %part number in LS-DYNA

% To translate more than one part just copy the above lines and add a 2 or
% 3 ... to the name of the variable
% To translate shell meshes uncomment the shell section

%%%%%%%%%%%%%%%%%%%%%%%%%%%%%%%%%%%%%%%%%%%%%%%%%%%%%%%%%%%%%%%%%%%%%%%%%%%%%%%%
disp('Writing start');
%%%%%%%%%%%%%%%%%%%%%%%%%%%%%%%%%%%%%%%%%%%%%%%%%%%%%%%%%%%%%%%%%%%%%%%%%%%%%%%%
fich=fopen('mesh.k','w');
%%%%%%%%%%%%%%%%%%%%%%%%%%%%%%%%%%%%%%%%%%%%%%%%%%%%%%%%%%%%%%%%%%%%%%%%%%%%%%%%
fprintf(fich,'*PART\n');% copy this section to add another part
fprintf(fich,'$# title\n');
fprintf(fich,'part name\n');%to be change to the name of the part
fprintf(fich,'$#       pid        secid         mid        eosid ...
hgid         grav       adpopt        tmid\n');
fprintf(fich,'%g,%g,%g,%g,%g,%g,%g,%g\n',partid1,0,0,0,0,0,0,0);
%%%%%%%%%%%%%%%%%%%%%%%%%%%%%%%%%%%%%%%%%%%%%%%%%%%%%%%%%%%%%%%%%%%%%%%%%%%%%%%%
disp('Part done');
%%%%%%%%%%%%%%%%%%%%%%%%%%%%%%%%%%%%%%%%%%%%%%%%%%%%%%%%%%%%%%%%%%%%%%%%%%%%%%%%
fprintf(fich,'*NODE\n');
fprintf(fich,'$#    nid                x                y ...
z        tc          rc\n');
for i=1:nnode(1,1)
fprintf(fich,'%g,%6d,%6d,%6d,%g,%g\n',node(i,1),node(i,2),...
    node(i,3),node(i,4),0,0);
end
% shift=nnode(1,1);
% for i=1:nnode2(1,1)
% fprintf(fich,'%g,%6d,%6d,%6d,%g,%g\n',node2(i,1)+shift,...
node2(i,2),node2(i,3),node2(i,4),0,0);
% end
```

```
%%%%%%%%%%%%%%%%%%%%%%%%%%%%%%%%%%%%%%%%%%%%%%%%%%%%%%%%%%%%%%%%%%%%%%%%
disp('Node done');
%%%%%%%%%%%%%%%%%%%%%%%%%%%%%%%%%%%%%%%%%%%%%%%%%%%%%%%%%%%%%%%%%%%%%%%%
fprintf(fich,'*ELEMENT_SOLID\n');
fprintf(fich,'$#    eid       pid       n1        n2        n3...
n4        n5        n6        n7        n8\n');
for i=1:nelement(1,1)
    fprintf(fich,'%g,%g,%g,%g,%g,%g,%g,%g,%g,%g\n',...
        element(i,1),partid1,element(i,2),element(i,3)...
        ,element(i,4),element(i,5),element(i,6),element(i,7)...
        ,element(i,8),element(i,9));
end
% element2(:,2:9)=element2(:,2:9)+shift;
% shift2 = nelement(1,1);
% for i=1:nelement2(1,1)
% fprintf(fich,'%g,%g,%g,%g,%g,%g,%g,%g,%g,%g\n',...
element2(i,1)+shift2,partid2,element2(i,2),element2(i,3),...
    element2(i,4),element2(i,5),element2(i,6),element2(i,7),...
    element2(i,8),element2(i,9));
% end
%%%%%%%%%%%%%%%%%%%%%%%%%%%%%%%%%%%%%%%%%%%%%%%%%%%%%%%%%%%%%%%%%%%%%%%%
disp('Volume element done');
%%%%%%%%%%%%%%%%%%%%%%%%%%%%%%%%%%%%%%%%%%%%%%%%%%%%%%%%%%%%%%%%%%%%%%%%
% fprintf(fich,'*ELEMENT_SHELL\n');
% fprintf(fich,'$#    eid       pid       n1        n2        n3        n4\n');
% for i=1:nelement(1,1)
%     fprintf(fich,'%g,%g,%g,%g,%g,%g\n',element(i,1),partid1,...
element(i,2),element(i,3),element(i,4),element(i,5));
% end
%%%%%%%%%%%%%%%%%%%%%%%%%%%%%%%%%%%%%%%%%%%%%%%%%%%%%%%%%%%%%%%%%%%%%%%%
disp('shell element done');
%%%%%%%%%%%%%%%%%%%%%%%%%%%%%%%%%%%%%%%%%%%%%%%%%%%%%%%%%%%%%%%%%%%%%%%%
fprintf(fich,'*END\n');
fclose(fich);
```

Appendix C

Finite element input files

The following sections include the input files used for the numerical simulations. The input files does not include the geometry of the simulations, i.e. the nodal coordinates and the elements. Only the main input files have been included, if changes were made in the simulations velocity or in a parameter in the material card to determine the analyses sensitivity, then these simulations have not been included. The nodes in the nodal sets have also been excluded.

C.1 LS-Dyna k-files

C.1.1 3mm uniaxile tensile-Reduced

```
$# LS-DYNA Keyword file created by LS-PrePost 4.0 - 28Jan2013(19:00)
$# Created on Nov-14-2013 (14:44:47)
*KEYWORD
*TITLE
$# title
LS-DYNA keyword deck by LS-PrePost
*CONTROL_TERMINATION
$#   endtim     endcyc      dtmin     endeng     endmas
 233.00000          0      0.000      0.000      0.000
*CONTROL_TIMESTEP
$#   dtinit     tssfac       isdo     tslimt      dt2ms       lctm      erode
ms1st
      0.000   0.700000          0      0.000      0.000          0          0
0
$#   dt2msf     dt2mslc      imscl     unused     unused      rmscl
      0.000          0          0                           0.000
*DATABASE_ELOUT
$#        dt      binary       lcur      ioopt    option1    option2    option3
option4
   1.000000          1          0          1          0          0          0
0
*DATABASE_GLSTAT
$#        dt      binary       lcur      ioopt
   1.000000          1          0          1
*DATABASE_NODFOR
$#        dt      binary       lcur      ioopt
   1.000000          0          0          1
*DATABASE_NODOUT
$#        dt      binary       lcur      ioopt    option1    option2
   1.000000          1          0          1      0.000          0
*DATABASE_RCFORC
$#        dt      binary       lcur      ioopt
   1.000000          1          0          1
*DATABASE_SECFORC
$#        dt      binary       lcur      ioopt
   1.000000          1          0          1
*DATABASE_BINARY_D3PLOT
$#        dt        lcdt       beam      npltc     psetid
 50.000000          0          0          0          0
$#     ioopt
          0
*DATABASE_EXTENT_BINARY
$#    neiph       neips     maxint     strflg     sigflg     epsflg     rltflg
engflg
```

```
            36             0             3             1             1             1             1
1
$#   cmpflg    ieverp    beamip     dcomp      shge     stssz    n3thdt
ialemat
             0             0             0             1             1             1             2
1
$#  nintsld   pkp_sen      sclp    unused     msscl     therm    intout
nodout
             8             0  1.000000                               0        0STRESS     STRESS
$#    dtdt    resplt
             0             0
*DATABASE_CROSS_SECTION_SET_ID
$#     csid
title
             1
$#    nsid      hsid      bsid      ssid      tsid      dsid        id
itype
             5             1             0             0             0             0             0
0
*SET_NODE_LIST_TITLE
Middle
$#      sid       da1       da2       da3       da4    solver
             5     0.000     0.000     0.000     0.000MECH
$#    nid1      nid2      nid3      nid4      nid5      nid6      nid7
nid8
*DATABASE_HISTORY_NODE_SET
$#     id1       id2       id3       id4       id5       id6       id7
id8
             7             0             0             0             0             0             0
0
*DATABASE_HISTORY_SOLID_SET
$#     id1       id2       id3       id4       id5       id6       id7
id8
             1             0             0             0             0             0             0
0
*BOUNDARY_PRESCRIBED_MOTION_SET_ID
$#      id
heading
         0move
$#    nsid       dof       vad      lcid        sf       vid     death
birth
             6             1             0             1  0.150000               01.0000E+28
0.000
*BOUNDARY_SPC_SET_BIRTH_DEATH
$#    nsid       cid      dofx      dofy      dofz     dofrx     dofry
dofrz
             1             0             1             1             1             0             0
0
```

271

```
$#      birth        death
     0.000         0.000
*SET_NODE_LIST_TITLE
LowerLeft
$#       sid         da1         da2         da3         da4      solver
          1        0.000       0.000       0.000       0.000MECH
$#      nid1        nid2        nid3        nid4        nid5        nid6        nid7
nid8
         14           0           0           0           0           0           0
0
*BOUNDARY_SPC_SET_BIRTH_DEATH
$#      nsid         cid        dofx        dofy        dofz       dofrx       dofry
dofrz
          2           0           1           0           0           0           0
0
$#      birth        death
     0.000         0.000
*SET_NODE_LIST_TITLE
LeftEnd
$#       sid         da1         da2         da3         da4      solver
          2        0.000       0.000       0.000       0.000MECH
$#      nid1        nid2        nid3        nid4        nid5        nid6        nid7
nid8
*BOUNDARY_SPC_SET_BIRTH_DEATH
$#      nsid         cid        dofx        dofy        dofz       dofrx       dofry
dofrz
          3           0           0           1           0           0           0
0
$#      birth        death
     0.000         0.000
*SET_NODE_LIST_TITLE
LowerEnd
$#       sid         da1         da2         da3         da4      solver
          3        0.000       0.000       0.000       0.000MECH
$#      nid1        nid2        nid3        nid4        nid5        nid6        nid7
nid8
*BOUNDARY_SPC_SET_BIRTH_DEATH
$#      nsid         cid        dofx        dofy        dofz       dofrx       dofry
dofrz
          4           0           0           0           1           0           0
0
$#      birth        death
     0.000         0.000
*SET_NODE_LIST_TITLE
Back
$#       sid         da1         da2         da3         da4      solver
          4        0.000       0.000       0.000       0.000MECH
```

```
$#       nid1         nid2         nid3         nid4         nid5         nid6         nid7
nid8
*PART
$# title
Core
$#       pid        secid          mid        eosid         hgid         grav       adpopt
tmid
           1            1            1            0            0            0            0
0
*SECTION_SOLID
$#     secid       elform          aet
           1            1            0
*MAT_USER_DEFINED_MATERIAL_MODELS
$        MID           RO           MT          LMC          NHV       IORTHO        IBULK
IG
           1  1.180e−01           44           27          114            0           12
13
$      IVECT        IFAIL       IHTERM       IHYPER         IEOS         LCMA
           1            1            0            1            0            0
$      EFLAG        YFLAG     RMAPFLAG        FFLAG        HFLAG        VFLAG        TFLAG
DFLAG
          14            1            1            1            1            1            0
1
$     STFLAG            E           PR         BULK        SHEAR       SIGMA0        ALPHA
BETA
           0  1.000e+03  4.000e−01  1.667e+03  3.570e+02  1.448e+01  1.170e+00  1.593e+00
$    THETAR1          QR1      THETAR2          QR2      THETAR3          QR3           CS
PS
 0.682e+03  5.140e+00  13.89e+00 −12.62e+00 −34.00e+00 −2.610e+00  3.798e−02  5.790e−04
$         DI          DCR        BETA0
 0.000e+00  9.000e−01  1.000e+00
*DEFINE_CURVE_SMOOTH
$#      lcid         sidr         dist       tstart         tend        trise           v0
           1            0  1.0000E+5        0.000        0.000     1.000000     1.000000
*SET_NODE_LIST_TITLE
RightEnd
$#        sid          da1          da2          da3          da4       solver
           6        0.000        0.000        0.000        0.000MECH
$#       nid1         nid2         nid3         nid4         nid5         nid6         nid7
nid8

*SET_NODE_LIST_TITLE
LowerRight
$#        sid          da1          da2          da3          da4       solver
           7        0.000        0.000        0.000        0.000MECH
$#       nid1         nid2         nid3         nid4         nid5         nid6         nid7
nid8
```

```
          10               0               0               0               0               0               0
0
*SET_SOLID_TITLE
Midd
$#       sid    solver
          1MECH
$#        k1          k2          k3          k4          k5          k6          k7
k8


*END
```

C.1.2   3mm uniaxial tensile-Full

```
$# LS−DYNA Keyword file created by LS−PrePost 4.0 − 28Jan2013(19:00)
$# Created on Nov−18−2013 (13:18:27)
*KEYWORD
*TITLE
$# title
LS−DYNA keyword deck by LS−PrePost
*CONTROL_TERMINATION
$#   endtim     endcyc      dtmin     endeng     endmas
  233.00000          0      0.000      0.000      0.000
*CONTROL_TIMESTEP
$#   dtinit     tssfac       isdo     tslimt      dt2ms       lctm      erode
ms1st
      0.000   0.700000          0      0.000      0.000          0          0
0
$#   dt2msf     dt2mslc      imscl     unused     unused      rmscl
      0.000          0          0                           0.000
*DATABASE_ELOUT
$#       dt     binary       lcur      ioopt    option1    option2    option3
option4
   1.000000          1          0          1          0          0          0
0
*DATABASE_GLSTAT
$#       dt     binary       lcur      ioopt
   1.000000          1          0          1
*DATABASE_NODFOR
$#       dt     binary       lcur      ioopt
   1.000000          0          0          1
*DATABASE_NODOUT
$#       dt     binary       lcur      ioopt    option1    option2
   1.000000          1          0          1      0.000          0
*DATABASE_RCFORC
$#       dt     binary       lcur      ioopt
   1.000000          1          0          1
*DATABASE_SECFORC
$#       dt     binary       lcur      ioopt
   1.000000          1          0          1
*DATABASE_BINARY_D3PLOT
$#       dt       lcdt       beam      npltc     psetid
  80.000000          0          0          0          0
$#    ioopt
          0
*DATABASE_EXTENT_BINARY
$#    neiph      neips     maxint     strflg     sigflg     epsflg     rltflg
engflg
         36          0          3          1          1          1          1
1
```

```
$#    cmpflg      ieverp      beamip       dcomp        shge       stssz      n3thdt
ialemat
          0           0           0           1           1           1           2
1
$#   nintsld     pkp_sen        sclp      unused       msscl       therm      intout
nodout
          8           0    1.000000                       0              0STRESS      STRESS
$#     dtdt      resplt
          0           0
*DATABASE_CROSS_SECTION_SET_ID
$#     csid
title
          1
$#     nsid        hsid        bsid        ssid        tsid        dsid          id
itype
          5           1           0           0           0           0           0
0
*SET_NODE_LIST_TITLE
Middle
$#      sid         da1         da2         da3         da4      solver
          5       0.000       0.000       0.000       0.000MECH
$#     nid1        nid2        nid3        nid4        nid5        nid6        nid7
nid8

*DATABASE_HISTORY_NODE_SET
$#      id1         id2         id3         id4         id5         id6         id7
id8
          7           8           9           0           0           0           0
0
*DATABASE_HISTORY_SOLID_SET
$#      id1         id2         id3         id4         id5         id6         id7
id8
          1           0           0           0           0           0           0
0
*BOUNDARY_PRESCRIBED_MOTION_SET_ID
$#      id
heading
         0move
$#     nsid         dof         vad        lcid          sf         vid       death
birth
          6           1           0           1    0.150000            01.0000E+28
0.000
*BOUNDARY_SPC_SET_BIRTH_DEATH
$#     nsid         cid        dofx        dofy        dofz       dofrx       dofry
dofrz
          1           0           1           1           1           0           0
0
$#    birth       death
```

```
     0.000        0.000
*SET_NODE_LIST_TITLE
LowerLeft
$#        sid         da1         da2         da3         da4       solver
           1        0.000       0.000       0.000       0.000MECH
$#     nid1        nid2        nid3        nid4        nid5        nid6        nid7
nid8
          14           0           0           0           0           0           0
0
*BOUNDARY_SPC_SET_BIRTH_DEATH
$#      nsid         cid        dofx        dofy        dofz       dofrx       dofry
dofrz
           2           0           1           0           0           0           0
0
$#     birth       death
     0.000        0.000
*SET_NODE_LIST_TITLE
LeftEnd
$#        sid         da1         da2         da3         da4       solver
           2        0.000       0.000       0.000       0.000MECH
$#     nid1        nid2        nid3        nid4        nid5        nid6        nid7
nid8

*BOUNDARY_SPC_SET_BIRTH_DEATH
$#      nsid         cid        dofx        dofy        dofz       dofrx       dofry
dofrz
           3           0           0           1           0           0           0
0
$#     birth       death
     0.000        0.000
*SET_NODE_LIST_TITLE
LowerEnd
$#        sid         da1         da2         da3         da4       solver
           3        0.000       0.000       0.000       0.000MECH
$#     nid1        nid2        nid3        nid4        nid5        nid6        nid7
nid8

*BOUNDARY_SPC_SET_BIRTH_DEATH
$#      nsid         cid        dofx        dofy        dofz       dofrx       dofry
dofrz
           4           0           0           0           1           0           0
0
$#     birth       death
     0.000        0.000
*SET_NODE_LIST_TITLE
Back
$#        sid         da1         da2         da3         da4       solver
           4        0.000       0.000       0.000       0.000MECH
```

```
$#       nid1         nid2         nid3         nid4         nid5         nid6         nid7
nid8

*PART
$# title
Core
$#       pid        secid          mid        eosid         hgid         grav       adpopt
tmid
           1            1            1            0            0            0            0
0
*SECTION_SOLID
$#     secid        elform          aet
           1            1            0
*MAT_USER_DEFINED_MATERIAL_MODELS
$        MID           RO           MT          LMC          NHV       IORTHO        IBULK
IG
           1  1.180e-01           44           30          114            0           12
13
$      IVECT        IFAIL       IHTERM       IHYPER         IEOS         LCMA
           1            1            0            1            0            0
$      EFLAG        YFLAG     RMAPFLAG        FFLAG        HFLAG        VFLAG        TFLAG
DFLAG
          14            1            1            1            1            1            0
1
$     STFLAG            E           PR         BULK        SHEAR       SIGMA0        ALPHA
BETA
           0  0.950e+03   3.500e-01    1.222e+03    4.074e+02    1.580e+01    1.175e+00   1.593e+00
$   THETAR1          QR1      THETAR2          QR2      THETAR3          QR3           CS
PS
 0.700e+03   4.072e+00    7.002e+00-3.395e+00-7.532e+01-2.390e+00    4.738e-02   5.968e-04
$         DI          DCR        BETA0         DMIN         DMAX         SDAM
 0.000e+00   9.000e-01    1.000e+00            0            1         0.08
*PART
$# title
Skin
$#       pid        secid          mid        eosid         hgid         grav       adpopt
tmid
           2            1            2            0            0            0            0
0
*MAT_USER_DEFINED_MATERIAL_MODELS
$        MID           RO           MT          LMC          NHV       IORTHO        IBULK
IG
           2  1.180e-01           44           30          114            0           12
13
$      IVECT        IFAIL       IHTERM       IHYPER         IEOS         LCMA
           1            1            0            1            0            0
$      EFLAG        YFLAG     RMAPFLAG        FFLAG        HFLAG        VFLAG        TFLAG
DFLAG
```

278

```
          14           1           1           1           1           1           0
1
$    STFLAG           E          PR        BULK       SHEAR      SIGMA0       ALPHA
BETA
           0  0.550e+03  4.000e−01  0.917e+03  1.964e+02  1.983e+01  1.175e+00  1.673e+00
$   THETAR1         QR1     THETAR2         QR2     THETAR3         QR3          CS
PS
 0.700e+03  4.072e+00  7.002e+00−3.395e+00−7.532e+01−2.390e+00  4.738e−02  5.968e−04
$          DI         DCR       BETA0        DMIN        DMAX        SDAM
 0.000e+00  9.000e−01  1.000e+00           0           1        0.08
*DEFINE_CURVE_SMOOTH
$#     lcid        sidr        dist      tstart        tend       trise          v0
          1           0  1.0000E+5       0.000       0.000    1.000000    1.000000
*SET_NODE_LIST_TITLE
RightEnd
$#      sid         da1         da2         da3         da4      solver
          6       0.000       0.000       0.000       0.000MECH
$#     nid1        nid2        nid3        nid4        nid5        nid6        nid7
nid8

*SET_NODE_LIST_TITLE
LowerRight
$#      sid         da1         da2         da3         da4      solver
          7       0.000       0.000       0.000       0.000MECH
$#     nid1        nid2        nid3        nid4        nid5        nid6        nid7
nid8
         10           0           0           0           0           0           0
0
*SET_NODE_LIST_TITLE
TopCenterLine
$#      sid         da1         da2         da3         da4      solver
          8       0.000       0.000       0.000       0.000MECH
$#     nid1        nid2        nid3        nid4        nid5        nid6        nid7
nid8

*SET_NODE_LIST_TITLE
SideCenterLine
$#      sid         da1         da2         da3         da4      solver
          9       0.000       0.000       0.000       0.000MECH
$#     nid1        nid2        nid3        nid4        nid5        nid6        nid7
nid8

*SET_SOLID_TITLE
Midd
$#      sid      solver
          1MECH
$#       k1          k2          k3          k4          k5          k6          k7
k8
```

$*$END

C.1.3 2mm uniaxial tensile-Full

```
$# LS−DYNA Keyword file created by LS−PrePost 4.0 − 28Jan2013(19:00)
$# Created on Nov−18−2013 (13:18:27)
*KEYWORD
*TITLE
$# title
LS−DYNA keyword deck by LS−PrePost
*CONTROL_TERMINATION
$#   endtim     endcyc      dtmin     endeng     endmas
 602.00000          0      0.000      0.000      0.000
*CONTROL_TIMESTEP
$#   dtinit     tssfac       isdo     tslimt      dt2ms       lctm      erode
ms1st
      0.000   0.700000          0      0.000      0.000          0          0
0
$#   dt2msf     dt2mslc      imscl     unused     unused      rmscl
      0.000          0          0                            0.000
*DATABASE_ELOUT
$#       dt     binary       lcur      ioopt    option1    option2    option3
option4
   2.000000          1          0          1          0          0          0
0
*DATABASE_GLSTAT
$#       dt     binary       lcur      ioopt
   2.000000          1          0          1
*DATABASE_NODFOR
$#       dt     binary       lcur      ioopt
   2.000000          0          0          1
*DATABASE_NODOUT
$#       dt     binary       lcur      ioopt    option1    option2
   2.000000          1          0          1      0.000          0
*DATABASE_RCFORC
$#       dt     binary       lcur      ioopt
   2.000000          1          0          1
*DATABASE_SECFORC
$#       dt     binary       lcur      ioopt
   2.000000          1          0          1
*DATABASE_BINARY_D3PLOT
$#       dt       lcdt       beam      npltc     psetid
600.000000          0          0          0          0
$#    ioopt
          0
*DATABASE_EXTENT_BINARY
$#    neiph      neips     maxint     strflg     sigflg     epsflg     rltflg
engflg
         36          0          3          1          1          1          1
1
```

```
$#    cmpflg      ieverp      beamip       dcomp        shge       stssz      n3thdt
ialemat
           0           0           0           1           1           1           2
1
$#   nintsld     pkp_sen        sclp      unused       msscl       therm      intout
nodout
           8           0    1.000000                               0      0STRESS      STRESS
$#      dtdt      resplt
           0           0
*DATABASE_CROSS_SECTION_SET_ID
$#      csid
title
           1
$#      nsid        hsid        bsid        ssid        tsid        dsid          id
itype
           5           1           0           0           0           0           0
0
*SET_NODE_LIST_TITLE
Middle
$#       sid         da1         da2         da3         da4      solver
           5       0.000       0.000       0.000       0.000MECH
$#      nid1        nid2        nid3        nid4        nid5        nid6        nid7
nid8
         326         345         364         383        1510        1529        1548
1567
        1586        1605        1624        1643        1662        1681        1700
1719
        1738        1757        1776        1795        1814        1833        2684
2703
        2722        2741        2760        2779        2798        2817        2836
2855
        2874        2893        2912        2931        3256        3294        4302
4321
        4340        4359        4378        4397        4416        4435        4454
5022
        5041        5060        5079        5098        5117        5136           0
0
*DATABASE_HISTORY_NODE_SET
$#       id1         id2         id3         id4         id5         id6         id7
id8
           7           8           9           0           0           0           0
0
*DATABASE_HISTORY_SOLID_SET
$#       id1         id2         id3         id4         id5         id6         id7
id8
           1           0           0           0           0           0           0
0
*BOUNDARY_PRESCRIBED_MOTION_SET_ID
```

```
$#        id
heading
        0move
$#      nsid           dof          vad          lcid            sf           vid         death
birth
         6             1            0             1     0.150000                    01.0000E+28
0.000
*BOUNDARY_SPC_SET_BIRTH_DEATH
$#      nsid           cid         dofx         dofy          dofz         dofrx         dofry
dofrz
         1             0            1             1             1             0             0
0
$#     birth        death
     0.000        0.000
*SET_NODE_LIST_TITLE
LowerLeft
$#       sid          da1          da2          da3           da4        solver
         1         0.000        0.000        0.000         0.000MECH
$#      nid1         nid2         nid3         nid4          nid5          nid6          nid7
nid8
        14             0            0             0             0             0             0
0
*BOUNDARY_SPC_SET_BIRTH_DEATH
$#      nsid           cid         dofx         dofy          dofz         dofrx         dofry
dofrz
         2             0            1             0             0             0             0
0
$#     birth        death
     0.000        0.000
*SET_NODE_LIST_TITLE
LeftEnd
$#       sid          da1          da2          da3           da4        solver
         2         0.000        0.000        0.000         0.000MECH
$#      nid1         nid2         nid3         nid4          nid5          nid6          nid7
nid8
*BOUNDARY_SPC_SET_BIRTH_DEATH
$#      nsid           cid         dofx         dofy          dofz         dofrx         dofry
dofrz
         3             0            0             1             0             0             0
0
$#     birth        death
     0.000        0.000
*SET_NODE_LIST_TITLE
LowerEnd
$#       sid          da1          da2          da3           da4        solver
         3         0.000        0.000        0.000         0.000MECH
$#      nid1         nid2         nid3         nid4          nid5          nid6          nid7
nid8
```

```
*BOUNDARY_SPC_SET_BIRTH_DEATH
$#      nsid         cid        dofx        dofy        dofz       dofrx       dofry
dofrz
           4           0           0           0           1           0           0
0
$#     birth       death
     0.000       0.000
*SET_NODE_LIST_TITLE
Back
$#       sid         da1         da2         da3         da4      solver
           4       0.000       0.000       0.000       0.000MECH
$#      nid1        nid2        nid3        nid4        nid5        nid6        nid7
nid8

*PART
$# title
Core
$#       pid       secid         mid       eosid        hgid        grav      adpopt
tmid
           1           1           1           0           0           0           0
0
*SECTION_SOLID
$#     secid       elform         aet
           1           1           0
*MAT_USER_DEFINED_MATERIAL_MODELS
$       MID          RO          MT         LMC         NHV      IORTHO       IBULK
IG
           1  1.180e−01          44          27         114           0          12
13
$     IVECT       IFAIL      IHTERM      IHYPER        IEOS        LCMA
           1           1           0           1           0           0
$     EFLAG       YFLAG    RMAPFLAG       FFLAG       HFLAG       VFLAG       TFLAG
DFLAG
          14           1           1           1           1           1           0
1
$    STFLAG           E          PR        BULK       SHEAR      SIGMA0       ALPHA
BETA
           0   0.950e+03   3.500e−01   1.222e+03   4.074e+02   1.580e+01   1.175e+00   1.593e+00
$   THETAR1         QR1     THETAR2         QR2     THETAR3         QR3          CS
PS
  0.700e+03   4.072e+00   7.002e+00−3.395e+00−7.532e+01−2.390e+00   4.738e−02   5.968e−04
$        DI         DCR       BETA0
  0.000e+00   9.000e−01   1.000e+00
*PART
$# title
Skin
```

```
$#        pid       secid         mid       eosid        hgid        grav      adpopt
tmid
            2           1           2           0           0           0           0
0
*MAT_USER_DEFINED_MATERIAL_MODELS
$         MID          RO          MT         LMC         NHV      IORTHO       IBULK
IG
            2  1.180e-01          44          27         114           0          12
13
$       IVECT       IFAIL      IHTERM      IHYPER        IEOS        LCMA
            1           1           0           1           0           0
$       EFLAG       YFLAG    RMAPFLAG       FFLAG       HFLAG       VFLAG       TFLAG
DFLAG
           14           1           1           1           1           1           0
1
$      STFLAG           E          PR        BULK       SHEAR      SIGMA0       ALPHA
BETA
            0  0.550e+03  3.500e-01  0.611e+03  2.037e+02  1.983e+01  1.175e+00  1.593e+00
$     THETAR1         QR1     THETAR2         QR2     THETAR3         QR3          CS
PS
 0.700e+03  4.072e+00  7.002e+00 -3.395e+00 -7.532e+01 -2.390e+00  4.738e-02  5.968e-04
$          DI         DCR       BETA0
 0.000e+00  9.000e-01  1.000e+00
*DEFINE_CURVE_SMOOTH
$#       lcid        sidr        dist      tstart        tend       trise          v0
            1           0  1.0000E+5       0.000       0.000    1.000000    1.000000
*SET_NODE_LIST_TITLE
RightEnd
$#        sid         da1         da2         da3         da4      solver
            6       0.000       0.000       0.000       0.000MECH
$#       nid1        nid2        nid3        nid4        nid5        nid6        nid7
nid8

*SET_NODE_LIST_TITLE
LowerRight
$#        sid         da1         da2         da3         da4      solver
            7       0.000       0.000       0.000       0.000MECH
$#       nid1        nid2        nid3        nid4        nid5        nid6        nid7
nid8
           10           0           0           0           0           0           0
0
*SET_NODE_LIST_TITLE
TopCenterLine
$#        sid         da1         da2         da3         da4      solver
            8       0.000       0.000       0.000       0.000MECH
$#       nid1        nid2        nid3        nid4        nid5        nid6        nid7
nid8
```

```
       326         327         344         345        1510        1511        1529
1530
      3256        3257        4302        4303           0           0           0
0
*SET_NODE_LIST_TITLE
SideCenterLine
$#       sid         da1         da2         da3         da4      solver
           9       0.000       0.000       0.000       0.000MECH
$#      nid1        nid2        nid3        nid4        nid5        nid6        nid7
nid8

*SET_SOLID_TITLE
Midd
$#       sid      solver
           1MECH
$#        k1          k2          k3          k4          k5          k6          k7
k8

*ELEMENT_SOLID
$#      eid         pid          n1          n2          n3          n4          n5          n6          n7
n8
*END
```

C.1.4   4mm uniaxial tensile-Full

```
$# LS−DYNA Keyword file created by LS−PrePost 4.0 − 28Jan2013(19:00)
$# Created on Nov−18−2013 (13:18:27)
*KEYWORD
*TITLE
$# title
LS−DYNA keyword deck by LS−PrePost
*CONTROL_TERMINATION
$#   endtim      endcyc        dtmin      endeng      endmas
 182.00000          0        0.000        0.000        0.000
*CONTROL_TIMESTEP
$#   dtinit      tssfac        isdo      tslimt        dt2ms        lctm        erode
ms1st
      0.000    0.700000          0        0.000        0.000          0          0
0
$#   dt2msf      dt2mslc      imscl      unused      unused        rmscl
      0.000          0          0                                  0.000
*DATABASE_ELOUT
$#       dt      binary        lcur       ioopt      option1     option2     option3
option4
   1.000000          1          0          1          0          0          0
0
*DATABASE_GLSTAT
$#       dt      binary        lcur       ioopt
   1.000000          1          0          1
*DATABASE_NODFOR
$#       dt      binary        lcur       ioopt
   1.000000          0          0          1
*DATABASE_NODOUT
$#       dt      binary        lcur       ioopt      option1     option2
   1.000000          1          0          1        0.000          0
*DATABASE_RCFORC
$#       dt      binary        lcur       ioopt
   1.000000          1          0          1
*DATABASE_SECFORC
$#       dt      binary        lcur       ioopt
   1.000000          1          0          1
*DATABASE_BINARY_D3PLOT
$#       dt        lcdt        beam       npltc      psetid
 80.000000          0          0          0          0
$#    ioopt
         0
*DATABASE_EXTENT_BINARY
$#    neiph       neips      maxint      strflg      sigflg      epsflg      rltflg
engflg
        36          0          3          1          1          1          1
1
```

```
$#    cmpflg     ieverp     beamip      dcomp       shge      stssz     n3thdt
ialemat
             0          0          0          1          1          1          2
1
$#   nintsld    pkp_sen       sclp     unused      msscl      therm     intout
nodout
             8          0   1.000000                          0     0STRESS     STRESS
$#      dtdt     resplt
             0          0
*DATABASE_CROSS_SECTION_SET_ID
$#      csid
title
             1
$#      nsid       hsid       bsid       ssid       tsid       dsid         id
itype
             5          1          0          0          0          0          0
0
*SET_NODE_LIST_TITLE
Middle
$#       sid        da1        da2        da3        da4     solver
             5      0.000      0.000      0.000      0.000MECH
$#      nid1       nid2       nid3       nid4       nid5       nid6       nid7
nid8

*DATABASE_HISTORY_NODE_SET
$#       id1        id2        id3        id4        id5        id6        id7
id8
             7          8          9          0          0          0          0
0
*DATABASE_HISTORY_SOLID_SET
$#       id1        id2        id3        id4        id5        id6        id7
id8
             1          0          0          0          0          0          0
0
*BOUNDARY_PRESCRIBED_MOTION_SET_ID
$#        id
heading
             0move
$#      nsid        dof        vad       lcid         sf        vid      death
birth
             6          1          0          1   0.150000             01.0000E+28
0.000
*BOUNDARY_SPC_SET_BIRTH_DEATH
$#      nsid        cid       dofx       dofy       dofz      dofrx      dofry
dofrz
             1          0          1          1          1          0          0
0
$#     birth      death
```

```
      0.000       0.000
*SET_NODE_LIST_TITLE
LowerLeft
$#      sid        da1        da2        da3        da4     solver
          1      0.000      0.000      0.000      0.000MECH
$#    nid1       nid2       nid3       nid4       nid5       nid6       nid7
nid8
         14          0          0          0          0          0          0
0
*BOUNDARY_SPC_SET_BIRTH_DEATH
$#    nsid        cid       dofx       dofy       dofz      dofrx      dofry
dofrz
          2          0          1          0          0          0          0
0
$#   birth      death
      0.000      0.000
*SET_NODE_LIST_TITLE
LeftEnd
$#      sid        da1        da2        da3        da4     solver
          2      0.000      0.000      0.000      0.000MECH
$#    nid1       nid2       nid3       nid4       nid5       nid6       nid7
nid8

*BOUNDARY_SPC_SET_BIRTH_DEATH
$#    nsid        cid       dofx       dofy       dofz      dofrx      dofry
dofrz
          3          0          0          1          0          0          0
0
$#   birth      death
      0.000      0.000
*SET_NODE_LIST_TITLE
LowerEnd
$#      sid        da1        da2        da3        da4     solver
          3      0.000      0.000      0.000      0.000MECH
$#    nid1       nid2       nid3       nid4       nid5       nid6       nid7
nid8

*BOUNDARY_SPC_SET_BIRTH_DEATH
$#    nsid        cid       dofx       dofy       dofz      dofrx      dofry
dofrz
          4          0          0          0          1          0          0
0
$#   birth      death
      0.000      0.000
*SET_NODE_LIST_TITLE
Back
$#      sid        da1        da2        da3        da4     solver
          4      0.000      0.000      0.000      0.000MECH
```

```
$#       nid1        nid2        nid3        nid4        nid5        nid6        nid7
nid8
*PART
$# title
Core
$#        pid       secid         mid       eosid        hgid        grav      adpopt
tmid
             1           1           1           0           0           0           0
0
*SECTION_SOLID
$#      secid       elform         aet
             1           1           0
*MAT_USER_DEFINED_MATERIAL_MODELS
$        MID          RO          MT         LMC         NHV      IORTHO       IBULK
IG
             1  1.180e−01          44          27         114           0          12
13
$      IVECT       IFAIL      IHTERM      IHYPER        IEOS        LCMA
             1           1           0           1           0           0
$      EFLAG       YFLAG    RMAPFLAG       FFLAG       HFLAG       VFLAG       TFLAG
DFLAG
            14           1           1           1           1           1           0
1
$     STFLAG           E          PR        BULK       SHEAR      SIGMA0       ALPHA
BETA
             0   0.950e+03   3.500e−01   1.222e+03   4.074e+02   1.580e+01   1.175e+00   1.593e+00
$    THETAR1         QR1     THETAR2         QR2     THETAR3         QR3          CS
PS
   0.700e+03   4.072e+00   7.002e+00−3.395e+00−7.532e+01−2.390e+00   4.738e−02   5.968e−04
$         DI         DCR       BETA0
   0.000e+00   9.000e−01   1.000e+00
*PART
$# title
Skin
$#        pid       secid         mid       eosid        hgid        grav      adpopt
tmid
             2           1           2           0           0           0           0
0
*MAT_USER_DEFINED_MATERIAL_MODELS
$        MID          RO          MT         LMC         NHV      IORTHO       IBULK
IG
             2  1.180e−01          44          27         114           0          12
13
$      IVECT       IFAIL      IHTERM      IHYPER        IEOS        LCMA
             1           1           0           1           0           0
$      EFLAG       YFLAG    RMAPFLAG       FFLAG       HFLAG       VFLAG       TFLAG
DFLAG
```

```
            14            1            1            1            1            1            0
1
$    STFLAG            E           PR         BULK        SHEAR       SIGMA0        ALPHA
BETA
            0  0.550e+03  3.500e−01  0.611e+03  2.037e+02  1.983e+01  1.175e+00  1.493e+00
$   THETAR1          QR1      THETAR2          QR2      THETAR3          QR3           CS
PS
 0.700e+03  4.072e+00  7.002e+00−3.395e+00−7.532e+01−2.390e+00  4.738e−02  5.968e−04
$         DI          DCR        BETA0
 0.000e+00  9.000e−01  1.000e+00
*DEFINE_CURVE_SMOOTH
$#     lcid         sidr         dist       tstart         tend        trise           v0
          1            0  1.0000E+5        0.000        0.000     1.000000     1.000000
*SET_NODE_LIST_TITLE
RightEnd
$#       sid          da1          da2          da3          da4     solver
          6        0.000        0.000        0.000        0.000MECH
$#      nid1         nid2         nid3         nid4         nid5         nid6         nid7
nid8

*SET_NODE_LIST_TITLE
LowerRight
$#       sid          da1          da2          da3          da4     solver
          7        0.000        0.000        0.000        0.000MECH
$#      nid1         nid2         nid3         nid4         nid5         nid6         nid7
nid8
         10            0            0            0            0            0            0
0
*SET_NODE_LIST_TITLE
TopCenterLine
$#       sid          da1          da2          da3          da4     solver
          8        0.000        0.000        0.000        0.000MECH
$#      nid1         nid2         nid3         nid4         nid5         nid6         nid7
nid8
        326          327          344          345         1510         1511         1529
1530
       3256         3257         4302         4303            0            0            0
0
*SET_NODE_LIST_TITLE
SideCenterLine
$#       sid          da1          da2          da3          da4     solver
          9        0.000        0.000        0.000        0.000MECH
$#      nid1         nid2         nid3         nid4         nid5         nid6         nid7
nid8
       3293         3294         4340         4341         4359         4360         4378
4379
       4397         4398         4416         4417         4435         4436         4454
4455
```

```
*SET_SOLID_TITLE
Midd
$#        sid      solver
          1MECH
$#        k1          k2          k3          k4          k5          k6          k7
k8

*END
```

C.1.5 Uniaxial compression

```
$# LS-DYNA Keyword file created by LS-PrePost 4.0 - 28Jan2013(19:00)
$# Created on Dec-19-2013 (11:12:07)
*KEYWORD
*TITLE
$# title
LS-DYNA keyword deck by LS-PrePost
*CONTROL_TERMINATION
$#   endtim    endcyc     dtmin    endeng    endmas
    36.00000         0     0.000     0.000     0.000
*CONTROL_TIMESTEP
$#   dtinit     tssfac      isdo    tslimt      dt2ms      lctm     erode
ms1st
     0.000   0.900000         0     0.000     0.000         0         0
0
$#   dt2msf    dt2mslc     imscl    unused    unused     rmscl
     0.000         0         0                          0.000
*DATABASE_BNDOUT
$#        dt    binary      lcur     ioopt
   0.100000         1         0         1
*DATABASE_ELOUT
$#        dt    binary      lcur     ioopt   option1   option2   option3
option4
   0.100000         1         0         1         0         0         0
0
*DATABASE_NODFOR
$#        dt    binary      lcur     ioopt
   0.100000         1         0         1
*DATABASE_NODOUT
$#        dt    binary      lcur     ioopt   option1   option2
   0.100000         1         0         1     0.000         0
*DATABASE_RCFORC
$#        dt    binary      lcur     ioopt
   0.100000         0         0         1
*DATABASE_SECFORC
$#        dt    binary      lcur     ioopt
   0.100000         0         0         1
*DATABASE_BINARY_D3PLOT
$#        dt      lcdt      beam     npltc    psetid
  30.000000         0         0         0         0
$#     ioopt
         0
*DATABASE_EXTENT_BINARY
$#    neiph     neips    maxint    strflg    sigflg    epsflg    rltflg
engflg
         0         0         3         1         1         1         1
1
```

293

$#	cmpflg	ieverp	beamip	dcomp	shge	stssz	n3thdt
ialemat							
	0	0	0	1	1	1	2
1							

$#	nintsld	pkp_sen	sclp	unused	msscl	therm	intout
nodout							
	1	0	1.000000		0	0STRESS	STRESS

$#	dtdt	resplt
	0	0

*DATABASE_CROSS_SECTION_SET_ID

$#	csid
title	
	1

$#	nsid	hsid	bsid	ssid	tsid	dsid	id
itype							
	7	2	0	0	0	0	0
0							

*SET_NODE_LIST_TITLE
Cross_Section

$#	sid	da1	da2	da3	da4	solver
	7	0.000	0.000	0.000	0.000MECH	

$#	nid1	nid2	nid3	nid4	nid5	nid6	nid7
nid8							

*DATABASE_NODAL_FORCE_GROUP

$#	nsid	cid
	7	0

*DATABASE_HISTORY_NODE_SET

$#	id1	id2	id3	id4	id5	id6	id7
id8							
	4	5	6	0	0	0	0
0							

*DATABASE_HISTORY_SOLID_SET

$#	id1	id2	id3	id4	id5	id6	id7
id8							
	1	0	0	0	0	0	0
0							

*BOUNDARY_PRESCRIBED_MOTION_RIGID_ID

$#	id
heading	
	1Compression

$#	pid	dof	vad	lcid	sf	vid	death
birth							
	3	3	0	1	−0.030000	0	1.0000E+28
0.000							

*BOUNDARY_SPC_SET_ID

$#	id
heading	

294

```
          0SymmetryPlane−Y
$#     nsid        cid       dofx       dofy       dofz      dofrx      dofry
dofrz
          1          0          0          1          0          1          0
1
*SET_NODE_LIST_TITLE
PP−xz
$#      sid        da1        da2        da3        da4     solver
          1      0.000      0.000      0.000      0.000MECH
$#     nid1       nid2       nid3       nid4       nid5       nid6       nid7
nid8

*BOUNDARY_SPC_SET_ID
$#       id
heading
          0SymmetryPlane−X
$#     nsid        cid       dofx       dofy       dofz      dofrx      dofry
dofrz
          2          0          1          0          0          0          1
1
*SET_NODE_LIST_TITLE
PP−yz
$#      sid        da1        da2        da3        da4     solver
          2      0.000      0.000      0.000      0.000MECH
$#     nid1       nid2       nid3       nid4       nid5       nid6       nid7
nid8

*CONTACT_AUTOMATIC_SINGLE_SURFACE
$#      cid
title
$#     ssid       msid      sstyp      mstyp     sboxid     mboxid        spr
mpr
          1          0          2          0          0          0          0
0
$#       fs         fd         dc         vc        vdc     penchk         bt
dt
  0.050000      0.000      0.000      0.000      0.000          0      0.0001.0000E+20
$#      sfs        sfm        sst        mst       sfst       sfmt        fsf
vsf
 10.000000   1.000000      0.000      0.000   1.000000   1.000000   1.000000   1.000000
*SET_PART_LIST_TITLE
Slave
$#      sid        da1        da2        da3        da4     solver
          1      0.000      0.000      0.000      0.000MECH
$#     pid1       pid2       pid3       pid4       pid5       pid6       pid7
pid8
          1          2          3          4          0          0          0
0
```

```
*PART
$# title
PP−Core
$#       pid      secid        mid      eosid       hgid       grav     adpopt
tmid
           1          1          1          0          0          0          0
0
*SECTION_SOLID
$#     secid     elform        aet
           1          2          0
*MAT_USER_DEFINED_MATERIAL_MODELS
$        MID         RO         MT        LMC        NHV     IORTHO      IBULK
IG
           1  1.180e−03         44         27        114          0         12
13
$      IVECT      IFAIL     IHTERM     IHYPER       IEOS       LCMA
           1          1          0          1          0          0
$      EFLAG      YFLAG    RMAPFLAG      FFLAG      HFLAG      VFLAG      TFLAG
DFLAG
          14          1          1          1          1          1          0
1
$     STFLAG          E         PR       BULK      SHEAR     SIGMA0      ALPHA
BETA
           0  0.950e+03  3.500e−01  1.222e+03  4.074e+02  1.580e+01  1.175e+00  1.593e+00
$    THETAR1        QR1    THETAR2        QR2    THETAR3        QR3         CS
PS
  0.700e+03  4.072e+00  7.002e+00−3.395e+00−7.532e+01−2.390e+00  4.738e−02  5.968e−04
$         DI        DCR      BETA0
  0.000e+00  9.000e−01  1.000e+00
*PART
$# title
PP−Skin
$#       pid      secid        mid      eosid       hgid       grav     adpopt
tmid
           2          1          2          0          0          0          0
0
*MAT_USER_DEFINED_MATERIAL_MODELS
$        MID         RO         MT        LMC        NHV     IORTHO      IBULK
IG
           2  1.180e−03         44         27        114          0         12
13
$      IVECT      IFAIL     IHTERM     IHYPER       IEOS       LCMA
           1          1          0          1          0          0
$      EFLAG      YFLAG    RMAPFLAG      FFLAG      HFLAG      VFLAG      TFLAG
DFLAG
          14          1          1          1          1          1          0
1
```

296

```
$    STFLAG           E          PR        BULK       SHEAR      SIGMA0       ALPHA
BETA
           0  0.550e+03  4.000e-01  0.917e+03  1.964e+02  1.983e+01  1.175e+00  1.493e+00
$   THETAR1         QR1     THETAR2         QR2     THETAR3         QR3          CS
PS
 0.700e+03  4.072e+00  7.002e+00 -3.395e+00 -7.532e+01 -2.390e+00  4.738e-02  5.968e-04
$         DI         DCR       BETA0
 0.000e+00  9.000e-01  1.000e+00
```
*PART
```
$# title
```
Machine top
```
$#      pid       secid        mid       eosid        hgid        grav      adpopt
tmid
           3           1           3           0           0           0           0
0
```
*MAT_RIGID_TITLE
Top
```
$#      mid          ro           e          pr           n      couple           m
alias
          35.0000E-10 10000.000    0.300000       0.000       0.000       0.000
$#      cmo        con1        con2
  1.000000           4           7
$# lco or a1          a2          a3          v1          v2          v3
     0.000       0.000       0.000       0.000       0.000       0.000
```
*PART
```
$# title
```
Machine bottom
```
$#      pid       secid        mid       eosid        hgid        grav      adpopt
tmid
           4           1           4           0           0           0           0
0
```
*MAT_RIGID_TITLE
Bottom
```
$#      mid          ro           e          pr           n      couple           m
alias
          45.0000E-10 10000.000    0.300000       0.000       0.000       0.000
$#      cmo        con1        con2
  1.000000           7           7
$# lco or a1          a2          a3          v1          v2          v3
     0.000       0.000       0.000       0.000       0.000       0.000
```
*DEFINE_CURVE_SMOOTH_TITLE
Load
```
$#     lcid        sidr        dist      tstart        tend       trise          v0
           1           0 10000.000       0.000 9000.0000    0.010000    1.000000
```
*SET_NODE_LIST_TITLE
Center_line
```
$#      sid         da1         da2         da3         da4      solver
           3       0.000       0.000       0.000       0.000MECH
```

```
$#      nid1      nid2      nid3      nid4      nid5      nid6      nid7
nid8

*SET_NODE_LIST_TITLE
Displacement
$#       sid       da1       da2       da3       da4    solver
           4     0.000     0.000     0.000     0.000MECH
$#      nid1      nid2      nid3      nid4      nid5      nid6      nid7
nid8
        3434      3603         0         0         0         0         0
0
*SET_NODE_LIST_TITLE
Surface_strains
$#       sid       da1       da2       da3       da4    solver
           5     0.000     0.000     0.000     0.000MECH
$#      nid1      nid2      nid3      nid4      nid5      nid6      nid7
nid8

*SET_NODE_LIST_TITLE
Top−Machine
$#       sid       da1       da2       da3       da4    solver
           6     0.000     0.000     0.000     0.000MECH
$#      nid1      nid2      nid3      nid4      nid5      nid6      nid7
nid8
        4861         0         0         0         0         0         0
0
*SET_PART_LIST_TITLE
Master
$#       sid       da1       da2       da3       da4    solver
           2     0.000     0.000     0.000     0.000MECH
$#      pid1      pid2      pid3      pid4      pid5      pid6      pid7
pid8
           3         4         0         0         0         0         0
0
*SET_SOLID_TITLE
Center
$#       sid    solver
           1MECH
$#        k1        k2        k3        k4        k5        k6        k7
k8
           1         8        15       325       326       327       328
329
         330       331       332       333       334       335       336
0
*SET_SOLID_TITLE
Cross_section
$#       sid    solver
           2MECH
```

$#	k1	k2	k3	k4	k5	k6	k7
k8							

*END

C.1.6 Notched-N1-Reduced

```
$# LS-DYNA Keyword file created by LS-PrePost 4.0 - 28Jan2013(19:00)
$# Created on Oct-25-2013 (09:55:34)
*KEYWORD
*TITLE
$# title
LS-DYNA keyword deck by LS-PrePost
$$$$$$$$$$$$$$$$$$$$$$$$$$$$$$$$$$$$$$$$ CONTROL $$$$$$$$$$$$$$$$$$$$$$$$$$$$$$$$$$$$$$$$$$$
*CONTROL_ACCURACY
$#      osu        inn     pidosu
          0          4          0
*CONTROL_ENERGY
$#     hgen       rwen     slnten      rylen
          2          2          2          2
*CONTROL_HOURGLASS
$#      ihq         qh
          1   0.100000
*CONTROL_SOLID
$#    esort    fmatrix    niptets     swlocl     psfail
          1          0          4          2          0
$#    pm1        pm2        pm3        pm4        pm5        pm6        pm7        pm8        pm9
pm10
          0          0          0          0          0          0          0          0          0
0
*CONTROL_TERMINATION
$#   endtim     endcyc      dtmin     endeng     endmas
    4.00000          0      0.000      0.000      0.000
*CONTROL_TIMESTEP
$#  dtinit     tssfac       isdo     tslimt      dt2ms       lctm      erode
ms1st
      0.000   0.700000          0      0.000      0.000          0          0
0
$#  dt2msf     dt2mslc      imscl     unused     unused      rmscl
      0.000          0          0                            0.000
*DATABASE_GLSTAT
$#       dt     binary       lcur      ioopt
    0.01000          1          0          1
*DATABASE_NODFOR
$#       dt     binary       lcur      ioopt
    0.01000          0          0          1
*DATABASE_NODOUT
$#       dt     binary       lcur      ioopt    option1    option2
    0.01000          0          0          1      0.000          0
*DATABASE_SECFORC
$#       dt     binary       lcur      ioopt
    0.01000          1          0          1
*DATABASE_BINARY_D3PLOT
```

```
$#        dt         lcdt        beam        npltc       psetid
   1.000000           0           0           0           0
$#    ioopt
            0
*DATABASE_EXTENT_BINARY
$#   neiph        neips       maxint       strflg       sigflg       epsflg       rltflg
engflg
          45           45            3            1            1            1            1
1
$#   cmpflg       ieverp       beamip        dcomp         shge        stssz       n3thdt
ialemat
           0            0            0            1            1            1            2
1
$#  nintsld      pkp_sen         sclp       unused        msscl        therm       intout
nodout
           8            0    1.000000                        0          0STRESS     STRESS
$#    dtdt        resplt
           0            0
*DATABASE_CROSS_SECTION_SET_ID
$#     csid
title
           1
$#    nsid         hsid         bsid         ssid         tsid         dsid           id
itype
           3            1            0            0            0            0            0
0
*DATABASE_HISTORY_NODE_SET
$#     id1          id2          id3          id4          id5          id6          id7
id8
           5            0            0            0            0            0            0
0
*BOUNDARY_PRESCRIBED_MOTION_SET_ID
$#       id
heading
           0move
$#    nsid          dof          vad         lcid           sf          vid        death
birth
           3            2            0            1     1.000000            01.0000E+28
0.000
*BOUNDARY_SPC_SET
$#    nsid          cid         dofx         dofy         dofz        dofrx        dofry
dofrz
           1            0            1            0            0            0            0
0
*BOUNDARY_SPC_SET
$#    nsid          cid         dofx         dofy         dofz        dofrx        dofry
dofrz
```

```
                2            0            0            0            1            0            0
0
*BOUNDARY_SPC_SET
$#      nsid          cid         dofx         dofy         dofz        dofrx        dofry
dofrz
                3            0            1            0            1            0            0
0
*BOUNDARY_SPC_SET
$#      nsid          cid         dofx         dofy         dofz        dofrx        dofry
dofrz
                4            0            1            1            1            0            0
0
*SECTION_SOLID
$#     secid       elform          aet
           1            1            0
*DEFINE_CURVE_SMOOTH
$#      lcid         sidr         dist       tstart         tend        trise           v0
           1            0   1.0000E+5        0.000        0.000     0.050000      2.00000
*MAT_USER_DEFINED_MATERIAL_MODELS
$         MID           RO           MT          LMC          NHV       IORTHO        IBULK
IG
           1   1.180e−04           44           27          114            0           12
13
$       IVECT        IFAIL       IHTERM       IHYPER         IEOS         LCMA
           1            1            0            1            0            0
$       EFLAG        YFLAG     RMAPFLAG        FFLAG        HFLAG        VFLAG        TFLAG
DFLAG
          14            1            1            1            1            1            0
1
$      STFLAG            E           PR         BULK        SHEAR       SIGMA0        ALPHA
BETA
           0    0.950e+03    3.500e−01    1.222e+03    4.074e+02    1.580e+01    1.175e+00    1.593e+00
$     THETAR1          QR1      THETAR2          QR2      THETAR3          QR3           CS
PS
    0.700e+03    4.072e+00    7.002e+00 −3.395e+00 −7.532e+01 −2.390e+00    4.738e−02    5.968e−04
$          DI          DCR        BETA0         DMIN         DMAX         SDAM
    0.000e+00    6.000e−01    1.000e+00
*PART
$# title
Notch
$#        pid        secid          mid        eosid         hgid         grav       adpopt
tmid
1,1,1,0,0,0,0,0

*SET_NODE_LIST_TITLE
symx
$#        sid          da1          da2          da3          da4       solver
1,0,0,0,0 MECH
```

```
$#       nid1       nid2       nid3       nid4       nid5       nid6       nid7
nid8
*SET_NODE_LIST_TITLE
symz
$#        sid        da1        da2        da3        da4     solver
2 ,0 ,0 ,0 ,0  MECH
$#       nid1       nid2       nid3       nid4       nid5       nid6       nid7
nid8

*SET_NODE_LIST_TITLE
load
$#        sid        da1        da2        da3        da4     solver
3 ,0 ,0 ,0 ,0  MECH
$#       nid1       nid2       nid3       nid4       nid5       nid6       nid7
nid8

*SET_NODE_LIST_TITLE
clamp
$#        sid        da1        da2        da3        da4     solver
4 ,0 ,0 ,0 ,0  MECH
$#       nid1       nid2       nid3       nid4       nid5       nid6       nid7
nid8

*SET_SOLID_TITLE
load
$#        sid     solver
          1MECH
$#         k1         k2         k3         k4         k5         k6         k7
k8

*SET_NODE_LIST_TITLE
Node  history
$#        sid        da1        da2        da3        da4     solver
5 ,0 ,0 ,0 ,0  MECH
$#       nid1       nid2       nid3       nid4       nid5       nid6       nid7
nid8
15 ,0 ,0 ,0 ,0 ,0 ,0 ,0
```

C.1.7 Notched-N2-Reduced

```
$# LS-DYNA Keyword file created by LS-PrePost 4.0 - 28Jan2013(19:00)
$# Created on Oct-25-2013 (09:55:34)
*KEYWORD
*TITLE
$# title
LS-DYNA keyword deck by LS-PrePost
$$$$$$$$$$$$$$$$$$$$$$$$$$$$$$$$$$$$$$$$$ CONTROL $$$$$$$$$$$$$$$$$$$$$$$$$$$$$$$$$$$$$$$$$$
*CONTROL_ACCURACY
$#      osu         inn      pidosu
          0           4           0
*CONTROL_ENERGY
$#     hgen        rwen      slnten       rylen
          2           2           2           2
*CONTROL_HOURGLASS
$#      ihq          qh
          1    0.100000
*CONTROL_SOLID
$#    esort     fmatrix     niptets      swlocl      psfail
          1           0           4           2           0
$#    pm1         pm2         pm3         pm4         pm5         pm6         pm7         pm8         pm9
pm10
          0           0           0           0           0           0           0           0           0
0
*CONTROL_TERMINATION
$#   endtim      endcyc       dtmin      endeng      endmas
    4.50000           0       0.000       0.000       0.000
*CONTROL_TIMESTEP
$#   dtinit      tssfac        isdo      tslimt       dt2ms        lctm       erode
ms1st
      0.000    0.700000           0       0.000       0.000           0           0
0
$#   dt2msf      dt2mslc       imscl      unused      unused       rmscl
      0.000           0           0                               0.000
*DATABASE_GLSTAT
$#       dt      binary        lcur       ioopt
   0.01000           1           0           1
*DATABASE_NODFOR
$#       dt      binary        lcur       ioopt
   0.01000           0           0           1
*DATABASE_NODOUT
$#       dt      binary        lcur       ioopt     option1     option2
   0.01000           0           0           1       0.000           0
*DATABASE_SECFORC
$#       dt      binary        lcur       ioopt
   0.01000           1           0           1
*DATABASE_BINARY_D3PLOT
```

```
$#        dt        lcdt        beam       npltc      psetid
   1.000000           0           0           0           0
$#   ioopt
          0
*DATABASE_EXTENT_BINARY
$#   neiph       neips      maxint      strflg      sigflg      epsflg      rltflg
engflg
         45          45           3           1           1           1           1
1
$#  cmpflg      ieverp      beamip       dcomp        shge       stssz      n3thdt
ialemat
          0           0           0           1           1           1           2
1
$#  nintsld     pkp_sen        sclp      unused       msscl       therm      intout
nodout
          8           0   1.000000                       0      0STRESS      STRESS
$#    dtdt      resplt
          0           0
*DATABASE_CROSS_SECTION_SET_ID
$#     csid
title
          1
$#    nsid        hsid        bsid        ssid        tsid        dsid          id
itype
          3           1           0           0           0           0           0
0
*DATABASE_HISTORY_NODE_SET
$#     id1         id2         id3         id4         id5         id6         id7
id8
          5           0           0           0           0           0           0
0
*BOUNDARY_PRESCRIBED_MOTION_SET_ID
$#      id
heading
         0move
$#    nsid         dof         vad        lcid          sf         vid       death
birth
          3           2           0           1   1.000000           01.0000E+28
0.000
*BOUNDARY_SPC_SET
$#    nsid         cid        dofx        dofy        dofz       dofrx       dofry
dofrz
          1           0           1           0           0           0           0
0
*BOUNDARY_SPC_SET
$#    nsid         cid        dofx        dofy        dofz       dofrx       dofry
dofrz
```

```
              2           0           0           0           1           0           0
0
*BOUNDARY_SPC_SET
$#      nsid         cid        dofx        dofy        dofz       dofrx       dofry
dofrz
              3           0           1           0           1           0           0
0
*BOUNDARY_SPC_SET
$#      nsid         cid        dofx        dofy        dofz       dofrx       dofry
dofrz
              4           0           1           1           1           0           0
0
*SECTION_SOLID
$#     secid      elform         aet
         1           1           0
*DEFINE_CURVE_SMOOTH
$#      lcid        sidr        dist      tstart        tend       trise          v0
         1           0  1.0000E+5       0.000       0.000    0.050000     1.00000
*MAT_USER_DEFINED_MATERIAL_MODELS
$         MID          RO          MT         LMC         NHV      IORTHO       IBULK
IG
         1  1.180e-04          44          27         114           0          12
13
$       IVECT       IFAIL      IHTERM      IHYPER        IEOS        LCMA
             1           1           0           1           0           0
$       EFLAG       YFLAG    RMAPFLAG       FFLAG       HFLAG       VFLAG       TFLAG
DFLAG
            14           1           1           1           1           1           0
1
$      STFLAG           E          PR        BULK       SHEAR      SIGMA0       ALPHA
BETA
             0   0.950e+03   3.500e-01   1.222e+03   4.074e+02   1.580e+01   1.175e+00   1.593e+00
$     THETAR1         QR1     THETAR2         QR2     THETAR3         QR3          CS
PS
  0.700e+03   4.072e+00   7.002e+00  -3.395e+00  -7.532e+01  -2.390e+00   4.738e-02   5.968e-04
$          DI         DCR       BETA0        DMIN        DMAX        SDAM
  0.000e+00   6.000e-01   1.000e+00
*PART
$# title
Notch
$#       pid       secid         mid       eosid        hgid        grav      adpopt
tmid
1,1,1,0,0,0,0,0
*SET_NODE_LIST_TITLE
symx
$#       sid         da1         da2         da3         da4      solver
1,0,0,0,0 MECH
```

```
$#       nid1       nid2       nid3       nid4       nid5       nid6       nid7
nid8
*SET_NODE_LIST_TITLE
symz
$#        sid        da1        da2        da3        da4     solver
2 ,0 ,0 ,0 ,0 MECH
$#       nid1       nid2       nid3       nid4       nid5       nid6       nid7
nid8
*SET_NODE_LIST_TITLE
load
$#        sid        da1        da2        da3        da4     solver
3 ,0 ,0 ,0 ,0 MECH
$#       nid1       nid2       nid3       nid4       nid5       nid6       nid7
nid8

*SET_NODE_LIST_TITLE
clamp
$#        sid        da1        da2        da3        da4     solver
4 ,0 ,0 ,0 ,0 MECH
$#       nid1       nid2       nid3       nid4       nid5       nid6       nid7
nid8

*SET_SOLID_TITLE
load
$#        sid     solver
          1MECH
$#         k1         k2         k3         k4         k5         k6         k7
k8

*SET_NODE_LIST_TITLE
Node history
$#        sid        da1        da2        da3        da4     solver
5 ,0 ,0 ,0 ,0 MECH
$#       nid1       nid2       nid3       nid4       nid5       nid6       nid7
nid8
21 ,0 ,0 ,0 ,0 ,0 ,0 ,0
*END
```

C.1.8 Notched-N3-Reduced

```
$# LS-DYNA Keyword file created by LS-PrePost 4.0 - 28Jan2013(19:00)
$# Created on Oct-25-2013 (09:55:34)
*KEYWORD
*TITLE
$# title
LS-DYNA keyword deck by LS-PrePost
$$$$$$$$$$$$$$$$$$$$$$$$$$$$$$$$$$$$$$$$ CONTROL $$$$$$$$$$$$$$$$$$$$$$$$$$$$$$$$$$$$$$$$$$
*CONTROL_ACCURACY
$#      osu         inn     pidosu
          0           4          0
*CONTROL_ENERGY
$#     hgen        rwen      slnten       rylen
          2           2           2           2
*CONTROL_HOURGLASS
$#      ihq          qh
          1    0.100000
*CONTROL_SOLID
$#    esort     fmatrix     niptets      swlocl      psfail
          1           0           4           2           0
$#    pm1        pm2        pm3         pm4         pm5         pm6         pm7         pm8         pm9
pm10
          0           0           0           0           0           0           0           0           0
0
*CONTROL_TERMINATION
$#   endtim      endcyc       dtmin      endeng      endmas
   8.35000           0       0.000       0.000       0.000
*CONTROL_TIMESTEP
$#  dtinit      tssfac        isdo      tslimt       dt2ms        lctm       erode
ms1st
      0.000    0.700000           0       0.000       0.000           0           0
0
$#  dt2msf      dt2mslc       imscl      unused      unused       rmscl
      0.000           0           0                                   0.000
*DATABASE_GLSTAT
$#       dt      binary        lcur       ioopt
   0.01000           1           0           1
*DATABASE_NODFOR
$#       dt      binary        lcur       ioopt
   0.01000           0           0           1
*DATABASE_NODOUT
$#       dt      binary        lcur       ioopt     option1     option2
   0.01000           0           0           1       0.000           0
*DATABASE_SECFORC
$#       dt      binary        lcur       ioopt
   0.01000           1           0           1
*DATABASE_BINARY_D3PLOT
```

```
$#         dt        lcdt        beam        npltc       psetid
  1.100000           0           0           0           0
$#    ioopt
          0
*DATABASE_EXTENT_BINARY
$#   neiph       neips      maxint      strflg      sigflg      epsflg      rltflg
engflg
         45          45           3           1           1           1           1
1
$#  cmpflg      ieverp      beamip       dcomp        shge       stssz      n3thdt
ialemat
          0           0           0           1           1           1           2
1
$# nintsld     pkp_sen        sclp      unused       msscl       therm      intout
nodout
          8           0    1.000000                               0        0STRESS      STRESS
$#    dtdt      resplt
          0           0
*DATABASE_CROSS_SECTION_SET_ID
$#     csid
title
          1
$#    nsid        hsid        bsid        ssid        tsid        dsid          id
itype
          3           1           0           0           0           0           0
0
*DATABASE_HISTORY_NODE_SET
$#     id1         id2         id3         id4         id5         id6         id7
id8
          5           0           0           0           0           0           0
0
*BOUNDARY_PRESCRIBED_MOTION_SET_ID
$#       id
heading
         0move
$#    nsid         dof         vad        lcid          sf         vid       death
birth
          3           2           0           1    1.000000              01.0000E+28
0.000
*BOUNDARY_SPC_SET
$#    nsid         cid        dofx        dofy        dofz       dofrx       dofry
dofrz
          1           0           1           0           0           0           0
0
*BOUNDARY_SPC_SET
$#    nsid         cid        dofx        dofy        dofz       dofrx       dofry
dofrz
```

| | 2 | 0 | 0 | 0 | 1 | 0 | 0 |
| 0 | | | | | | | |

*BOUNDARY_SPC_SET
$#	nsid	cid	dofx	dofy	dofz	dofrx	dofry
dofrz							
	3	0	1	0	1	0	0
0							

*BOUNDARY_SPC_SET
$#	nsid	cid	dofx	dofy	dofz	dofrx	dofry
dofrz							
	4	0	1	1	1	0	0
0							

*SECTION_SOLID
| $# | secid | elform | aet |
| | 1 | 1 | 0 |

*DEFINE_CURVE_SMOOTH
| $# | lcid | sidr | dist | tstart | tend | trise | v0 |
| | 1 | 0 | 1.0000E+5 | 0.000 | 0.000 | 0.050000 | 1.50000 |

*MAT_USER_DEFINED_MATERIAL_MODELS
$	MID	RO	MT	LMC	NHV	IORTHO	IBULK
IG							
	1	1.180e−04	44	27	114	0	12
13							
$	IVECT	IFAIL	IHTERM	IHYPER	IEOS	LCMA	
	1	1	0	1	0	0	
$	EFLAG	YFLAG	RMAPFLAG	FFLAG	HFLAG	VFLAG	TFLAG
DFLAG							
	14	1	1	1	1	1	0
1							
$	STFLAG	E	PR	BULK	SHEAR	SIGMA0	ALPHA
BETA							
	0	0.950e+03	3.500e−01	1.222e+03	4.074e+02	1.580e+01	1.175e+00	1.593e+00
$	THETAR1	QR1	THETAR2	QR2	THETAR3	QR3	CS
PS							
	0.700e+03	4.072e+00	7.002e+00	−3.395e+00	−7.532e+01	−2.390e+00	4.738e−02	5.968e−04
$	DI	DCR	BETA0	DMIN	DMAX	SDAM	
	0.000e+00	6.000e−01	1.000e+00				

*PART
$# title
Notch
| $# | pid | secid | mid | eosid | hgid | grav | adpopt |
| tmid | | | | | | | |
1,1,1,0,0,0,0,0
*NODE
| $# | nid | x | y | z | tc | rc |

*SET_NODE_LIST_TITLE
symx
| $# | sid | da1 | da2 | da3 | da4 | solver |

```
1 ,0 ,0 ,0 ,0 MECH
$#     nid1        nid2        nid3        nid4        nid5        nid6        nid7
nid8
*SET_NODE_LIST_TITLE
symz
$#      sid        da1         da2         da3         da4      solver
2 ,0 ,0 ,0 ,0 MECH
$#     nid1        nid2        nid3        nid4        nid5        nid6        nid7
nid8

*SET_NODE_LIST_TITLE
load
$#      sid        da1         da2         da3         da4      solver
3 ,0 ,0 ,0 ,0 MECH
$#     nid1        nid2        nid3        nid4        nid5        nid6        nid7
nid8

*SET_NODE_LIST_TITLE
clamp
$#      sid        da1         da2         da3         da4      solver
4 ,0 ,0 ,0 ,0 MECH
$#     nid1        nid2        nid3        nid4        nid5        nid6        nid7
nid8

*SET_SOLID_TITLE
load
$#      sid     solver
          1MECH
$#       k1         k2          k3          k4          k5          k6          k7
k8

*SET_NODE_LIST_TITLE
Node history
$#      sid        da1         da2         da3         da4      solver
5 ,0 ,0 ,0 ,0 MECH
$#     nid1        nid2        nid3        nid4        nid5        nid6        nid7
nid8
11 ,0 ,0 ,0 ,0 ,0 ,0 ,0
*END
```

C.1.9 Notched-N1-Full

```
$# LS-DYNA Keyword file created by LS-PrePost 4.0 - 28Jan2013(19:00)
$# Created on Jan-24-2014 (10:20:28)
*KEYWORD
*TITLE
$# title
LS-DYNA keyword deck by LS-PrePost
$$$$$$$$$$$$$$$$$$$$$$$$$$$$$$$$$$$$$$$$ CONTROL $$$$$$$$$$$$$$$$$$$$$$$$$$$$$$$$$$$$$$$$
*CONTROL_ACCURACY
$#       osu         inn      pidosu
           0           4           0
*CONTROL_ENERGY
$#      hgen        rwen      slnten       rylen
           2           2           2           2
*CONTROL_HOURGLASS
$#       ihq          qh
           1    0.100000
*CONTROL_SOLID
$#     esort     fmatrix     niptets      swlocl      psfail
           1           0           4           2           0
$#   pm1       pm2       pm3       pm4       pm5       pm6       pm7       pm8       pm9
pm10
           0         0         0         0         0         0         0         0         0
0
*CONTROL_TERMINATION
$#    endtim      endcyc       dtmin      endeng      endmas
    6.000000           0       0.000       0.000       0.000
*CONTROL_TIMESTEP
$#  dtinit      tssfac        isdo      tslimt       dt2ms        lctm       erode
ms1st
       0.000    0.700000           0       0.000       0.000           0           0
0
$#  dt2msf      dt2mslc       imscl      unused      unused       rmscl
       0.000           0           0                               0.000
*DATABASE_GLSTAT
$#        dt      binary        lcur       ioopt
    0.010000           1           0           1
*DATABASE_NODFOR
$#        dt      binary        lcur       ioopt
    0.010000           0           0           1
*DATABASE_NODOUT
$#        dt      binary        lcur       ioopt     option1     option2
    0.010000           0           0           1       0.000           0
*DATABASE_SECFORC
$#        dt      binary        lcur       ioopt
    0.010000           1           0           1
*DATABASE_BINARY_D3PLOT
```

312

```
$#        dt        lcdt        beam       npltc      psetid
  10.000000           0           0           0           0
$#    ioopt
          0
*DATABASE_EXTENT_BINARY
$#   neiph       neips      maxint      strflg      sigflg      epsflg      rltflg
engflg
         45          45           3           1           1           1           1
1
$#  cmpflg      ieverp      beamip       dcomp        shge       stssz      n3thdt
ialemat
          0           0           0           1           1           1           2
1
$# nintsld     pkp_sen        sclp      unused       msscl       therm      intout
nodout
          8           0    1.000000                           0      0STRESS      STRESS
$#    dtdt      resplt
          0           0
*DATABASE_CROSS_SECTION_SET_ID
$#     csid
title
          1
$#    nsid        hsid        bsid        ssid        tsid        dsid          id
itype
          3           1           0           0           0           0           0
0
*SET_NODE_LIST_TITLE
load
$#     sid         da1         da2         da3         da4      solver
          3       0.000       0.000       0.000       0.000MECH
$#    nid1        nid2        nid3        nid4        nid5        nid6        nid7
nid8

*DATABASE_HISTORY_NODE_SET
$#     id1         id2         id3         id4         id5         id6         id7
id8
          5           0           0           0           0           0           0
0
*BOUNDARY_PRESCRIBED_MOTION_SET_ID
$#       id
heading
          0move
$#    nsid         dof         vad        lcid          sf         vid       death
birth
          3           1           0           1    1.000000           01.0000E+28
0.000
*BOUNDARY_SPC_SET
```

```
$#       nsid          cid         dofx         dofy         dofz        dofrx        dofry
dofrz
            1            0            0            1            0            0            0
0
*SET_NODE_LIST_TITLE
symy
$#        sid          da1          da2          da3          da4       solver
            1        0.000        0.000        0.000        0.000MECH
$#       nid1         nid2         nid3         nid4         nid5         nid6         nid7
nid8

*BOUNDARY_SPC_SET
$#       nsid          cid         dofx         dofy         dofz        dofrx        dofry
dofrz
            2            0            0            0            1            0            0
0
*SET_NODE_LIST_TITLE
symz
$#        sid          da1          da2          da3          da4       solver
            2        0.000        0.000        0.000        0.000MECH
$#       nid1         nid2         nid3         nid4         nid5         nid6         nid7
nid8

*BOUNDARY_SPC_SET
$#       nsid          cid         dofx         dofy         dofz        dofrx        dofry
dofrz
            3            0            0            1            1            0            0
0
*BOUNDARY_SPC_SET
$#       nsid          cid         dofx         dofy         dofz        dofrx        dofry
dofrz
            4            0            1            1            1            0            0
0
*SET_NODE_LIST_TITLE
clamp
$#        sid          da1          da2          da3          da4       solver
            4        0.000        0.000        0.000        0.000MECH
$#       nid1         nid2         nid3         nid4         nid5         nid6         nid7
nid8

*PART
$# title
Notch
$#        pid        secid          mid        eosid         hgid         grav       adpopt
tmid
            1            1            1            0            0            0            0
0
*SECTION_SOLID
```

314

```
$#     secid      elform         aet
            1           1           0
*MAT_USER_DEFINED_MATERIAL_MODELS
$        MID          RO          MT         LMC         NHV      IORTHO       IBULK
IG
$#       mid          ro          mt         lmc         nhv      iortho       ibulk
ig
            1  1.1800E-4          44          27         114           0          12
13
$      IVECT       IFAIL      IHTERM      IHYPER        IEOS        LCMA
$#     ivect       ifail       itherm      ihyper        ieos        lmca      unused
unused
            1           1           0           1           0           0
$      EFLAG       YFLAG    RMAPFLAG       FFLAG       HFLAG       VFLAG       TFLAG
DFLAG
$# p1              p2          p3          p4          p5          p6          p7
p8
           14           1           1           1           1           1           0           1
$     STFLAG           E          PR        BULK       SHEAR      SIGMA0       ALPHA
BETA
$# p1              p2          p3          p4          p5          p6          p7
p8
            0      0.950e+03   3.500e-01   1.222e+03   4.074e+02   1.580e+01   1.175e+00  1.593e+00
$    THETAR1         QR1     THETAR2         QR2     THETAR3         QR3          CS
PS
$# p1              p2          p3          p4          p5          p6          p7
p8
    0.700e+03   4.072e+00   7.002e+00  -3.395e+00 -7.532e+01  -2.390e+00 4.738e-02  5.968e-04
$         DI         DCR       BETA0        DMIN        DMAX        SDAM
$# p1              p2          p3          p4          p5          p6          p7
p8
    0.000e+00   6.000e-01   1.000e+00
*PART
$# title
Notch
$#       pid       secid         mid       eosid        hgid        grav      adpopt
tmid
            2           1           2           0           0           0           0
0
*MAT_USER_DEFINED_MATERIAL_MODELS
$        MID          RO          MT         LMC         NHV      IORTHO       IBULK
IG
$#       mid          ro          mt         lmc         nhv      iortho       ibulk
ig
            2  1.1800E-4          44          27         114           0          12
13
$      IVECT       IFAIL      IHTERM      IHYPER        IEOS        LCMA
```

315

```
$#      ivect      ifail      itherm     ihyper      ieos       lmca      unused
unused
              1          1          0          1          0          0
$    EFLAG      YFLAG   RMAPFLAG      FFLAG      HFLAG      VFLAG      TFLAG
DFLAG
$# p1             p2         p3         p4         p5         p6         p7
p8
14          1          1          1          1          1          0          1
$   STFLAG          E         PR       BULK      SHEAR     SIGMA0      ALPHA
BETA
$# p1             p2         p3         p4         p5         p6         p7
p8
0          0.550e+03  4.000e−01  0.917e+03  1.964e+02  1.983e+01  1.175e+00  1.493e+00
$  THETAR1        QR1     THETAR2        QR2     THETAR3        QR3         CS
PS
$# p1             p2         p3         p4         p5         p6         p7
p8
0.700e+03  4.072e+00  7.002e+00  −3.395e+00−7.532e+01−2.390e+004.738e−02  5.968e−04
$        DI        DCR      BETA0
$# p1             p2         p3         p4         p5         p6         p7
p8
0.000e+00  6.000e−01  1.000e+00
*DEFINE_CURVE_SMOOTH
$#     lcid       sidr       dist     tstart       tend      trise         v0
          1          0  1.0000E+5      0.000      0.000   0.050000    2.00000
*SET_NODE_LIST_TITLE
Node history
$#      sid        da1        da2        da3        da4     solver
          5      0.000      0.000      0.000      0.000MECH
$#     nid1       nid2       nid3       nid4       nid5       nid6       nid7
nid8
       1844          0          0          0          0          0          0
0
*SET_SOLID_TITLE
load
$#      sid     solver
          1MECH
$#       k1         k2         k3         k4         k5         k6         k7
k8

*END
```

C.1.10 Notched-N2-Full

```
$# LS-DYNA Keyword file created by LS-PrePost 4.0 - 28Jan2013(19:00)
$# Created on Jan-24-2014 (10:03:39)
*KEYWORD
*TITLE
$# title
LS-DYNA keyword deck by LS-PrePost
$$$$$$$$$$$$$$$$$$$$$$$$$$$$$$$$$$$$$$$$$ CONTROL $$$$$$$$$$$$$$$$$$$$$$$$$$$$$$$$$$$$$$$$$$
*CONTROL_ACCURACY
$#      osu        inn     pidosu
         0          4          0
*CONTROL_ENERGY
$#     hgen       rwen     slnten      rylen
         2          2          2          2
*CONTROL_HOURGLASS
$#      ihq         qh
         1   0.100000
*CONTROL_SOLID
$#    esort    fmatrix    niptets     swlocl     psfail
         1          0          4          2          0
$#   pm1        pm2        pm3        pm4        pm5        pm6        pm7        pm8        pm9
pm10
         0          0          0          0          0          0          0          0          0
0
*CONTROL_TERMINATION
$#   endtim     endcyc      dtmin     endeng     endmas
  6.000000          0      0.000      0.000      0.000
*CONTROL_TIMESTEP
$#  dtinit     tssfac       isdo     tslimt      dt2ms       lctm      erode
ms1st
     0.000   0.700000          0      0.000      0.000          0          0
0
$#  dt2msf     dt2mslc      imscl     unused     unused      rmscl
     0.000          0          0                            0.000
*DATABASE_GLSTAT
$#       dt     binary       lcur      ioopt
  0.010000          1          0          1
*DATABASE_NODFOR
$#       dt     binary       lcur      ioopt
  0.010000          0          0          1
*DATABASE_NODOUT
$#       dt     binary       lcur      ioopt    option1    option2
  0.010000          0          0          1      0.000          0
*DATABASE_SECFORC
$#       dt     binary       lcur      ioopt
  0.010000          1          0          1
*DATABASE_BINARY_D3PLOT
```

```
$#        dt        lcdt        beam       npltc      psetid
   1.000000           0           0           0           0
$#    ioopt
          0
*DATABASE_EXTENT_BINARY
$#   neiph       neips       maxint      strflg      sigflg      epsflg      rltflg
engflg
         45          45           3           1           1           1           1
1
$#  cmpflg      ieverp       beamip       dcomp        shge       stssz      n3thdt
ialemat
          0           0           0           1           1           1           2
1
$# nintsld     pkp_sen         sclp      unused       msscl       therm      intout
nodout
          8           0    1.000000                       0        0STRESS      STRESS
$#    dtdt      resplt
          0           0
*DATABASE_CROSS_SECTION_SET_ID
$#    csid
title
          1
$#    nsid        hsid        bsid        ssid        tsid        dsid          id
itype
          3           1           0           0           0           0           0
0
*SET_NODE_LIST_TITLE
load
$#     sid         da1         da2         da3         da4      solver
          3       0.000       0.000       0.000       0.000MECH
$#    nid1        nid2        nid3        nid4        nid5        nid6        nid7
nid8

*DATABASE_HISTORY_NODE_SET
$#     id1         id2         id3         id4         id5         id6         id7
id8
          5           0           0           0           0           0           0
0
*BOUNDARY_PRESCRIBED_MOTION_SET_ID
$#       id
heading
          0move
$#    nsid         dof         vad        lcid          sf         vid       death
birth
          3           1           0           1    1.000000           01.0000E+28
0.000
*BOUNDARY_SPC_SET
```

```
$#       nsid          cid         dofx         dofy         dofz        dofrx        dofry
dofrz
            1            0            0            1            0            0            0
0
*SET_NODE_LIST_TITLE
symy
$#        sid          da1          da2          da3          da4       solver
            1        0.000        0.000        0.000        0.000MECH
$#       nid1         nid2         nid3         nid4         nid5         nid6         nid7
nid8

*BOUNDARY_SPC_SET
$#       nsid          cid         dofx         dofy         dofz        dofrx        dofry
dofrz
            2            0            0            0            1            0            0
0
*SET_NODE_LIST_TITLE
symz
$#        sid          da1          da2          da3          da4       solver
            2        0.000        0.000        0.000        0.000MECH
$#       nid1         nid2         nid3         nid4         nid5         nid6         nid7
nid8

*BOUNDARY_SPC_SET
$#       nsid          cid         dofx         dofy         dofz        dofrx        dofry
dofrz
            3            0            0            1            1            0            0
0
*BOUNDARY_SPC_SET
$#       nsid          cid         dofx         dofy         dofz        dofrx        dofry
dofrz
            4            0            1            1            1            0            0
0
*SET_NODE_LIST_TITLE
clamp
$#        sid          da1          da2          da3          da4       solver
            4        0.000        0.000        0.000        0.000MECH
$#       nid1         nid2         nid3         nid4         nid5         nid6         nid7
nid8

*PART
$# title
Core
$#        pid        secid          mid        eosid         hgid         grav       adpopt
tmid
            1            1            1            0            0            0            0
0
*SECTION_SOLID
```

```
$#       secid      elform         aet
            1           1           0
*MAT_USER_DEFINED_MATERIAL_MODELS
$         MID          RO          MT         LMC         NHV      IORTHO       IBULK
IG
$#        mid          ro          mt         lmc         nhv      iortho       ibulk
ig
            1  1.1800E-4          44          27         114           0          12
13
$       IVECT       IFAIL      IHTERM      IHYPER        IEOS        LCMA
$#      ivect       ifail      itherm      ihyper        ieos        lmca      unused
unused
            1           1           0           1           0           0
$       EFLAG       YFLAG    RMAPFLAG       FFLAG       HFLAG       VFLAG       TFLAG
DFLAG
$# p1             p2          p3          p4          p5          p6          p7
p8
14          1           1           1           1           1           0           1
$      STFLAG           E          PR        BULK       SHEAR      SIGMA0       ALPHA
BETA
$# p1             p2          p3          p4          p5          p6          p7
p8
0          0.950e+03   3.500e-01   1.222e+03   4.074e+02   1.580e+01   1.175e+00   1.593e+00
$     THETAR1         QR1     THETAR2         QR2     THETAR3         QR3          CS
PS
$# p1             p2          p3          p4          p5          p6          p7
p8
0.700e+03   4.072e+00   7.002e+00  -3.395e+00 -7.532e+01 -2.390e+00 4.738e-02   5.968e-04
$          DI         DCR       BETA0        DMIN        DMAX        SDAM
$# p1             p2          p3          p4          p5          p6          p7
p8
0.000e+00   6.000e-01   1.000e+00
*PART
$# title
Skin
$#        pid       secid         mid       eosid        hgid        grav      adpopt
tmid
            2           1           2           0           0           0           0
0
*MAT_USER_DEFINED_MATERIAL_MODELS
$         MID          RO          MT         LMC         NHV      IORTHO       IBULK
IG
$#        mid          ro          mt         lmc         nhv      iortho       ibulk
ig
            2  1.1800E-4          44          27         114           0          12
13
$       IVECT       IFAIL      IHTERM      IHYPER        IEOS        LCMA
```

```
$#     ivect        ifail       itherm       ihyper        ieos         lmca       unused
unused
            1           1           0           1           0           0
$    EFLAG       YFLAG    RMAPFLAG       FFLAG       HFLAG       VFLAG       TFLAG
DFLAG
$# p1           p2          p3          p4          p5          p6          p7
p8
14          1           1           1           1           1           0           1
$   STFLAG        E          PR        BULK       SHEAR      SIGMA0       ALPHA
BETA
$# p1           p2          p3          p4          p5          p6          p7
p8
0          0.550e+03 4.000e-01 0.917e+03 1.964e+02 1.983e+01 1.175e+00 1.493e+00
$  THETAR1       QR1     THETAR2        QR2     THETAR3        QR3          CS
PS
$# p1           p2          p3          p4          p5          p6          p7
p8
0.700e+03 4.072e+00 7.002e+00 -3.395e+00-7.532e+01-2.390e+004.738e-02 5.968e-04
$        DI         DCR       BETA0
$# p1           p2          p3          p4          p5          p6          p7
p8
0.000e+00 6.000e-01 1.000e+00
*DEFINE_CURVE_SMOOTH
$#    lcid        sidr        dist      tstart        tend       trise          v0
         1           0 1.0000E+5       0.000       0.000    0.050000    1.000000
*SET_NODE_LIST_TITLE
Node  history
$#     sid         da1         da2         da3         da4      solver
         5       0.000       0.000       0.000       0.000MECH
$#    nid1        nid2        nid3        nid4        nid5        nid6        nid7
nid8
         5           0           0           0           0           0           0
0
*SET_SOLID_TITLE
load
$#     sid      solver
         1MECH
$#      k1          k2          k3          k4          k5          k6          k7
k8

*END
```

C.1.11   Notched-N3-Full

```
$# LS-DYNA Keyword file created by LS-PrePost 4.0 - 28Jan2013(19:00)
$# Created on Jan-24-2014 (11:49:40)
*KEYWORD
*TITLE
$# title
LS-DYNA keyword deck by LS-PrePost
$$$$$$$$$$$$$$$$$$$$$$$$$$$$$$$$$$$$$$$$ CONTROL $$$$$$$$$$$$$$$$$$$$$$$$$$$$$$$$$$$$$$$$$$
*CONTROL_ACCURACY
$#       osu         inn      pidosu
          0           4           0
*CONTROL_ENERGY
$#      hgen        rwen      slnten       rylen
          2           2           2           2
*CONTROL_HOURGLASS
$#       ihq          qh
          1    0.100000
*CONTROL_SOLID
$#     esort     fmatrix     niptets      swlocl      psfail
          1           0           4           2           0
$#    pm1        pm2        pm3        pm4        pm5        pm6        pm7        pm8        pm9
pm10
          0           0           0           0           0           0           0           0           0
0
*CONTROL_TERMINATION
$#    endtim      endcyc       dtmin      endeng      endmas
   7.000000           0       0.000       0.000       0.000
*CONTROL_TIMESTEP
$#   dtinit      tssfac        isdo      tslimt       dt2ms        lctm       erode
ms1st
      0.000    0.700000           0       0.000       0.000           0           0
0
$#   dt2msf      dt2mslc       imscl      unused      unused       rmscl
      0.000           0           0                                0.000
*DATABASE_GLSTAT
$#        dt      binary        lcur       ioopt
   0.010000           1           0           1
*DATABASE_NODFOR
$#        dt      binary        lcur       ioopt
   0.010000           0           0           1
*DATABASE_NODOUT
$#        dt      binary        lcur       ioopt     option1     option2
   0.010000           0           0           1       0.000           0
*DATABASE_SECFORC
$#        dt      binary        lcur       ioopt
   0.010000           1           0           1
*DATABASE_BINARY_D3PLOT
```

```
$#          dt         lcdt        beam       npltc      psetid
  2.000000            0           0           0           0
$#    ioopt
           0
*DATABASE_EXTENT_BINARY
$#    neiph        neips       maxint      strflg      sigflg      epsflg      rltflg
engflg
          45           45           3           1           1           1           1
1
$#   cmpflg       ieverp      beamip       dcomp        shge       stssz      n3thdt
ialemat
           0            0           0           1           1           1           2
1
$#   nintsld      pkp_sen        sclp       unused       msscl       therm      intout
nodout
           8            0    1.000000                                0        0STRESS      STRESS
$#     dtdt       resplt
           0            0
*DATABASE_CROSS_SECTION_SET_ID
$#      csid
title
           1
$#     nsid         hsid        bsid        ssid        tsid        dsid          id
itype
           3            1           0           0           0           0           0
0
*SET_NODE_LIST_TITLE
load
$#      sid          da1         da2         da3         da4      solver
           3        0.000       0.000       0.000       0.000MECH
$#     nid1         nid2        nid3        nid4        nid5        nid6        nid7
nid8

*DATABASE_HISTORY_NODE_SET
$#      id1          id2         id3         id4         id5         id6         id7
id8
           5            0           0           0           0           0           0
0
*BOUNDARY_PRESCRIBED_MOTION_SET_ID
$#       id
heading
           0move
$#     nsid          dof         vad        lcid          sf         vid       death
birth
           3            1           0           1    1.000000           01.0000E+28
0.000
*BOUNDARY_SPC_SET
```

```
$#       nsid         cid        dofx        dofy        dofz       dofrx       dofry
dofrz
           1           0           0           1           0           0           0
0
*SET_NODE_LIST_TITLE
symy
$#        sid         da1         da2         da3         da4      solver
           1       0.000       0.000       0.000       0.000MECH
$#       nid1        nid2        nid3        nid4        nid5        nid6        nid7
nid8

*BOUNDARY_SPC_SET
$#       nsid         cid        dofx        dofy        dofz       dofrx       dofry
dofrz
           2           0           0           0           1           0           0
0
*SET_NODE_LIST_TITLE
symz
$#        sid         da1         da2         da3         da4      solver
           2       0.000       0.000       0.000       0.000MECH
$#       nid1        nid2        nid3        nid4        nid5        nid6        nid7
nid8

*BOUNDARY_SPC_SET
$#       nsid         cid        dofx        dofy        dofz       dofrx       dofry
dofrz
           3           0           0           1           1           0           0
0
*BOUNDARY_SPC_SET
$#       nsid         cid        dofx        dofy        dofz       dofrx       dofry
dofrz
           4           0           1           1           1           0           0
0
*SET_NODE_LIST_TITLE
clamp
$#        sid         da1         da2         da3         da4      solver
           4       0.000       0.000       0.000       0.000MECH
$#       nid1        nid2        nid3        nid4        nid5        nid6        nid7
nid8

*PART
$# title
Notch
$#        pid       secid         mid       eosid        hgid        grav      adpopt
tmid
           1           1           1           0           0           0           0
0
*SECTION_SOLID
```

```
$#     secid      elform         aet
           1           1           0
*MAT_USER_DEFINED_MATERIAL_MODELS
$        MID          RO          MT         LMC         NHV      IORTHO       IBULK
IG
$#       mid          ro          mt         lmc         nhv      iortho       ibulk
ig
           1  1.1800E-4          44          27         114           0          12
13
$      IVECT       IFAIL      IHTERM      IHYPER        IEOS        LCMA
$#     ivect       ifail       itherm      ihyper        ieos        lmca      unused
unused
           1           1           0           1           0           0
$      EFLAG       YFLAG    RMAPFLAG       FFLAG       HFLAG       VFLAG       TFLAG
DFLAG
$# p1              p2          p3          p4          p5          p6          p7
p8
14           1           1           1           1           1           0           1
$     STFLAG           E          PR        BULK       SHEAR      SIGMA0       ALPHA
BETA
$# p1              p2          p3          p4          p5          p6          p7
p8
0        0.950e+03  3.500e-01  1.222e+03  4.074e+02  1.580e+01  1.175e+00  1.593e+00
$    THETAR1         QR1     THETAR2         QR2     THETAR3         QR3          CS
PS
$# p1              p2          p3          p4          p5          p6          p7
p8
0.700e+03  4.072e+00  7.002e+00 -3.395e+00-7.532e+01-2.390e+004.738e-02  5.968e-04
$         DI         DCR       BETA0        DMIN        DMAX        SDAM
$# p1              p2          p3          p4          p5          p6          p7
p8
0.000e+00  6.000e-01  1.000e+00
*PART
$# title
Notch
$#       pid       secid         mid       eosid        hgid        grav      adpopt
tmid
           2           1           2           0           0           0           0
0
*MAT_USER_DEFINED_MATERIAL_MODELS
$        MID          RO          MT         LMC         NHV      IORTHO       IBULK
IG
$#       mid          ro          mt         lmc         nhv      iortho       ibulk
ig
           2  1.1800E-4          44          27         114           0          12
13
$      IVECT       IFAIL      IHTERM      IHYPER        IEOS        LCMA
```

```
$#      ivect       ifail      itherm      ihyper        ieos        lmca      unused
unused
             1           1           0           1           0           0
$     EFLAG       YFLAG    RMAPFLAG       FFLAG       HFLAG       VFLAG       TFLAG
DFLAG
$# p1                 p2          p3          p4          p5          p6          p7
p8
14           1           1           1           1           1           0           1
$    STFLAG           E          PR        BULK       SHEAR      SIGMA0       ALPHA
BETA
$# p1                 p2          p3          p4          p5          p6          p7
p8
0          0.550e+03 4.000e−01 0.917e+03 1.964e+02 1.983e+01 1.175e+00 1.493e+00
$   THETAR1         QR1      THETAR2         QR2     THETAR3         QR3          CS
PS
$# p1                 p2          p3          p4          p5          p6          p7
p8
0.700e+03 4.072e+00 7.002e+00 −3.395e+00−7.532e+01−2.390e+004.738e−02 5.968e−04
$         DI         DCR       BETA0
$# p1                 p2          p3          p4          p5          p6          p7
p8
0.000e+00 6.000e−01 1.000e+00
*DEFINE_CURVE_SMOOTH
$#     lcid        sidr        dist      tstart        tend       trise          v0
          1           0 1.0000E+5       0.000       0.000    0.050000    1.500000
*SET_NODE_LIST_TITLE
Node history
$#      sid         da1         da2         da3         da4      solver
          5       0.000       0.000       0.000       0.000MECH
$#     nid1        nid2        nid3        nid4        nid5        nid6        nid7
nid8
          8           0           0           0           0           0           0
0
*SET_SOLID_TITLE
load
$#      sid      solver
          1MECH
$#       k1          k2          k3          k4          k5          k6          k7
k8

*END
```

C.2 Abaqus input file

C.2.1 Drop tower

Main

```
*Heading
** Job name: solid_drop Model name: Model−1
** Generated by: Abaqus/CAE 6.11−1
*Preprint, echo=NO, model=NO, history=NO, contact=NO
**
** PARTS
**
*Part, name=Plate
*Elset, elset=symx
*Elset, elset=symz
*Nset, nset=skin
*Elset, elset=skin
*Nset, nset=core
*Elset, elset=core, generate
 14743, 73710,      1
** Section: skin
*Solid Section, elset=skin, material=skin
,
** Section: core
*Solid Section, elset=core, material=Core
,
*End Part
**
*Part, name=impactor
*End Part
**
**
** ASSEMBLY
**
*Assembly, name=Assembly
**
*Instance, name=Plate−1, part=Plate
*End Instance
**
*Instance, name=impactor−1, part=impactor
*Node
      1, −0.00999999978, 0.0287500005, −1.22464679e−18
*Nset, nset=impactor−1−RefPt_, internal
1,
*Nset, nset=refpt
 1,
*Surface, type=REVOLUTION, name=impacotr
```

```
START,            0.01,  0.0287500000279397
 LINE,            0.01,            0.01
 CIRCL,              0.,              0.,              0.,            0.01
*Rigid Body, ref node=impactor−1−RefPt_, analytical surface=impacotr
*Element, type=MASS, elset=refpt_mass_
1, 1
*Mass, elset=refpt_mass_
1.26125,
*End Instance
**
*End Assembly
**
** MATERIALS
**
*include,input=mat.inp
**
** INTERACTION PROPERTIES
**
*Surface Interaction, name=IntProp−1
*Friction
 0.3,
*Surface Behavior, pressure−overclosure=HARD
**
** BOUNDARY CONDITIONS
**
** Name: disp_impactor Type: Displacement/Rotation
*Boundary
impactor−1.refpt, 1, 1
impactor−1.refpt, 3, 3
impactor−1.refpt, 4, 4
impactor−1.refpt, 5, 5
impactor−1.refpt, 6, 6
** Name: enc Type: Symmetry/Antisymmetry/Encastre
*Boundary
Plate−1.clamp, ENCASTRE
** Name: symx Type: Symmetry/Antisymmetry/Encastre
*Boundary
Plate−1.symx, XSYMM
** Name: symz Type: Symmetry/Antisymmetry/Encastre
*Boundary
Plate−1.symz, ZSYMM
**
** PREDEFINED FIELDS
**
** Name: Predefined Field−1   Type: Velocity
*Initial Conditions, type=VELOCITY
impactor−1.refpt, 1, 0.
impactor−1.refpt, 2, −4.411
```

```
impactor −1.refpt , 3 , 0.
** ————————————————————————————————————————————————————————————
**
** STEP: loading
**
*Step , name=loading
*Dynamic , Explicit
, 0.0140
*Bulk Viscosity
0.06 , 1.2
**
** INTERACTIONS
**
** Interaction : Int −1
*Contact , op=NEW
*Contact Inclusions , ALL EXTERIOR
*Contact Property Assignment
 , , IntProp −1
**
** OUTPUT REQUESTS
**
*Restart , write , number interval=1, time marks=NO
**
** FIELD OUTPUT: F−Output −1
**
*OUTPUT, FIELD , NUMBER INTERVAL=150 ,TIME MARKS=YES
*ELEMENT OUTPUT
ER, PEEQ, S , PE, LE , E , ENER, STATUS, SDV
*NODE OUTPUT
U, V, RF
*Output , history , variable=PRESELECT, time interval=0.000106667
*END STEP
```

Materials

```
** MATERIALS
**
*Material, name=skin
*Density
1180.,
*INCLUDE,INPUT=./DEPVAR_SPM.inc
*User material, Constants = 25
**  EFLAG,     YFLAG, RMAPFLAG,   FFLAG,    HFLAG,    VFLAG,   TFLAG,     DFLAG
       1,         1,        1,        1,        1,        1,       0,         1
** STFLAG,        E,       PR, SIGMA0,    ALPHA,    BETA,THETAR1,       QR1
       0,    0.55e8,     0.40, 1.98e7,    1.175,    1.49,   0.7e9,  4.072e+6
**THETAR2,      QR2,   THETAR3,     QR3,       CS,      PS,      DI,       DCR
  7.002e6,-3.395e6,- 7.532e7,-2.39e6,4.738e-2,5.968e-4,       0,6.000e-01
**   BETA0
       1
*Material, name=core
*Density
1180.,
*INCLUDE,INPUT=./DEPVAR_SPM.inc
*User material, Constants = 25
**  EFLAG,     YFLAG, RMAPFLAG,   FFLAG,    HFLAG,    VFLAG,   TFLAG,     DFLAG
       1,         1,        1,        1,        1,        1,       0,         1
** STFLAG,        E,       PR, SIGMA0,    ALPHA,    BETA,THETAR1,       QR1
       0,    0.95e9,     0.35, 1.58e7,    1.175,    1.59,   0.7e9,  4.072e+6
**THETAR2,      QR2,   THETAR3,     QR3,       CS,      PS,      DI,       DCR
  7.002e6,-3.395e6,- 7.532e7,-2.39e6,4.738e-2,5.968e-4,       0,6.000e-01
**   BETA0
       1
```